STUDIES ON FLUIDISED BED DRYING

by

ISMAIL MOSTAFA, B.Sc., M.Sc., D.I.C.

Thesis submitted in part fulfilment of the regulations for Ph.D. degree of the University of London.

Dept. of Chemical Engineering and
Chemical Technology,
Imperial College,
University of London.

September, 1977.



TEXT BOUND INTO

THE SPINE

To

my wife Avis

my daughter Bianca

and my mother.

ABSTRACT

A three-dimensional fluidised bed was designed, constructed and operated to study the drying of different materials (e.g. silica gel, molecular sieves and exfoliated vermiculite).

An experimental study was conducted to analyse the effect of air flow rate and temperature, particle size and bed height, and indirectly, the bubbling behaviour of the bed on the solids drying rate.

The variation in minimum fluidising velocity with solids moisture content was studied experimentally. A simple agglomeration model is suggested to explain the moist particles' behaviour - at incipient fluidisation- during the drying period, in which it is assumed that at higher solids moisture content than a critical value, the bed is composed of spherical agglomerates where particles are held together mainly by surface tension forces, and below this critical value the variation in minimum fluidising velocity is directly related to the single particles density variation with moisture content. The model was tested and showed a qualitative agreement with the experimental results.

The effect of both air velocity and particle diameter on the overall heat and mass transfer coefficient was studied experimentally. The results obtained showed that all the transfer occurs in the first few centimeters above the distributor where bubbles, if they exist, are extremely small, - and hence the gas may be treated as one homogeneous phase represented by particle Reynolds' number. The results from both heat and mass transfer studies showed

an analogy during the drying period, where both of Nusselt and Sherwood's numbers are proportional to Reynold's number raised to the power (1·3).

Finally, a simple bubbling model, combined with a homogeneous model in the entry zone was developed and discussed, to represent the fluidised bed dryer. The proposed modle shows good agreement with the experimental results and supports Walker's (1975) results of the significance of the distributor on the bed performance. From the experimental results it is clear that an earlier model in the literature is in error, largely because the entry zone effect was ignored in fluidised bed drying.

ACKNOWLEDGEMENTS

I would like to thank Dr. D.L. Pyle, who has done so much to guide this work, and provided an endless source of energy for all his students. I would also like to acknowledge my debt to Professor R. Sargent, whose vital assistance revived the project during its most critical stage.

Finally, I am grateful to The Old Centralians, for their financial support during the final stage of the project.

LIST OF CONTENTS

		PAGE
Chapter 1	INTRODUCTION	1
Chapter 2	EQUIPMENT AND EXPERIMENTAL DETAILS	8
2-1	Introduction	8
2-2	Design consideration	8
2-3	Apparatus	11
	2-3-1 Air filter	11
	2-3-2 Pressure reducing valve	11
	2-3-3 Dehumidifier	11
	2-3-4 Heater	12
	2-3-5 Fluidised beds	13
	2-3-6 Dust separating unit	14
2-4	Measurements	15
	2-4-1 Flow rate measurement	15
	2-4-2 Pressure measurement	15
	2-4-3 Temperature measurement	15
	2-4-4 Air humidity measurement	16
	2-4-5 Solids moisture content	17
2-5	Fluidising materials	18
2-6	Start-up procedure	19

Chapter 3		MINIMUM FLUIDISING VELOCITY	21
	3-1	Introduction	21
	3-2	Pressure drop and minimum fluidising velocity	21
	3-3	Factors affecting fluidising behaviour	22
		3-3-1 Inter-particle forces	23
		1- Surface tension force	25
		2- London/Van der Waal's force	27
		3- Electrostatic force	28
		3-3-2 Hydrodynamic forces	28
	3-4	Agglomeration model	30
	3-5	Experimental study on (U^*)	38
	3-6	Results	38
Chapter 4		HEAT TRANSFER IN FLUIDISED BED DRYING	43
	4-1	Introduction	43
	4-2	Fluid/particle heat transfer	44
		4-2-1 Review	44
		4-2-2 Mechanism	44
		4-2-3 Experimental study on ($h_{g/p}$)	52
		4-2-4 Results and correlations	54
	4-3	Bed/wall heat transfer	56
		4-3-1 Review	56
		4-3-2 Mechanism	62
		4-3-3 Experimental study on ($h_{B/w}$)	63
		4-3-4 Results and correlations	65

Chapter 5 MASS TRANSFER IN FLUIDISED BED DRYING 69

5-1 Introduction 69

5-2 Overall mass transfer in fluidised bed drying 69

5-3 Mass transfer to rising bubbles in aggregative fluidisation 77

5-4 Mechanism 85

5-5 Experimental study on the overall mass transfer coefficient $\bar{K}_g$ 88

5-6 Results and correlations 91

Chapter 6 SOLIDS DRYING CURVES IN SHALLOW FLUIDISED BEDS 94

6-1 Introduction 94

6-2 Basic principles 94

6-2-1 Humidification process 94

6-2-2 Hygrothermal equilibrium 96

6-2-3 Drying curves 97

6-2-4 Pore diffusion 98

6-3 Solids drying mechanisms 101

6-3-1 Moisture diffusion model 101

6-3-2 Pore diffusion model 102

6-3-3 Simultaneous mass and heat transfer model 105

6-4 Experimental study on drying of solids in fluidised bed 107

6-4-1 Effect of bed height 108

6-4-2 Effect of gas flow rate 109

6-4-3 Effect of particle size 110

6-4-4 Effect of gas temperature 111

6-4-5 Effect of bubble exchange factor 112

6-5	Results and correlations	113
6-6	Discussion	118
Chapter 7	MODELLING	120
7-1	Introduction	120
7-2	Fluidised bed models review	122
7-3	Theoretical considerations in fluidised bed drying	125
7-4	Model for simultaneous heat and mass transfer	127
	A- Entry zone	127
	B- Top section	130
7-5	Experimental study on bed performance	133
7-6	Results	135
	A- Entry zone	135
	B- Comparison with model	135
	C- Effect of air flow rate on bed performance	137
	D- Effect of bed height on bed performance	137
Chapter 8	DISCUSSION AND CONCLUSIONS	139
8-1	Minimum fluidising velocity	139
8-2	Entry zone effect	141
8-3	Analogy between heat and mass transfer	142
8-4	Solids drying rate	143
8-5	Fluidised bed dryer model	144
8-6	Implications	145

FIGURES 147

Figures (2) Equipment 147

Figures (3) Minimum fluidising velocity 150

Figures (4) Heat transfer 161

Figures (5) Mass transfer 183

Figures (6) Solids drying curves 190

Figures (7) Modelling 218

APPENDICES

Appendix (1) Hygrothermal properties of saturated humid air 243

Appendix (2) Equipment 245

Appendix (3) Particle size determination 252

Appendix (4) Heat transfer calculations 254

Appendix (5) Air humidity calculations 280

Appendix (6) Drying curves 308

Appendix (7) Model results 345

Appendix (8) Modelling of top section in fluidised bed dryer 355

NOMENCLATURE 362

REFERENCES 368

CHAPTER (1)

INTRODUCTION

Drying is one of the oldest unit operations discovered by man. In the early stages of life on earth; crops and seeds were dried using the sun as the direct source of energy. Later, the need for more sophisticated methods became apparent: not only to dry crops and seeds efficiently and under unfavourable weather conditions but also to dry the different industrial products (e.g. chemicals, powders, granules) as well as natural resources (e,g. iron ores, phosphate rocks, salts). Drying methods have been extended not only to cover solid phase meterials but also to cover liquids and gases, hence new types of drying medium have been explored such as molecular sieves and silica gel.

Many drying methods have been used to cover the wide range of varieties of the industrial products. These methods can be classified into two main groups: direct and indirect drying; both of these two groups can be either batch or continuous. Under the first group where the drying is carried out by contacting hot dry gases with the wet materials, we can mention: continuous tray dryers such as continuous metal belts or vibrating trays, utilizing hot gases; continuous sheeting dryers where a continuous sheet of material passes through the dryer; pneumatic conveying dryers where often in conjuction with grinding, materials are conveyed in a stream at high temperature and velocity gases to a cyclone collector; rotary dryers where materials are conveyed and showered inside the rotating cylinder through which hot gases flow; tunnel dryers where materials on trucks are moved through a tunnel then contacted with hot gases; and spray dryers where wet fine powders are sprayed from nozzles at the top of the dryer

to contact hot gases flowing upwards.

Under the second group, where hot gases and wet solids do not come into a direct contact, we find cylinder dryers where continuous sheets are dried by passing over rotating cylinders which are generally steam heated; drum dryers which may be heated with steam or hot water; steam tube rotary dryers where also steam or hot water can be used; vibrating tray dryers where heat is supplied by either steam or hot water and the vibration improves heat transfer coefficients; agitated pan dryers which can handle small quantities of one batch of granules agitated in a horizontal stationary steam heated shell; and vacuum tray dryers where wet solids are dried on shelves heated by steam or hot water.

More advanced drying methods have been developed such as infra-red or radiant heat dryers, where the operation depends on the generation, transmission and absorption of infra-red rays. Dielectric heat dryers operate on the principle of heat generation within solids by placing them in a high frequency electric field.

Each method mentioned above has its own applications, advantages and disadvantages, but in general there are a number of problems associated with most of drying methods discussed above. One of the major problems in drying of granules is the thermal gradient inside the solids which creates thermal stresses and leads to cracks in the final product. Another problem is the uneven distribution of heat inside the dryers, which produces different drying rates for the same product and produces a distribution of final moisture content in the same product. One problem associated with drying of chemical powders - especially heat sensitive types - is that "hot spots" inside the bulk of product can ruin the whole batch. In engineering terms, most of the drying methods discussed above are characterised by low overall heat transfer coefficients

(of the order of 10 $\frac{\text{Watt}}{m^2\ {}^oK}$), high power consumption and relatively high capital cost.

Mathur and Gishler (1955) started a new technique for wheat drying using a spouted bed, in which a jet of hot air is blown through a shallow bed of wheat. In small dryers, the grain nearest to the hot air stream is the first to dry and most severely heated. In large dryers, mixing may be promoted by the use of rotating metal shafts.

Peterson (1963) produced the first commercial spouted bed dryers in Canada to dry three types of peas, lentils and flux. The commercial dryer had a 60 cm diameter heater and a 90 cm diameter cooler side by side, the heater contained a 210 cm deep spouted bed while the cooler contained a moving packed bed. Wet feed flowed through an adjustable slide door from a storage bin into the side of the heater; the hot partially dried product overflowed to the cooler with counter-current air flow, where further drying occured. The final dried product flowed through a regulating orifice at the bottom of the cooler.

Peck et al (1974) used a spouted bed for the batch drying of barley malt in Brazil. The column used was an upright cylinder of 30 cm diameter with a conical base terminating in an air inlet pipe; the air was supplied by a centrifugal blower through a heater into a metallic gauze at the bottom of the bed.

Spouted bed dryers have proved to have useful applications in the drying of coarse materials which do not fluidise properly. There are some problems associated with drying in spouted beds, such as : particle agglomeration inside the bed, non-uniform temperature distribution, "hot spots" in the bed, and the moisture content distribution of the final product.

The monograph by Davidson and Harrison (1963) succeeded in attracting the attention of many scientists and engineers to the importance of fluidised beds applications in the different areas of heat and mass transfer, chemical reactions, combustion, solids mixing, mineral separation, and powder technology. Fluidised beds proved to have advantages in many fields; with higher conversion levels and bed performance as chemical reactors, as well as facilitating high solid surface areas and better mixing in the bed. One major advantage of fluidised beds is the uniform temperature distribution in the bed, which helps to avoid thermal cracks in particles and "hot spots" in the bulk of the bed. The high heat and mass transfer coefficients in fluidised bed leads to better performance and lower power consumption, in addition to the ease and safety of operation and control of these beds.

Since the 1940's the industrial research laboratories started working on the commercial application of fluidised bed dryers.

Wall and Ash (1949) managed to manufacture a commercial fluidised bed dryer and sizer for lime stone and dolomite using a 180 cm diameter by 480 cm high bed of 45 (ton/hr) capacity. The drying medium was hot air of 400°C. The air was heated by an oil burner and passes through the bed to the cyclons.

Beeker (1958) showed the significance of fluid bed dryers in the industry. A fluo solids dryer was supplied to the Marguette Cement Manufacturing Co. of Rockmart, Georgia, for drying of limestone replacing two 12 meters long rotary drying units. The first coal dryer was erected at the Lynnville-Indiana where a preparation plant for Lynnville Coal Co. was designed to handle 70 (ton/hr) and to remove 10% moisture from 4 mm coal particles.

Beeken (1960) reviewed the commercial application of fluidised bed dryers in the industry. One of the main applications was limestone and dolomite drying and a plant was erected for New England Lime Co. Ltd. to dry 50 (ton/hr) dolomite. Another main application for fluidised bed dryers was to handle the blast furnace slag which is used in the cement industry. A commercial plant of 240 cm diameter bed was erected in the Detroit area to handle 35 (ton/hr) slag of moisture content 10% - 20% (dry basis) and dry it up to 0.1% at an operating temperature of 100°C. A new application of fluidised bed dryers in the chemicals industry took place in Hastelloy U.S.A. The dryer was 150 cm in diameter and could reduce the moisture content of chemicals from 30% to 0.5% under operating temperatures of 100 - 120°C. Fluidised bed dryers have been applied to dry phosphate rock by Dorr - Olliver Co. and can handle up to 300 (ton/hr).

Scott et al (1963) introduced fluidised bed dryers to the pharmaceutical industry and concluded that drying in fluidised beds is fifteen times faster than conventional tray drying methods. They used lactose placebo made with solution of methyl cellulose as the binding agent and the second test granulation was an anti-acid, consisting primarily of magnesium trisilicate with syrup as the binding agent.

Davis and Glazier (1965) applied a large scalefluidised bed dryer to iron-ore concentrate. The dryer plant had two identical fluidised bed units, each one consisting of two compartments separated by a refractory dome constriction plate containing Tuyeres for gas distribution into the bed. The wind box compartment below the constriction plate is a 420 cm diameter combustion zone, where air enters through a bustle pipe and oil is injected and burned to produce hot gases for fluidisation and drying in the upper compartment of the bed. Moisture laden gases and entrained solids are disengaged in the free board above the bed, and off-gas passes through ductwork to a cyclone system and stack.

Commercial fluidised bed drying proved to have advantages compared with other drying methods in different industrial areas, (e.g. limestone, dolomite, blast furnace slag, cement, chemicals, iron-ore, posphate rocks), hence a detailed study of fluidised bed drying was required to enable us to estimate the parameters involved in the process, and to evaluate their importance, on both the dryer performance and heat and mass transfer rates in the bed. In practice there have been relatively few theoretical studies of fluidising bed operation. In some early work, Kettenring, Manderfield and Smith (1950) studied mass and heat transfer in fluidised bed drying and produced correlations for those coefficients.

Heertjes, De Boer and Haas Van Dorsser (1953) produced a report on experimental measurements of humidity and temperature in fluidised bed drying using Foxboro dew point meter.

Heertjes and Mc. Kibbins (1955) tried to correlate the partial heat transfer coefficient from air to solids in fluidised bed drying.

Heertjes (1962) tried to explore the analogy between heat and mass transfer in fluidised bed drying and to correlate the simultaneous mass and heat transfer coefficients in the bed.

Wormald and Burnell (1971) tried to discuss the different engineering aspects in the design of fluidised bed dryers (e.g. throughputs, residence time, operating temperature range, feed moisture content, product moisture content).

Hoebink and Rietema (1974) produced a simple mathematical model for moisture transfer from solids to gas in fluidised bed drying, based on Rowe and Partridge's "Cloud Model" in fluid bed reactor.

These studies are described critically and in more details in subsequent sections of this work. However, in general it can be said that there has been no definitive study of the various factors involved in the transfer process, nor is there

a clear picture of the relative importance of the different physical processes involved. In this project a study of the effect of some parameterson the dryer performance is carried out, and experimental data are obtained and correlated on the processes of heat and mass transfer in the bed. The effect of solids moisture content on minimum fluidising velocity is studied experimently, and a simple agglomeration model is developed for drying offine particles. The effect of different factors on drying rates of solids is analysed experimently and a general correlation is produced. Finally, a simple mathematical model is developed to explain the behaviour of fluidised bed dryer on the light of the simultaneous heat and mass transfer occuring at the entry zone, taking into account the role of bubbles in the bed.

CHAPTER (2)

EQUIPMENT AND EXPERIMENTAL DETAILS

2-1 INTRODUCTION

A 10 cm diameter fluidised bed was designed and constructed to dry different materials such as silica gel, molecular seives and exfoliated vermiculite. A 2-dimensional bed was also used for some ancillary studies.

A line diagram of the equipment is shown in figure (2-1). Compressed air at a nominal 100 PSI (6.8 bar) passes through two air filters to remove traces of oil or condensed water. The clean air passes through a pressure reducing valve, leaving at a pressure of 20 PSI (1.4 bar) and then flows through a series of flowmeters. The air is divided into two independently controlled streams, one of which is fed directly to the fluidised bed distributor while the other passes through a fluidised bed dehumidification unit. The dry clean air passes through an electrically heated unit where it is heated up to the required temperature before it enters the bed. A temperature controller connected to the electric heater was used to control the air temperature entering either the three or two dimensional bed.

2-2 DESIGN CONSIDERATION

The main design objective was to achieve a wide range of bed performance during the drying period, and a large number of practical problems associated with operating the bed had also to be solved.

The following points summarize some of the factors taken into account in the design of the fluidised bed dryer:

1. Choice of fluidising materials - One of the major problems is to find suitable materials which can be fluidised whilst drying. Some materials such as sand, coke, potassium permanganate and calcium carbonate do not fluidise properly at high initial moisture contents, due to large interparticle forces or solids agglomeration, leading to slugging and channelling in the bed. On the other hand silica gel, molecular sieves and exfoliated vermiculite have excellent fluidising properties during drying; in addition, the change in colour of silica gel (from pink to blue during drying) gives an additional sensitive observation for the drying period in a fluidised bed.

2. Sampling points - 2 cm diameter holes were drilled at different heights in the bed to enable measurements of the solids moisture content. The fluidised solids were sampled via 1.5 cm diameter on/off valves. The size of sampling points was chosen on the basis of the largest particle size handled by the bed. The sampling points were arranged at vertical intervals of 10 cm starting at a height of 3 cm above the distributor, to enable measurements of the moisture profiles in the bed, as well as the degree of solids mixing for different fluidising materials.

3. Temperature measurements - Gas and solids temperatures are important parameters in the analysis of fluidised bed drying. Shielded Copper / Constantan thermo-couples were fitted into the bed at heights of 5 mm, 1 cm, 2 cm, 5 cm and 10 cm above distributor. Suction lines were connected to the thermo-couples to measure the air temperature profile in the bed. Further details are given in section 2-4-3.

4. Humidity measurement - A (Shaw) hygrometer was used to measure both inlet and outlet air conditions. Air sampling points were installed 10 cm apart to measure the variation in air humidity with bed height via Suction lines, manifold and a vacuum centrifugal pump.

5. Flowrate measurement and control - Air flowrates up to 1000 l/min were used to fluidise different solids with average particle diameters of 106, 940, 2247 and 4470 microns. It was noticed in a preliminary study that the minimum fluidising velocity for the same particles depends strongly on the initial moisture content, and thus a mercury manometer was connected above the distributor to enable the measurement of the exact flowrate required for minimum fluidisation, using the pressure drop across the bed as an indicator of the onset of fluidisation.

6. Temperature control - This was based on two major measurements : first, the temperature of the air leaving the heating unit; secondly, the air temperature at the base of the distributor. A secondary electric heater was installed next to the dehumidifier to give an additional heating load, and to allow operation of higher flowrates up to 1000 l/min at operating temperature of 150°C; at the same time the heater served as a stand-by for the primary heating unit.

7. Charging and discharging the bed - The fresh wet solids were fed from the top of 200 cm high bed at the beginning of the operation, and were discharged at the end of the drying period from 3 holes of 2 cm diameter at the bottom of the bed.

8. Solids elutriation - An air filter was installed at the top of the three dimensional bed, to remove all the dust escaped from the bed and recover the

fine particles elutriated during the operation.

2-3 APPARATUS

The equipment consists of six major units as shown in figure (2-1): an air filter, pressure reducing valve, dehumidifier, heater, fluidised beds and dust separating unit . In the following section, a brief discussion of the design, function and operation of each unit is given, taking into account the practical problems associated during operation and the choice of a range of operating conditions to obtain the maximum bed performance.

2-3-1 AIR FILTER

In order to remove the oil and water from the air supply, an air filter was necessary. Two automatic drain filters were fitted to the air line before the reducing valve. The first separates all the oil from the air stream, while the second reduces the condensed moisture down to 10 gm water/Kg air.

2-3-2 PRESSURE REDUCING VALVE

The clean air coming from the filters at a nominal pressure of 100PSI (6.8 bar) enters a 2.5 cm inlet-outlet pressure reducing valve, and leaves it at 20 PSI (1.4 Bar). The pressure reducing valve can handle flowrates upto 1000 l/min.

2-3-3 DEHUMIDIFIER

A fluidised bed dehumidifier was designed to reduce the air humidity in the input stream to a minimum of 4.439 gm water/Kg air. The bed was 10 cm diameter and 60 cm high with 2.5 cm inlet and outlet tubes. The dehumidifier was made of brass, while its distributor was sintered stainless steel. A 100 micron mesh gauze was fixed at the top of the bed to prevent solids elutriation.

The fluidising material used was silica gel having an average particle size of 4 mm - based on particle size distribution function shown in Appendix 3 - and the total bed height was 40 cm. The air leaving the dehumidifier was sampled using the "Shaw" hygrometer, if the outlet humidity exceeded 4.439 gm water/ Kg air, the process was stopped and the $silica_{gel}$ was regenerated inside the bed using a 2.5 KW heating element wound around the dehumidifier and controlled by voltage regulator and temperature controller.

2.3.4 HEATER

The dry clean air entering the electrically heated unit was divided into two streams, using 1.2 cm diameter red brass tubes, to follow a coiled path through the unit.

The electrical heating element used was electrothermal quartz cord insulation/ high voltage loading (HC 505), of 488 cm in length and 1600 wattage, with a surface loading of 6.2 Watt/cm^2 and a linear loading of 4 Watt/cm with 230 V supply. The element temperature reaches up to 800°C. Because of the high surface loading of the element, a temperature controller was used as well as a voltage regulator. The element was made of nickel/chrome around an inorganic Core, and covered witha tough external sheath of braided quartz fibre of an approximate outside diameter of 5 mm.

Two elements were used in the heating unit togive an overall electrical power of 3 KW. To reduce heat losses, a quartz fibre sheet was used for insulating the heating unit which was packed in a mild steel box. To achievethe necessary performance and maintain safe operation the following precautions were used:

1. Voltage regulator - The electric current passing through the heating elements was controlled by a voltage regulator. The output voltage was increased to 80% of the fed value over a period of one hour.

2. Air temperature control - The temperature of the air leaving the heater varies with the operating conditions. The air flow rate is one of the major factors affecting the maximum temperature obtained (e.g. for an air flowrate of 100 l/min, its temperature could reach 300°C; on the other hand for larger flowrates (e.g. up to 1000 l/min the maximum air temperature obtained was 150°C). A Copper/Constantan thermo-couple at the heater outlet measured the air temperature and was connected to an on-off solid state temperature controller.

3. Element temperature control - The temperature of the element should not exceed 800°C. To avoid damage a nickel-chromium/nickel-aluminium thermo-couple connected to a pyrometer was fixed along the element surface inside the heating unit. The operating conditions were restricted to give a maximum element temperature of 700°C.

2-3-5 FLUIDISED BEDS

A cylindrical section fluidised bed was designed to study the different parameters affecting solids drying rates as well as mass and heat transfer in the bed. A temperature-resistant glass bed was chosen to allow for observing bubble formation and behaviour. It also enabled us to study solids mixing and circulation in the bed, as well as the change of colour of silica gel from pink to blue during drying.

The bed was 10 cm diameter and the total height of the glass tube was 200 cm. The hot dry clean air enters the bed through a 1 cm thick sintered stainless steel distributor plate. The solids sampling points are separated vertically by 10 cm intervals, while the bottom one is 3 cm above distributor. The bed also has 5 valves to sample the air rising in the bed. Both air and solids temperatures are measured in the bed, using suction and covered Copper/Constantan thermo-couples at different heights in the bed (e.g. 5mm 1 cm, 2 cm, 5 cm and 10 cm above the distributor.)

A two-dimensional fluidised bed was installed next to the main rig for qualitative experiments. A three way valve in the air supply controlled the air flow to each bed.

2-3-6 DUST SEPARATING UNIT

Solids elutriation and dust formation is one of the problems associated with operating fluidised beds. A two-section dust separator was designed to overcome this problem consisting of a cylindrical brass base of 10 cm outside diameter and 15 cm high to fit tightly on the top of the fluidised bed. An aluminium box of 40x40x60 cm was welded to the brass cylinder to increase the separator cross sectional area; hence the air velocity drops in this region to enable fine particles to settle in the separator. A 50 micron mesh gauze was also provided at the top of each section to separate any escaped particles. The design proved to be highly efficient for particle sizes larger than 100 microns diameter, but less satisfactory for particles of less than 50 microns diameter.

2.4 MEASUREMENTS

The following variables were measured at different parts of the rig: air flow rate and pressure before the dehumidifier, solids and air temperature at 5mm, 1 cm, 2 cm, 5 cm, and 10 cm above the bed distributor, the humidity of the air entering and leaving the bed and the average solids moisture content of the bed.

2-4-1 AIR FLOW RATE MEASUREMENT

A series of rotameters (Metric 7A, 18A and 47A) were installed after the pressure reducing valve, to measure the air flow rate up to 1000 l/min. Calibration charts were constructed for ther three rotometers under different operating conditions (e.g. atmospheric pressure and 15°C, 1.7 bar and 25°C, 2.4 bar and 15°C).

2-4-2 PRESSURE MEASUREMENT

Spiral bourdon pressure gauges were used to measure the air pressure at different points in the supply line. A mercury manometer was connected above the distributor to measure the pressure drop across the bed and to enable the minimum fluidising velocity to be measured.

2-4-3 TEMPERATURE MEASUREMENT

The analysis of fluidised bed drying depends strongly on the air and solids temperatures in the bed.

Copper/Constantan thermo-couples in stainless steel sheath were chosen, covering a total range of -100°C to 400°C. The thermo-couple measuring circuit consisted of hot and cold junctions, connected to a potentiometer with its accessories (e.g. galvonometer, standard cell and 2V battery). The calibration of the Copper/Constantan thermo-couples is given in Appendix (2-2).

Three different methods were used to measure the following temperatures:

(1) Average bed temperature - This was measured directly by fitting the shielded Copper/Constantan thermo-couples into the bed. This measurement represents an average temperature between the air and the solids at the bed.

(2) Air temperature - To measure the air temperature in the bed, it was necessary to isolate the particles from the thermo-couples using a 50 micron mesh gauze to cover the thermo-couple cap heads. A vacuum line was connected to the thermo-couple so that a small flow of air was sucked past the thermo-couple to give a measurement of the air temperature inside the bed. The temperature of the air entering the bed is measured and controlled by a temperature controller as shown in figure (2-2).

(3) Solids temperature - Two methods were used for this purpose: one of them was using an adhesive material on the thermo-couple to cover it with solids and prevent any contact with air; the second method was to use thermo-couple cap heads filled with fresh particles to insulate it from the air stream. The first method mentioned above showed a false higher solids temperature; mainly because of the different specific heat capacity of the adhesive material from the fluidised particles.

2-4-4- AIR HUMIDITY

The humidity of the air leaving the fluidised bed dryer is a sensitive indicator of the bed performance. A 6 mm copper tube was used to sample the air from different points in the rig; this was connected to a "Shaw" hygrometer for humidity measurement. The air was sampled from the following points in the rig:

(1) After the dehumidifier - The air was sampled to indicate the efficiency of the dehumidifier and the need for regeneration of silica gel.

(2) After the heater - The air was sampled to check its humidity.

(3) Three dimensional bed - The air was sampled from five different points in the bed with 10 cm vertical intervals to give the air humidity profile in the bed. The results obtained were not satisfactory and hence the humidity of the air leaving the bed was measured directly by the sensor element.

(4) Two dimensional bed - The air was sampled from the top of the bed to give a qualitative analysis of the bed performance.

The "Shaw" hygrometer has two scales : one which reads dew points (-80°C to - 20°C) and is used for very dry gases; the second scale gives the gas relative humidity (0-100%) using the normal sensing element.

The sensing element is an idealised hygroscopic system, only a few microns in thickness, in which there is a dynamic equilibrium between the liquid water contained in the pores and the water vapour pressure outside the element. Because of the small size of pores, large molecules cannot enter the pores and the element is specific for water vapour molecules. The capacitance of the system varies with its water content and this is indicated on the dial - in the front panel of the equipment - and recorded using chart recorder.

2-4-5 SOLIDS MOISTURE CONTENT

In this work the moisture content determination of silica gel was carried out using a sensitive micro balance (10^{-6}gm). The solids were

sampled through an on/off valve 5 cm above distributor, and the sample was isolated from the air by means of a sealed tube. The moisture content was calculated by weighing the sample before and after complete oven drying using the prepared micro balance.

2-5 FLUIDISING MATERIALS

A preliminary study of fluidised bed drying, showed that some wet solids have very poor fluidising properties, especially at high initial moisture content. Examples of such materials are :

(1) Sand : different particle sizes were tried (e.g. 100, 250, 350, and 500 microns) at different initial moisture content, up to 0.30 gm Water/gm dry sand.

(2) Coal .: pulverized coal of 100 microns particle size was tried. Unfortunately the drying process was accompanied by agglomeration of the particles inside the bed which leads to channelling.

(3) Potassium Permanganete : a series of preliminary experiments were carried out to dry wet potassium permanganate of 500 micron particle size and 0.10 initial moisture content. The bed did not fluidise properly till the solids moisture content dropped to 0.0015 gm water/gm dry solids.

Further experimental study showed that there are some other materials which have excellent fluidising properties during drying such as:

(1) Exfoliated vermculite - It is used in ion-exchange packed bed, and can be fluidised well during drying at 20% gm water/ gm solids for a batch of 400 microns average particle size.

(2) Molecular sieves - Particles up to 500 microns average particle size can fluidise easily at initial moisture content of 0.10 gm water/gm solids.

(3) Silica gel - From preliminary experimental study on fluidised bed drying it was shown that silica gel is one of the ideal materials for analysis of the dryer performance. The pink wet silica gel changes its colour to blue to determine when the process should be stopped.

The majority of our experimental work was carried out using silica gel of different particle sizes (e.g. 106, 940, 2247 and 4067 microns).

2-6 START-UP PROCEDURE

To start-up the fluidised bed dryer, the following steps should be followed to ensure a safe operation:

(1) Air from the main supply is vented to drain the condensed water and oil in the line.

(2) The pressure reducing valve is set and adjusted to the required operating pressure.

(3) The required flowrate is set using the rotometers and allowed to pass through the equipment.

(4) First, cold air flows through the empty bed to atmosphere while the valve to humidifier is shut.

(5) The humidifier heater is switched on to allow for silica gel regeneration.

(6) The heater is switched on and the voltage output is increased from 10% to 70% over a period of one hour.

(7) Once the heater and the dehumidifier are at the operating conditions, the air is switched through them.

(8) The air temperature entering the bed is governed by the temperature controller setting; it is allowed to pass for one hour before it reaches

steady state conditions.

(9) The air is then switched to the 2-Dimensional bed while wet solids are charged to the cylindrical bed.

(10) The drying experiment starts when the hot dry clean air is allowed to enter the bed.

CHAPTER (3)

MINIMUM FLUIDISING VELOCITY

3-1 INTRODUCTION

The poor fluidising characteristics of certain powders and solids is well known from the literature. In fluidised bed drying, it is clear that the moisture content of the solids plays an important role on the bed behaviour; for example, a preliminary study on drying of wet sand showed that the bed does not fluidise until the sand moisture content drops to 0.001 gmwater/gm solids. It is clear that this behaviour must be related to the balance of inter-particle forces as a function of solids moisture content.

The resultant of different inter-particle forces acting such as surface tension, London - Van der Waal's and electrostatic forces produce an attractive potential between the particles to form agglomerates. On the other hand, the fluid flow past the touching particles creates a hydrodynamic force which tends to break these agglomerates.

The balance between inter-particle forces and hydrodynamic forces in the bed will govern the solids behaviour during the drying period.

3-2 PRESSURE DROP AND MINIMUM FLUIDISING VELOCITY

The pressure drop whilst a fluid flows through fluidised or packed particles has been studied by many workers (e.g. some classic early studies were carried out by Blake (1922) , Kozeny (1927), Carman (1937) and Ergun (1952)).

Richardson (1971) presented a comprehensive review on minimum fluidising velocity and its derivation from the existing pressure drop relationships. He showed that for fine spherical particles, using the Carman-Kozeny equation for pressure drop, the minimum fluidising velocity can be expressed as*:

$$U_o = 0.00059 \frac{dp^2 (\rho_s - \rho_f) g}{\mu} \qquad (3\text{-}1)$$

For larger particles, using Ergun equation for pressure drop, the following relationship is obtained:

$$\frac{\rho_f (\rho_s - \rho_f) g\, dp^3}{\mu^2} = 150 \frac{(1 - \varepsilon_o)}{\varepsilon_o^3} \frac{\rho_f \cdot dp}{\mu} U_o + \frac{1.75}{\varepsilon_o^3} \left[\frac{\rho_f \cdot dp}{\mu}\right]^2 U_o^2 \qquad (3\text{-}2)$$

3-3 FACTORS AFFECTING FLUIDISING BEHAVIOUR

As seen from Geldart (1973) and Geldart and Baeyens (1974); the fluidising behaviour of fine particles depends on both the mean particle size and the particle density. They classified the solids fluidised by gas into four major groups depending on their behaviour: Group (A) where dense phase expansion occurs in the region between minimum fluidisation and bubble commencement, group (B) where bubbling starts at the minimum fluidising velocity , group (C) which contains solids difficult to fluidise and group (D) where a stable spouted bed is formed. In group (C) they showed that the inter-particle cohesive forces are greater thatn those exerted by the fluid on particles.

Vanecek et al (1967) studied the effect of initial moisture content on minimum fluidising velocity. They used particle size of 0.1 - 0.7 mm for different sand types (e.g. river, glass and recirculation foundary sand).

---

* A complete set of symbols can be found in the nomenclature section

They showed that the wet sand does not fluidise until the moisture content drops to a certain value below 0.04 gm W/gm S depending on the type of sand used. They also mentioned the variation of minimum fluidising velocity with the sand moisture content over their short drying period (0.04 gm water/gm solids), but they failed to relate the bed behaviour to the cohesive forces between the particles.

In fluidised bed drying, the free moisture existing in the bed creates surface tension forces between the particles which plays its role in particle agglomeration. The agglomerate behaviour is governed by the balance between two major forces: inter-particle forces which create adhesion between the particles inside the agglomerate and is mainly due to surface tension forces - figure (3-1-a) and hydrodynamic forces which are created by the fluid flow in and around the agglomerate and tends to separate the particles and break the agglomerate - figure (3-2).

In the following section these latter two forces will be discussed in an attempt to illustrate its effect on the fluidising behaviour of the bed.

3-3-1 INTER-PARTICLE FORCES

For small particles of average diameter 100 microns or less, inter-particle forces are important and are of the same order as gravitational forces (Donsi and Massimilla 1973 - 1975).

Henszelmann et al (1967) studied the industrial problem of agglomeration of fine pigments in fluidised beds. They used a 3.9 cm bed to fluidise lead chromate, paris blue, chromium oxide and iron oxide for a range of particle sizes of 0.06 - 0.6 microns. Their results showed a large value for minimum

voidage fraction (0.8 - 0.9) which is much greater than expected (0.3-0.4) and they explained that as a result of particles agglomeration in the bed.

Cheng (1968) developed a theory for the tensile strength of fine particles in fluidised beds, taking into account powder density, particle size distribution and inter-particle forces. He showed that the surface of each particle consists of surface portrusions and the physical contact between particles is made by the micro contacts between these portrusions, which prevent the particles from coming into intimate contact and give a space for liquid to fill between particles. He mentioned the effect of inter-particle forces (e.g. surface tension, Van der Waal's, electrostatic and magnetic forces) on particle agglomeration. Unfortunately, there is no experimental proof of the theory.

Sastry and Fuerstenau (1972) tried to explain the mechanism of agglomerate growth in pelletization. They showed that the physical forces contributing to the formation of an agglomerate are:

(1) Attractive forces between particles, including surface tension, Van der Waal's and electrostatic forces.

(2) An inter-locking effect between particles, which depends largely on the particles shape.

(3) Adhesional and cohesional forces which lead to bridges between particles.

(4) Interfacial and capillary forces which depend on the solids moisture content. For fluidised bed drying, the first force mentioned is applicable.

Rietema and Mutsers (1973) studied the effect of inter-particle forces on the elasticity of fluidised beds. They used a two dimensional tilting bed (100 x 26 x 1 cm) to fluidise cracking catalyst, polypropylene and glass beads

of particle sizes 18-128 microns with different fluidising media: air, hydrogen, neon and propane. Their results showed that, at low fluidising velocity, the inter-particle forces give the fluidised bed a sufficientely stable structure to prevent it from sliding-off when the bed is tilted around an axis perpendicular to it. In their discussion they ignored the effect of friction force-between the bed and its wall-on the stability of the bed structure, which has a special importance in case of very narrow two dimensional beds.

Donsi and Massimilla (1973 & 1976) studied particle to particle forces in fluidised beds of fine particles. They showed that for coarse particles (dp $\nearrow$ 500 microns), bubbles appear as soon as the fluid velocity exceeds the minimum fluidising velocity, on the other hand for fine particles (dp $\searrow$ 50 microns) bubbles do not appear when the velocity exceeds the minimum fluidising conditions and channelling occurs instead. They suggested that for fine particles of average particle diameter less than 100 microns, the intensity of inter-particle forces is proportional to the radius of curvature of particles aspherities at contact points. For very small aspherities less than 0.1 micron, the inter-particle forces are comparable with the weight of particles in the 40-100 micron size range.

In the following section, inter-particle forces in fluidised bed drying are discussed. We will consider the role of surface tension, London - Van der Waal's and electrostatic forces in particles agglomeration.

1. SURFACE TENSION FORCES

The presence of liquid between solid particles creates certain forces mainly due to surface tension. A pendular liquid shape between particles

represents the general case for the moisture in a non-hygroscopic bed, where water is retained as separate lens-shaped rings at the points of contact between particles. For hygroscopic materials; the excess moisture over the saturation conditions will stay in a pendular state.

From figure (3-1-a), a general picture of the cohesive forces between two particles in the agglomerate is shown where:

(1) A surface tension force (T)dynes, between the spherical particles of radius (R)cm, due to the presence of moisture of surface tension (σ)dyne/cm, is represented by:

$$T = 2 \pi b . \sigma \qquad (3\text{-}3)$$

and acts along the air/water interface.

(2) A pressure force (P) , due to the hydrostatic pressure in the water being lower than that in the air, with which the remainder of the particle is in contact; as shown by Conway-Jones (1957):

$$P = \pi b^2 \sigma \left(\frac{1}{c} - \frac{1}{b} \right) \qquad (3\text{-}4)$$

The overall surface tension force (F_s)dynes, is produced by adding equations (3-3) and (3-4) to give:

$$F_s = \frac{2 \pi R}{1 + \text{Tan} (\theta/2)} \qquad (3\text{-}5\text{-}a)$$

where (θ) is the angle corresponding to the free moisture content between the two particles (figure 3-1-a).

For an average particle size of 100 microns and using $\sigma_{water} = 73$ dyne/cm (at 18°C), the surface tension forces between two particles can be calculated at the beginning of the drying - assuming that the two particles are over saturated with water hence ($\theta = \pi /2$).

The overall surface tension force = 1.146 dynes

It is important to realize that - from equation (3-5) - the surface tension

force is proportional to the particle size.

2- LONDON- VAN DER WAAL S FORCES

The adhesive forces created by the presence of one particle next to another has been studied by different workers, Corn (1966) reviewed it showing that London-Van der Waal·s force can be represented in the following form:

$$F_v = \frac{\pi m_o^2 \lambda}{24} \quad \frac{dp}{r^2} \qquad (3\text{-}5)$$

where

F_v: London-Van der Waal/s force (dynes)

m_o: Number of particles in 1 cm^3 (—)

λ: Van der Waal s constant (ergs)

dp: particle diameter (cm)

r : the distance of approach of surfaces (cm)

To apply equation (3-5) to the particles inside the agglomerate during drying, we shall use the results discussed by Corn (1966) for the Constant in Van der Waal s equation where($\frac{\pi m_o^2 \lambda}{24} = 5 \times 10^{-10}$ ergs) for spherical particles. The assumption for the distance of approach of surfaces (r) is extremely difficult because of the irregularity of particles surface.

To give an estimate for the order of magnitude of the forces involved, we shall assume that (r = 1000 Å), using an average particle diameter of 100 microns, from equation (3-5):

London- Van der Waal s force = 5×10^{-2} dynes

This force becomes less significant as the particle size increases.

3- ELECTROSTATIC FORCES

If the particle carries a charge (g) e.s.u., and is separated by a distance (r) cm from the adhering particle by a dielectric medium (ε), the induced electrical force on the particle can be represented by:

$$F_E = \frac{\varepsilon\ g^2}{r^2} \qquad (3\text{-}6)$$

For the same particles discussed for London-Van der Waal s forces, we shall assume opposite charges of 100 e.s.u. on each particle and the medium in between is air, then for an average particle diameter of 100 micron and the distance of approach of surfaces is assumed 1000 Å equation 3-6 produces:

Electrostatic force = 2.2×10^{-6} dynes

Comparing these results, it is clear that the surface tension forces is 100 times larger than London-Van der Waal s which is already 10000 times larger than the electrostatic forces• the surface tension force is the major contributing factor for the overall inter-particle forces in the bed.

3-3-2 HYDRODYNAMIC FORCES

The forces created by a uniform viscous flow past touching or close particles is a famous problem which has been studied in a range of application areas.

Stimson and Jeffery (1926) were the first to study the motion set up in a viscous fluid at rest at infinity by two spheres (equal or unequal) moving with equal small velocities par allel to their line of centre. The same analysis applies to the corresponding problem in which spheres are fixed and an infinite fluid streams past them with a constant velocity. They managed to derive mathematically the forces created by a viscous

irrotational incompressible fluid moving with velocity (U) at infinity, on two touching spheres of radius (r). Based on Stokes' stream lines function for fluid motion, they derived:

$$F = (\lambda)\ (6\pi\mu r)\ U \qquad (3\text{-}7)$$

where:

F: hydrodynamic force in the same dirrection of the fluid flow and acts at the centre of each particle.

μ: fluid viscosity.

λ: is function of (α) which is the ratio between the centre distance between the two particles and the particle diameter (e.g. for α=1.1; λ= 0.663 and for $\alpha=\infty$; λ=1 leading to Stokes' law).

r: spherical particle radius

U: fluid velocity at infinity

Happel and Brenner (1965) gave a detailed mathematical analysis of fluid flow at low Reynold s' numbers around two touching spheres, using solid spherical harmonic function. They derived the following form for the hydrodynamic force exerted by a viscous fluid on two touching equal-sized spheres not free to rotate, with their line of centres parallel to the fluid flow direction:

$$F = (0.647)\ (6\pi\mu r)\ U \qquad (3\text{-}8)$$

where: F, μ, r and U are defined as in equation (3-7)

Goren (1970) studied the normal force exerted by creeping flow past two touching spheres of arbitrary sizes and parallel to the line of centres. Using an axisymmetric stagnation flow with no-slip boundary conditions, he derived the same form of hydrodynamic force:

$$F = (K)\ (6\pi\mu r)\ U \qquad (3\text{-}9)$$

where (K) is a function of the distance between the spheres (e.g. K=0.645 for touching spheres).

Rowe and Hen wood (1961) and Rowe (1961) measured the drag forces on a sphere in water stream, and showed how these drag forces vary with the proximity of neighbouring spheres. Using 1.3 and 1.6 cm in diameter polythene spheres and flow conditions of Reynolds' numbers in the range 10 to 1000, they studied the effect different particles arrangements on the drag forces. The experimental results showed an increase in the drag forces of almost two order of magnitude when the sphere forms part of a regular packed array.

In the next section, a simple agglomeration model is presented to illustrate the effect of both hydrodynamic and surface tension forces on the stability of agglomerates during the drying period.

3-4 AGGLOMERATION MODEL

The results of an experimental study of the effect of the moisture content on the minimum fluidising velocity of silica gel are shown in figures (3.4,5 and 6). By drawing two straight lines, the idealised behaviour can be represented as shown in figures (3.7,8 and 9) where the asymptotes intersect at a critical point (X_{cr}, U_{cr}) which depends strongly on the particle size.

A possible explanation is that for solids moisture contents higher than the critical value (X_{cr}) , there is sufficient free moisture for particles to agglomerate, and below the value (X_{cr}) the moisture is largely contained within the particles.

To find the effect of different parameters on the agglomerate behaviour, the following assumptions are made:

(1) All the particles in the bed are spherical and have an average diameter dp.

(2) For hygroscopic materials, at higher moisture contents than the critical value ($X > X_{cr}$), all the micro pores are penetrated with water and excess water exists in pendular state between particles as free moisture.

(3) Above (X_{cr}) particles bind together because of surface tension forces and form agglomerates, with an average equivalent diameter of $\bar{D}_A$, containing N particles per agglomerate.

(4) The average moisture content of the agglomerate is the same as the solid particles in the bed.

(5) When drying proceeds, the solids moisture content decreases until it reaches a critical value (X_{cr}), at which the surface tension forces are no longer strong to resist the hydrodynamic forces, hence the agglomerate breaks.

From figures (3-7, 8 and 9), the bed behaviour is classified into two regions: (AB), where the bed is assumed to be composed of spherical agglomerates, in which particles are held together by the inter-particle forces, and (BC), where single particles only exist and the change in minimum fluidising velocity is mainly due to the variation in density with the moisture content.

1- REGION BC (Single Particles)

When the solids moisture content reaches the critical value X_{cr}; the surface tension forces are no longer strong enough to resist the hydrodynamic forces, hence the agglomerates break.

In this region, the variation in minimum fluidising velocity of moist solids U* is mainly due to the moist solids density variation during drying. At any solids moisture content X (where $X < X_{cr}$), the moist solids density

$$\rho_s^* = \rho_s (1 + A X) \qquad (3\text{-}10)$$

where:

ρ_s: solids density of bone dry particles

A: fractional moisture content contained inside particles.

The minimum fluidising velocity for bone dry particles U_o can be represented by:

$$U_o = \frac{K g}{\mu} \; dp^2 \; (\rho_s - \rho_f) \qquad (3\text{-}11)$$

where:

K = constant depends on the theory (e.g. for Carman - Kozeny equation: K = 0.00059)

For moist particles, the minimum fluidising velocity U* can be written as:

$$U^* = \frac{Kg}{\mu} \; dp^2 \; (\rho_s^* - \rho_f) \qquad (3\text{-}12)$$

using equation (3-10) and (3-11), the following form for equation (3-12) is obtained (by ignoring ρ_f compared with ρ_s):

$$U^* = U_o + BX \qquad (3\text{-}13)$$

where

$B = U_o . A$

To find the relationship between the fractional moisture content contained inside the particle A and the particle size dp, we shall assume that particles have a shape factor $\Phi = 1$, and an average internal pore fraction (E). Assuming that moisture penetrates a distance Δ inside the particle of diameter dp, hence the following relationships are written:

$$\text{Particle mass} = \frac{\pi}{6} dp^3 \rho_s$$

$$\text{Mass of moisture} = \frac{\pi}{6} (dp^3 - (dp - \Delta)^3) \rho_w E$$

by ignoring the higher powers of (Δ), the following equation is obtained:

$$A X = \frac{3 \rho_w \cdot \Delta \cdot E}{\rho_s} \cdot \frac{1}{dp} \qquad (3\text{-}13\text{-}a)$$

From equation (3-13-a), it is clear that for the same adsorbing materials (i.e. Δ = constant) and for the same solids moisture content X (where $X < X_{cr}$), the following simple relationship can be obtained:

$$A = K \frac{1}{dp} \qquad (3\text{-}13\text{-}b)$$

(for $X < X_{cr}$)

2 - REGION A B (Agglomeration)

When solids moisture content is higher than the critical value (X_{cr}) the excess moisture above saturation conditions exists in a pendular state between the particles and exerts surface tension forces. In this region we assume, as a first approximation, that the bed is composed of spherical agglomerates where the particles are held together by inter-particle forces (principally surface tension).

To estimate the number of particles N inside an agglomerate, which is assumed to have an average diameter $\bar{D}_A$, volume V and to contain mass W of particles and has an internal voidge fraction ϕ, then the effective diameter of the aggregate is related to N by:

$$\frac{\pi}{6} \bar{D}_A^3 (1 - \phi) = \frac{\pi}{6} N dp^3 \qquad (3\text{-}14)$$

for hexagonal packing of particles, $\phi = 0.395$ and hence equation (3-14) can be reduced to:

$$N = 0.605 \quad R_A^{\,3} \tag{3-15}$$

where:

R_A = ratio between the agglomerate and particle diameters

$$= \frac{\bar{D}_A}{dp}$$

To find the dry bulk agglomerate density ρ_A

$$\rho_A = \frac{N \left(\frac{\pi}{6} \quad dp^3\right) \rho_s}{\frac{\pi}{6} \quad \bar{D}_A^{\,3}}$$

$$\rho_A = 0.605\, \rho_s \tag{3-16}$$

Since all the moisture is assumed to be contained inside the agglomerate, the bulk density of the moist agglomerate ρ_A^* can be related to the dry solids density ρ_s by the following equation:

$$\rho_A^* = 0.605\, \rho_s \quad (1+X) \tag{3-17}$$

The minimum fluidising velocity for the moist agglomerate U^*, for $Re < 20$, can be represented in the following form:

$$U^* = \frac{K\, g}{\mu} \quad \bar{D}_A^2 \quad (\rho_A^* - \rho_f) \tag{3-18}$$

Using equation (3-17) and substituting $R_A = \frac{\bar{D}_A}{dp}$ in equation (3-18) gives:

$$U^* = \frac{K\, g}{\mu} \; dp^2 \; R^2 \quad (0.605\, \rho_s\, (1 + X) \quad - \rho_f) \tag{3-19}$$

At the critical moisture content X_{cr}, the critical minimum fluidising velocity for the agglomerate U_{cr} can be represented by:

$$U_{cr} = \frac{K\, g}{\mu} \quad dp^2\, R^2\, (\, 0.605\, \rho_s\, (1 + X_{cr}) - \rho_f\,) \tag{3-20}$$

Assuming that the properties of the fluidising air does not change during drying period; then substracting equation (3-20) from (3-19) gives:

$$U^* - U_{cr} = \frac{0.605\ K\ g}{\mu} dp^2\ R^2\ \rho_s\ (X - X_{cr}) \qquad (3\text{-}21)$$

$$U^* - U_{cr} = 0.605\ U_o\ R^2\ (X - X_{cr}) \qquad (3\text{-}22)$$

$$(\text{for } X > X_{cr})$$

where

U_o: minimum fluidising velocity of bone dry particles

Relationship between the particle size and its critical point

Consider the simplest case of agglomeration, where only two particles of the same radius r bind together because of surface tension forces, as shown in figure (3-3), with their line of centres parallel to the fluid flow direction. The forces acting on the top particle are : hydrodynamic force, F_h, (upwards) and surface tension, T, and gravitional, mg, forces (downwards).

During the drying period, the angle (Θ), corresponding to the free moisture binding the two particles together, decreases until it reaches a critical value Θ_{cr} at which the surface tension is no longer strong enough to resist the hydrodynamic force, hence the agglomerate breaks.

At this critical point, the following force balance is written for the top particle:

$$F_h = mg + T$$

$$6\lambda\pi\mu\ r\ U_{cr} = \frac{4}{3}\ \pi r^3 \rho_s g + 2\pi\sigma\ r \sin\Theta_{cr} \qquad (3\text{-}23)$$

where

λ : hydrodynamic force constant

μ : air viscosity

r : particle radius

U_{cr}: air critical velocity at which the agglomerate breaks

ρ_s : solids density of bone dry particles

σ : Surface tension of moisture

θ_{cr}: critical angle at which the agglomerate breaks.

The relationship between the free moisture of volume V and the angle θ , can be obtained as follows (figure 3-3):

$$V = \pi b^2 h - 2 \left(\frac{\pi}{6} \frac{h}{2} \left(3 b^2 + \left(\frac{h}{2}\right)^2\right)\right) \tag{3-24}$$

This can be reduced to

$$V = \frac{2\pi}{3} r^3 \left(1 - \cos\theta\right)^2 \left(1 + 2\cos\theta\right) \tag{3-25}$$

Since the mass of two spheres M_s is:

$$M_s = 2 \left(\frac{4}{3} \pi r^3 \rho_s\right)$$

free moisture content X_F can be represented as:

$$X_F = \left(1 - A X_{cr}\right) = \frac{\rho_w}{4 \rho_s} \left(1 - \cos\theta_{cr}\right)^2 \left(1 + 2\cos\theta_{cr}\right) \tag{3-26}$$

where

ρ_w : water density

ρ_s : bone dry solids density

From equation (3-23) and substituting for U_{cr}

$$U_{cr} = U_o + B X_{cr}$$

$$U_{cr} = K_1 r^2 + B X_{cr}$$

The following formula is obtained

$$X_{cr} = K_2 r^2 + K_3 \sin\theta_{cr} \tag{3-27}$$

Solving equation (3-26) and (3-27) to eliminate θ_{cr} , and utilising equation (3-13-a)

the following relationship is obtained between (X_{cr}) and (dp):

$$X_{cr} - \frac{K}{dp} = K_4 \left(1 - \sqrt{1 - K_o r^4}\right)^2 \left(1 + 2\sqrt{1 - K_o r^4}\right) \qquad (3\text{-}28)$$

where:

X_{cr} = critical moisture content (—)

r = particle radius (cm)

dp = particle diameter (cm)

The left hand side in equation (3-28) is nearly zero because $\sqrt{1 - K_o r^4} \sim 1$ (where $K_o = 144$), hence the previous equation can be approximated to:

$$X_{cr} = \frac{K}{dp} \qquad (3\text{-}29)$$

3-5 EXPERIMENTAL STUDY

An experimental programme was designed to study the effect of solids moisture content on the minimum fluidising velocity of moist solids at different air temperatures.

A 20 cm high silica gel bed was used with initial moisture content up to 40% gm water/gm solids and of different particle sizes (106, 940 and 2247 microns) and fluidised by air at different temperatures (40, 60 and 80°C).

The minimum fluidising velocity of bone dry silica gel U_o was measured using a manometer connected above the distributor, while the variation in the minimum fluidising velocity of the moist solids U^* with solids moisture content X was measured using calibrated rotameters. The moisture content of solids was measured every 5 minutes during the experiments by weighing moist samples before and after complete drying using a micro-balance. Details of particle size measurement are given in Appendix (3).

3-6 RESULTS

The results obtained in this chapter are classified into two groups: first, showing the effect of different parameters on the minimum fluidising velocity of the moist solids, while in the second group the model discussed before in (3-4) is examined.

1- Factors affecting U^*

The effect of solids moisture content, air temperature and particle size on the minimum fluidising velocity of the moist particles are shown in figures (3-4, 5 and 6).

The relationship between solids moisture content and minimum fluidising velocity is reproduced for the nine curves of particle sizes (106, 940 and 2247 microns) at different temperatures (40, 60 and 80°C). The flow rate required for minimum fluidisation of wet solids decreases rapidly with the decrease in moisture content in the early stages of drying and then decreases steadily until it reaches a minimum value.

From the experimental results, the variation of U^* with solids moisture content X for different batches follows the same trend. On the other hand, the air temperature has a slight effect on the flow rate required for minimum fluidisation after taking into account the correction to the flow rate, which supports the early assumption that the average air properties are constant during the drying period.

2- Agglomeration model

To check the agglomeration model for fine particles at low Reynolds numbers a detailed study took place on the 106 micron batch using a shallow bed of 20 cm high, at different air temperatures (40, 60 and 80°C). The results obtained are shown in figures (3-7, 8 and 9) where the minimum fluidising velocity of the moist solids U^* is plotted versus solids moisture content X. The relationship is idealised by two straight lines representing the best fit to equations of the form:

$$U^* = U_o + B\,X \qquad (\text{for } X < X_{cr}) \tag{3-30}$$

and

$$U^* - U_{cr} = \alpha\,(X - X_{cr}) \qquad (\text{for } X > X_{cr}) \tag{3-31}$$

In region B C

Where solids moisture content X is lower than the critical value X_{cr}, the results showed a constant slope B of 0.5357 $\frac{\text{cm / s}}{\text{gm W/ gm S}}$ for the three sets of data.

This shows that the variation of minimum fluidising velocity of moist solids, in this region, is a direct functionof the hygroscopic solids density variation which varies here as a result of drying as predicted earlier by the model (equation 3-13).

To check the relationship between the fraction of moisture penetrated inside the particle A and the particle diameter dp, the following table is constructed:

dp (cm)	B slope	U_o (cm/s)	A $= B/U_o$	$1/dp\ (cm)^{-1}$
0.0106	0.5357	12.85	4×10^{-2}	94.5
0.0940	0.5357	30	1.8×10^{-2}	10.6
0.2247	0.5357	58	9.2×10^{-3}	4.5

Comparing the results obtained with the theory proposed earlier (equation 3-13-b), as shown in figure (3-10), a general agreement is obtained,nevertheless the deviation between the experimental values of A and the model is a direct result of ignoring the higher terms of penetration depth Δ in equation (3-13-a). from figure (3-10) the constant K in equation (3-13-b) is fo und to be equal to 9.5×10^{-4} for silica gel particles.

Region A B

Where solids moisture content is higher then the critical value X_{cr}, the relationship between $(U^* - U_{cr})$ and $(X - X_{cr})$ can be represented by a straight line.

Taking an average value for the critical moisture content of (X_{cr} = o.28 gmwater/ gm solids), and measuring the slope of best linear fit for each experiment, the average agglomerate diameter $\bar{D}_A$ was calculated and tabulated below:(for d_p=106 μ)

T (°C)	U_o Exp (cm/s)	U_{cr} (cm/s)	X_{cr} (av.) gm W/ gmS	Slope (α)	$R_A = \left(\frac{\alpha}{.605\ U_o}\right)^{1/2}$	$\bar{D}_A$ (microns)
40	12-85	13	0.28	297.8	6.189	656
60	12-85	13	0.28	375.6	6.951	737
80	12-85	13	0.28	536.0	8.303	880

For 106 microns silica gel, the results showed that the moist particles tend to agglomerate because of surface tension forces, producing larger aggregates of an average diameter $\bar{D}_A$ of 650-880 microns which is held constant during drying until the solids moisture content drops to a critical value X_{cr} (0.28 gm water/ gm solids) at which the surface tension forces is weaker than the hydrodynamic forces hence the agglomerate breaks into single particles.

From the results shown in figures (3-4, 5 and 6), it is clear that increasing the particle diameter shifts the critical moisture content to a lower value. Plotting the results obtained for critical moisture content X_{cr} of different particle size dp in figure (3-11) shows a qualitative agreement with the

model proposed earlier (equation 3-29).

From the different results obtained in this section, it is possible to explain the variation of minimum fluidising velocity of moist particles with its moisture content by the agglomeration model discussed earlier in section 3-4. At higher solids moisture content than the critical value ($X > X_{cr}$), the bed is composed of spherical agglomerates in which the particles are held together by surface tension mainly and when the solids moisture content drops to its critical value: surface tension forces are no longer strong enough to resist the hydrodynamic forces, hence the agglomerate breaks and the variation in minimum fluidising velocity in this region ($X < X_{cr}$) is mainly due to the hygroscopic material density variation with moisture content.

In the following chapter, both gas-to-particle and bed-to-wall heat transfer are studied experimentally in fluidised bed drying, in order to explore the different parameters affecting the heat transfer coefficients during the drying period.

CHAPTER (4)

HEAT TRANSFER IN FLUIDISED BED DRYING

4-1 INTRODUCTION

Solids drying in fluidised beds is ultimately linked to heat transfer which occurs by one of the following three forms: air to particle, particle to particle and bed to wall transfer.

In the first case, heat is transfered from hot air to the wet particles in the bed, and this is the major factor controlling solids drying. This transfered heat is used mainly for two purposes: one is to raise the temperature of the particles and the moisture associated with them to the required temperature, and second, to supply the heat required for evaporation.

In the second case, heat is transferred by conduction from hot particles to the neighbouring cold particles. This often happens when the wall is heated externally, hence heat is transferred from the external layer of particles to the next by conduction. In fluidised bed drying, particles are generally well mixed with a uniform temperature, hence particle to particle transfer is insignificant compared with heat required for drying of solids.

In the third case, heat is transferred from the hot bed to the wall where, due to bubble-induced solids circulation, the hot fluidised particles come into contact with the wall and heat exchange occurs before they are pushed away by fresh hot particles. In the case of externally heated walls,

the transfer takes place in the opposite direction of the mentioned above as shown by Botterill (1975).

In this chapter, heat transfer for both of fluid to particle and bed to wall is studied for fluidised bed drying. In each section, some of the work done by other workers is discussed followed by the mechanisms proposed. The correlations for our experimental results are shown and discussed at the end of each section.

4-2 FLUID TO PARTICLE HEAT TRANSFER

4-2-1 REVIEW

Kettenring, Manderfield and Smith (1950) were the first to study heat transfer in fluidised bed drying. They used a 6 cm in diameter bed to fluidise (14-20, 20-28, 28-35 and 35-48 mesh) silica gel using hot air.

Their experimental results were correlated to give:

$$\frac{h_{g/p}\, dp}{K} = 0.0135 \left(\frac{dp\ G}{\mu}\right)^{1.30} \qquad (4\text{-}1)$$

Their calculations were based on the assumption that the air leaving the bed is in thermal equilibrium with the particles in the bed. They did not measure the particles temperature and used the outlet air temperature instead

Heertjes et al (1953) gave a detailed experimental study of heat transfer in fluidised bed drying of silica gel (0.3 - 0.5 mm). They illustrated the importance of the distributor in supplying heat to the bed by conduction. They showed that the transfer between gas and particles takes place only in the first 5 mm above the distributor and recommended that solids temperature at the

bottom of the bed is higher than the top of the bed because of the distributor effect.

Heertjes and Mc Kibbins (1956) used a 6 cm diameter bed of (0.36 - 1.1 mm) silica gel and fluidised by hot air. To calculate air to particle heat transfer coefficients $h_{g/p}$, they assumed that solids are perfectly mixed and have the same temperature of the air leaving the bed. Their results were correlated as:

$$h_{g/p} = 1.31\ (Re)^{0.76} \qquad (4\text{-}2)$$

Heertjes (1962) discussed gas to particle heat transfer in fluidised bed drying. He correlated the transfer coefficient $h_{g/p}$ to the voidage fraction ε_o, superficial velocity U, particle size dp and tube diameter D_t in the following form:

$$Nu = 10\ (\varepsilon_0)^3\ (Fr)^{-0.49}\ (Pr)^{1/3}\ \left(\frac{dp}{D_t}\right)^{0.17}\ (Re)^{0.97} \qquad (4\text{-}3)$$

where:

$$Fr : \text{Froude number} = \frac{U^2}{\varepsilon_o^2} \cdot \frac{1}{dp\ g}$$

$$Nu : \text{Nusselt number} = \frac{h_{g/p}\ dp}{K}$$

$$Pr = \text{Prandtl number} : \frac{C_p\ \mu}{K}$$

$$Re: \text{Reynolds number} = \frac{\rho\ dp\ \ U}{\mu\ \ \varepsilon_o}$$

His correlation is based on the gas interstitial velocity using the voidge fraction at minimum fluidisation conditions which is physically confusing, because it assumes that all the gas in the bed is in the dense phase which is not correct for higher velocities than minimum fluidisation.

Wamsley and Johanson (1954) studied heat transfer from gas to particles in a 6 cm diameter column, using different solids of glass beads (32 -115 mesh), crushed alumina (16-65 mesh) and Dowex-50 (20 up to 35 mesh). Their heat transfer coefficient calculations were based on two assumptions: (1) The gas is perfectly mixed in the bed, hence the gas outlet temperature represents the gas temperature inside the bed; (2): the solids temperature was not measured and was taken as the adiabatic saturation temperature. They correlated their results in the following form:

$$h_{g/p} = 1,270 \quad dp^{1.27} \tag{4-4}$$

Frantz (1961) produced a comprehensive review of work on gas to particle heat transfer, up to that date,he proposed a theory for heat transfer in fluidised beds between the gas and particles based on conduction through a thin gas film around the particle ; hence the average heat transfer coefficient is a function of the average effective film thickness which can be obtained by integrating the point thickness over the entire surface area of the particle. For a single particle, the theory was developed to give

$$Nu = 2 + \frac{dp}{X} \qquad \text{where } dp = \text{particle size}, \; X = \text{film thickness} \tag{4-5}$$

Experimentally this theory did not have much success.

Ferron and Watson (1962) studied convective heat transfer between gas and particles in the dense phase. They mentioned the significance of distributor effect on bed performance, where the gas temperature drops from the inlet condition to the bed temperature in less than 2.5 cm. They used 7.5 and 20 cm diameter beds with silica aluminium cracking catalyst of 60 microns particle size, fludised by hot air. They correlated their results in the following form :

$$h_{g/P} = 0.0029 \; (U)^{0.5} \quad (D_t)^{-0.7} \quad \left(\frac{L}{Dt}\right)^{-0.7} \tag{4-6}$$

They measured solids temperature by a bare thermo-couple which is incorrect because the measured value represents an average between both gas and solids temperature. They also assumed that the gas temperature is constant in the bed and equal to the outlet temperature, which does not hold true in case of low flow rates; moreover they neglected the importance of particle size dp on the transfer coefficients.

Chang and Wen (1966) studied heat transfer in a baffled fluidised bed at high Reynolds' numbers. They measured the air and solids temperatures using a suction and miniature thermo-couples. Their experimental results showed an axial temperature gradient at the lower section of the bed, with a uniform temperature at the top. Their results showed that gas to particle heat transfer coefficients were independent of Reynolds' number, which contradicts most of the other workers. This strange relationship could be a result of the method of particle temperature measurement, where the miniature thermo-couple readings do not strictly represent the particle temperature, especially for larger particles of low thermal conductivity.

Gupta et al. (1973) summarized the data obtained by other workers, and correlated it in term of heat transfer factor J_h. Assuming that the gas in the bed is one homogeneous phase of superficial velocity U, they correlated the different data in the following form:

$$J_h \cdot \varepsilon = \frac{2.876}{Re} + \frac{0.3023}{Re^{0.35}} \qquad (4\text{-}7)$$

In this correlation, although Reynolds' number is based on the gas superficial velocity, the effect of voidge fraction is included in the correlation.

Equation (4-7) shows that all the gas in the bed is in contact with particles, hence the bubbles effect on the transfer rate is excluded.

Botterill (1975) gives a detailed study of heat transfer in fluidised beds, showing that although gas to particle heat transfer coefficients are not high ($6\text{-}23 \frac{W}{m^2\,{}^\circ K}$) the rates of heat transfer are very high, mainly because of the very large surface area exposed by particles (3,000 - 45,000 m^2/m^3). He illustrated the difficulty of measuring both gas and particle temperatures in the bed, and concluded that there is a very rapid change in the gas temperature at the entry zone of the bed where it is most difficult to take accurate measurements.

The large variations between the different correlations discussed in the lit'erature, indicate the complexity of the problem and show the limitations of the models proposed. Gas and particle

temperature measurement is one of the difficult problems in gas to particle heat transfer: for example, Kettenring et al (1950), Heertjes and Mc Kibbins (1956) assumed that the solids were in thermal equilibrium with the air leaving the bed and that the particle temperature was equal to the air at the outlet; this assumption is not strictly correct especially at low gas flow rates. Ferron and Watson (1962) measured the particle temperature using a bare thermo-couple, which does not represent solids temperature and then assumed that the gas temperature is constant in the bed and equal to the outlet temperature, which again is completely different from the actual gas temperature especially at the entry zone. Wamsley and Johanson (1954) did not measure particle temperature and it was taken as the adiabatic saturation temperature, which

does not agree with the experimental values. Chang and Wen (1966) used a suction thermo-couple to measure the gas temperature, and a miniature thermo-couple for particle temperature which could be misleading in case of larger particles with internal temperature gradients.

On the other hand, all the models proposed by different workers assumed that the gas fluidising the bed is one homogeneous phase, hence the effect of bubbles rising in the bed on the heat transfer between gas and particles is neglected; this could be a misleading approach especially for very fine particles (<50 microns) where each bubble is isolated from the dense-phase gas by a cloud, hence its temperature could be much higher than the gas in contact with the moist cold particles.

Finally, from the different data available in the literature, it is clear that no single correlation can describe gas to particle heat transfer in fluidised beds, which leads to the need for extra care for handling the results obtained from different designs.

4-2-2 MECHANISM

From the two-phase theory (Davidson and Harrison 1963), the air passing through the fluidised bed dryer is divided into two phases:

the dense-phase air, which is in direct contact with the moist solids, and the bubble phase, which represents the air in excess of minimum fluidisation and contains particles only in the bubble wakes. Since the dense-phase air supplies the heat required for vaporization to the wet particles, the bubble air will be at a higher temperature than the dense-phase.

The importance of bubbles on gas to particle heat transfer in freely bubbling fluidised bed drying, depends on the bed characteristics, particle diameter, bubble size and velocity and on the ratio α ($= \frac{U_b}{U_o}$) which determines if the bubble is surrounded by a cloud or not.

For ($\alpha < 1$), the bubble rises in the bed without a cloud and exchanges its heat content with the dense-phase air by convection as well as by conduction through its boundary. For higher number of transfer units X, both the bubble and the dense-phase air are expected to reach a thermal equilibrium, hence the main resistance controlling gas to particle heat transfer lies in the conduction step through a laminar fluid layer around each particle.

For ($\alpha > 1$), the bubble rising in the cylindrical bed dryer is surrounded by a cloud of radius R_c where $(\frac{R_c}{R_b}^3 = \frac{\alpha+2}{\alpha-1})$ as shown by Davidson (1961).

In this case, three different terms contribute to the overall gas to particle heat transfer in the bed:

(1) bubble to cloud heat transfer, which occurs by convection due to the volumetric exchange as well as by conduction through the bubble/cloud boundary.

(2) cloud to dense-phase heat transfer by conduction through the cloud/dense-phase boundary layer which has an average thermal conductivity(Ke).

(3) dense-phase to particles heat transfer, and this mainly controlled by conduction through a thin laminar fluid layer around each particle.

Realising all the complications of gas to particle heat transfer in fluidised bed drying, the following assumptions are made to analyse our results:

(1) Air to particle heat transfer occurs mainly at the entry zone of the bed (i.e the first few centimeters above the distributor), where the air temperature drops dramatically.

(2) Bubbles are not established at the entry zone, hence we shall treat the air as one homogeneous phase exchanging its heat with the moist solids.

(3) Both air and solids temperatures vary with the bed height.

(4) The particles are assumed to have a spherical shape and to have an average diameter dp.

To calculate air to particle overall heat transfer coefficient $h_{g/p}$, the following equation is used:

$$h_{g/p} = \frac{q_{HT}}{A' \int_0^H (Tg - Ts)\, d z} \qquad (4\text{-}8)$$

where

q_{HT}: Rate of heat transfer from air to particle $(\frac{Cal}{S})$

A' : Area of fluidised particles per unit bed height

$$= \frac{6\,(1-\varepsilon)\,\pi\, D_t^2}{4\,dp}\ (\frac{H_o}{H})\qquad (\frac{cm^2}{cm})$$

H_o : Bed height before expansion (cm)

H : Bed height after expansion (cm)

T_g : Gas temperature (°C)

T_s : Solids temperature (°C)

A dimensionless analysis is used subsequently to correlate the different factors (e.g. particle size dp, air velocity U, air physical properties: density ρ_f, viscosity μ and thermal conductivity K) with the overall gas to particle heat transfer coefficient $h_{g/p}$.

4-2-3 EXPERIMENTAL STUDY ON $h_{g/p}$

To study the effect of air flow rate and particle size on the overall gas to particle heat transfer coefficient, a series on twelve experiments were carried out on 10 cm high bed of silica gel fluidised by hot air with an average inlet temperature of 65°C at different air flow rates as shown below in table (4-1)

Group	Particle size (microns)	Inlet air temperature (°C)	X_i (Initial) (gmW/gmS)	Air flow rate Q (l/min)	Superficial Air velocity U (cm/S)
1	106	65	0.2016	35	7.4
			0.2795	60	12.7
			0.1851	85	17.9
			0.1867	150	31.8
2	940	65	0.1396	85	17.9
			0.2023	150	31.8
			0.1682	275	58.4
			0.1648	500	106.2
3	2247	65	0.2549	150	31.8
			0.1343	275	58.4
			0.2091	375	79.6
			0.1529	500	106.2

Table (4-1)

The air temperature profile in the bed was measured using four suction thermo-couples (Copper/Constantan) fitted at 5 mm, 1 cm, 2 cm and 10 cm above the distributor. The solids temperatures were measured at the same heights using shielded Copper/Constantan thermo-couples with mesh gauze cap heads and filled up with fresh moist solids.

To measure the heat transfer rate q_{HT} between air and particles, two different methods were used based on the solids drying rate and the air temperature.

In the solids drying rate method the drying curve for the solids was established and the drying rate was measured over the constant rate period, then the transfer rate q_{HT} was calculated using the following equation:

$$q_H = R. (-\Delta H_{vap}) \qquad (4-9)$$

where

R : constant drying rate (gm water/S)

ΔH_{vap}: latent heat of vaporization(cal/gm water)

This method showed higher values than predicted,mainly because of interference between heat transfer by conduction from the distributor to particles with gas to particle heat transfer.

In the second method the measured change in air temperature between the inlet and outlet of the bed is used to calculate the heat transfer rate q_{HT} utilizing the following equation:

$$q_{HT} = G. c_g (T_{in} - T_{out}) \qquad (4-10)$$

where

G: mass flow rate of air (gm/S)

c_g: specific heat capacity of air (cal/gm . °C)

A preliminary experimental study showed that the heat losses through the bed wall are less than 7% of the total heat transferred from the gas to the particle hence we shall assume that our bed operates under adiabatic conditions to utilise equation (4-10) in calculating gas to particle overall heat transfer coefficient.

The area of fluidised particles per unit bed height $\grave{A}$ was calculated by measuring the bed heights before and after expansion and using an average particle diameter dp calculated by the size distribution function method shown in Appendix (3).

The integral $\int_0^H (Tg - Ts)\, dZ$ in equation (4-8) was evaluated for each experiment by graphical integration using both gas and solids temperature profiles in the bed.

4-2-4 RESULTS AND CORRELATIONS

Typical experimental results for the air temperature drop in the entry zone are shown in figures (4-1 and 2). At the early stages of drying, an average of 10-15°C temperature drop occurs within the first two centimeters above the distributor. For the 940 micron particles, an air temperature gradient throughout the bed exists at low air flow rates (100 l/min), but increasing the air flow rate to 500 l/min shows a constant air temperature above the entry zone, which suggests that the air may be assumed to be perfectly mixed in this region as a result of particles mixing induced by the vigorously rising bubbles in the bed. From the results it is clear that the entry zone effect is independent of air flow rate.

The overall gas to particle heat transfer coefficients are calculated as shown in Appendix (4). The following table summarizes the results obtained from the different batches:

Particle size dp (microns)	Minimum fluidising velocity U_o (l/min)	Flow rate Q_o (l/min)	Superficial air velocity U (cm/s)	$h_{g/p}$ $\frac{W}{m^2 . {}^oK}$	Re = $\frac{\rho U\, dp}{\mu}$	Nu = $\frac{h_{g/p}\, dp}{K}$	Correlation
		35	7.4	0.634	0.483	0.024	Nu
106	12.8	60	12.8	1.178	0.829	0.045	=
		85	18.1	2.045	1.181	0.078	$0.06137\, Re^{1.315}$
		150	31.8	4.241	2.075	0.162	
		85	18	8.333	10.4	0.275	Nu
940	30	150	31.8	25.000	18.4	0.825	=
		275	58.4	45.830	33.7	1.513	$0.02290\, Re^{1.149}$
		500	106.2	66.662	61.36	11.667	
		150	31.8	27.059	43.98	2.194	Nu
2247	58	275	58.4	72.540	80.78	5.882	=
		375	79.6	97.498	110.11	7.906	$0.01397\, Re^{1.351}$
		500	106.2	138.700	146.91	11.247	

Table (4-2)

For 106 micron particles, the variation of $h_{g/p}$ with air flow rate is shown in figures (4-3 and 4), and the following correlation is obtained from figure (4-5) using least square fit:

$$Nu = 0.06137 \cdot Re^{1.315} \qquad (4\text{-}11)$$

$$(0.1 < Re < 10)$$

The results obtained from the 940 micron diameter batch are plotted in figures (4-6, 7 and 8) to show the effect of air flow rate on gas to particle heat transfer coefficient, and the following correlation is obtained:

$$Nu = 0.02290\, Re^{1.149} \qquad (4\text{-}12)$$

$$(10 < Re < 50)$$

For 2247 micron batch, the effect of air flow rate on $h_{g/p}$ is shown in figures (4-9 and 10) and using figure (4-11) the following correlation is obtained:

$$Nu = 0.01397\ Re^{1.351} \qquad (4\text{-}13)$$
$$(50 < Re < 200)$$

In our correlations Reynolds' number is based on the air superficial velocity; since it is found that most of gas to particle heat transfer occurs at the first few centimeters above the distributor where we assumed that bubbles are not established and the gas flows in one homogeneous phase. This model as first approximation, gives reasonable results when applied to similar operating and design conditions. On the other hand,it is clear that ignoring the effect of bubbles on gas to particle heat transfer could produce misleading results especially in the case of very fine particles (<50 microns say) where the bubble temperature is likely to be higher than in the dense phase because of the cloud isolation effect.

For the experimental results, increasing the particle size increases the overall gas to particle heat transfer coefficient, i.e. for 106 micron batch ($h_{g/p} \sim 1 - 4 \frac{W}{m^2 . {}^oK}$), for 940 microns batch ($h_{g/p} \sim 25\text{-}66 \frac{W}{m^2 . {}^oK}$) and for 2247 microns batch ($h_{g/p} \sim 72 - 138 \frac{W}{m^2 . {}^oK}$). On the other hand, the effect of air velocity on $h_{g/p}$ is constrained by the particle size as shown in table (4-2), although the experimental results showed that value of $h_{g/p}$ is nearly doubled by changing the state of the bed from fixed to minimum fluidisation conditions.

4-3 BED TO WALL HEAT TRANSFER

4-3-1 REVIEW

Heat transfer from a fluidised bed to the wall or an immersed surface is of special importance in industry, especially for fluidised bed heat exchangers and fluidised bed combustion systems.

Baerg , Klassen and Gishler (1950) studied the factors affecting heat transfer coefficients between the bed and its wall using a 14 cm diameter bed of solids height 25 cm. The fluidising air passed through different materials (iron powder, sand, jagged silica, glass beads, cracking catalyst and alumina). Their experimental results showed a de crease in the bed/wall heat transfer coefficient, with the increase of particle size. They correlated their results in the following form

$$h_{B/w} = h_{max} - 55\ e^{-0.012\ (G\ -\ 0.71\ \rho_g)} \qquad (4.14)$$

where

$$h_{max} = 49\ \log \frac{0.00037}{dp}\ \rho_g \qquad (4\text{-}15)$$

Dow and Jackob (1951) reported their experimental work for heat transfer from vertical tubes 5 and 8 cm diameter to fluidise a mixture of solids (Aerocate, coke and iron powder), using hot air. Experimental data were correlated in the following form:

$$Nu = 0.5\ (\frac{Dt}{L})^{0.65}\ (\frac{Dt}{dp})^{0.17}\ (\frac{\rho_s}{\rho_g}\ .\ \frac{C_s}{C_g})^{0.25}\ (Re)^{0.80}_{Tube} \qquad (4\text{-}16)$$

Van Heerden, Nobel and Van Krevelen (1951), used a small scale apparatus, to analyse heat transfer between dense phase and bed wall using different fluidising media (e.g. air, mixture of hydrogen and nitrogen, carbon dioxide, argon, town gas and methane) and different mixtures of solids (e.g. carborundum, iron oxide, coke lead and fly ash).

Their results were correlated as follow,

For $(2 < \frac{G}{Go} < 20)$

$$\frac{Nu}{Pr^{0.5}}\ (\frac{\rho_s}{\rho_g})^{0.18}\ (\frac{\rho_g}{\rho_s}\ .\ \frac{Cs}{Cg})^{0.36} = \Psi\ (B.Re) \qquad (4\text{-}17)$$

where

$$\text{for } Re < 5 \qquad \Psi\ (B.Re) = 0.58\ (B.Re)^{0.45} \qquad (4\text{-}18)$$

One of their interesting results is the increase of (bed/wall) heat transfer coefficient with the increase of the particle size, which disagrees with most other workers.

Levenspiel and Walton (1954) studied the effect of particle size, gas flow rate, bed temperature, particle shape on bed to wall heat transfer coefficients. They used hot air to fluidise different materials of glass beads, soya beads, bead catalyst and fine coal in 11 cm diameter tube. Their experimental results showed that $h_{B/W}$ is proportional to air flow rate, while it decreased with the increase of particle size, their data fit the following three correlations

$$Nu)_r = 0.0018\ (Re)\ \left(\frac{dp}{Dt}\right)^{-1.16} \qquad (4\text{-}19)$$

$$\frac{h_{B/W}}{Cp \cdot G} = 10\left(\frac{D_t \cdot G}{\mu}\right)^{-0.65} \qquad (4.20)$$

$$\frac{h_{B/W}}{Cp \cdot G} = 0.6\ (Re)^{0.7} \qquad (4\text{-}21)$$

Wen and Leva (1956) tried to generalize the dense phase to wall heat transfer correlations, on the basis of the principle that heat transfer from the gas to wall is accured by conduction through alaminar film stagnant to the wall. The effect of particle size on ($h_{B/W}$) was not clear in their analysis and figures 4 and 5 in their paper contradict each other. They used dimension less analysis to get the following relationship

$$Nu = 0.16\left[\frac{\zeta_s \cdot \rho_s \cdot dp.^{1.5}\ g^{0.5}}{K}\right]^{0.4}\left(\frac{G \cdot dp.\gamma}{\mu \cdot R}\right)^{0.36} \qquad (4\text{-}22)$$

where

R: expansion ratio of fluidised bed

γ: fluidisation efficiency

Wender and Cooper (1958) produced a paper to correlate the different data obtained on bed to wall heat transfer. In their correlation, they tried to take into account the effect of height over diameter ratio $(\frac{LH}{Dt})$, gas physical properties (ρ_g, Cg, K, μ), solids characteristics (dp, ρ_s, Cs), and gas flow rates on ($h_{B/W}$). They used dimensionless analysis for nine independent sets of data, and they derived the following correlations:

For $(0.001 < Re < 1)$

$$\left[\frac{h\ dp\ /\ K\ (1-\varepsilon)\ (\ \frac{C_s}{C_g}\ \cdot\ \frac{\rho_s}{\rho_g}\ )\qquad \times 10^4}{1 + 7.5\ e^{-0.44\,(\frac{LH}{Dt})\ /\ (\frac{Cs}{Cg})}}\right] \propto Re^{1.2} \qquad (4\text{-}23)$$

For $(1 < Re < 100)$

$$\frac{F}{Y} \propto Re^{0.36} \qquad (4\text{-}24)$$

Drinkenburg (1967) used a 30 cm diameter fluidised bed to study the fluctuations in (bed/wall) heat transfer coefficients, using a thermistor 600 micron diameter as a heating element mounted near the wall, and its resistance variation was recorded using a wheatstone bridge. Fluctuations in local (bed/wall) heat transfer coefficients were recorded, which he tried to explain by a "slip and stick" mechanism on the wall.

Gabor (1970) proposed two mechanisms for (bed/wall) heat transfer: a "string of spheres" model and "alternate slabs" model. In his model of alternate slabs, he assumed that the bed is approximated by a series of alternate slabs representing the solid and gas phases. The numerical solution to this model is based on the assumptions that all heat flows through alternating series of gas and solid phases, and the heat removed by gas convection can be neglected, and that there is no heat transfer in directions parallel to the wall. He assumed

that the thickness of the gas slab between the wall and the first layer of particles is (0.1 dp), but the author admits that the agreement between the theory and experimental data for gases other than air is not very good.

Botterill (1970) proposed a model for heat transfer between fluidised bed and the wall. He illustrated the dependence of ($h_{B/W}$) on the frequency of particles exchange between the bulk of the bed and the wall. His model is based on neglecting any heat transfer by conduction because of the short time of contact between particles and surface and predicts that the fluidising gas thermal conductivity is a limiting factor in the process. More details about the model will be discussed in section 4-3-2.

Baskakov et al (1973), studied heat transfer between the fluidised bed and the wall or immersed object in the bed. They used a modified "packet model" to describe the process, taking into account both the effective heat resistance in the gap between the packet of particles and surface as well as the convective term for heat transferred from the gas to the surface. One of the interesting results is the relationship between ($h_{B/W}$) and the particle size, where they found that in the range of (50 up to 3000 microns dp), $h_{B/W}$ decreases rapidly and then start increasing slowly for larger ranges of particle size (dp > 3000 microns).

Tuot and Clift (1973) presented an interesting paper describing instantaneous local wall to bed heat transfer coefficients around bubble rising in 2 - dimension bed. They used spherical glass beads of particle diameter (177 - 250 microns) fluidised by air in a (120 x 50 x 1.2 cm) bed. They showed two different groups of results to explain the effect of bubbles on

(bed/wall) heat transfer coefficients. The first group describes the effect of a bubble whose vertical axis coincides with the measuring probe, while the second one shows bubbles whose central line is 0.8 bubble diameter away from the probe. The maximum (bed/wall) heat transfer coefficient occurs some distance behind the bubble, while the minimum value recorded was at the bubble side of the indented region. They showed that the predicted values of $h_{B/W}$ from the present models of film penetration or string of particles model, are much larger than the values obtained experimentaly. To interpretate their results in terms of particle motion around the bubble, they found that Bingham-plastic behaviour in the particulate phase, which predicts an asymetric distribution of particle velocities around the bubble, is consistent with the results obtained in their work.

Baeyens and Goossens (1973) tried to explain the wide variation in results obtained on (bed/wall) heat transfer coefficients by checking three different items, the average radial temperature profile, the transient heat transfer effects around a single rising bubble and the temperature fluctuations in freely bubbling fluidised bed. Their experimental results for radi al temperature profile suggest that the mechanisms of Levenspiel and Walton (1954) are in error and suggest that the film penetration models should give more realistic results, although the problem of estimating the thickness of the thermal layer is still in question.

Botterill (1973) warned that any design correlation should only be used in cases very close to the original experimental condition on which they were based. He explained the good heat transfer properties of gas fluidised systems as a result of the high heat capacity of particles as well as their mobility in the bed.

Vitovec (1975) studied the heat transfer between a heated wall and fluidised bed during sublimation. He used ammonium terephthalate mixed with inert particles of corundum ceramic fluidised by air. His results showed high values for heat transfer (in the range of 270-420 $\frac{W}{m^2 \cdot {}^oK}$) and he correlated the results in the following simple form:

For $1 < Re < 12$

$$Nu = 2.3\ Re^{0.3} \qquad (4\text{-}25)$$

Zabrodsky, Antonishin and Parnas (1976) reviewed the work on (bed/wall) heat transfer, trying to illustrate the concept of unsteady heat diffusion from the wall to the bed, which depends on both of particle velocity(v) and concentration (ϵ) near the surface, bearing in mind the importance of the themal properties of the gas in this region.

Harrison and Bhattacharya (1976) studied heat transfer in a pulsed fluidised bed. They used a 200 mm square in cross section and 800 mm high bed; to fluidise three different batches of sand of particle size (43-63, 200-250, and 500-600 microns) using pulsed air of frequencies varying from (zero to 4HZ). Their results showed a large improvement (80%) of (bed/wall) heat transfer in pulsed bed of larger particles just above fluidisation.

4-3-2 MECHANISM

Quantative models have been proposed by different workers (Van Heerden et al (1953), Wen and Leva (1956), Yoshida et al (1969), Gabor (1970) and Baskakov et al (1973)), but unfortunately the ratio between the predicted values of bed to wall heat transfer coefficient and the experimental one is often of order ten or more.

In the laminar layer model proposed by Levenspiel and Walton (1954), it is assumed that the resistance to heat transfer between the fluidised bed and the wall is due to a laminer layer of fluid formed at the interior bed wall; this laminer layer is destroyed when solids particles pass through it, and hence the average laminer layer in fluidised bed. is thinner than in a corresponding empty tube which explains the higher values of $h_{B/W}$ in the fluidised beds. The estimation of this film thickness is the major problem in the model since their assumption that particles are stationary is not realistic in fluidised beds.

The packet model developed by Mickley and Fairbanks (1955) is based on the unsteady-state heat flow by conduction from the bed to the wall. In this model they assumed that a thermal equilibrium is established between the gas and particles within the bed and that packets of gas and solids having uniform thermal properties with conductivity $(K_b)_{mf}$ are swept into the wall under the bubble-induced particle motion, to exchange its heat content with the surface and then are renewed by further packets. Botterill and Williams (1963) used a similar model to solve the problem of heat transfer from spherical particle to the wall, then Botterill (1967) extended the work to study heat transfer from two particles in depth of the bed to the wall.

All the mechanisms proposed require some estimates of the particle residence time on the surface, the renewal rate and the film thickness which depends strongly on the experimental details and the bed design.

4-3-3 EXPERIMENTAL STUDY ON $h_{B/W}$

Nine experiments were carried out in a 10 cm high bed of bone dry silica gel fluidised by hot air at 50 °C to study the overall bed to wall heat transfer

The following table summarizes the different operating conditions:

Group	Particle Size dp (microns)	Bed height (cm)	Inlet Air temperature (°C)	Air Flow rate Q (l/min)	Air velocity U (cm/s)
1	106	10	50	15	3.2
	106	10	50	35	7.4
	106	10	50	60	12.7
2	940	10	50	150	31.8
	940	10	50	275	58.4
	940	10	50	500	106.2
3	2247	10	50	275	58.4
	2247	10	50	375	79.6
	2247	10	50	500	106.2

Table (4-3)

The overall bed to wall heat transfer coefficient was calculated from the following equation:

$$h_{B/W} = \frac{q_{HT}}{\bar{A} \int_0^H (T_b - T_w)\, dZ} \qquad (4\text{-}26)$$

Where

q_{HT} : rate of heat transfer from the bed to the wall (cal/S)

$\bar{A}$: wall surface area per unit bed height (cm^2/cm)

T_b : bed temperature (°C)

T_w : wall temperature (°C)

The rate of heat transfer between the bed and the wall was calculated using the following equation:

$$q_{HT} = G.\ Cg\ (T_{in} - T_{out}) \qquad (4\text{-}27)$$

where

The inlet and the outlet air temperatures are measured at steady state conditions for the bone dry silica gel bed.

The bed temperature T_b was measured using shielded Copper/Constantan thermo-couples fixed at 5 mm, 1 cm, 2 cm and 10 cm above the distributor. The wall temperature T_w was measured from outside using two thermometres fixed at 2 and 8 cm above the distributor, which showed a close reading, hence we used an average wall temperature in equation (4-26). The integral $\int_0^H (T_b - T_w)\, dZ$ in the mentioned equation was evaluated using graphical integration for each experiment. Each experiment was run for 2 hours, taking measurements each 10 minutes andthe overall bed to wall heat transfer coefficient was taken as an average over the whole experiment.

4-3-4 RESULTS AND CORRELATIONS

The effect of the air flow rate on the overall bed to wall heat transfer coefficient is shown in figures (4-15, 16 and 17) for the three different batches. It is clear that increasing the air flow rate increases $h_{B/W}$ until it reaches a maximum value $(h_{B/W})_{max}$ and then decreases as predicted by most of the other workers. On the other hand the effect of particle size on $h_{B/W}$ is shown in figure (4-18); from which the maximum value of bed to wall heat transfer coefficient $(h_{BW/})$ max decreases with increasing particle size until it reaches

a minimum value and then start increasing; this result supports the early work of Baskakov et al (1973) although it does not agree with most other workers.

Applying Dow and Jackob : (1951) dimensionless groups to our results based on particle diameter, table (4-4) is obtained and plotting those results in figure (4-20), the following correlation is poraucel:

for $0.1 < Re < 150$

$$Nu = 0.025 \left(\frac{Dt}{L}\right)^{0.65} \left(\frac{Dt}{dp}\right)^{0.17} \left((1-\varepsilon) \left(\frac{\rho_s}{\rho_g} \cdot \frac{Cs}{Cg}\right) \right)^{0.2} Re^{0.925}$$

correlation coefficient = 93% (4-28)

dp (microns)	$(h_{B/W})_{Max}$ $(\frac{W}{m^2 . ^oK})$	U (cm/S)	Re = $(\frac{\rho u\, dp}{\mu})$	Nu = $(\frac{h\, dp}{K})$	$(\frac{D_t}{L})^{0.65}$	$(\frac{D_t}{dp})^{0.17}$	$(\frac{\rho_s}{\rho_g} \cdot \frac{Cs}{Cg})^{0.25}$	$(1-\varepsilon)^{0.25}$
106	70	3-2	.208	.103	1	3·2	5.342	.88
		7-4	.483	.072	1	3·2	5.342	.88
		12-8	.829	.829	1	3·2	5.342	.88
940	60	31-8	18.40	.972	1	2·2	5.342	.88
		58.4	33.70	1.618	1	2·2	5.342	.88
		106.2	61.36	1.717	1	2·2	5.342	.88
2247	85	58.4	80.78	3.099	1	1·9	5.342	.88
		79.6	110.11	3.926	1	1·9	5.342	.88
		106.2	146.91	6.976	1	1·9	5.342	.88

Table (4-4)

Modified Dow and Jackob correlation

TEXT BOUND INTO

THE SPINE

Wender and Cooper (1958) modified groups are applied to our results in table (4-5), and from figure (4-21) the following correlation is obtained

For 0.1 Re 150

$$Nu \times 10^4 = 3.882\,(1-\epsilon)\left(\frac{Cs}{Cg}\cdot\frac{\rho_s}{\rho_g}\right)\left(1+7.5\,e^{-0.44\left(\frac{L_H}{Dt}\cdot\frac{Cs}{Cg}\right)}\right)Re^{0.805}$$

correlation coefficient = 93% (4-29)

Group	dp (microns)	$(h_{B/W})_{max}$ $(\frac{W}{m^2.^oK})$	U (cm/s)	Re= $(\frac{\rho u\ dp}{K})$	Nu= $(\frac{h\ dp}{K})$	$\frac{Nu \times 10^4}{(1-\epsilon)(\frac{Cs}{Cg}\cdot\frac{\rho_s}{\rho_g})}$	$(\frac{LH}{D_t})$	$(\frac{Cs}{Cg})$
1	106	70	3-2	.208	.103	2.108	1	.781
			7-4	.483	.072	1.474	1	.781
			12-7	.829	.829	5.833	1	.781
2	940	60	31-8	18.40	.972	19.893	1	.781
			58.4	33.70	1.618	33.115	1	.781
			106.2	61.36	1.717	35.141	1	.781
3	2247	87	58.4	80.78	3.099	63.425	1	.781
			79.6	110.11	3.926	80.351	1	.781
			106.2	146.91	6.976	142.774	1	.781

Table (4-5)

Modified Wender and Cooper Correlation

Both equations (4-28) and (4-29) showed a high correlation coefficient of 93% which suggests their application to similar operating condition.

It is clear that both the gas flow rate and particle size are crucial parameters on both gas-to-particle and bed-to-wall heat transfer in fluidised beds. $h_{g/p}$ is linearly proportional to the air velocity while $h_{B/W}$ increases with the increase in air velocity until it reaches a maximum and then decreases. Increasing particle size increases gas to particle heat transfer and decreases bed to wall heat transfer coefficient until it reaches a minimum and then increases.

In the next chapter we shall discuss mass transfer in fluidised bed drying, which is a direct result of gas to particle heat transfer discussed in this chapter.

CHAPTER (5)

MASS TRANSFER IN FLUIDISED BED DRYING

5-1 INTRODUCTION

In fluidised bed drying, mass transfer takes place in two steps, first, moisture transfer from the wet solids to the dense-phase gas in contact with solids; second, the transfer of water vapour from the dense-phase gas to the bubbles rising in the bed. To determine which step is rate-controlling, we shall first discuss these two processes and then investigate the effects of phase segregation on mass transfer in fluidised bed drying.

The overall process of mass transfer depends on: molecular diffusion, eddy diffusion, pore diffusion, interphase transfer and simultaneous heat and mass transfer. During the constant rate period, pore diffusion is insignificant and the moisture is transferred from wet solids to the dense-phase gas as a result of the simultaneous heat and mass transfer process. On the other hand, water vapour transfer from the dense-phase gas to the bubbles rising in the bed occurs by molecular diffusion when the bubble is surrounded by a cloud ($\alpha = \frac{U_b}{U_o} > 1$), and by diffusion and convection in case of through flow ($\alpha = \frac{U_b}{U_o} < 1$).

5-2 OVERALL MASS TRANSFER IN SINGLE-PHASE MODELS

In this section weshall discuss the attempts at correlating overall mass transfer based on single-phase models, in which it is assumed that all the gas passing through the bed is one homogeneous phase in contact with the

particles.

Kettenring et al (1950) were the first to study mass transfer in fluidised bed drying. They used an 8 cm diameter bed to fluidise silica gel of 0.297 - 1.19 mm particle size using hot air. They correlated their results for the overall mass transfer coefficients Kg in terms of the air mean partial pressure p_m, molecular weight M and mass velocity G in the following form:

$$Kg \left(\frac{p_m \cdot Ma}{G}\right) = 0.0018 \, (Re)^{0.30} \qquad (5\text{-}1)$$

Their calculations for Kg were based on the assumption that the equilibrium pressure of water vapour on the particle surface is equal to the partial pressure of water vapour in the air leaving the bed. Experimentally this assumption is proved to be not strictly correct where the equilibrium humidity depends on both of solids moisture content and bed temperature as shown by Rietema and Hoebink (1973).

Thoenes and Kramers (1958) studied mass transfer from spheres, in various regular packings, soaked with liquids to the flowing gas (air, CO_2 and H_2). Their experimental results showed the relative importance of diffusion as compared with convection. They correlated their results in the following way:

$$Sh = 1.0 \, Sc^{1/3} \, Re^{\frac{1}{2}} \qquad (5\text{-}2)$$

$$\text{for } 40 < Re < 4000$$

Carberry (1960) proposed a boundary layer model for fluid to particle mass transfer, in which the process is controlled by molecular diffusion within the boundary layer, which is developed and destroyed repeatedly as the fluid flows through the bed, and the following equation is obtained:

$$Jd = 1.15\ Re^{-\frac{1}{2}} \qquad (Re < 1000) \qquad (5\text{-}3)$$

where

Jd : mass transfer factor

Re : Reynolds' number based on interstitial velocity.

Riccetti and Thodos (1961) studied mass transfer in gas fluidised beds. They used 1.5 cm bed to fluidise alumina particles of 3 mm average diameter. They studied the evaporation of water and nitro benzene to air in the bed and correlated their results in the following form:

$$Jd = \frac{1}{Re^{`0.40} - 1.5} \qquad (100 < Re < 6000) \qquad (5\text{-}4)$$

where

Jd : mass transfer factor

Re` : modified Reynolds' number $= \frac{U\ dp\ \rho}{\mu(1-\varepsilon)}$

Richardson and Szekely (1961) presented an experimental paper on mass transfer in a small fluidised bed. They used 30 mm diameter bed to fluidise silica alumina catalyst of (88 - 2576 microns) particle size. The fluidising medium was air containing iso-octane or tolune vapour, and the adsorption of the vapour on the particles was measured experimentally. Their results showed that all the transfer took place in a very shallow zone just above the distributor. They correlated their results in the following form:

$$Sh = 0.374\ Re^{1.18} \qquad (0.1 < Re < 15) \qquad (5\text{-}5)$$

or

$$Sh = 2.01\ Re^{0.5} \qquad (15 < Re < 250) \qquad (5\text{-}6)$$

where $Re = \frac{\rho U\ dp}{\mu}$

Mc Connachie and Thodos (1963) studied mass transfer from a sphere saturated with water to the air in both of packed and distended beds and obtained a similar relationship to that of (5-4)

$$Jd = \frac{1.192}{Re^{0.41} - 1.52} \qquad (5\text{-}7)$$

They compared their results with data available from fluidised bed and concluded that the distended bed results are consistent with those obtained from fluidised beds, hence the particle motion does not have any effect on mass transfer. The conclusion is not strictly correct as shown by Beek (1971) because the controlling step in mass transfer lies between the segregated phases in aggregative fluidisation which they ignored during their discussion.

Rowe and Claxton (1965) generalised the correlations obtained from mass and heat transfer in fluidised bed. To overcome the problem that most of the data in literature reported values for Sherwood and Nusselt numbers less than the theoretical lower limit of 2.0. They correlated data in the following general form:

$$Nu \text{ (or } Sh) = A + B\ Pr^{1/3} \text{ (or } Sc^{1/3})\ Re^{n} \qquad (5\text{-}8)$$

where

A,B : are functions of voidge fraction (ε)

n : function of Reynolds' number

Ziegler and Holmes (1966) studied mass transfer of water vapour from a saturated porous sphere into various air fluidised beds. They showed that the model of forced convection mass transfer predicted lower values than the results

obtained in fluidised beds. They introduced a new term $\psi(Y)$ to represent the effect of particle motion on mass transfer. They correlated their results in the following way:

$$Sh = Sh_2 + \psi(Y) \qquad (5\text{-}9)$$

where $$Sh_2 = 2 + 0.60\ Sc^{1/3}\ Re^{\frac{1}{2}} \qquad (5\text{-}10)$$

$$Y = \frac{G - G_{mf}}{(\phi dp)^2\ (\rho_s - \rho_g)\ \rho_g}$$

ρ_g, ρ_s : gas and solids density

ϕ : sphericity

G : mass velocity of gas

Petrovic and Thodos (1967) studied the evaporation of water, n- decane, n - dodecane and n- tetradecane from the surface of celite particles into air. The results obtained supported the early work of Rowe and Claxton (1965) and showed higher mass transfer coefficients in packed beds than in fluidised beds for the same particle Reynolds' number.

Kato et al (1970) studied mass transfer in fixed and fluidised bed, by subliming naphthalene into an air stream in a 2.5 cm diameter bed using inert particles of arcyl and glass beads of (0.4 - 0.016 cm) particle size. Their experimental results showed that the Sherwood number is not only a function of Schmidt and Reynolds' numbers, but also depends on the ratio of particle diameter to bed height.

Beek (1971) gives a comprehensive discussion of the work on mass transfer in fluidised bed. For particulate fluidisation, he showed that the effect of fluidising velocity U and the voidge fraction ε on mass transfer coefficient $K_{g/p}$ tends to compensate each other, hence the overall effect will be in the order of ($K_{g/p} \propto U^{0.15 - 0.24)}$.

Based on these results, he was able to explain the slower rates of mass transfer in fluidised beds than packed beds. He also discussed the effect of phase segregation on mass transfer in fluidised beds, and showed that those workers who concluded that $K_{g/p}$ increases with increasing gas flow rates should reinterpretate their results on the basis of K_B instead of $K_{g/p}$.

Yoon and Thodos (1972) studied the evaporation of n-decane from the surface of celite particles into air in fluidised beds.

They measured the concentration profile in the bed and correlated their results in the following way:

$$J_d \varepsilon = \frac{0.947}{Re^{0.50}} \qquad (5\text{-}11)$$

$$(100 < Re < 450)$$

Their results showed that all the mass transfer occurs in the first 2.5 cm above the distributor.

Pfafflin et al (1974) presented simplified models for mass and heat transfer in fluidised beds. They assumed that all the gas flowing in the bed is one homogeneous phase, hence the following equations are derived:

For heat transfer $\qquad Nu = K_1 \, Pr \, Re \qquad (5\text{-}12)$

and for mass transfer

$$Sh = K_2 \, Sc \, Re \qquad (5\text{-}13)$$

where Reynolds' number is based on the particle diameter and superficial velocity. The prediction did not agree with the experimental results because of ingoring the effect of bubbles on both of heat and mass transfer in the bed.

The wide range of correlations obtained on the basis of single-phase model and the different data obtained by various workers, is a result of ignoring the significance of bubbles on mass transfer in fluidised bed where in general, the resistance to mass transfer between the segregated phases exist as shown by Beek (1971).

The following table (5-1) summarizes of the data and correlations obtained by different workers.

and for mass transfer

$$Sh = K_2 \, Sc \, Re \qquad (5\text{-}13)$$

where Reynolds' number is based on the particle diameter and superficial velocity. The prediction did not agree with the experimental results because of ingoring the effect of bubbles on both of heat and mass transfer in the bed.

The wide range of correlations obtained on the basis of single-phase model and the different data obtained by various workers, is a result of ignoring the significance of bubbles on mass transfer in fluidised bed where in general, the resistance to mass transfer between the segregated phases exist as shown by Beek (1971).

The following table (5-1) summarizes of the data and correlations obtained by different workers.

Table (5-1)

Overall mass transfer correlations in fluidised bed.

Reference	Correlation	Transfer	Particle Size (microns)	$\overline{Kg}_{overall}$ (cm/s)
Kettenring et al (1950)	$Kg\left(\frac{p_m \cdot M_a}{G}\right) = 0.0018\ Re^{0.30}$	water/air	silica gel (297-1190)	2·7
Richardson and Szekely (1961)	$Sh = 0.374\ Re^{1.18}$ $(0.1 < Re < 15)$ $Sh = 2.01\ Re^{0.5}$ $(15 < Re < 250)$	Carbon tetra Chloride/air	Charcoal 128 (88-2567)	5·5
Mc Connachie and Thodos (1963)	$Jd = \frac{1.192}{Re^{0.41} - 1.52}$	water/air	Porous sphere (1588)	4·6
Riccetti and Thodos (1961)	$Jd = \frac{1}{Re^{0.40} - 1.5}$ $100 < Re < 600$	water/air nitrobenze/air dichloro- -benzene/air	alumina particles (3000)	25·4 13·1 8·3
Petrovic and Thodos (1967)	$Jd = \frac{0.589}{Re^{0.427}}$	water/air n-decane/air n-dodecane/air n-tetradecane/ air	celite particles (182-309)	20·1 5·3 5·1 5·1
Yoon and Thodos (1972)	$Jd. = \frac{0.947}{Re^{0.50}}$ $100 < Re < 450$	decane/air	celite particles (182-309)	5·4

From table (5-1) for overall mass transfer in fluidised bed, it is clear that there is a wide range of correlations and results reported in literature, which suggests that representing fluidised bed by single phase models is not strictly correct especially in cases where the resistance to mass transfer lies between the dense-phase and the bubble rising in the bed, which we shall discuss in the next section.

5-3 MASS TRANSFER TO BUBBLES RISING IN FLUIDISED BED

Recent work has shown that mass transfer in bubbling fluidised beds does not depend only on the transfer between particles and the gas in contact, but also on the transfer step between the segregated phases.

Davidson (1961) studied the gas exchange between a rising bubble and the surrounding particulate phase. From his theory, the volumetric flow rate into and out of each bubble is given by:

$$q = \tfrac{3}{4}\pi U_o De^2 \qquad (5\text{-}14)$$

where

U_o : minimum fluidising velocity

De : equivalent bubble diameter

Orcutt, Davidson and Pigford (1962) developed the first bubble model representing fluidised bed reactor and studied experimentally ozone decomposition in an iron oxide bed. They showed that ozone transfer between the bubble and the dense phase gas occurs by convection (equation 5-14) as well as molecular diffusion (which is represented by a mass transfer coefficient K_g) , hence the total rate of exchange of ozone between the bubble and the surrounding dense

phase is represented by:

$$Q = \pi De^2 (K_G + \tfrac{3}{4} U_o) \qquad (5\text{-}15)$$

Davidson and Harrison (1963) assumed that both convective and diffusional flows - between the bubble and the dense-phase gas - are additive to give an equivalent flow rate to and from the bubble Q.

$$Q = q + K_G S \qquad (5\text{-}16)$$

where

$$q = \tfrac{3}{4} \pi U_o \quad De^2$$

$$S = \pi D_e^2$$

K_G = bubble to dense phase mass transfer coefficient based on surface area of sphere of diameter D_e(cm/s)

Using the analogy between mass transfer from bubbles in fluidised bed and liquid-film controlled diffusion from a rising bubble of spherical cap shape with flat bottom and having an angle $\Theta = 50^o$ between its rim and polar axis, the coefficient K_G can be calculated from the following equation:

$$K_G = 0.975 \quad D_G^{\frac{1}{2}} \left(\frac{g}{D_e} \right)^{\frac{1}{4}} \qquad (5\text{-}17)$$

where

D_G : gas phase diffusion coefficient (cm^2/s)

Kun ii and Levenspiel (1968) proposed a new model for estimating the mass transfer coefficient between bubble and dense-phase based on the cloud model suggested earlier by Partridge and Rowe (1966). They assumed that the transfer occurs via two steps: bubble to cloud transfer and cloud to emulsion phase transfer.

They assumed that the mass transfer coefficient between the bubble and the cloud $K_{B/C}$ can be represented in terms of gas exchange coefficient per unit volume of the bubble.

Using Davidson and Harrison's (1963) results of equation (5-16) and dividing by the bubble volume they obtained:

$$K_{B/C} = 4.5 \left(\frac{U_o}{D_e}\right) + 5.85 \left(\frac{D_G^{\frac{1}{2}} \; g^{\frac{1}{4}}}{D_e^{5/4}}\right) \qquad (5\text{-}15)$$

To calculate the mass transfer coefficient between the cloud and the emulsion phase $K_{C/E}$, they assumed that the Higbie penetration model is applicable, hence by analogy to the contacting of a bubble by liquid, they derived:

$$K_{C/E} = 6.78 \left(\frac{D_G \; \varepsilon_o \; U_b}{D_e^{\,3}}\right)^{\frac{1}{2}} \qquad (5\text{-}19)$$

Thus the overall mass transfer coefficient between the bubble and emulsion phase K_B based on unit volume of bubble can be represented as:

$$\frac{1}{K_B} = \frac{1}{K_{B/C}} + \frac{1}{K_{C/E}} \qquad (5\text{-}20)$$

Chiba and Kabayashi (1970) presented a model for mass transfer between the bubble and e mulsion phase, in which they assumed that the main resitance to mass transfer lies in the transfer step between the cloud and the emulsion phase. Using the solution derived by Murray (1965) for the fluid flow around rising bubble in fluidised bed, they calculated the mass transfer coefficient between the bubble and dense phase based on unit volume of the bubble:

$$K_B = K_{C/E} = \left(\frac{6.78}{1-fw}\right)\left(\frac{\alpha}{\alpha - 1}\right)\left(\frac{D_G\ \varepsilon_o^{\,2}\ U_b}{De^3}\right)^{\frac{1}{2}} \qquad (5\text{-}21)$$

where:

f_w : volume fraction of bubble wake

α : ratio of bubble rising velocity to that of interstitial gas in emulsion phase $\left(= \frac{U_b}{U_o} \right)$

D_G : diffusion coefficient of the tracer gas in fluidising gas (cm^2/S)

ε_o : voidge fraction at incipient fluidisation

Experimental results for ozone and helium mass transfer to air fluidised beds were reported and showed reasonable agreement with the theory, despite the fact declared by Harrison and Guedes de Carvalho (1975) that some of the bubbles diameters were very close to the tube diameter which suggested slugging in the bed.

Pyle and Hargreaves (1971) studied the gas flow out of the bubble rising in fluidised bed and derived a relationship between the through flow q and the voidge fraction ε at the bubble surface.

From their theory they derived the following equation for flow through a spherical bubble in a cylindrical bed:

$$Q = \frac{\pi}{3}\ \varepsilon\ \left(\frac{n}{n_o}\right)\left(\frac{I3_o}{I3}\right) U_o\ a^2 \qquad (5\text{-}22)$$

where

ε : voidge fraction

n, n_o: particle number density, (at incipient fluidisation)

$I3, I3_o$: drag force function, (at incipient fluidisation)

U_o : interstitial minimum fluidising velocity

a : bubble radius

Using equation (5-22) and assuming various, but constant, values for ε they predicted under certain conditions a reduction in the flow through the bubble from the flow through the same void when filled with particles.

Beek (1971) proposed a sophisticated two-phase model to predict mass transfer in aggregative fluidisation, in which the bed performance is represented as a function of four dimensionless groups $\left(\frac{U_o}{U}, \frac{(1-\varepsilon_b)\,E_f}{U\,H}, \frac{U}{K_{g/p}\,a\,H}\right.$ and $\left.\frac{K_B\,a_b}{K_{g/p}\,a}\right)$.

where

ε_b : fraction of bed occupied by bubbles

E_f : dispersion coefficient of fluid in the dense phase (m^2/S)

$K_{g/p}$: gas to particle mass transfer coefficient (m/S)

K_B : overall bubble to dense phase mass transfer coefficient (m/S)

a : surface area of particles per unit volume of bed (m^{-1})

a_b : surface area of bubbles per unit volume of bed (m^{-1})

In his model he used the same relationship obtained by Davidson and Harrison (1963) for mass transfer between the bubble and dense phase, hence his overall mass transfer coefficient between bubble and dense phase K_B based on unit surface area (πD_e^2) is represented in the following form:

$$K_B = \frac{3}{4} U_o + \left(\frac{g\,D_G^2}{D_e}\right)^{\frac{1}{4}} \qquad (5\text{-}22)$$

Pyle (1972) presented a comprehensive review on mass transfer between bubbles and emulsion phase in gas fluidised beds. He discussed the work done by both Kunii and Levenspiel (1968) and Chiba and Kobayashi (1970), illustrating the significance of the effect of container walls on bubbles of larger diameter (near to the tube size) and the limits on those models when the bubbles rise as slugs.

Harrison and Guedes de Carvalha (1975) studied mass transfer from a slug rising in gas fluidised bed. They used 0.051 m diameter tube, fluidising glass ballotini of 77 microns particle size by nitrogen. A slug of either nitrogen or helium was injected and the variation in the tracer concentration in the slug as it rises through the bed was measured using gas chromatography. The experimental results for Argon showed a good agreement with the theory developed earlier by Hovmand and Davidson (1971) in which both diffusion and through flow are additive, but unfortunately the results obtained for helium showed a considerable deviation. From the results it is clear that the diffusion term in the exchange rate is a vital parameter for beds of fine particles.

Rietema and Hoebink (1975) studied mass transfer between rising bubbles and the dense phase in gas fluidised beds. They used a 45 cm diameter tube and 95 cm high bed, fluidising glass beads and cracking catalyst of 51 and 61 microns average particle size. Their results for the overall bubble to dense phase gas mass transfer coefficient K_B showed an increase with increasing the bubble diameter D_e which contradicts all the other theories.

Chavarie and Grace (1975 - 1976) measured the overall interphase mass transfer coefficient between the bubble and the dense phase K_B corrected

for bubble growth in the bed in two-dimensional bed. The experimental results showed that the convective transfer due to adsorption of tracer gas on the particles surface in the bubble wake played a negligible role in the transfer process. They also showed that failure to allow for bubble growth in the bed, may lead to an overestimation of K_B by a factor of 2.5 as proved experimentally. For the conditions employed in this work (i.e. glass beads with U_o = 5.3 cm/S, ε_o = 0.46, bubbles injected at an average equivalent diameter ~ 20 cm, U_b = 40-60 cm/s and bubbles area at 200-400 cm^2 in two dimensional bed of 245 x 56 x 1 cm) they predicted overall mass transfer coefficients from the different devised models as shown in the following table (5-2)

Table (5-2)

Reference	Basis of model at bubble boundary	at cloud boundary	K_B -predicted (cm/s)
Higbie (1935)	No resistance	penetration theory	0.50
Partridge and Rowe (1966)	No resistance	cloud acts like cylinder in liquid	0.20
Chiba and Kobayashi (1970)	No resistance	diffusion	0.30
Kunii and Levenspiel (1968)	Through flow and molecular diffusion	penetration theory	0.51
Davidson and Harrison(1963)	Through flow and molecular diffusion (additives)	no resistance	4.1
Hovmand and Davidson (1971)	Through flow and molecular diffusion	No resistance	5.0
Chavarie and Grace (1975 & 1976)	Experimental (allowing for bubble linear growth)		1.7

From this table it is clear that models which assume that diffusion from the cloud interface is rate-controlling under-estimate the mass transfer coefficient K_B , on the other hand those models which assume that molecular diffusion and through fl ow at the bubble interface are additive, ignoring the resistance at the cloud boundary, lead to over prediction of K_B .

The large variation in the different models proposed and the resulting correlations means that their use should be handled with great care.

5-4 MECHANISM

Many workers have found that mass transfer between the dense phase gas and rising bubbles dominates the transfer process.

It is convenient to work in terms of transfer units in other words if the transfer for the bubbles is limiting the overall process, the height of a transfer unit between the bubble and dense phase gas $(HTU)_B$ is larger than the one between the particles and dense phase gas $(HTU)_P$.

Preliminary experiments on mass transfer between air and silica gel particles at incipient fluidisation showed very low gas/particle mass transfer coefficients ($K_{g/p} \sim 0.002 - 0.166$ cm/s), hence it is convenient to work in terms of height of transfer units to find out the main resistance controlling mass transfer in fluidised bed drying.

Following the same analysis of Beek (1971) particle to dense phase gas $(HTU)_p$ and dense phase gas to bubble $(HTU)_B$ can be written in the following form:

$$(HTU)_p = \frac{U}{A_p \cdot K_{g/p}} \qquad (5\text{-}23)$$

$$(HTU)_B = \frac{U - U_o}{A'_b \cdot K_B}$$

$$= \frac{U - U_o + 0.67 \sqrt{g D_e}}{6 (0.75 U_o + (g D_G^2 / D_e)^{\frac{1}{4}})} \cdot D_e \quad (5.24)$$

on the basis of Davidson and Harrison's Theory (1963).

where

A'_p : surface area of particles per unit volume of bed (cm^2/cm^3)

A'_b : surface area of bubble per unit volume of bed (cm^2/cm^3)

D_e : diameter of sphere having the same bubble volume (cm)

For an estimated average bubble diameter of 1 cm, based on observing the bubble size at the top of the bed, the ratio between $(HTU)_p$ and $(HTU)_B$ is found to be of order 10. This suggests that the resistance to transfer between particle and dense phase gas is controlling the overall mass transfer in fluidised bed drying as a direct result of the low transfer coefficient ($K_{g/p}$).

To calculate the overall mass transfer coefficient $\bar{K}g$ in fluidised bed drying, a simple model is proposed in which it is assumed that the gas flowing in the bed is one homogeneous phase. The following unsteady state energy balance may be written to describe the gas phase:

$$\frac{G}{U} C_g \frac{\partial Tg}{\partial t} = - G C_g \frac{\partial Tg}{\partial Z} + G (-\Delta H) \frac{\partial Y}{\partial Z} - dq_s \quad (5\text{-}25)$$

where:

G	:	air mass flow rate	(gm A /S)
U	:	air superficial velocity	(cm /S)
Cg	:	air specific heat	$(\frac{cal}{gm.\ ^{o}C})$
Tg	:	air temperature	(^{o}C)
t	:	time	(s)
Z	:	height over distributor	(cm)
Δ H	:	Latent heat of vaporisation	$(\frac{cal}{gm\ W})$
q_s	:	heat transfer rate from air to solids per unit bed height	$(\frac{cal}{S.\ cm})$
Y_g	:	air humidity	$(\frac{gm\ W}{gm\ A})$

Boundary conditions:

at Z = 0 : Tg = Tin Yg = Yin

at Z = H : Tg = Tout Yg = Yout

For quasi steady-state conditions ($\frac{\partial Tg}{\partial t}$ is negligible), and using the boundary conditions mentioned above, equation (5.25) can be approximated by the following equation:

at any height Z cm above the distributor:

$$C_g\ (T_{in} - T_g) = (\Delta H)\ (Y_g - Y_{in}) + \frac{Q_s}{G} \qquad (5\text{-}26)$$

where

G : gas mass flow rate (gm/s)

T_g, Y_g : gas temperature and humidity at certain height

Z cm (^oC, $\frac{gm\ W}{gm\ A}$)

Q_s : rate of heat transfer from gas to heat-up solids up to height Z cm

$$= \bar{h}_{g/p}\ \bar{A} \int_0^Z (T_g - T_s)\ dZ \qquad (Cal/s)$$

From equation (5-26) it is clear that by measuring the gas temperature profile in the bed the air humidity profile can be calculated using an average value for gas to particle heat transfer coefficient $\bar{h}_{g/p}$ measured for each experiment by the same method discussed before in chapter (4), hence the overall mass transfer coefficient $\bar{K}_g$ can be evaluated.

5-5 EXPERIMENTAL STUDY ON THE OVERALL MASS TRANSFER COEFFICIENT $\bar{K}_g$

Based on a humidity driving force ($Y^* - Y_g$), an overall mass transfer coefficient $\bar{K}_g$ can be calculated using the following relationship:

$$\bar{K}_g = \frac{W}{\bar{A} \int_0^H (Y^* - Y_g)\ dZ} \qquad (5\text{-}27)$$

where

W : rate of moisture evaporation (gm W/S)

$\bar{A}$: surface area of fluidised particles (cm^2/cm) per unit bed height

$$= \frac{6\ Ws}{\rho_s \cdot dp \cdot H}$$

Y_g : air humidity as function of bed height - calculated from equation (5-26) (gmW/Kg A)

Y^* : humidity of the air at equilibrium with particle surface (gm W/ Kg A)

To calculate the air equilibrium humidity Y^*, the solids moisture content X was measured and applied to the silica gel hygrothermal equilibrium curve (figure 6-1), hence the air equilibrium $(RH)^*$ is obtained and corrected to give the air equilibrium humidity at the corresponding temperature using the following relationship:

$$Y^* = \frac{(RH)^* \cdot p_o}{(P - (RH)^* \cdot p_o)} \cdot \frac{M_w}{M_A} \cdot \frac{1}{1000} \quad \text{(gmW/Kg A)}$$

where

P : operating bed pressure (bar)

p_o : saturation vapour pressure of moisture in air (bar)

M_w : molecular weight of moisture

M_A : molecular weight of air

An experimental programme was designed to study the effect of air velocity and particle size on the overall mass transfer coefficient $\bar{K}_g$. The following table (5-3) summarizes the different operating conditions during this study;

Table (5-3)

Group	Particle size dp (microns)	Minimum fluidising velocity U_o (cm/s)	Initial bed height H_o (cm)	Average bed temperature T (°C)	Air flow rate Q (l/min)	Superficial air velocity U (cm/s)	Initial solids moisture content (—)
1	106	12·8	10	50	35	7·4	0.201
	106	12·8	10	50	60	12·8	0.279
	106	12·8	10	50	150	31·8	0.186
2	940	30	10	50	150	31·8	0.202
	940	30	10	50	275	58·3	0.168
	940	30	10	50	500	106	0.164
3	2247	58	10	50	275	58·3	0.134
	2247	58	10	50	375	79.5	0.209
	2247	58	10	50	500	106	0.152

5-6 RESULTS AND CORRELATIONS

The variation of air humidity as a function of the bed height is shown in figures (5-1,2 and 3) for the three different particle sizes (106, 940 and 2247 microns). The results obtained from the different batches are consistent and support the earlier work of Kettenring et al (1950), Heertjes et al (1953) and Richardson and Szekely (1961). It is clear that in fluidised bed drying moisture transfer takes place at the entry zone of the bed (within 2 cm above the distributor) and that there is a little or no transfer to the air passing through the rest of the bed.

The effect of air velocity on the overall mass transfer $\bar{K}_g$ in the bed is shown in figure (5-4), from which it is clear that increasing the air flow rate improves the moisture transfer from the silica gel to the air. The variation in $\bar{K}_g$ with the particle size is shown in figure (5-5); from which it is clear that the overall mass transfer coefficient $\bar{K}_g$ increases with increasing particle size up to 1000 microns, but $\bar{K}_g$ does not change for higher particle sizes. The effect of particle size on $\bar{K}_g$ is difficult to investigate experimentally because of the elutriation of fine particles at higher air flow rates.

The results obtained for the overall mass transfer coefficient $\bar{K}_g$ in fluidised bed drying are correlated in terms of Sherwood Sh and Reynolds' Re numbers based on the particle diameter dp, and the following correlation is obtained from figure (5-6):

$$Sh = 0.004 \quad Re^{1.33} \qquad (5\text{-}28)$$

$$\text{for} \quad 10 < Re < 100$$

Our experimental study on the overall mass transfer coefficient $\bar{K}_g$ showed lower values (0.002 - 1.104 cm/s) compared with other workers (table 5-1). This could be explained by the sensitivity of the calculations to the integral $\int_o^H (Y^* - Y_g)\, dZ$ in equation (5-27).

Kettenring et al (1950) assumed that Y^* is constant in the bed and equal to the air humidity at the outlet which proved to be incorrect, while Thodos et al (1961 and 1963) used a log mean partial pressure difference of the moisture $(\Delta P)_m$ in the bed using the same previous assumption, which lead to overestimating $\bar{K}_g$ as expected.

From our experimental results we can conclude that during the constant rate period for drying of hygroscopic materials, moisture transfer from particles to gas occurs via two steps: first, in the entry zone within the first two centimeters above the distributor, the gas looses most of its heat in direct evaporation of moisture from the solids, hence the transfer process in this region is governed by simultaneous heat and mass transfer and hence the bubble effect is insignificant in this region. In the second step, since the gas leaving the entry zone is unsaturated, we would expect some moisture transfer between the segregated phases - as shown from the two phase theory - which could not measure by simple single-phase model proposed earlier in section (5-4). This shows the need to develop a model representing fluidised bed drying which takes into account the role of bubble in the bed, which we shall discuss in details in chapter (7).

In the next chapter, solids drying curves are discussed, showing the effect of different parameters (e.g. air flow rate, particle size, bed height,

bed temperature, number of transfer units of the bubble and gas thermal characteristics) on the drying rates of solids; and these effects are correlated to enable us to predict the drying rates of solids in fluidised bed drying under different operating conditions.

CHAPTER (6)

SOLIDS DRYING CURVES IN SHALLOW FLUIDISED BED

6-1 INTRODUCTION

Drying of powders and granules in fluidised bed has proved to be highly efficient in many industries. Despite the lack of academic studies on the behaviour of fluidised bed dryers and on the factors affecting the bed performance, industrial applications of fluidised bed dryers are widespread (e.g. Wall and Ash (1949), Beeken (1958-1960), Scott et al (1963), Davis and Glazier (1965)).

In this chapter; we shall present an experimental study on the effect of different parameters (e.g. air flow rate, particle size, bed height, air temperature, bubble exchange factor and gas thermal characteristics) on the solids drying curves with the aim of showing how to achieve the highest drying rate by optimizing between the different operating factors.

6-2 BASIC PRINCIPLES

In the following section we shall discuss the basic principles of four different processes which occur during drying: humidification, hygrothermal equilibrium, solids drying curves and pore diffusion.

6-2-1 Humidification Process

Moisture evaporating from wet solids humidifies the air in contact. This increase in air humidity decreases the humidity driving force between solids

and air, and limits the maximum drying rate. The extent of humidification can be used as a measure of the bed performance, which can be represented in terms of rehumidity driving force ψ :

$$\psi = (Y^* - Y_g)$$

where

Y_g : gas humidity (Kg water/Kg air)

Y^* : humidity of the gas in equilibrium with particle surface (Kg water/ Kg air)

(It is important to realise that Y^* is a function of both solids moisture content and gas temperature).

Three limiting cases can occur in the bed:

(a) Isenthalpic change: where the air follows constant-enthalpy line $(\frac{\Delta i}{\Delta Y})_G = 0$,

(b) Isohumid change: where the air humidity remains constant - which often occurs during heating or cooling - $(\frac{\Delta i}{\Delta Y})_G = \infty$,

(c) Isothermal change: where the processes occur under constant temperature conditions.

For the air/water system, the adiabatic saturation temperature of the air and the wet bulb temperature of the solids are the same, hence the famous Grosvenor equation for air temperature, humidity and enthalpy changes can be written in the following form:

$$(T_{g2} - T_{g1}) = \frac{-(\Delta H)_{vap}}{C_g} (Y_{g2} - Y_{g1}) \qquad (6\text{-}2)$$

6-2-2 Hygrothermal Equilibrium

A material is said to be non-hygroscopic as long as the interstitial micro pore radii are greater than around one micron, so that no significant lowering of vapour pressure of the diffusant occurs.

On the other hand, the moisture in hygroscopic materials is either totally free, partially bound or totally bound, and does not exert its full vapour pressure. In this case the change in moisture/solid bond free energy can be represented in the following form - as shown by Keey (1970):

$$- \Delta G' = - RT \ Ln \frac{P}{P_o}$$

where

G' : Gibbs free energy

P : Vapour pressure exerted by moisture in a hygroscopic material

P_o : Saturation vapour pressure of moisture at a temperature (T).

From the hygrothermal equilibrium curve of silica gel shown in figure (6-1)- discussed by Keey (1972) and Rietema and Hoebink (1973) - it is clear that the equilibrium relative humidity of the air (Y^*) during drying is lower than its value during wetting as a result of the vapour pressure at the surface of hygroscopic materials which is always less than that for a "free moisture" surface.

From the silica gel hygrothermal curve, it is expected that the retained moisture content will not diffuse to the air in contact, until the relative humidity of the air Ψ decreases to a lower value than the equilibrium

relative humidity ψ^* : hence it is necessary to heat the air for the drying of moist silica gel in fluidised bed to proceed.

6-2-3 Drying Curves

The mechanism of solids drying may be characterised by a drying curve which depends strongly on two major factors: the particle nature (e.g. hygroscopic or non-hygroscopic) and the orientation of the particles in the equipment in question as discussed in Keey (1970).

For a non-hygroscopic capillary-porous bed, a typical drying curve is shown in figure (6-2). This can be explained by a "two-pore capillary" model, in which the superficial moisture gives a constant drying rate period (AB), followed by two falling rate periods which correspond to the moisture state in the bed: funicular state (BC) followed by pendular state(CD).

For a hygroscopic capillary-porous material, a typical drying curve is given in figure (6-3). The constant rate period (AB) exists when there is enough superficial moisture, then followed by three falling rate periods which correspond to : totally free moisture region (BC), followed by partially bound moisture region (CD) and ending with totally bound moisture region (DE).

For hygroscopic non-porous materials, the moisture is distributed throughout each particle as if were dissolved in it, hence air cannot penetrate the wet particle. The moisture moves by diffusion under an ever disminishing concentration gradient, and the drying rate decreases without the appearance of a sharp critical point as shown in figure (6-4).

The drying of silica gel in fluidised bed gives similar drying curves to figure (6-4). This can be explained by the nature of solids drying in fluidised bed, where each particle behaves like a hygroscopic sphere suspended in an air stream : hence the moisture diffuses through the micropores of the particles to the surface, where the difference between the equilibrium relative humidity at the surface and the gas relative humidity will represent the driving force for moisture transfer from the solids to the air in contact.

6-2-4- Pore Diffusion

Moisture diffusion in the pores of the particles occurs via three different routes, Bulk (molecular) diffusion, Knudson diffusion and surface pore diffusion as discussed by Sherwood, Pigford and Wilke (1975).

Bulk pore diffusion occurs when the pore size is larger than the mean free path of moisture in the air. In this case the resistance to moisture diffusion lies in the collision of water molecules together inside the pores. The bulk diffusion coefficient (D_p) can be calculated on the basis of a molecular diffusion coefficient in the gas phase (D_G) from the following relationship:

$$D_p = \frac{D_G \cdot \Theta}{\tau} \qquad (6\text{-}4)$$

where

Θ : Free fraction of cross sectional area of the pore

τ : Tortuosity factor, which is a correction factor to allow for the difference in diffusion path (which is longer than the distance travelled normally to the surface). It also accounts for the variation in the pore cross section area as well as the difference in the pore shape.

Knudson diffusion occurs when the pore size is smaller than the mean free path of moisture diffusion in the air. Here, the main resistance to moisture transfer is due to the collision of molecules with the pore walls. The Kinetic theory of diffusion non-adsorbing round pores, predicts: Knudson diffusion coefficients (D_{Kp}) from the following equation:

$$D_{Kp} = 19400 \frac{\Theta^2}{\Sigma \cdot \delta_g \cdot \rho_b} \left(\frac{T}{M}\right)^{\frac{1}{2}} \qquad (6\text{-}5)$$

where

δ_g : Brunauer- Emmett-Teller Isotherm (surface/gm)

ρ_b : bulk density (gm/cm^3)

M : molecular weight of diffusing material

T : gas temperature (^oK)

In the transition region, where both bulk and Knudson pore diffusion interact, the overall pore diffusion coefficient ($\bar{D}_p$) can be represented as

$$\bar{D}_p = \frac{1}{\left(\frac{1}{D_p}\right) + \left(\frac{1}{D_{Kp}}\right)} \qquad (6\text{-}6)$$

Surface pore diffusion occurs when the diffusing moisture is adsorbed by the pore wall, and hence a surface concentration gradient is developed, of the same sign and direction as the concentration gradient of the diffusing vapour in the pore. Although capillary condensation may cause the pores

to fill up with liquid moisture, we can still assume that the adsorber layer is so thin that the cross section of the pores available for gas diffusion is not greatly reduced and since the gas and surface diffusions are parallel, so the overall pore diffusion flux can be represented by equation (6-7) for a linear adsorbtion isotherm:

$$J = -(\bar{D}p + K D_{sp}) \frac{dc}{dy} \qquad (6\text{-}7)$$

where

J : overall pore diffusion flux

$\bar{D}_p$: defined in equation (6-6)

D_{sp} : pore surface diffusion coefficient

K : adsorbtion isotherm constant

$\frac{dc}{dy}$: moisture gradient in the pore

Depending on both pore size and mean free path of water molecules in the air, the controlling step in pore diffusion can be determined (i.e. for larger pore size than the mean free path of water molecules, bulk pore diffusion controls, while for smaller pore size than the mean free path of water molecules, Knudson diffusion control). Surface pore diffusion occurs only when the water molecules are adsorbed by the pore walls, which is the case in most hygroscopic materials.

6-3 SOLIDS DRYING MECHANISM

In this section, three different models are discussed for moisture transfer from solids during drying : (a) moisture diffusion, (b) water vapour diffusion and (c) simultaneous mass and heat transfer model.

6-3-1 Moisture Diffusion Model

Becker and Sallans (1955 - 1960) and Becker (1959) proposed a moisture diffusion model to describe the drying of wheat Kernels. The model is based on the assumption that, during the constant-rate period, the drying of solids is controlled by liquid moisture diffusion in the solids. By applying Fick's law for diffusion of moisture in spherical particles they derived the following general equation for the average moisture concentration $\bar{c}$ in the solids as a function of time t, in the following form:

$$\bar{c} = \frac{6}{\pi^2} \sum_{n=1}^{\infty} \frac{1}{n^2} \exp\left(-\frac{n^2 \pi^2}{q} X^2\right) \qquad (6\text{-}8)$$

where

$$X = \frac{S}{V} \sqrt{Dt}$$

D : moisture diffusivity (cm^2/s)

S : exposed surface area of solids (cm^2)

V : solids volume (cm^3)

For spherical particles, equation (6-8) can be approximated to the following form:

$$\frac{C_o - \bar{c}}{\sqrt{t}} = \frac{2}{\sqrt{\pi}} \frac{S}{V} \sqrt{D} (C_o - C_s) - \frac{f(o)}{2} \left(\frac{S}{V}\right)^2 D (C_o - C_s) \sqrt{t}$$

$$\frac{K}{\sqrt{t}} = K_o - b \sqrt{t} \qquad (6\text{-}8 - a)$$

where

C_o : initial moisture content

C_s : moisture content at the particle surface

They applied the model to the drying of wheat in a spouted bed and showed that the diffusion coefficient of moisture in solids is independent of the moisture concentration.

6-3-2 Pore Diffusion Model

Philip and De Vries (1957) were the first to report a comprehensive study of vapour and liquid diffusion during the drying of a column of porous medium under ambient conditions.

The theory is based on the fact that vapour diffusion in the pores is the controlling step in moisture transfer between solids and gas. They showed that the vapour flux q_{vap} $(\frac{gm}{cm^2 \cdot s})$ can be represented by:

$$q_{vap} = - D_G \nabla \tau a \qquad (\nabla \rho) \qquad (6\text{-}10\text{-}a)$$

where

D_G : moisture molecular diffusion coefficient (cm^2/s)

V : mass flow factor

τ : tortuosity factor

a : internal voidge fraction of solids

ρ : water vapour density (gm/cm^3)

For liquid diffusion, they showed the liquid flux q_{liq} ($\frac{gm}{cm^2 . s}$) can be written in the following form:

$$q_{liq} = - K \rho (\nabla \phi) \qquad (6\text{-}10\text{-}b)$$

where

K : unsaturated hydraulic conductivity (cm/s)

ϕ : total potential (cm)

They proved that the thermal liquid diffusion can be ignored compared with the vapour diffusion especially at solids moisture contents less than 30 % ($\frac{gm\ W}{gm\ S}$), and finally they derived a general differential equation, to describe moisture movement in porous media under combined temperature and moisture gradients, in the following general form:

$$\frac{\partial X}{\partial t} = \nabla \cdot (D_T \nabla T) + \nabla \cdot (D_X \nabla X) + \frac{\partial K}{\partial Z} \qquad (6\text{-}10\text{-}c)$$

where

X : solids moisture content (gmW/gmS)

T : temperature (^oC)

t : time (S)

Z	: distance	(cm)
K	: defined in equation (6-10-b)	(cm/s)
D_T	: thermal moisture diffusivity	(cm^2/s)
D_x	: Isothermal vapour diffusivity	(cm^2/s)

This model predicts solids drying rates in both constant-rate and falling--rate periods based on the assumption of liquid-vapour equilibrium in the porous media.

Novak and Coulman (1975) reviewed the different theories of moisture transfer in rigid porous materials and they proposed a general mechanism to describe moisture movement during the drying of a column of sand under ambient conditions.

The model accounts for four different parameters contributing to moisture transfer : (a) liquid movement which is controlled by capillary flow, (b) vapour transfer - this is controlled by gas diffusion in the pores, (c) simultaneous heat and moisture transfer which is controlled by conduction of heat to solids, and (d) interphase mass transfer between liquid and vapour which is controlled by the gas film resistance.

Assuming that vapour-liquid equilibrium is established in the porous medium, the model can be reduced to the following form:

$$\frac{\partial \bar{s}}{\partial t} = -\frac{1}{\varepsilon} \frac{\partial}{\partial Z} \left(U^{\rho} + \frac{M_w N_w}{\rho_w} \right) \qquad (6\text{-}11)$$

where

$\bar{s}$: volume of moisture per volume of gas and liquid in the porous media

ε : voidge fraction

Z	: column height	(cm)
U^o	: volumetric flux of liquid water	(cm/day)
M_w	: molecular weight of moisture	
N_w	: molar flux of water vapour	(gm mole/cm^2- day)
ρ_w	: liquid water density	(gm/cm^3)

6-3-3 Simultaneous Mass and Heat Transfer Model

Myklestad (1968) studied the transient flow of heat and moisture, during drying in packed granular beds. His drying curves showed four different stages, a constant drying rate period , an increasing rate period and two falling rate periods. During the constant-drying rate periods, he assumed that simultaneous mass and heat transfer is the controlling step, and he developed the following equations to describe the packed bed:

Gas temperature:

$$T_g\Big)_z = T_s + (T_{in} - T_s)\, e^{-\alpha z} \qquad (6\text{-}12)$$

Gas humidity:

$$Y_g\Big)_z = Y^* + (Y_{in} - Y^*)\, e^{-\beta z} \qquad (6\text{-}13)$$

Solids moisture content:

$$\frac{dX}{dt} = -\frac{\bar{K}}{\rho_s} \int_o^Z (Y^* - Y_g)\, dz \qquad (6\text{-}14)$$

where

$$\alpha = \frac{\bar{h}}{G \cdot C_g}$$

$$\beta = \frac{\bar{K}}{G}$$

$\bar{h}$ = overall gas to particle heat transfer coefficient

$\bar{K}$ = overall gas to particle mass transfer coefficient

Peck, Max and Ahluwalia (1971) developed a theory to predict solids drying curves, based on heat and mass transfer correlations. The model is based on the following assumptions (a) internal resistance to liquid flow is negligible , (b) moisture evaporation takes place only on the surface of the particle, (c) heat transfer to solids is small compared with latent heat required for evaporation, (d) solids surface temperature is equal to the wet bulk temperature.

Based on these assumptions, they derived the following form for drying rate of solids in packed beds:

$$\left(\frac{d X}{d t}\right) = - K_g \grave{A} \left(\frac{X}{X_{cr}}\right)^{2/3} (P_s - P_R) \qquad (6\text{-}15)$$

where

X : solids moisture content

t : time

K_g : overall mass transfer coefficient

$\grave{A}$: particle surface area

X_{cr} : critical moisture content

P_s : saturation water vapour pressure

P_R : partial pressure of water vapour in the air

From the different basic mechanisms of solids drying, discussed above, it is clear that moisture transfer from wet solids to the drying gas depends on both the moisture state in solids and the particle orientation in the drying equipment.

In fluidised bed drying, particles behave like suspended spheres in the hot air stream during the drying period, hence the applicability of the pore diffusion model (Philip and De Vries (1957) and Novak and Coulman (1975)) is very difficult especially during the constant-rate period where the pore diffusion is insignificant.

Both the moisture diffusion model (Becker and Sallans (1955-1960))and the simultaneous heat and moisture transfer model (Myklestad (1968) and Pecketal (1971)) may be applied to fluidised bed drying after taking into account the effect of bubbles on the mass transfer process during the drying period.

6-4 EXPERIMENTAL STUDY ON DRYING OF SOLIDS IN FLUIDISED BED

The effect of the air flow rate, particle size, air temperature and thermal characteristics, bed height and bubble exchange factor on the drying rate of solids in fluidised bed was studied experimentally using wet silica gel particles. The drying curves for different experiments were obtained by sampling the solids every ten minutes.

6-4-1 Bed Height (H_o)

Four different experiments were run on 940 micron silica gel particles to study the variation of solids drying rate with bed height. The following table summarizes the experimental operating conditions:

Run	Initial bed height H_o (cm)	Particle size dp (microns)	Minimum fluidising velocity U_o (cm/s)	Average bed temperature T (^oC)	Air flow rate Q (l/min)	Superficial air velocity U (cm/s)
1	5	940	30	50	150	31·8
2	10	940	30	50	150	31·8
3	15	940	30	50	150	31·8
4	20	940	30	50	150	31·8

6-4-2 Air Flow Rate (Q)

The effect of air flow rate on solids drying rate was studied by conducting 28 experiments under different operating conditions as shown in the following table using silica gel particles.

Run	Air flow rate Q (l/min)	Superficial air velocity U (cm/s)	Particle size dp (microns)	Minimum fluidising velocity U_o (cm/s)	Average bed temperature T (°C)	Initial bed height H_o (cm)
5	35	7.4	106	12·8	50	10
6	60	12·8	106	12·8	50	10
7	85	18·1	106	12·8	50	10
8	150	31·8	106	12·8	50	10
9	85	18·1	940	30	50	10
10	150	31·8	940	30	50	10
11	275	58·4	940	30	50	10
12	500	106·2	940	30	50	10
13	150	31·8	2247	58	50	10
14	275	58·4	2247	58	50	10
15	375	79·6	2247	58	50	10
16	500	106.2	2247	58	50	10
17	150	31·8	940	30	40	10
18	275	58·4	940	30	40	10
19	400	84·9	940	30	40	10
20	500	106·2	940	30	40	10
21	150	31·8	940	30	60	10
22	275	58·4	940	30	60	10
23	400	84·9	940	30	60	10
24	600	127·4	940	30	60	10
25	150	31·8	940	30	80	10
26	275	58·4	940	30	80	10

(Con t.)

27	400	84.9	940	30	80	10
28	600	127.4	940	30	80	10
29	150	31.8	940	30	100	10
30	275	58.4	940	30	100	10
31	400	84.9	940	30	100	10
32	600	127.4	940	30	100	10

6-4-3 Particle Size (dp)

To study the effect of particle diameter on solids drying rate, a nine experiment programme was run on the three different batches available of silica gel particles. The different operating condition are shown in the following table:

Run	Particle size dp (microns(	Minimum fluidising velocity U_o (cm/s)	Air flow rate Q (l/min)	Superficial Air velocity U (cm/s)	Average bed temperature T (^oC)	Initial bed height H_o (cm)
33	106	12.8	150	31.8	50	10
34	940	30	150	31.8	50	10
35	2247	58	150	31.8	50	10
36	106	12.8	275	58.4	50	10
37	940	30	275	58.4	50	10
38	2247	58	275	58.4	50	10
39	106	12.8	500	127.4	50	10
40	940	30	500	127.4	50	10
41	2247	58	500	127.4	50	10

6-4-4 Air Temperature (T_{in})

The effect of inlet air temperature on solids drying rate was studied for silica gel particles. The different operating conditions for the experiments are shown in the following table:

Run	Inlet air temperature T_{in} (°C)	Particle size dp (microns)	Minimum fluidising velocity U_o (cm/s)	Air flow rate Q (l/min)	Superficial air velocity U (cm/s)	Initial bed height H_o (cm)
42	40	940	30	150	31-8	10
43	60	940	30	150	31-8	10
44	80	940	30	150	31-8	10
45	100	940	30	150	31-8	10
46	40	940	30	275	58-4	10
47	60	940	30	275	58-4	10
48	80	940	30	275	58-4	10
49	100	940	30	275	58-4	10
50	40	940	30	400	84-9	10
51	60	940	30	400	84-9	10
52	80	940	30	400	84-9	10
53	100	940	30	400	84-9	10
54	40	940	30	500	106-2	10
55	60	940	30	500	106-2	10
56	80	940	30	500	106-2	10
57	100	940	30	500	106-2	10

6-4-5 Bubble Exchange Factor

To study the effect of bubbles rising in fluidised bed drying on solids drying rate, it was convenient to analyse the results in terms of the number of"bubble transfer units" - $(NTU)_B$. Following the same analysis of Davidson and Harrison (1963), as discussed in the last chapter (section 5-3), the number of bubble transfer units $(NTU)_B$ can be written in the following form:

$$(NTU)_B = \frac{6.34\ H_o}{D_e\ (g\ De)^{\frac{1}{2}}}\ \left(U_o + \frac{1.3\ D_G^{\frac{1}{2}}\ g^{\frac{1}{4}}}{D_e^{\frac{1}{4}}} \right) \qquad (6.16)$$

It is clear that $(NTU)_B$ depends on both particle size (which controls the minimum fluidising velocity U_o) and the assumed bubble flow rate per unit cross section area of the bed $(U - U_o)$ which is related to the bubble diameter by:

$$U - U_o = N\ V\ U_A \qquad (6\text{-}17)$$

as shown by Davidson and Harrison (1963) from the two-phase theory, where

V	: bubble volume	$(\frac{\Pi}{6} D_e^{\,3})$	(cm^3)
N	: number of bubbles per unit volume		
U_A	: absolute bubble rising velocity	$(U - U_o + K\ \sqrt{g\ D_e})$	
D_e	: equivalent bubble diameter	(cm)	
U	: air superficial velocity	(cm/s)	
U_o	: minimum fluidising velocity	(cm/s)	

Because of the difficulty of measuring the effect of $(NTU)_B$ on solids drying rate directly, two sets of experiments were run: the first group, to study the effect of $(NTU)_B$ at constant bubble flow rate ($U - U_o$) on solids drying rate and in the second group, the effect of $(NTU)_B$ at constant particle diameter on solids drying rate was studied. In all the experiments, the bubble diameter was estimated by observing the bubble size at the top of the bed, mainly because the bed used in drying was so shallow that the bed expansion method for determining the average bubble diameter was not very accurate in these experiments. It is clear from the previous chapters (4) and (5) that drying of solids in fluidised bed is dominated by simultaneous heat and mass transfer above the distributor, where the gas is nearly one homogeneous phase and hence the drying rate of solids is insensitive to the bubble diameter.

6-5 RESULTS AND CORRELATIONS

The effect of bed height on the solids drying curves is shown in figure (6-5). The overall drying rate of the solids, R, decreases on increasing the bed height. Figure (6-6) shows that the drying rate is proportional to the reciprocal of bed height,

$$R \propto \left(\frac{H_o}{D}\right)^{-1} \qquad (6\text{-}17)$$

where for convenience the bed height has been made dimensionless by scaling by bed diameter.

The effect of air flowrate on the drying curves of the solids is illustrated in figures (6-7, 8 and 9) for the different particle sizes (106, 940 and 2247 microns) respectively. The overall effect is shown in figure (6-10), from which, it is clear that the drying rate increases on increasing air flow rate.

The effect of air flow rate on solids drying rate at different temperatures is also shown in figures (6-11, 12, 13 and 14) for the different air temperatures (40, 60, 80 and 100 °C) respectively.

Figure (6-15) illustrates the linear relationship between air flow rate and solids drying rate.

Typical drying curves showing the effect of particle size on solids drying rate are given in figures (6-16, 17 and 18) at different air flow rates (150, 275 and 500 l/min). All the results showed a slight increase in the drying rate of solids on increasing the particle size. Figure (6-19) shows the logarithmic relationship between dimensionless particle diameter represented at (dp/D) and solids drying rate, which can be represented as:

$$R \quad \alpha \quad \left(\frac{dp}{D}\right)^{0.105} \qquad (6\text{-}18)$$

The effects of air temperature on the drying curves of solids are shown in figures (6-20, 21, 22 and 23) for different air flow rates (150, 275, 400 and 500 l/min). The results show the direct effect of heat transfer on the drying rate of solids which increases with the increase in air temperature. This effect can be represented , from figure (6-24), in the following form:

$$R \quad \alpha \quad \left(\frac{T}{T_R}\right)^{1.15} \qquad (6\text{-}19)$$

where

T : inlet air temperature

T_R : room temperature

The relationship between the drying rate of solids and the air thermal characteristics expressed in terms of Prandtl number ($Pr = \frac{C_g \mu}{K}$) is shown in figure (6-25), and can be represented in the following form:

$$R \quad \alpha \quad Pr^{5.14} \qquad (6\text{-}20)$$

The effect of bubble exchange $(NTU)_B$ on the drying rate of solids was studied for two different cases: first, at constant bubble flow rate $(U - U_o)$, second, at constant particle diameter dp. The following table summarizes the results obtained in the first case where $(U - U_o)$ is kept constant, and the change in $(NTU)_B$ is mainly due to the change in particle size which controls (U_o) in equation (6-16).

Run	Particle size dp (microns)	Minimum fluidising velocity U_o (cm/s)	Superficial air velocity U (cm/s)	Bubble flow rate /A $(U-U_o)$ (cm/s)	Bubble diameter (observed) De (cm)	Bubble exchange (eqn 6.16) $(NTU)_B$ (—)	Drying rate $R \times 10^3$ ($\frac{gmW}{gm\ dry\ S}$/min
58	106	12·8	32·8	20	2	20	2·86
59	940	30	50	20	1	65	4·00
60	2247	58	78	20	1	122	4·50

The results obtained are plotted in figure (6-26), from which it appears that there is a linear increase in the drying rate on increasing $(NTU)_B$ at

constant $(U - U_o)$ as a result for increasing the particle diameter dp.

For the second case, where particle diameter is kept constant, the change in $(NTU)_B$ was obtained by changing the air flow rate which changes the bubble size De.

The following table summarizes the results obtained for three different batches of silica gel (106, 940 and 2247 microns).

Run	Particle size dp (microns)	Minimum fluidising velocity U_o (cm/s)	Superficial air velocity U (cm/s)	Bubble diameter (observed) De (cm)	Bubble exchange (eq^n 6.16) $(NTU)_B$ (—)	Drying rate R X 10^3 ($\frac{gmW}{gm\ dry\ S}$ /min)
61	106	12·8	15·8	0·5	88	2
62	106	12·8	18·1	1	30	2·5
63	106	12·8	31·8	2	20	2·86
64	940	30	35·5	0·5	188	3·333
65	940	30	58·4	1	65	4·00
66	940	30	106·2	2	44	4·333
67	2247	58	63·4	0·5	351	2·667
68	2247	58	79·6	1	122	4·50
69	2247	58	106·2	2	83	6·00

The results obtained are plotted in figure (6-26-a), from which it is clear that, for constant particle diameter, increasing the air velocity, which increases the average estimated bubble diameter and consequently decreases

$(NTU)_B$, shows an increase in solids drying rate.

From these two sets of results, it is clear that solids drying rate, in figure (6-26), is dominated by particle size when the air flow rate is kept constant, on the other hand it is governed by the direct effect of air flow rate when the particle diameter is kept constant (figure 6-26-a). The apparently contradictory effects of $(NTU)_B$ on the solids drying rate are, it is suggested, a result of the fact that R is directly affected by air velocity and particle diameter and only indirectly (since these parameters affect $(NTU)_B$) by the bubbling behaviour. This can be explained on the light of entry zone effect, where solids drying rate is governed by simultaneous heat and mass transfer. It ia clear from the previous chapter that most of the mass transfer occurs in the first few centimeters above the distributor and because the height of transfer unit between particle and dense-phase gas is much higher than the one between the segregated phases, it is expected that the transfer in the entry zone is dominated by the resistance between gas and particle, and hence the bubble exchange $(NTU)_B$ is relatively unimportant in the bed where the transfer is controlled by Reynolds' number in the entry zone, which will be discussed in more details in the next chapter.

From the various results obtained, showing the effect of different parameters on the drying of solids, figure (6-27) is plotted to represent the general solids drying rate correlations, which is expressed in the following form:

a- for $Re < 10$

$$R = 0.07 \times 10^{-3} \left(\frac{D}{H_o}\right) \left(\frac{T}{T_R}\right)^{1.15} \left(\frac{dp}{D}\right)^{0.105} Pr^{5.14} Re^{1.51} \qquad (6\text{-}21)$$

b-for $10 < Re < 100$

$$R = 0.005 \times 10^{-3} \left(\frac{D}{H_o}\right) \left(\frac{T}{T_R}\right)^{1.15} \left(\frac{dp}{D}\right)^{0.05} Pr^{5.14} Re^{0.604} \qquad (6\text{-}22)$$

where the drying constant has the same dimensions as the solids drying rate R $\left(\frac{\text{gm Water}}{\text{gm dry Solids}} / S\right)$.

6-6 DISCUSSION

From the results obtained in this chapter, we can examine the moisture transfer mechanism proposed earlier by Becker and Sallans (1955-1960) which is based on the assumption that water liquid diffusion in the solids is the controlling step for moisture transfer during the drying period (discussed earlier in section 6-3-1). Our experimental results do not agree with this model, and support the earlier results of Peck et al (1974) on drying of barley malt which also do not agree with the Becker-Sallans model. It is clear from both sets of results that liquid water diffusion in the particle is not the controlling step in moisture transfer during the drying period, and we suggest that the drying rate in fluidised bed is governed by the simultaneous heat and mass transfer at the entry zone of the bed which is discussed in more details in the next chapter.

The effect of different parameters on the drying rate of solids R can be explained in terms of the overall mass transfer coefficients $\bar{K}g$ in the bed. For example, increasing the air flow rate improves the overall mass transfer coefficient $\bar{K}_g$ and hence the solids drying rate, R , is

expected to improve automatically. The effect of particle size on the overall mass transfer coefficient $\bar{K}_g$ is shown in figure (5-5), from which it is seen that increasing the particle size (for dp $<$1000 microns) increases $\bar{K}_g$, and hence the solids drying rate R is expected to increase. From these different results, we can see the direct effect of the overall mass transfer coefficient on solids drying rate; nevertheless, from the drying experiments it is clear that increasing the air temperature improves the drying rate of solids, which can be explained as a direct result of increasing the heat transfer from the gas to the moist particles in the bed, and hence the overall drying rate of solids in fluidised bed is concluded to be directly affected by the simultaneous heat and mass transfer occuring at the entry zone of the bed. Both the relative unimportance of bubble exchange $(NTU)_B$ and the effect of bed height on solids drying rate are a direct resultof the entry zone effect in the bed as discussed in more details in the next chapter.

CHAPTER (7)

MODELLING

7-1 INTRODUCTION

The wide application of fluidised beds in different industrial areas requires a full understanding of the effect of different design parameters on the bed performance. Different models have been proposed to explain the behaviour of fluidised beds as catalytic reactors and these models can be classified into four groups: homogeneous flow models (e.g. Shen and Johnstone 1955 up to 1960s), single-parameter bubble models (e.g. Davidson and Harrison 1963), bubble coalescence models (e.g. Calderbank and Toor 1971) and back-mixing models (e.g. Fryer and Potter 1973-1976).

In homogeneous flow models, fluidised bed behaviour is treated as an extension of packed or distended beds, where it is assumed that all the gas passes through the bed as one homogeneous phase, and hence all the single phase relationships are applicable.

In both the single-parameter bubble and bubble coalescence models, it is agreed that the major characteristic of gas fluidised bed is the appearance of bubbles in the bed, which play a crucial role in solids mixing, determining the thermal properties of the bed, as well as heat and mass transfer between the segregated phases.

These models are based mainly on the mechanics of bubbles rising in the bed and have the following general features: the gas passing through the bed consists of a dense-phase, which is in direct contact with solids and rises at the minimum fluidising velocity, and the bubble-phase which represents the rest of the gas and rises with its own characteristic bubble velocity U_b. If the bubble rising velocity U_b is less than the interstitial velocity at incipient fluidisation u_o (i.e α ($= \frac{U_b}{u_o}$) is less than 1), the bubble exchanges its gas with the dense-phase by convection as well as diffuison (through flow) as shown by Davidson and Harrison (1963). On the other hand, if the bubble rising velocity U_b is larger than the interstitial u_o, hence ($\alpha > 1$) the bubble is surrounded by a cloud of radius R_c, depending on the bubble radius, a, as well as the ratio α, and the gas exchange between the bubble and dense-phase occurs by diffusion and cloud-shedding as shown by Rowe and Partridge (1966).

The major difference between the single-parameter and coalescence bubble models lies in the assumption that all the bubbles have the same equivalent diameter, De, and that bubble distribution is uniform throughout the whole bed in the first model (e.g. Davidson and Harrison 1963); the other model accounts for bubble growth in the bed by coalescence and shows that the bubble distribution function depends on position in the bed (e.g. Calderbank and Toor 1971).

In the last group - back-mixing models (e.g. Fryer and Potter 1973-1976) - it is assumed that when the gas velocity exceeds a critical value U_{cr}, the dense-phase gas will flow downwards with the recirculating solids

while the bubbles rise upwards in the bed. The model predicts an axial concentration profile which passes through a minimum value within the bed.

It is important to recognise the difficulty in analysing fluidised bed performance as a result of the interaction between the different parameters; moreover, there is a lack of experimental data with which the available models can be tested to explore in depth other factors which could affect the bed performance, such as distributor performance, bubble growth and coalescence and particle mixing.

7-2 FLUIDISED BED MODELS REVIEW

Orcutt, Davidson and Pigford (1962) were the first to analyse fluidised bed performance on the basis of bubble mechanics. The model is based on the two-phase theory, where the gas in excess of that needed for incipient fluidisation passes through the bed as bubbles, which are assumed not to contain any solids and have constant bubble diameter throughout the whole bed.

Davidson and Harrison (1963) studied first-order catalytic reactions in fluidised beds. They showed that with the assumption of perfect mixing in the dense-phase, the model predicts the limiting behaviour of the bed to be a continuous stirred tank reactor for slow reactions and fast exchange between the segregated phases; on the other hand, for fast reactions the model predicts a by-passing effect which controls the overall bed performance.

Pyle and Rose (1965) studied the fluid flow through a bubble rising in fluidised bed. They discussed three different models to describe the overall reactor performance based on bubble mechanics. The bubble models suggested were : (a) stream line flow in the bubble and the dense-phase, (b) perfect mixing within the bubble and stream line flow in the dense-phase, (c) complete mixing of fluid between the bubble and the cloud when $\alpha > 1$.

Partridge and Rowe (1966) studied bubbling models of very fine particles They showed that when $\alpha > 1$, the bubble rising in the bed is surrounded by a cloud where the gas is in intimate contact with particles. Their model is based on the assumption that the bubble and the cloud gas are in perfect mixing, and the resistance to the transfer between the bubble and dense phase gas lies in the diffusion step at the cloud boundary.

Latham and Potter (1970) examined the back-mixing model, where it is assumed that the down-flow gas can occur when the velocity of the descending particles exceeds the interstitial gas velocity in the dense-phase, and they defined the gas superficial velocity at which back-mixing occurs in terms of a critical velocity (U_{cr}).

Calderbank and Toor (1971) discussed bubble coalescence models, where the bubble size varies as it rises in the bed because of the coalescence with other bubbles. Because of the bubble size variation in the bed, all the other parameters affecting the bed performance (e.g. exchange between bubble and dense phase gas Q, number of bubbles per unit volume of the bed N, bubble volume V and the exchange factor X) will change in

the bed as a function of bubble position. The complicated mathematical formula for the bed performance can be solved numerically.

Pyle (1972) reviewed some of the important bubbling models in fluidised bed. He showed that the results obtained by Toor and Calderbank (1967-1968)on the insignificance of bubble coalescence is doubtful and hence the fluidised bed performance cannot be characterised by single-parameter models. He also highlighted the importance of bubble inception at the distributor, bubble coalescence and growth, the distributor design, bubble distribution in large beds and the importance of particle mixing on the bed performance.

Chiba and Kobayashi (1973) proposed a bubble coalescence model, in which they assumed that bed can be divided into " n " compartments where the bubble size and gas exchange are constants within the same compartment. Using a semi-emperical relationship for bubble size variation between one compartment and the next, they showed that bed performance can be calculated using a numerical technique.

Fryer and Potter (1973-1976) modified the back-mixing model to include the bubble size variation with bed height. The theoretical model predicts an axial concentration profile which passes through a minimum value within the bed. Studying the catalytic decomposition of ozone in 22.9 cm bed of 107 microns catalyst, the measured concentration profile showed a minimum concentration within the bed, which supports the model in question.

The different models mentioned above show the degree of complexity in describing the bubbling beds, and highlight the effect of different parameters (e.g. bubble diameter, bubble size distribution function, bubble coalescence, bubble exchange factor, bubble inception at the distributor, the design of the distributor, entry zone effect, particle velocity and the overall particle circulation) on the bed performance.

7-3 THEORETICAL CONSIDERATION IN FLUIDISED BED DRYING MODELLING

To consider the theoretical aspects of fluid bed drying, we shall discuss the model of Hoebink and Rietema (1973), which is the only bubbling model in the literature analysing solids drying in fluidised bed.

The model is based on the two-phase theory, and the dense-phase gas is assumed to be in perfect mixing and in equilibrium conditions with the moist particles, hence its humidity is Y^* . The bubble rising in the bed is surrounded by a cloud of radius R_c (where $\alpha > 1$), and the bubble gas is assumed to be perfectly mixed and at humidity Y_b which depends on the bubbles position in the bed. The gas in the cloud is assumed to be in plug flow and leaves the bubble at the top with humidity Y_b and re-enters it at the bottom with humidity Y_{in}. They assumed that moisture transfer to bubbles occurs via diffusion from dense-phase gas to the bubble cloud as well as by the direct drying of solids descending through the cloud.

The model predicts that the bubble gas will also have an equilibrium humidity Y^* , and hence the overall gas leaves the bed with equilibrium humidity Y^* regardless of the moisture content of solids in the bed.

The attempt of Hoebink and Rietema (1973) to characterise fluid bed drying by a single-parameter bubble model did however show disagreement with their experimental results.

To discuss the reasons for the large deviation between the model and their experimental results, first, consider some limitations in the model for the bubbling bed: the model does not consider the effect of bubble coalescence in the bed which can overestimate the bubble mass transfer coefficient in their calculations as shown by Chavarie and Grace (1976). The assumption that moisture transfer from solids is limited to a part of the cloud ($\frac{\pi}{4} < \theta < 3\frac{\pi}{4}$) ignores the large effect of direct drying of solids in the bubble wake which represents around ($\frac{1}{3}$) of the bubble volume. The assumption that diffusive transfer between the bubble and cloud can be ignored, represents a serious error for fine particles where the diffusive term is the major contributor to the total transfer especially at higher temperatures where moisture diffusivity doubles in value.

Considering now the drying model: the assumption that the bed can be trated as an isothermal dryer is strictly incorrect as shown earlier in figures (4-1) and (4-2), and hence ignoring the entry zone effect where the simultaneous heat and moisture transfer occurs, as shown in chapters(4) and (5), can produce misleading results.

Their experiments showed much lower values of humidity for the gas leaving the bed than the predicted equilibrium values, which can be explained by ther relative unimportance of the bubble exchange in the bed compared with the direct drying of solids by simultaneous heat and moisture

transfer in the entry zone and which they ignored in the model.

7-4 MODEL FOR SIMULTANEOUS HEAT AND MASS TRANSFER

The model disaussed here for shallow fluidised bed drying is based on two major observations: first, the dramatic temperature drop of the gas entering the bed when it contacts the cold moist particles, which results from the simultaneous heat and mass transfer occuring in the entry zone. Secondly, we showed in chapter (5) that the mass transfer coefficient $K_{g/p}$ is low;resulting in a larger height of transfer unit between particles and dense-phase gas than the one between the segregated phases, which suggests that bubbles are of relative insignificance compared with the simultaneous heat and mass transfer in the entry zone.

Based on those two observations, a simple model is proposed, to take into account the entry zone effect on the dryer performance, in which the fluidised bed dryer is assumed to consist of two sections: an entry zone, where the drying is governed by simultaneous heat and mass transfer, and the bubbles if they exist at all, are extremely small, and hence the bubbles' role in mass transfer can be ignored within this section, and the top section, where the bed is isothermal and hence bubbles are expected to have a role in moisture transfer within this zone.

A - Entry Zone $(0 < Z < \zeta)$

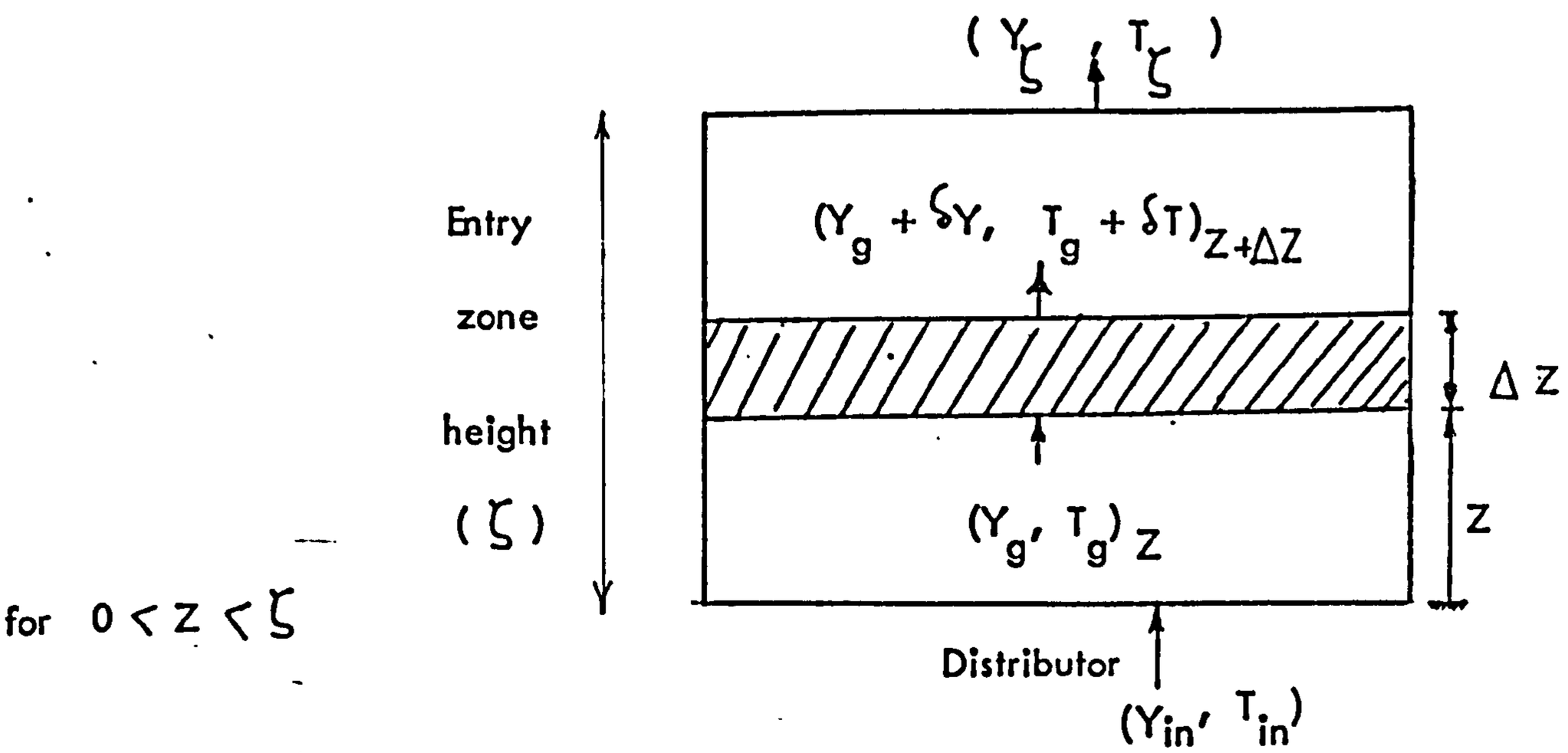
In this section, the gas temperature drops dramatically within the first few centimeters, ζ , above the distributor and the height of this entry zone

dpends on the experimental details and on the distributor design. In this zone the following assumptions are made:

1- No stable bubbles are established and hence the gas can be treated as a single homogeneous phase passing in plug flow.

2- Both conductive heat transfer from the distributor to solids and heat losses through the wall are negligible compared with the convective heat transferred from gas to solids.

Since the process is controlled by simultaneous heat and mass transfer within this region, a unsteady state differential energy balance can be written, for a gas plug, in the following form:



for $0 < Z < \zeta$

$$A \varepsilon \rho_g C_g \frac{\partial T_g}{\partial t} = - A \varepsilon U \rho_g C_g \frac{\partial T_g}{\partial Z} + A \varepsilon U \rho_g (\Delta H)_{vap} \frac{\partial Y_g}{\partial Z} - d q_s \qquad (7\text{-}1)$$

Assuming quasi- steady state solution ($\frac{\partial T_g}{\partial t}$ is negligible), equation (7-1) gives, at any height Z above the distributor ($0 < Z < \zeta$), the following relation:

$$C_g (T_{in} - T_g) = (\Delta H)_{vap} (Y_g - Y_{in}) + \frac{Q_s}{G} \qquad (7\text{-}2)$$

where

C_g:	gas specific heat capacity	$(\frac{cal}{gm \cdot {}^oC})$
T_{in}:	Inlet gas temperature above the distributor	$({}^oC)$
T_g :	gas temperature at theight Z	$({}^oC)$
$(\Delta H)_{vap}$:	latent heat of vaporisation	$(\frac{cal}{gm})$
Y_g :	gas humidity at height Z	$(\frac{gm\ Water}{gm\ Air})$
Y_{in} :	gas inlet humidity	$(\frac{gm\ Water}{gm\ Air})$
G :	air mass flow rate	(gm Air / S)
Q_s:	heat transfer rate to solids $= h_{g/p} \bar{A} \int_0^z (T_g - T)dz$	(cal/S)
T_o:	air temperature at the outlet of the bed	$({}^oC)$

At any time (t), by measuring: the inlet gas conditions (T_{in}, Y_{in}) as well as gas and solids temperatures at theight Z cm above the distributor (T_g, $T_s)_Z$, and using a measured value for $h_{g/p}$, equation (7-2) can be used to compute the corresponding gas humidity $(Y_g)_Z$ at this moment of time and at that specific height Z ($0 < Z < \zeta$), and hence the gas humidity curves cam be computed over the entry zone (as shown in Appendix (7))

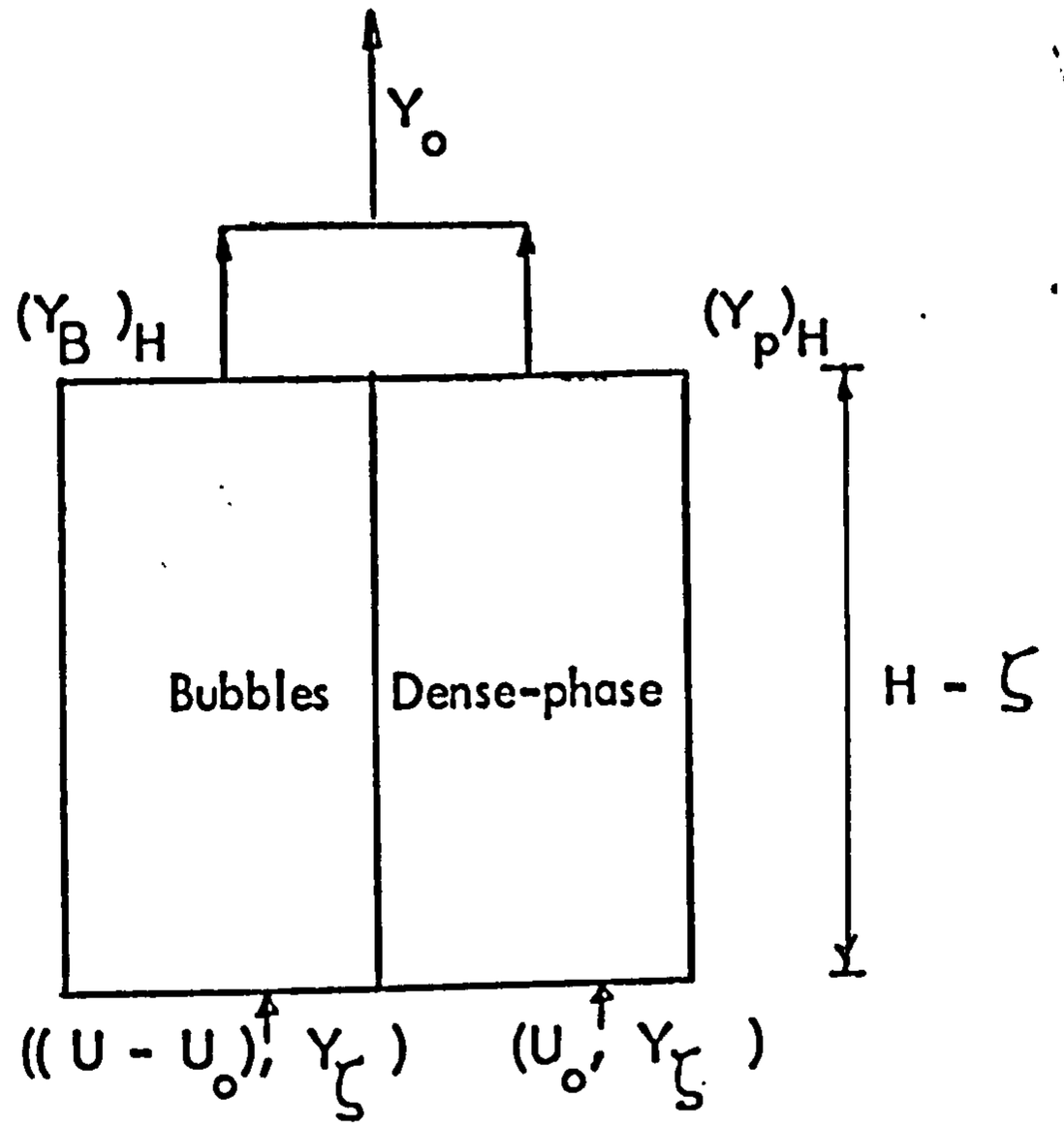
The gas humidity at the top of the entry zone Y_ζ , can be calculated from equation (7-2) at any time (t) to give:

$$Y_\zeta = Y_{in} + \frac{C_g}{\Delta H}(T_{in} - T_\zeta) - \frac{(Q_s)_\zeta}{G \cdot \Delta H} \qquad (7\text{-}2\text{-}a)$$

Since the rest of the bed is isothermal (i.e. $T_\zeta = T_o$), equation (7-2-a) can be written as:

$$Y_\zeta = Y_{in} + \frac{C_g}{\Delta H}(T_{in} - T_0) - \frac{(Q_s)_\zeta}{G \cdot \Delta H} \qquad (7\text{-}3)$$

B- Top Section ($\zeta < Z < H$)



In this region, it is assumed that:

1- The gas at the top of the entry zone with humidity Y_ζ , is assumed to be divided into dense phase gas and bubbles, following the two-phase theory.

2- The bubbles established are assumed to have a constant equivalent diameter D_c , and the bubble distribution is assumed to be uniform

over the whole top section.

3- Since the top section of the bed is isothermal, particles to dense-phase moisture transfer is controlled by diffusion, while the dense-phase to bubbles moisture transfer can be described by Davidson and Harrison's model (1963), where diffusion and convection are additive.

4- Particles are assumed to be perfectly mixed and have an average moisture content X, since the temperature is constant within this region, theequilibrium air-humidity at the particle surface Y^* is constant for the whole top section.

A detailed description of the different models describing the top section of fluidised bed dryer and based on the same analysis of Davidson and Harrison, is shown in Appendix (8).

In the first model, where the dense phase gas is assumed to be perfectly mixed, the bed performance η(the ratio between the outlet air humidity Y_o and the air equilibrium humidity at the particle surface Y^*) can be represented in the following form:

$$\eta = 1 - \beta_1 \left(1 - \frac{Y_\zeta}{Y^*} \right) \qquad (7\text{-}4)$$

where

$$\beta_1 = 1 - \frac{K_{g/p} \bar{A} \left(1 - \left(\frac{U - U_o}{U} \right) e^{-X} \right)}{K_{g/p} \bar{A} + U_o + (U - U_o)\left(1 - e^{-X} \right)} \qquad (7\text{-}5)$$

$K_{g/p}$: gas to particle mass transfer coefficient (cm/s)

$\bar{A}$: particles surface area per unit cross sectional area of the bed (cm^2/cm^2)

U : gas superficial velocity (cm/s)

X : bubble exchange factor $\left(\frac{Q}{V} \cdot \frac{H'}{U_A}\right)$

H' : top section height $(H - \zeta)$ (cm)

Y_ζ : air humidity at the top of entry zone given by equation (7-3) $\left(\frac{\text{gm Water}}{\text{Kg Air}}\right)$

In the second model, where the dense-phase gas is assumed to be in plug flow, the dryer performance can be represented by:

$$\eta = 1 - \beta_2 \left(1 - \frac{Y_\zeta}{Y^*}\right) \qquad (7\text{-}6)$$

where

$$\beta_2 = \left(\frac{-m_2}{m_1 - m_2}\right)\left(1 - \frac{U_o \quad m_1 \quad H'}{U \qquad X}\right) e^{-m_1 H'}$$

$$- \quad + \quad \left(\frac{m_1}{m_1 - m_2}\right)\left(1 - \frac{U_o \quad m_2 \quad H'}{U \qquad X}\right) e^{-m_2 H'} \qquad (7\text{-}7)$$

$$\begin{matrix} m_1 \\ m_2 \end{matrix} = \frac{+A_2 \pm \sqrt{A_2^2 - 4 A_1 A_3}}{2 A_1}$$

$$A_1 = \frac{U_o \quad H'}{X}$$

$$A_2 = U + \frac{K_{g/p} \quad \overline{A} \quad H'}{X}$$

$$A_3 = K_{g/p} \quad \overline{A}$$

X : bubble exchange factor $\left(\frac{Q}{V} \cdot \frac{H'}{U_A}\right)$

H' : top section height $(H - \zeta)$ (cm)

Y_ζ : air humidity at the top of entry zone given by equation (7-3) $\left(\frac{\text{gm Water}}{\text{Kg Air}}\right)$

In the second model, where the dense-phase gas is assumed to be in plug flow, the dryer performance can be represented by:

$$\eta = 1 - \beta_2 \left(1 - \frac{Y_\zeta}{Y^*}\right) \qquad (7\text{-}6)$$

where

$$\beta_2 = \left(\frac{-m_2}{m_1 - m_2}\right)\left(1 - \frac{U_o}{U}\frac{m_1 H'}{X}\right) e^{-m_1 H'}$$

$$- + \left(\frac{m_1}{m_1 - m_2}\right)\left(1 - \frac{U_o}{U}\frac{m_2 H'}{X}\right) e^{-m_2 H'} \qquad (7\text{-}7)$$

$$\frac{m_1}{m_2} = \frac{+A_2 \pm \sqrt{A_2^2 - 4 A_1 A_3}}{2 A_1}$$

$$A_1 = \frac{U_o H'}{X}$$

$$A_2 = U + \frac{K_{g/p} \overline{A} H'}{X}$$

$$A_3 = K_{g/p} \overline{A}$$

From both equations (7-4) and (7-6), the general form of fluidised bed dryer performance can be represented by:

$$\eta = 1 - \beta \left(1 - \frac{Y_\zeta}{Y^*} \right) \qquad (7\text{-}8)$$

where

$$(0 < \beta < 1)$$

From the general equation (7-8), the dryer performance is characterised by two factors, first, the entry zone effect which is represented by (Y_ζ / Y^*) and is governed by simultaneous mass and heat transfer; secondly, the bubbling effect represented by the factor (β) and which determines the relative importance of the bubbles.

For very low values of β ($<<1$), equation (7-8) predicts a higher outlet air hunidity Y_o ,which means that the bubbles improve the drying of solids at the top section of the bed, on the other hand, for higher values of β (~ 1): equation (7-8) predicts that the outlet air humidity Y_o will be equal to Y_ζ which shows the insignificant role of bubbles in the bed.

7-5 EXPERIMENTAL STUDY ON BED PERFORMANCE

Two groups of experiments were run in the cylindrical bed: first, to examine the model proposed earlier in section (7-4); secondly, to study the effect of bed height on the dryer performance and hence to examine the entry zone effect.

In the first group of experiments, three different batches of silica gel were dried (106, 940 and 2247 microns). The air humidity at inlet and outlet was measured by a "Shaw" hygrometer, while gas and solids temperatures were measured at 0.5, 1, 2, 5 and 10 cm above the distributor. Solids moisture content was measured by sampling during the drying period.All the measurements were carried out at constant time intervals of 10 minutes. The following table summarizes the different operating conditions during those experiments:

Table (7-1)

Experimental Group (1)

Group	Particle diameter dp (microns)	Minimum fluidising velocity U_o (cm/s)	Average air temperature T_{in} (°C)	Initial bed height H_o (cm)	Air flow rate Q (l/min)	Superficial air velocity U (cm/s)
1	106	12.8	50	10	90	20
		12.8	50	10	150	31.8
		12.8	50	10	275	58.3
2	940	30	50	10	200	40
		30	50	10	275	58.3
		30	50	10	500	106
3	2247	58	50	10	325	68.9
		58	50	10	375	80
		58	50	10	500	106

In the second group of experiments, the humidity of the air leaving the bed with heights of 1, 2, 3, 4, 5 and 10 cms for the three silica gel batches were measured at incipient fluidisation conditions.

7-6 RESULTS

A- Entry Zone

The entry zone height ζ is measured experimentally from two independent experiments: first, by measuring the gas temperature in the bed as shown in a typical figure (4-1); secondly, by measuring the humidity of air leaving the bed at different heights as shown in figure (7-19). Both results are in good agreement showing an average value of ζ around 2 cm above the distributor. Other workers studying entry zone effects reported different results for the height (e.g. in Kettenring et al (1950) $\zeta = 5$ cm, Heertjes et al (1953) $\zeta = 1$ cm, Richardson and Szekely (1961) $\zeta = 2$ mm and in Yates and Constans (1973) $\zeta < 5$ cm). From all these different results, it is clear that the entry zone height depends largely on the distributor design which supports the earlier work of Walker (1975) on the importance of distributor design.

The sensitivity of the bed performance η to the entry zone height can be seen from equations (7-8 and 7-3). It will be seen that the height "ζ" enters directly only in the term representing the heat transfer rate from gas to solids, Q_s ; and hence in gas/solid systems with low heat transfer coefficients, the entry zone height will often be irrelevant to the overall bed performance.

B- Comparison with Model

The experimental values of bed performance η from the different nine

experiments (table 7-1) are shown in figures (7-1 to 7-9). At constant time intervals of 10 minutes, inlet and outlet air humidities were measured directly (Y_{in} and Y_{out}), solids moisture content (X) was measured and hence the equilibrium air humidity at the particle surface (Y^*) was calculated using the hygrothermal equilibrium curve for silica gel; air and solids temperatures were measured at different points in the bed and hence (Y_ζ) was calculated. By plotting the experimental values of η versus ($1 - Y_\zeta / Y^*$), a good agreement between the different results and the theory is obtained as shown in figures (7-1 to 7-9).

The general model proposed earlier (equation 7-8) predicts a linear relationship between η and ($1 - Y_\zeta / Y^*$) with a slope ($-\beta$) which depends on the flow pattern in the dense-phase gas. Calculating the factor (β) in both cases of the dense-phase gas - i.e. perfectly mixed or plug flow - using equations (7-5) and (7-7) and using the measured values of $K_{g/p}$, $\bar{A}$, U and U_o for the different experiments and using an average bubble diameter of 1 cm estimated by observing the bubble at the top of the bed, gives predicted values of (β) very close to 1 ($\beta = 0.998$); moreover the results show very little sensitivity to the estimated bubble diameter D_e .

Plotting the predicted bed performance in figures (7-1 to 7-9) gives a very good fit to the experimental data points. The results obtained show the insignificance of the bubbles in these experiments on fluidised bed drying where the process is governed by simultaneous heat and mass transfer in the entry zone of the bed.

Figures (7-10 to 7-18) show the measured values of the humidity of the air leaving the bed as a function of time during batch drying. The predicted values from the model show a general agreement with the experiments; the deviation between them can be explained as a result of the assumption of quasi-steady state conditions during the drying period which is not strictly true in batch drying.

C- Effect of Air Flow Rate on "η"

The effect of air flow rate on bed performance is shown in figures (7-21, 7-22 and 7-23). For the three different particle size groups, increasing the air flow rate decreases the relative humidity of the air coming out of the bed. This effect can be related to the decrease in air residence time in the bed, and hence a decrease in the bed performance as a humidifier and an increase in the bed performance as a dryer is expected.

D- Effect of Bed Height on "η"

The maximum relative humidity achieved by the air leaving the fluidised bed dryer is shown for the three different groups (106, 940 and 2247 microns), in figure (7-19).

Each curve represents six individual experiments starting from one centimeter high up to ten centimeters. The results show the significance of solids drying in shallow beds since the air humidity hardly changes after the first two centimeters. These results support the earlier ones on the air humidity profiles which are discussed in chapter (5).

All the results obtained from the different experiments are consistent with the model discussed earlier in section (7-4). The relative unimportance of the bubbles in these experiments show that the major factor contributing for moisture transfer in the fluidised bed drying is the simultaneous heat and mass transfer occuring in the entry zone of the bed. The statement that bubble interchange is unimportant does not lessen the bubble role in producing solids mixing and the uniform thermal properties of the bed.

CHAPTER (8)

DISCUSSION AND CONCLUSIONS

For convenience, the discussion covers the different aspects discussed in previous chapters in the order: minimum fluidising velocity, entry zone effect, analogy between heat and mass transfer, solids drying rate and modelling of fluidised bed dryer. The general implication of the results is then discussed.

8-1 MINIMUM FLUIDISING VELOCITY

The variation in minimum fluidising velocity with solids moisture content, discussed in chapter (3), is explained satisfactorily in the light of the role of inter-particle forces in the bed and their dependance on solids moisture content.

A typical experimental result shows that in the early stages of drying the minimum fluidising velocity U^* decreases rapidly with the decrease in solids moisture content until it reaches a critical value X_{cr}, dependant on the particle size dp, after which there is a slight decrease in U^* with solids moisture content until it reaches a constant value U_o corresponding to bone dry solids.

The agglomeration model proposed in chapter (3) is based on the assumption that at higher values of solids moisture content ($X > X_{cr}$), the

bed is composed of spherical agglomerates in which particles are held together mainly because of surface tension forces.

During drying, when the solids moisture content drops to a critical value X_{cr} , the surface tension forces are no longer strong enough to resist the hydrodynamic force and hence the agglomerate breaks; then in the lower range of solids moisture content ($X < X_{cr}$), the variation in the minimum fluidising velocity is a direct result of the variation of particle density withs solids moisture content.

Using the experimental results obtained from 106 microns silica gel particles, the model predicts an average agglomerate size of 660-880 microns. It is clear that at higher values of solids moisture content ($X > X_{cr}$) the model can be applied to both hygroscopic and non-hygroscopic materials, and hence the results obtained earlier by Vanecek et al (1967), for the variation of minimum fluidising velocity of the wet sand, can be explained in the light of the agglomeration model.

Considering the case where only two particles agglomerate, and assuming that the moisture penetrates only a distance Δ from the surface of the particle, the model predicts a decrease in the critical moisture content X_{cr} with increasing particle diameter dp . The experimental results obtained from the three available silica gel batches (106, 440 and 2247 microns) showed a qualitative agreement with the model.

Further work is recommended in this area to develop a general model where n-particles agglomerate together and hence the effect of neighbouring

particles on the critical moisture content (X_{cr}) cannot be ignored. Such a model will also have to develop a more realistic picture for the fluid motion in and around the agglomerate. I t is also suggested that a parallel experimental approach to the problem should be carried out to study the effect of liquid penetration in particle surfaces on the behaviour of agglomerates in fluidised beds.

8-2 ENTRY ZONE EFFECT

The experimental results on the air temperature profile in fluidised bed drying, discussed in chapter (4), showed a dramatic temperature drop over the first few centimeters above the distributor. The entry zone effect in fluidised beds is well known in the literature and depends strongly on the distributor design.

Our experimental results on gas to particle heat transfer in fluidised bed drying, discussed in chapter (4), showed that the process is dominated by the entry zone, where the driving force for heat transfer ($T_g - T_s$) is very large compared with the conditions in the rest of the bed. This result supports the earlier work of Heertjes and McKibbins (1956), Kettenring et al (1950) and Heertjes (1962); although their measured gas temperatures were in fact average bed temperatures.

The results discussed in chapter (5), for mass transfer in fluidised bed drying, showed that the controlling step in the process lies in the resistance to transfer between particles and gas, which occurs mainly in the entry zone

of the bed as a result of simultaneous heat and moisture transfer. This can explain the earlier concentration profiles in the bed measured by other workers (e.g. Heertjes et al 1953, Richardson and Szekely 1961 and Yates and Constans 1973) which showed that all the transfer takes place within the first few centimeters above the distributor.

Now it is clear that the entry zone effect, which is a direct result of the distributor design, plugs its role in most processes where there is an interaction between heat and mass transfer in the bed.

It is recommended that the effect of the distributor design on the overall fluidised bed performance should be studied in much more quantitative detail following the preliminary evidence of Walker (1975) on its importance.

8-3 ANALOGY BETWEEN HEAT AND MASS TRANSFER IN FLUIDISED BED DRYING

The effect of different operating parameters on both overall gas to particle heat and mass transfer coefficients are discussed in chapters (4) and (5). From the experimental results it is clear that the two factors affecting both $\bar{h}_{g/p}$ and $\bar{K}_{g/p}$ during the constant rate period are the air velocity and particle diameter. Increasing either the air velocity or the particle diameter improves both the gas to particle heat and mass transfer coefficients, although the effect of air velocity on both coefficients is much stronger than the particle diameter.

An average correlation of overall gas to particle heat transfer coefficient, for the three different particle sizes, shows that the Nusselt number is proportional

to $Re^{1.3}$ which agrees with the results obtained from the mass transfer studies (chapter 5) that the Sherwood number is proportional to Reynolds'number raised to the same power. The results obtained earlier by Sen Gupta and Thodos (1963) which showed the ratio between heat and mass transfer factors is nearly 1 for distended beds, suggest that:in cases where bubbles are relatively unimportant in mass transfer,the distended bed may produce similar results for the fluidised bed.

Since the resistance to transfer lies in the step between gas and particle as discussed in chapter (5), the analogy between heat and mass transfer in the bed can be explained by a laminer layer model where heat transfer is controlled by conduction through a thin layer of fluid around the particle while the corresponding moisture transfer occurs by diffusion in the opposite direction. Most of our results on both $\bar{h}_{g/p}$ and $\bar{K}_{g/p}$ agree with the revised data in literature as shown in chapters (4) and (5).

8-4 SOLIDS DRYING RATE

This work reports the first data on the effect of different parameters on solids drying rate in shallow fluidised bed.

The overall effect of air flow rate on the drying rate of solids, as discussed in chapter (6), shows that increasing the air velocity improves the drying rate as a direct result of the increase in particle to gas mass transfer coefficient. The slight increase in the drying rate of solids with increasing

particle diameter can be explained from the effect of particle size on the overall gas-to-particle mass transfer coefficient. The strong influence of air temperature and thermal properties on the drying rate of solids proves that, during the constant-rate period, solids drying in fluidised bed is governed by simultaneous heat and mass transfer.

The decrease in solids drying rate with increasing bed height may be explained as a result of the entry zone effect in the bed, where most of the heat and mass transfer occurs; consequently the drying of solids takes place within this very shallow zone, and as a result of that, increasing the bed height while the potential zone for drying is constant, decreases the overall dryer performance as shown from the experiments.

8-5 FLUIDISED BED DRYER MODEL

The model proposed earlier in chapter (7) is based on our experimental observation for the entry zone effect in fluidised bed drying. The model takes into account both simultaneous heat and mass transfer occuring above the distributor and the bubble exchange with the dense-phase gas above the entry zone. In this model it is assumed that gas passing through the entry zone is one homogeneous phase in plug flow, while the bubbles are only established above the entry zone. Using a quasi steady-state solution for the gas in the entry zone and following the same analysis of Davidson and Harrison (1963) for a single-parameter bubbling two-phase model in the top section of the bed, the dryer performance is expressed in the following general form:

$$\eta = 1 - \beta\left(1 - \frac{Y\zeta}{Y^*}\right)$$

where the bubbling effect (β) depends on the flow pattern in the dense-phase gas and is given by equations (7-5) and (7-7). The height of the entry zone ζ depends on the distributor design as shown by different workers (e.g. Kettenring et al 1950, Heertjes et al 1953, Richardson and Szekely 1961, Yates and Constans 1973).

The predicted value of the factor (β) based on our experimental conditions gives a good fit to the experimental results of the bed performance , and shows the relative unimportance of the bubbles on the dryer performance during these experiments; nevertheless these results do not lessen the significant bubble role in solids mixing and uniform thermal properties in the bed during the drying period.

8-6 IMPLICATIONS

From the different results discussed earlier, it is clear that the entry zone effect in fluidised bed generally plays an important role in determining the bed performance. In special cases where there is an interaction between heat and mass transfer in the bed, the effect of the entry zone may govern the process, and the results obtained by different workers (e.g. Heertjes at al (1953) in evaporating water to air, Richardson and Bakhtiar (1955) in adsorption of iso-octane and tolune vapour on silica-aluminium catalyst, Yates and Constans

(1967) in isomerization of butene-1 to butene-2) show typical examples of the significance of the entry zone effect on the bed performance.

On the other hand, it is important to realise that any model describing fluidised bed dryer which ignores the entry zone effect can be in error, as discussed in chapter (7), for Hoebink and Rietema's (1973) model where their experiments showed a large deviation from the model.

Fluidised bed has proved to be an efficient tool for drying solids, especially for powders where the drying rate improves rapidly with air flow rate. The cylindrical bed can be operated under a wide range of operating conditions of air flow rate, temperature, particle size and bed height and showed satisfactory results, as discussed in chapter (6). shallow fluidised beds are recommended for drying of fine particles.

As a result of drying experiments, it is suggested that the designer of fluidised bed dryer should consider carefully the effect of the distributor design on the dryer performance and more research is required in the area of the influence of distributor design on the bed performance.

From the different highlighted areas in this work, it is important to realise that the lack of data in different aspects in fluidised bed - such as: particles agglomeration in fluidised bed, the entry zone effect, the significance of the distributor design, particles mixing, the bubble role in heat transfer, incipition of bubbles at the distributor and the variation in bubble diameter and distribution in the bed - represent a continuous challenge to workers in the field.

FIGURES (2)

EQUIPMENT

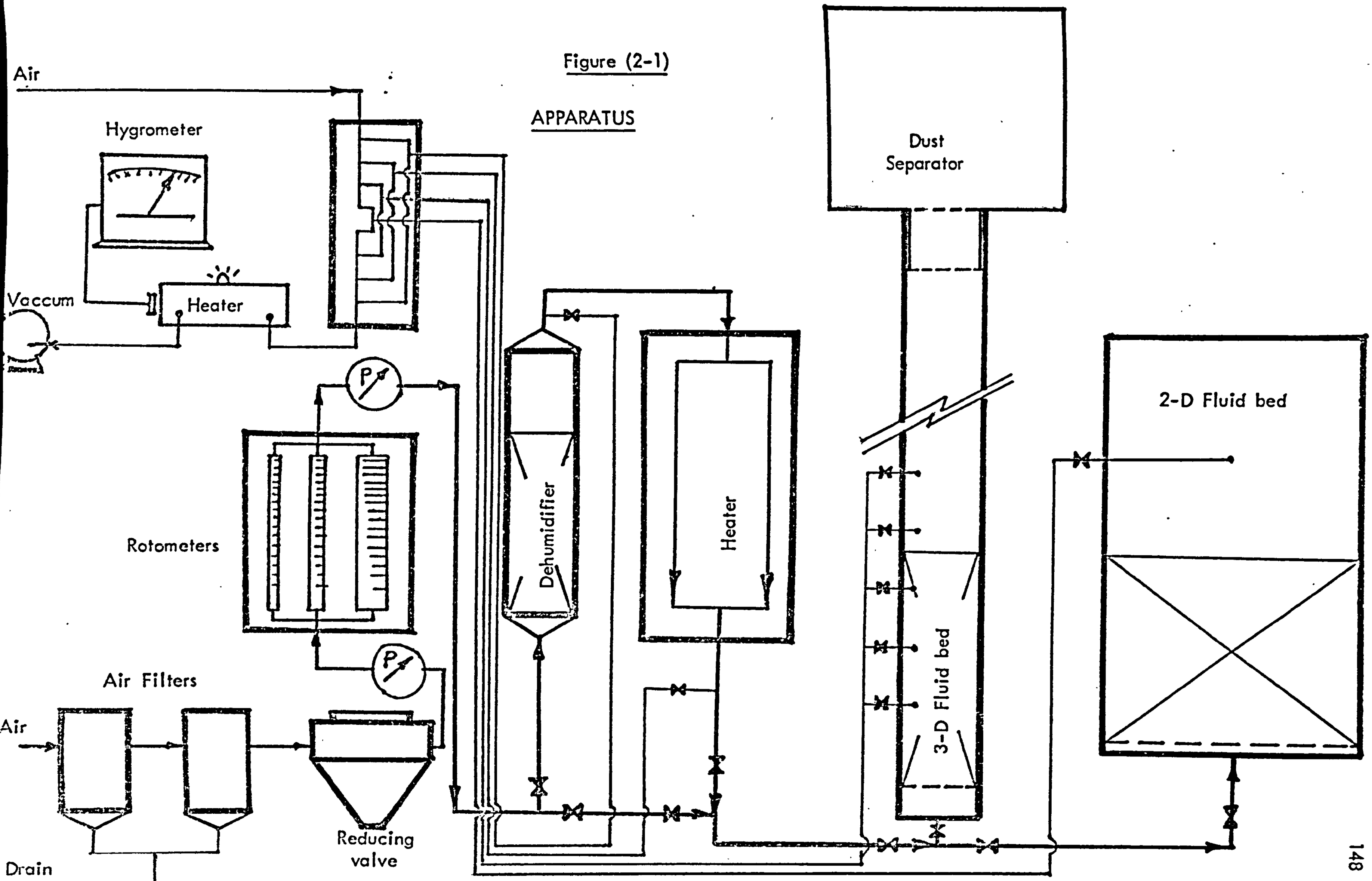
Figure (2-1) APPARATUS

Figure (2-2) TEMPERATURE CONTROLLER WIRING

Figure (2-3) HUMIDITY MEASUREMENT

Figure (2-1)

APPARATUS



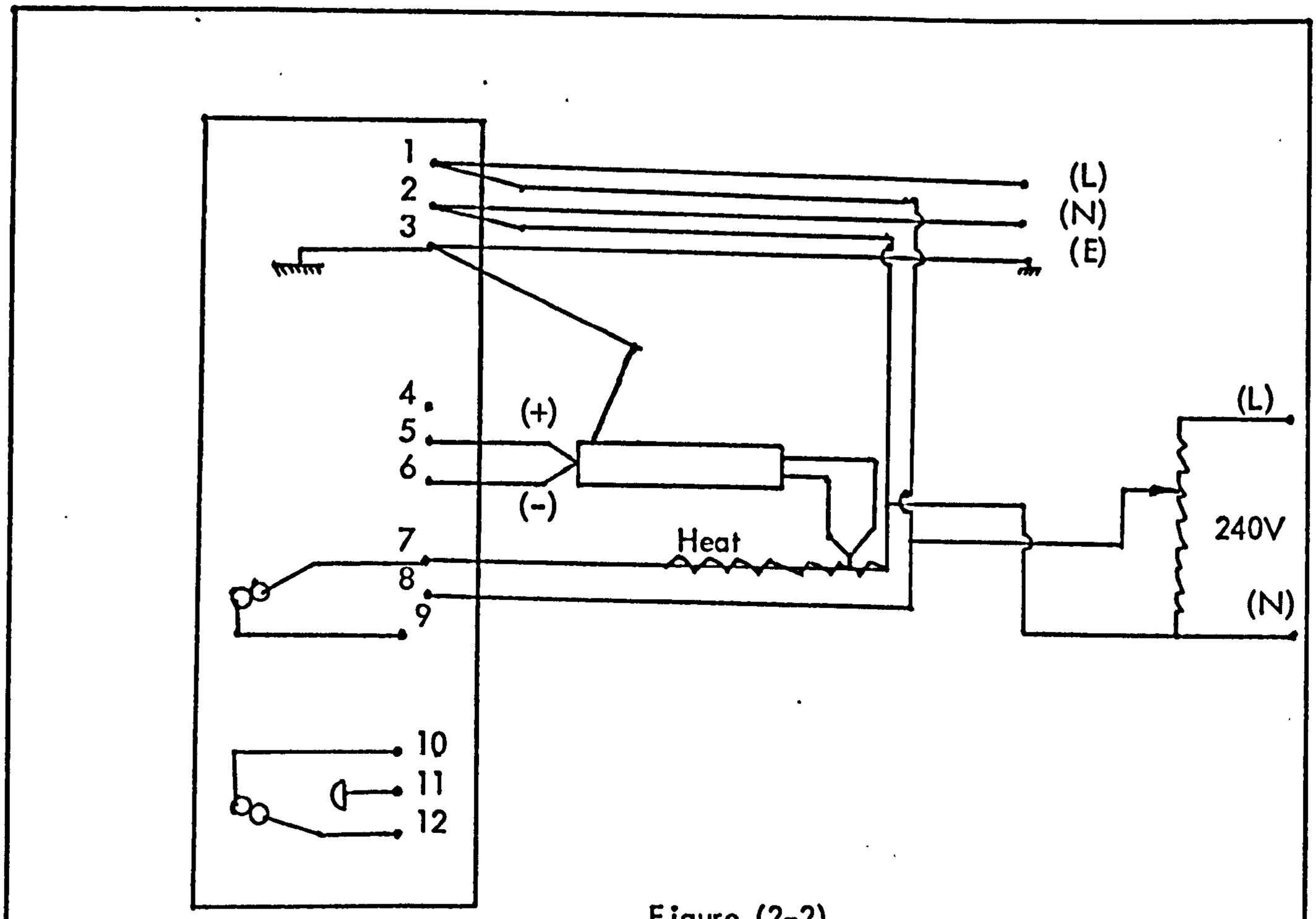


Figure (2-2)

Temperature Controller Wiring

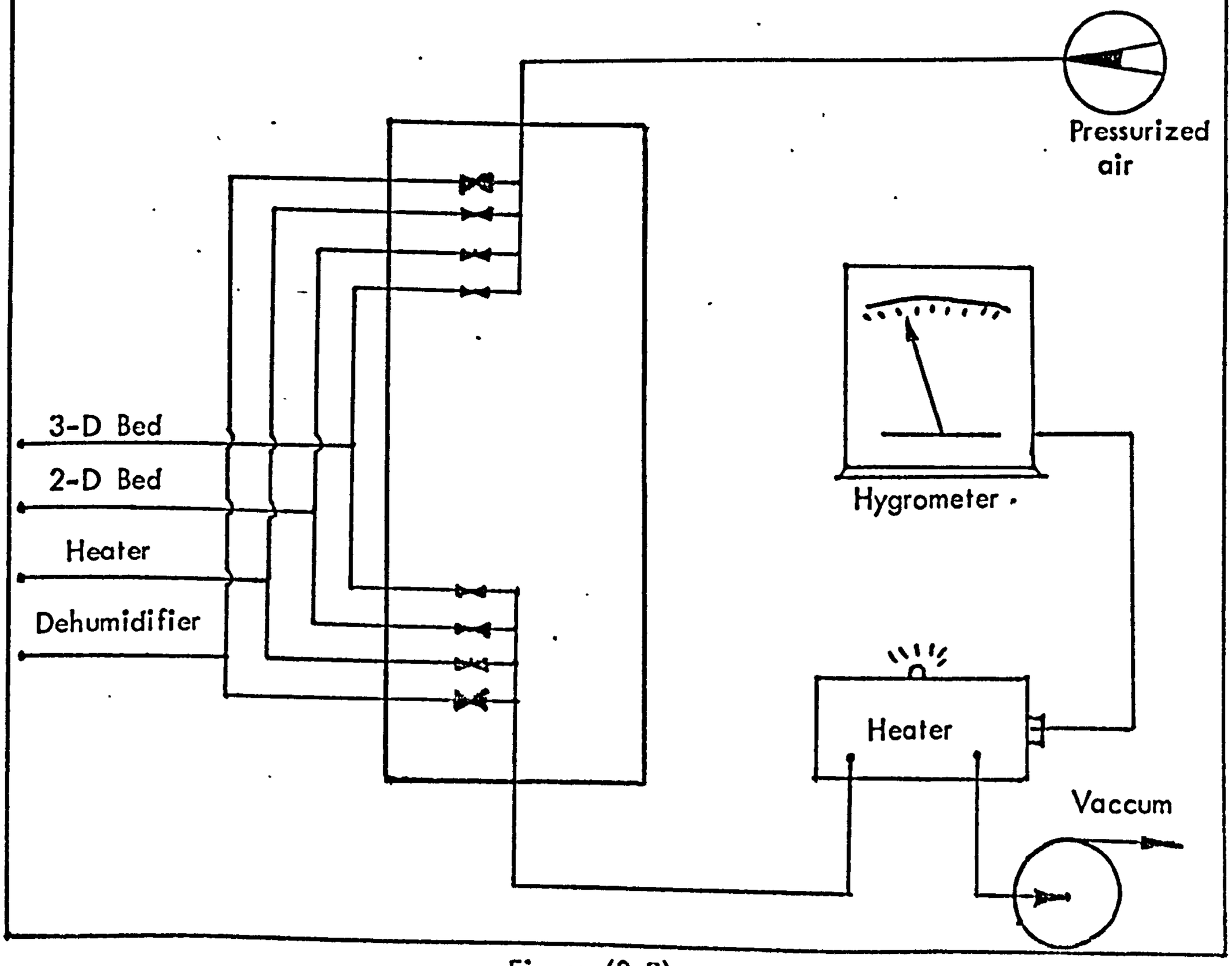


Figure (2-3)

Air Humidity Measurement

FIGURES (3)

"MINIMUM FLUIDISING VELOCITY"

Figure (3-1 a) Cohesive Forces between Particles

Figure (3-1 b) Size and Accumulative Distribution Functions

Figure (3-2) Hydrodynamic Forces on two Spheres

Figure (3-3) Agglomeration Model

Figure (3-4) (U^*) vs. (X) At 40°C

Figure (3-5) (U^*) vs. (X) At 60°C

Figure (3-6) (U^*) vs. (X) At 80°C

Figure (3-7) Agglomeration Model Results - At 40°C

Figure (3-8) Agglomeration Model Results - At 60°C

Figure (3-9) Agglomeration Model Results - At 80°C

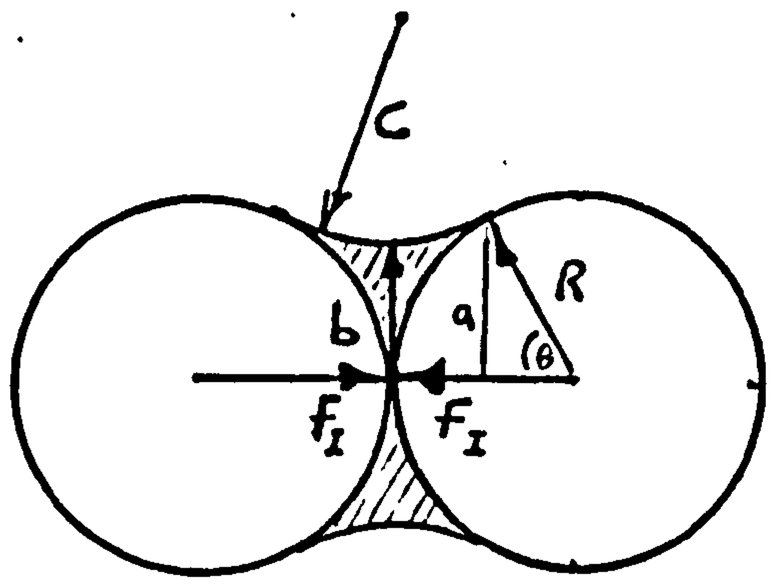


Figure (3.1-a)

Cohesive Forces between two Particles

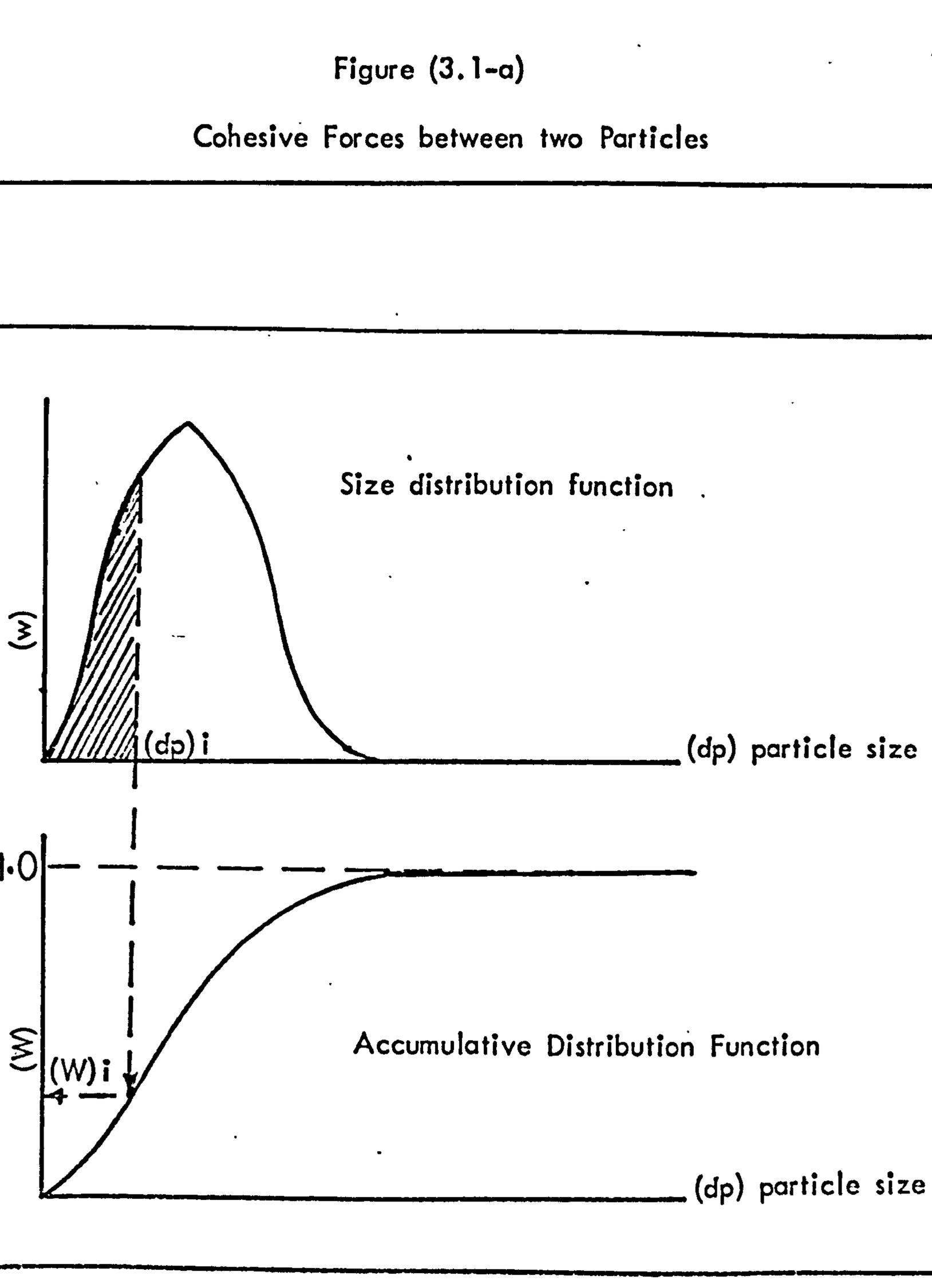


Figure (3-1-b)

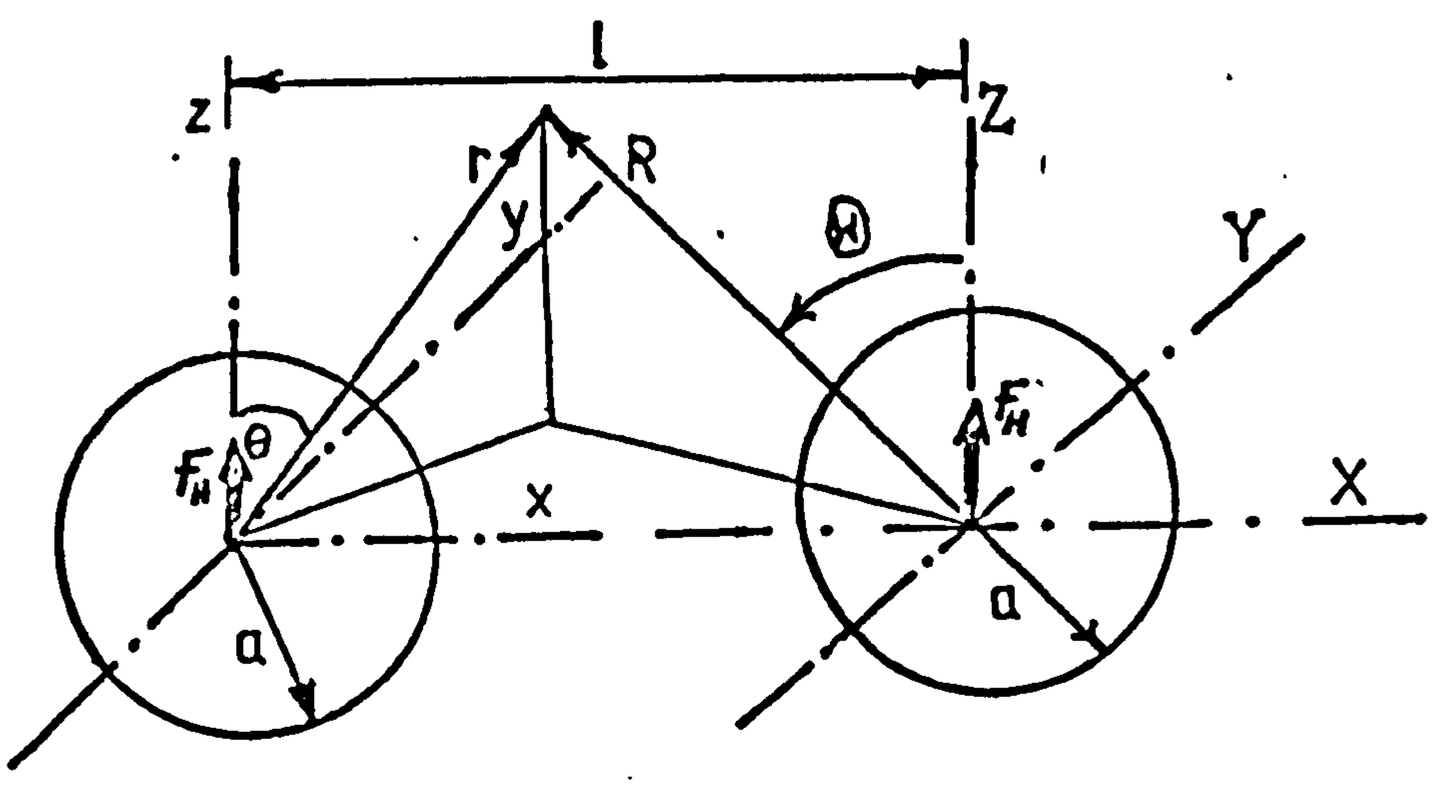


Figure (3-2)

Hydro dynamic Forces

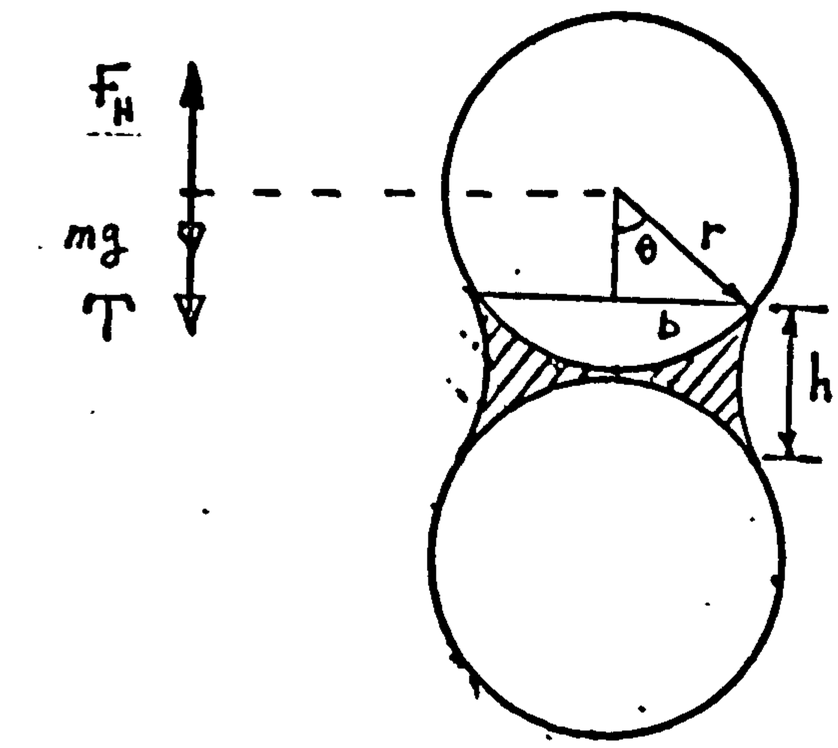


Figure (3-3)

Agglomeration Model

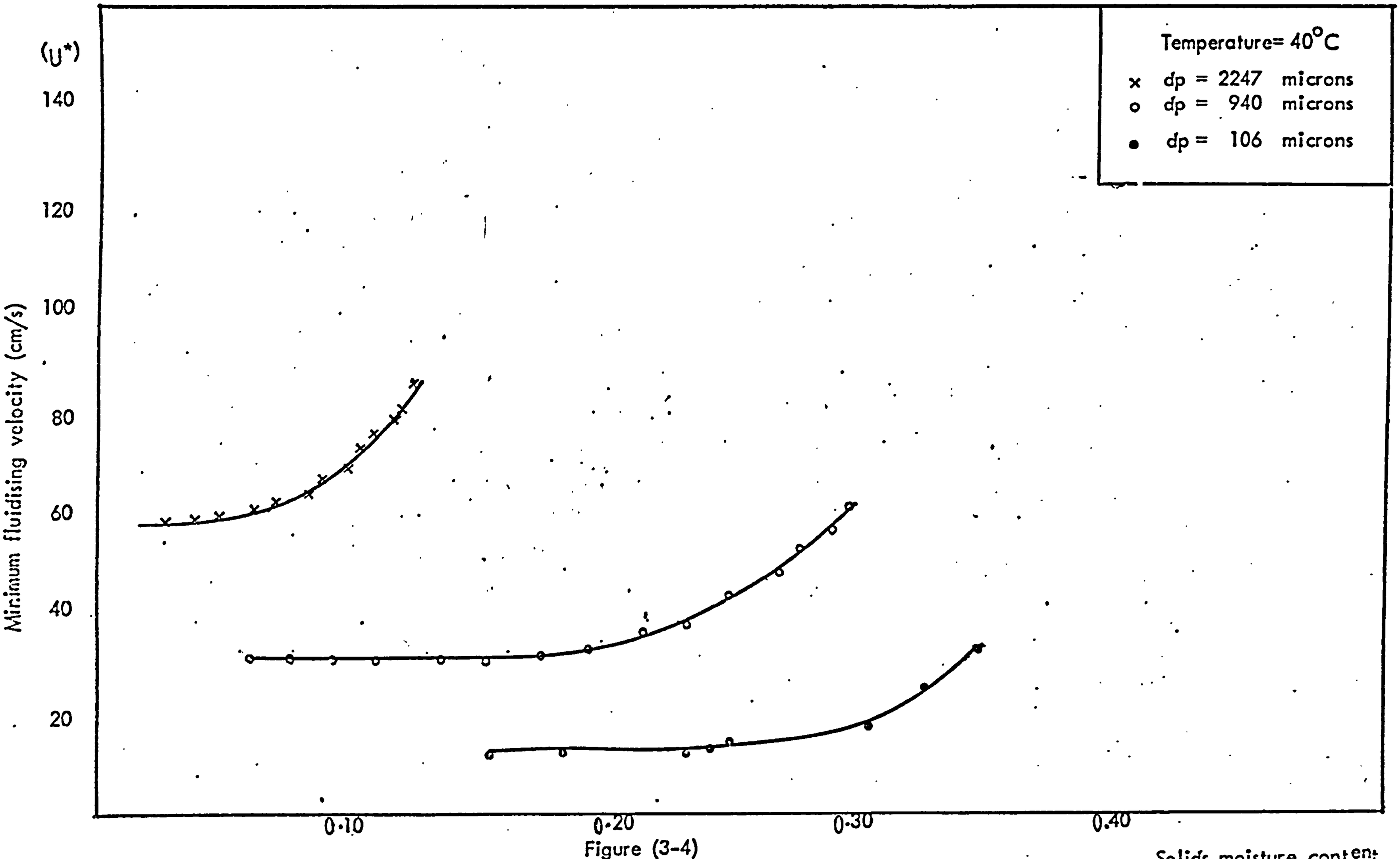


Figure (3-4)

(U*) Versus (X)- AT 40°C

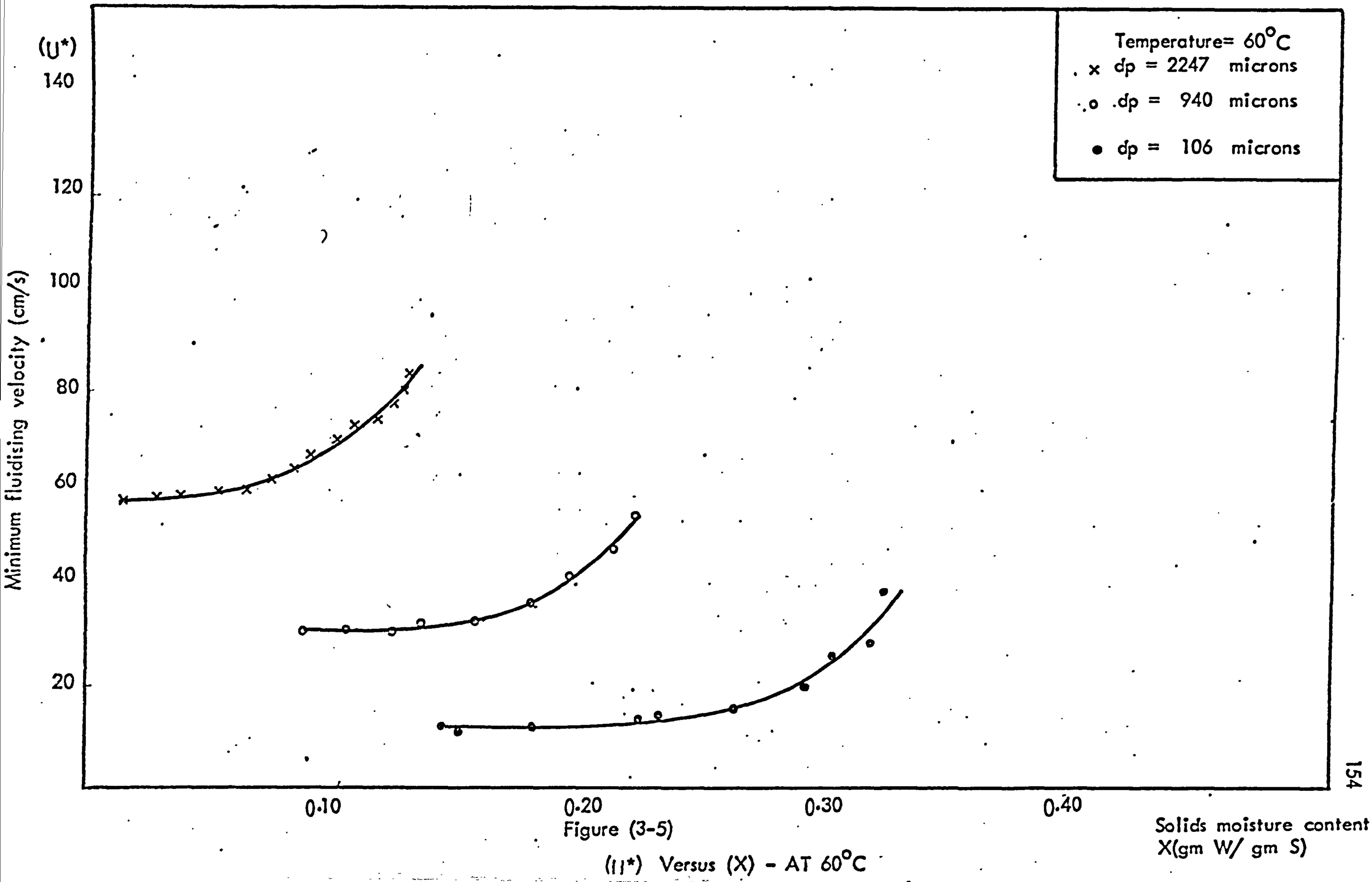


Figure (3-5)

(U*) Versus (X) - AT 60°C

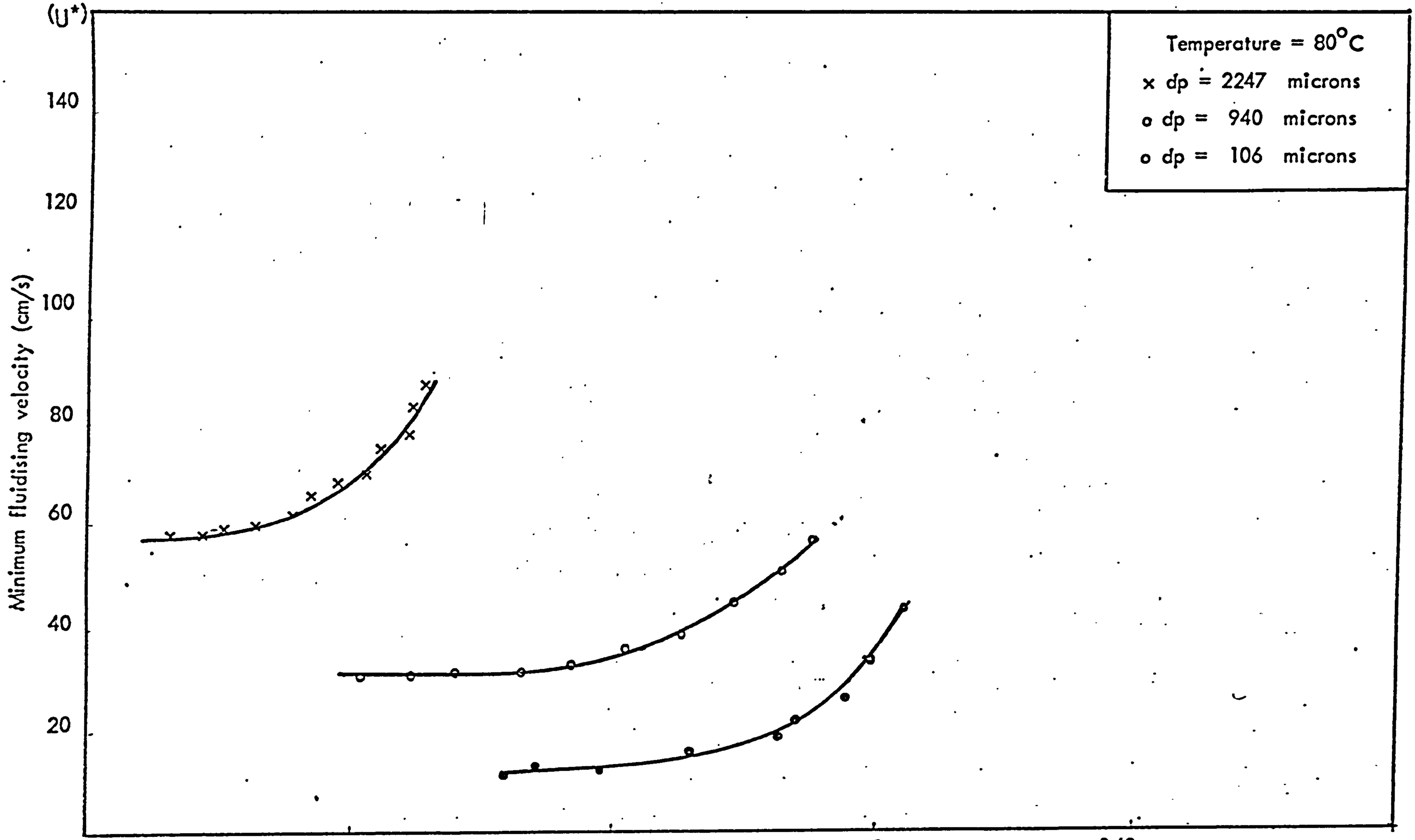


Figure (3-6)
(U*) Versus (X) - AT 80°C

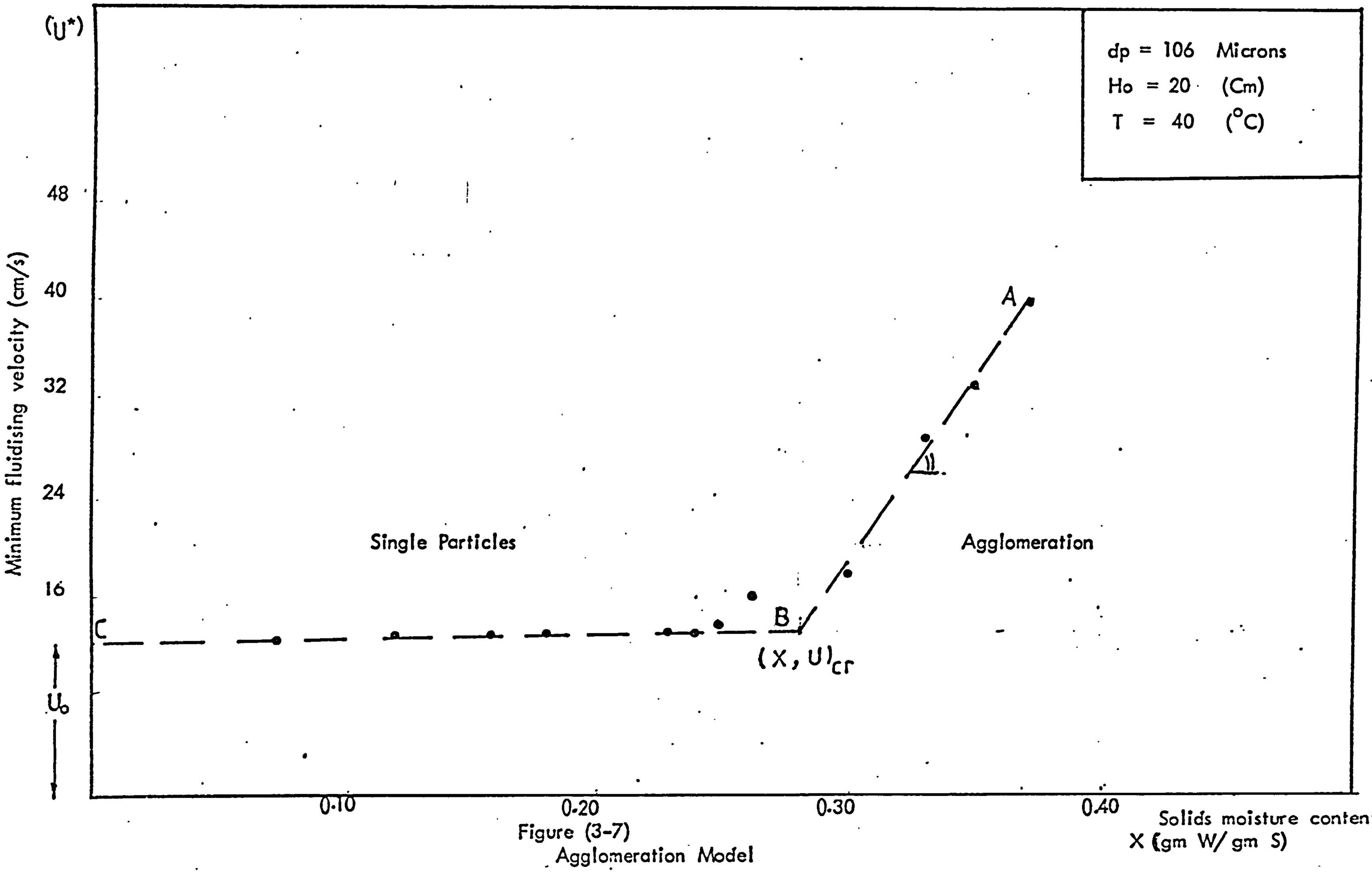


Figure (3-7)
Agglomeration Model

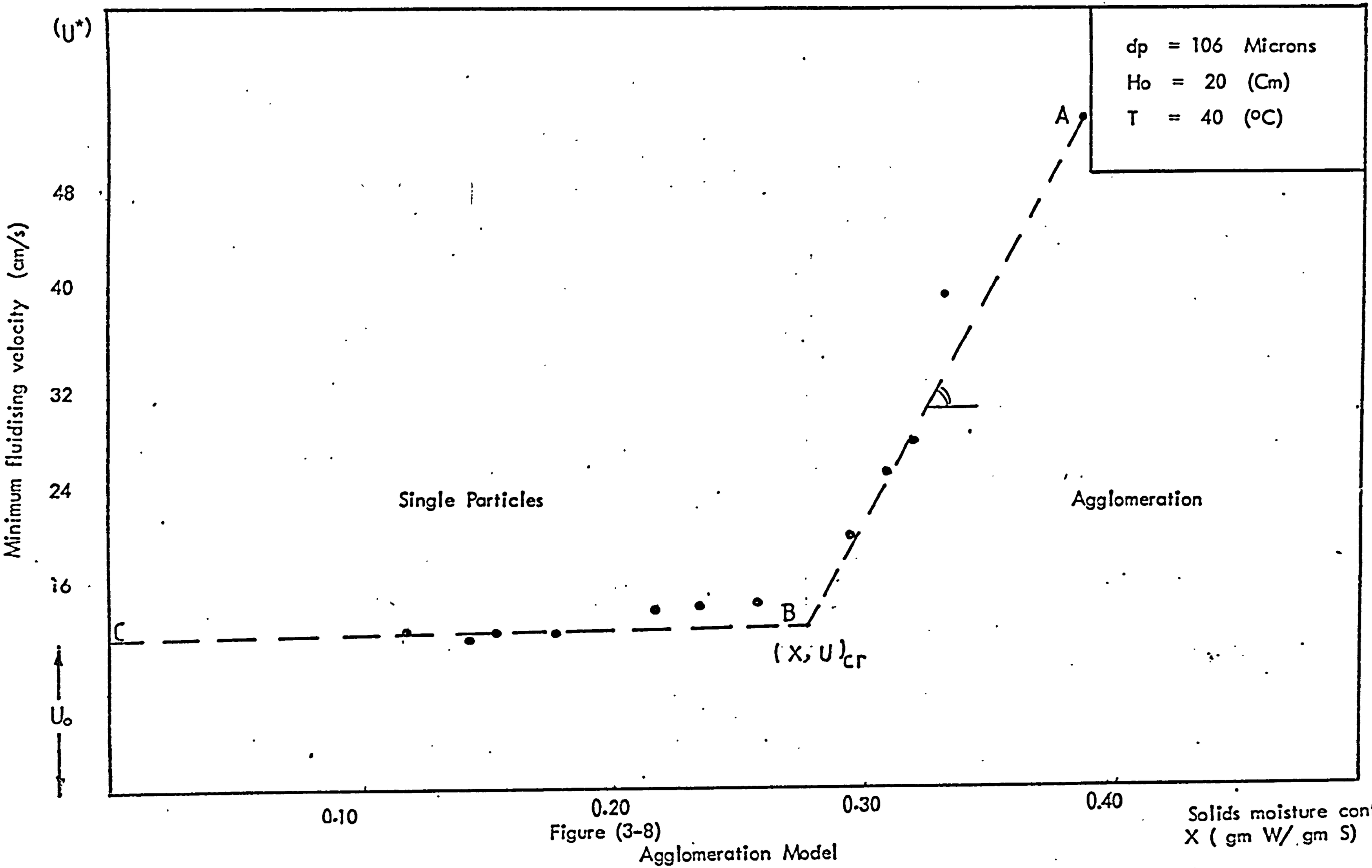


Figure (3-8)
Agglomeration Model

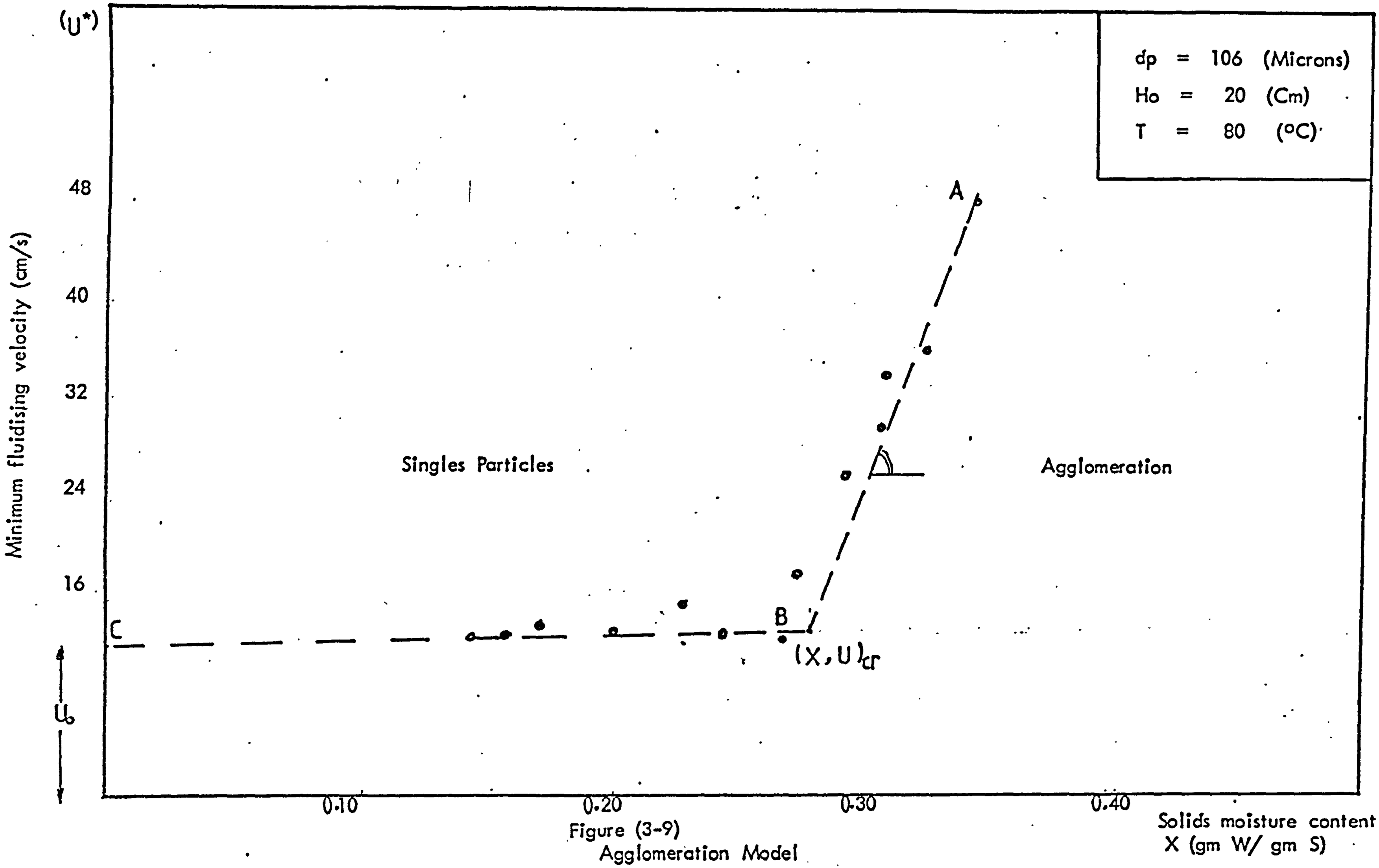


Figure (3-9)
Agglomeration Model

figure (3 . 10)

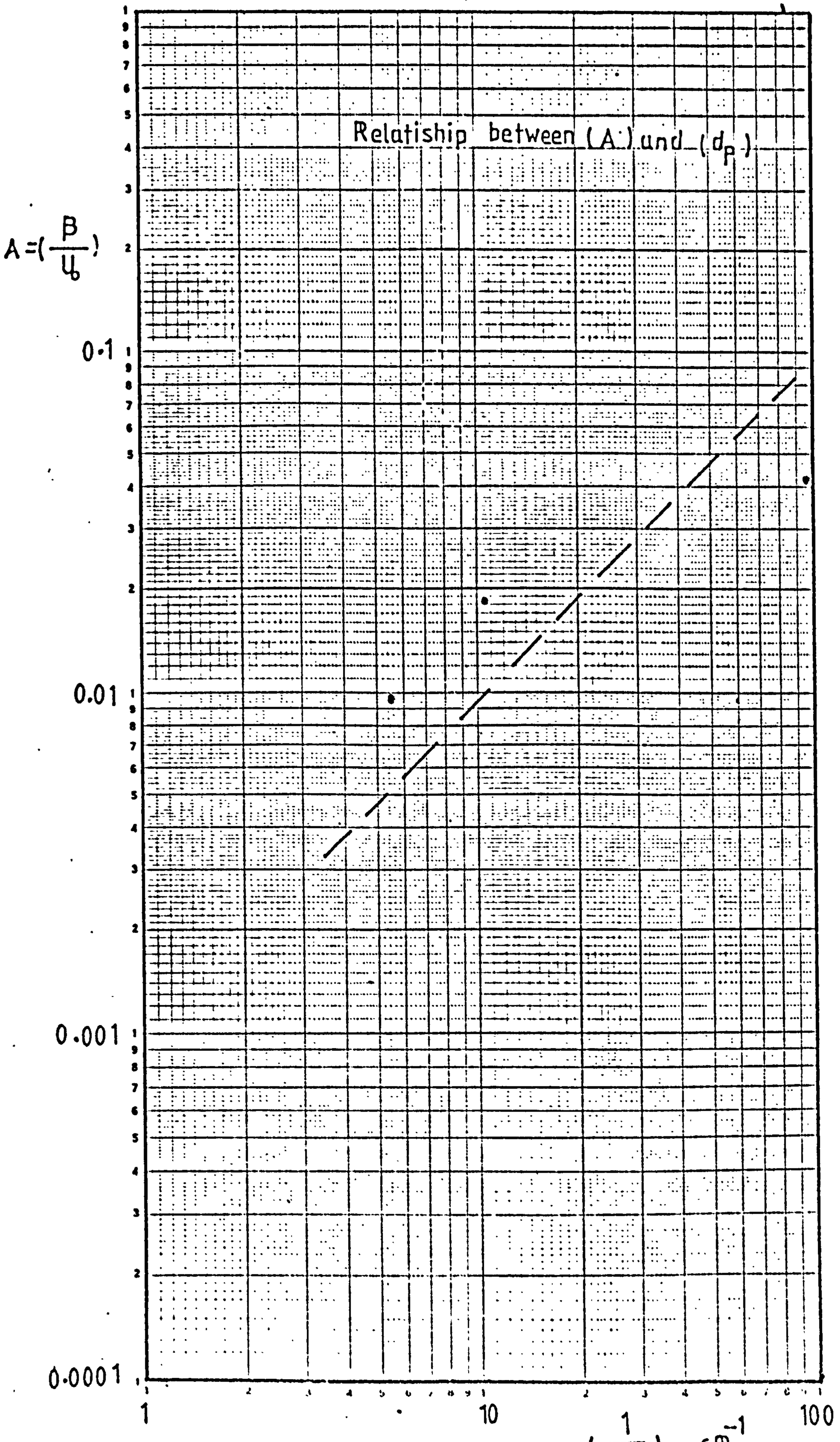
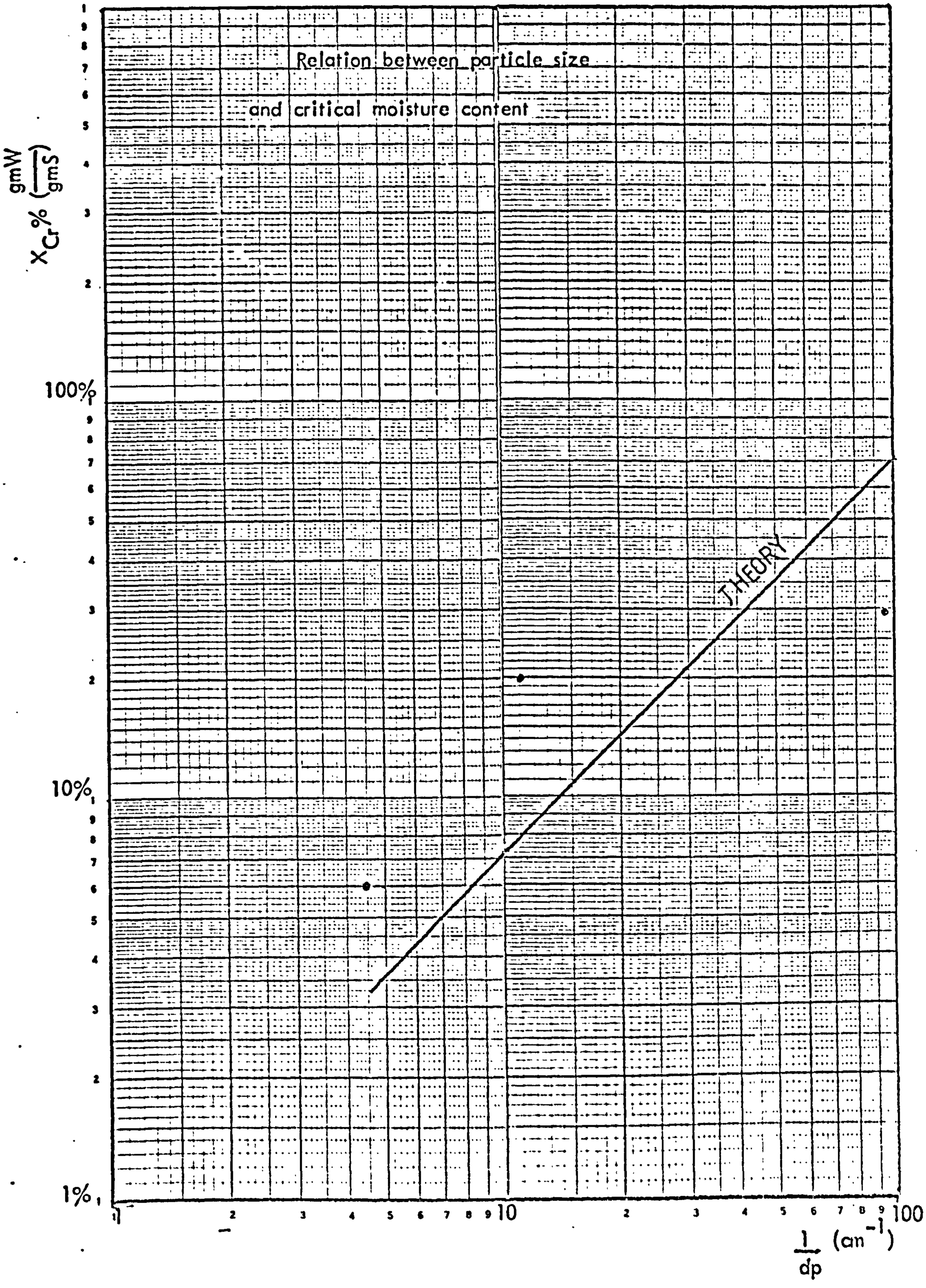

Relatiship between (A) and (d_p)
$A=(\frac{B}{U_b})$
0.1
0.01
0.001
0.0001
1
10
100
$(\frac{1}{l})$ cm^{-1}

Figure (3-11)


Relation between particle size
and critical moisture content
$X_{Cr}\%$ $\left(\frac{gmW}{gmS}\right)$
100%
10%
1%
THEORY
1 2 3 4 5 6 7 8 9 10 2 3 4 5 6 7 8 9 100
$\frac{1}{dp}$ (cm^{-1})

FIGURES (4)

HEAT TRANSFER

Figure (4-1) Air Temperature Profile At 100 (l /min)

Figure (4-2) Air Temperature Profile At 500 (l /min)

Figure (4-3) ($h_{g/p}$) vs. (X) at Different Flowrates - for 106 (μ)

Figure (4-4) Effect of Air Velocity on ($h_{g/p}$) " "

Figure (4-5) Gas to Particles Heat Transfer " "

Figure (4-6) ($h_{g/p}$) vs. (X) at different Flowrates -for 940 (μ)

Figure (4-7) Effectof Air velocity on ($h_{g/p}$) " "

Figure (4-8) Gas to particle heat transfer " "

Figure (4-9) ($h_{g/p}$) vs. (X) at different flowrates - for 2247 (μ)

Figure (4-10) Effect of air velocity on ($h_{g/p}$) " "

Figure (4-11) Gas to particles heat transfer " "

Figure (4-12) Effect of particle size on ($h_{g/p}$)

Figure (4-13) Effect of airvelocity on ($h_{g/p}$)

Figure (4-14) An overall heat transfer correlation

Figure (4-15) Effect of air flowrate on ($h_{b/w}$) - for 106 (μ)

Figure (4-16) Effect of air flowrate on ($h_{b/w}$) -for 940 (μ)

figure (4-17) Effect of air flowrate on ($h_{b/w}$) for 2247 (μ)

Figure (4-18) Effect of particle . size on $(h_{b/w})_{Max.}$

Figure (4-19) Levenspeil & Walton modified correlation

Figure (4-20) Dow & Jackob modified correlation

Figure (4-21) Wender & Cooper modified correlation

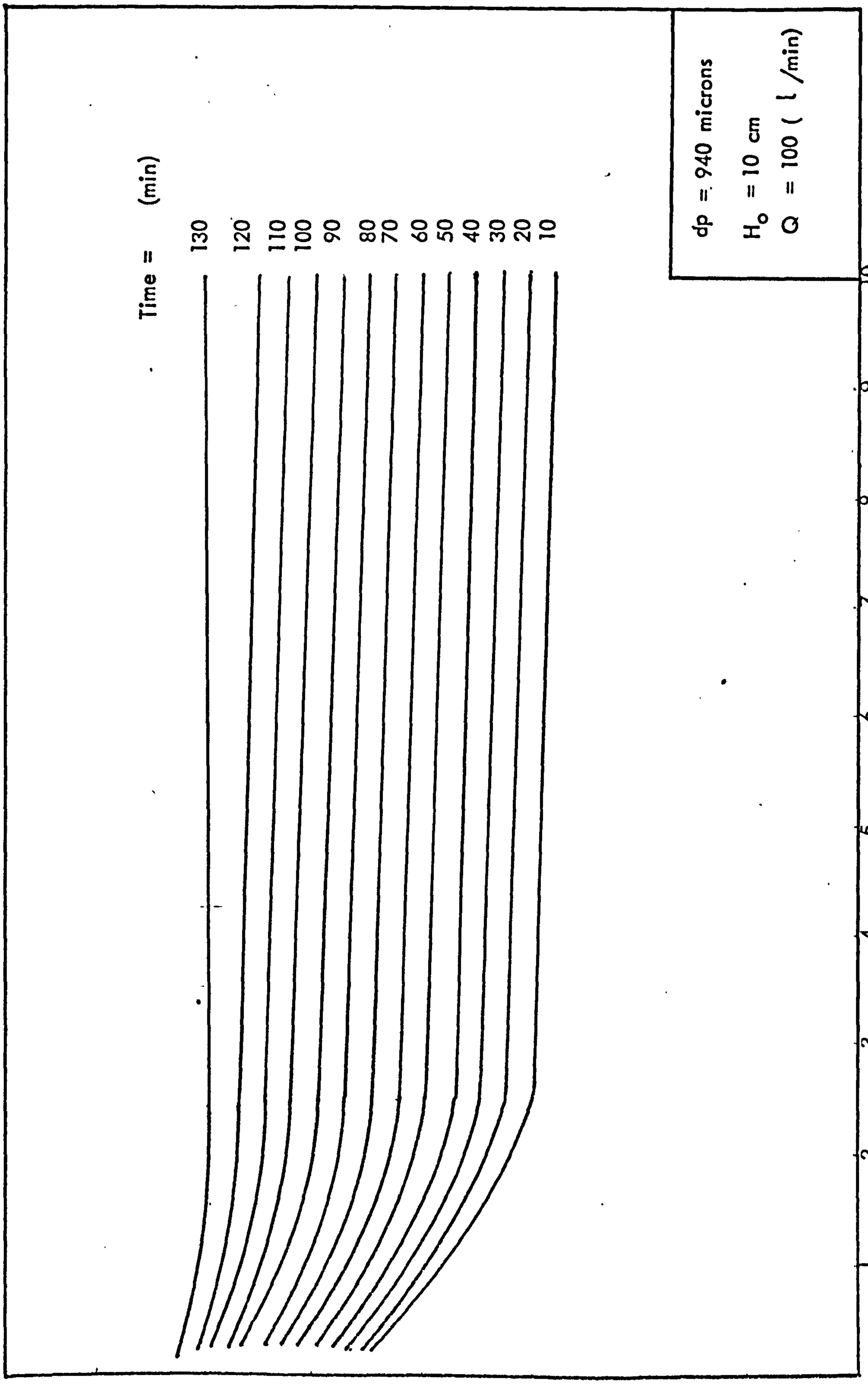


Figure (4-1)
Air Temperature Profile

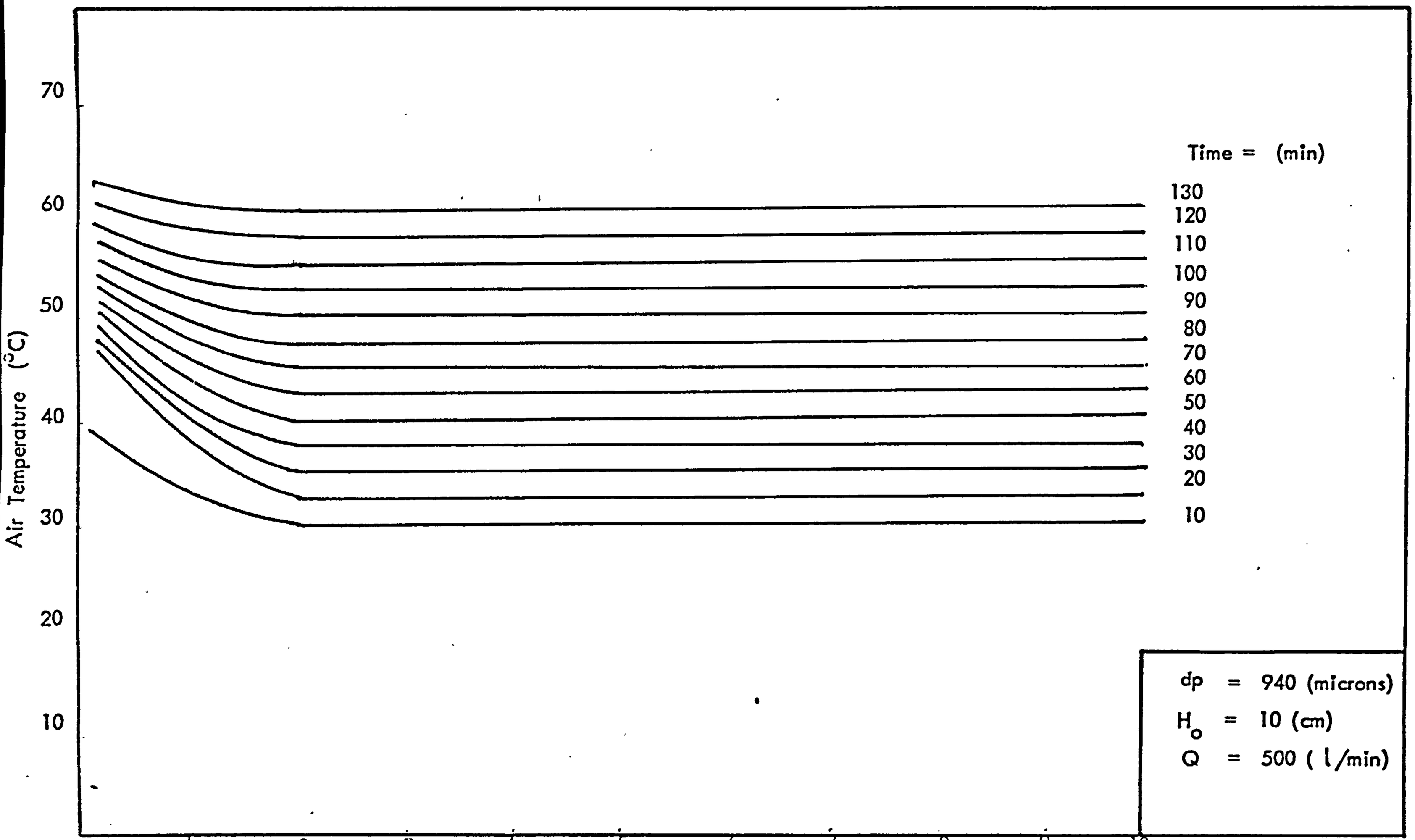


Figure (4-2)
Air Temperature Profile

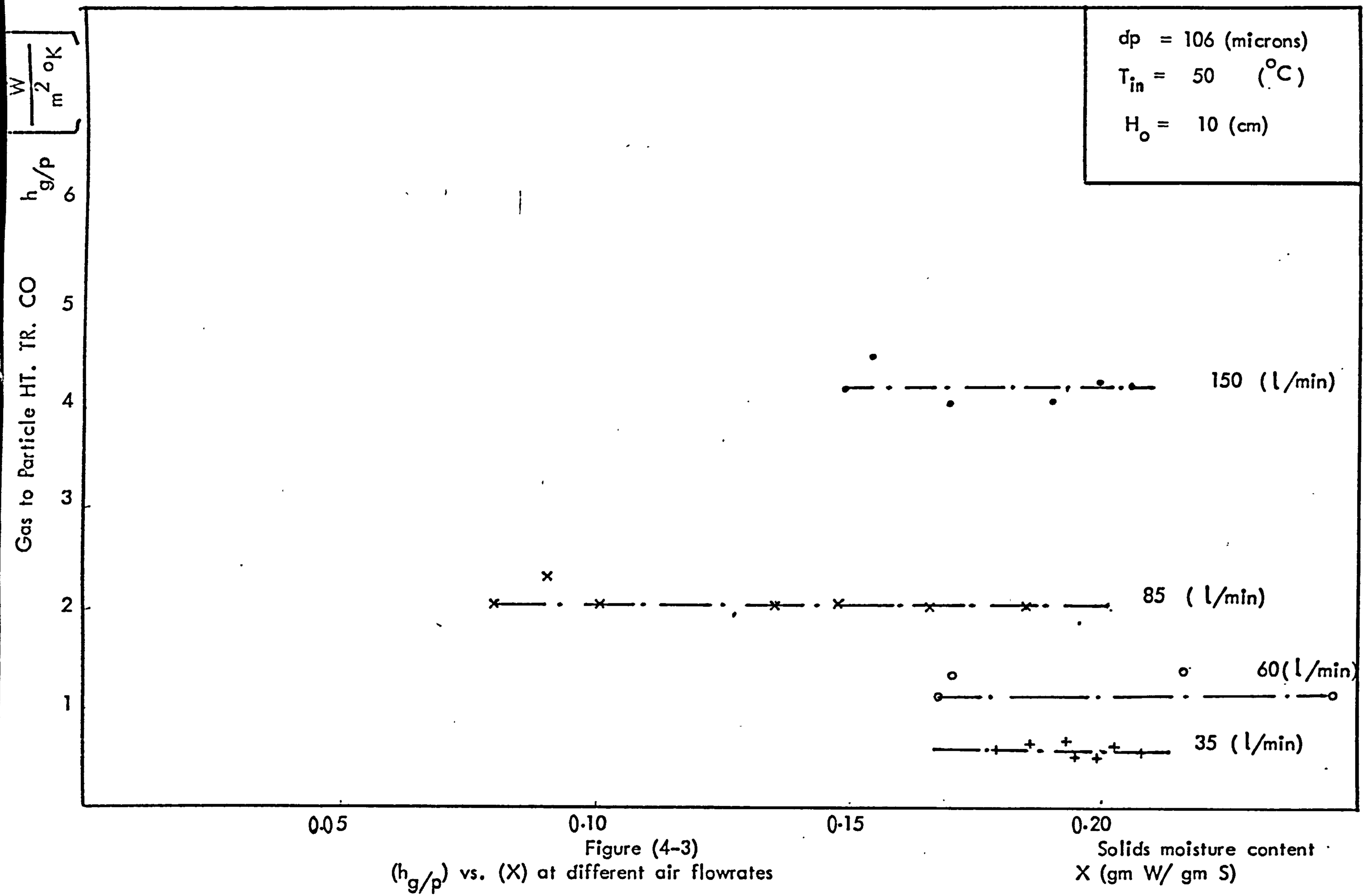


Figure (4-3)
($h_{g/p}$) vs. (X) at different air flowrates

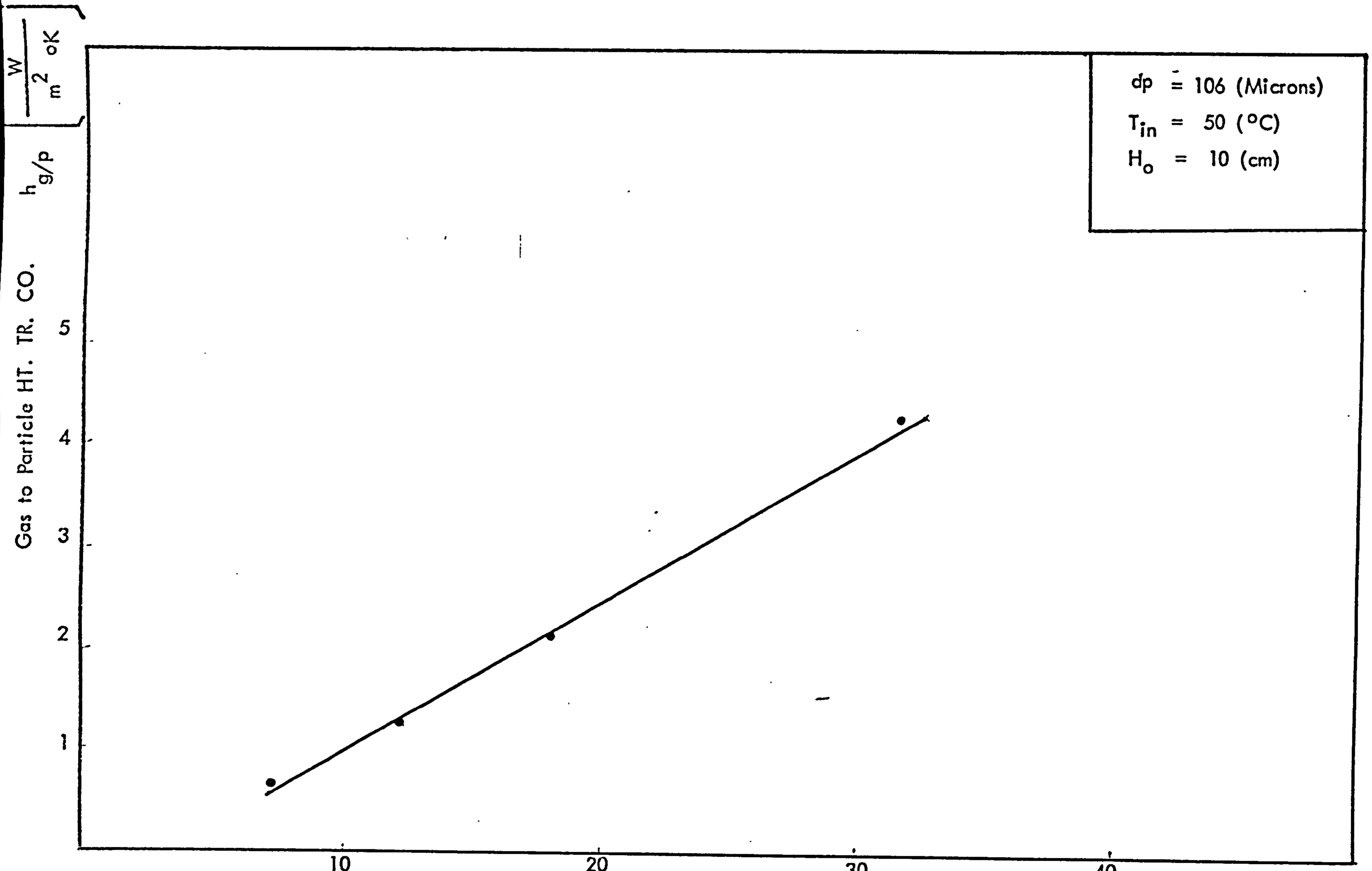


Figure (4-4)
Effect of air velocity on $h_{g/p}$

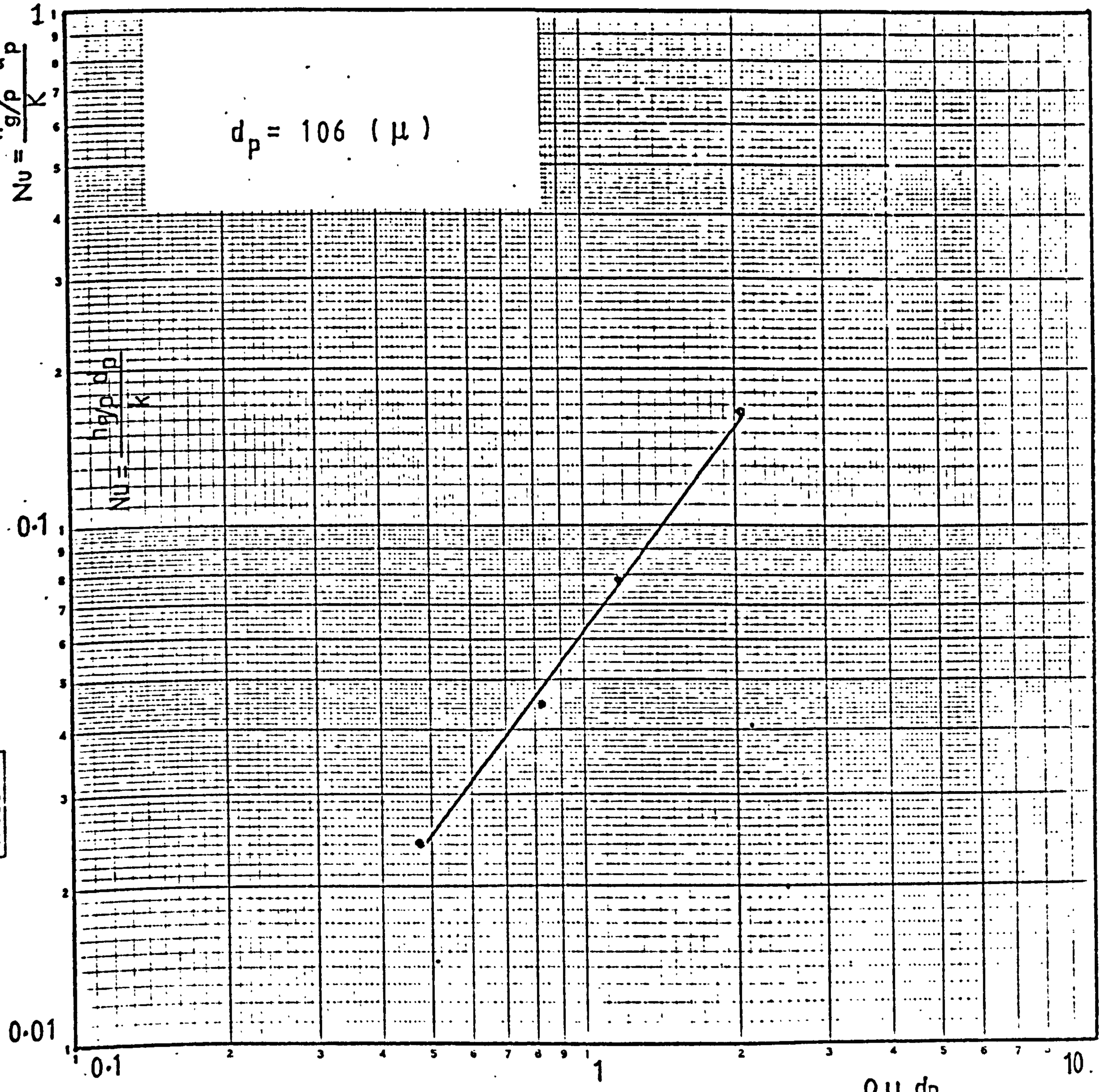


Figure (4-5)

gas to particle heat transfer
dp = 106 microns

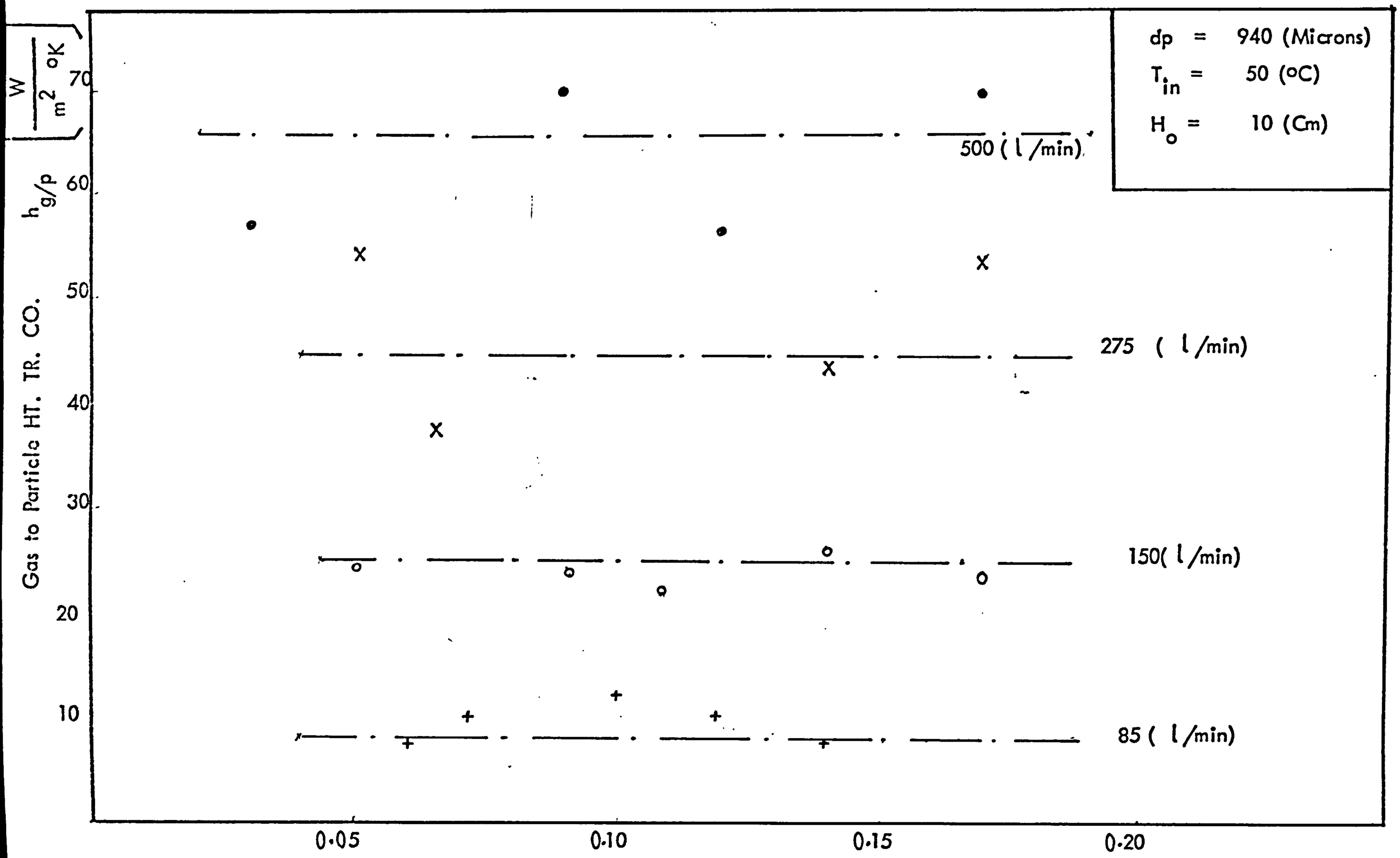


Figure (4-6)
($h_{g/p}$) vs. (X) at different air flowrates

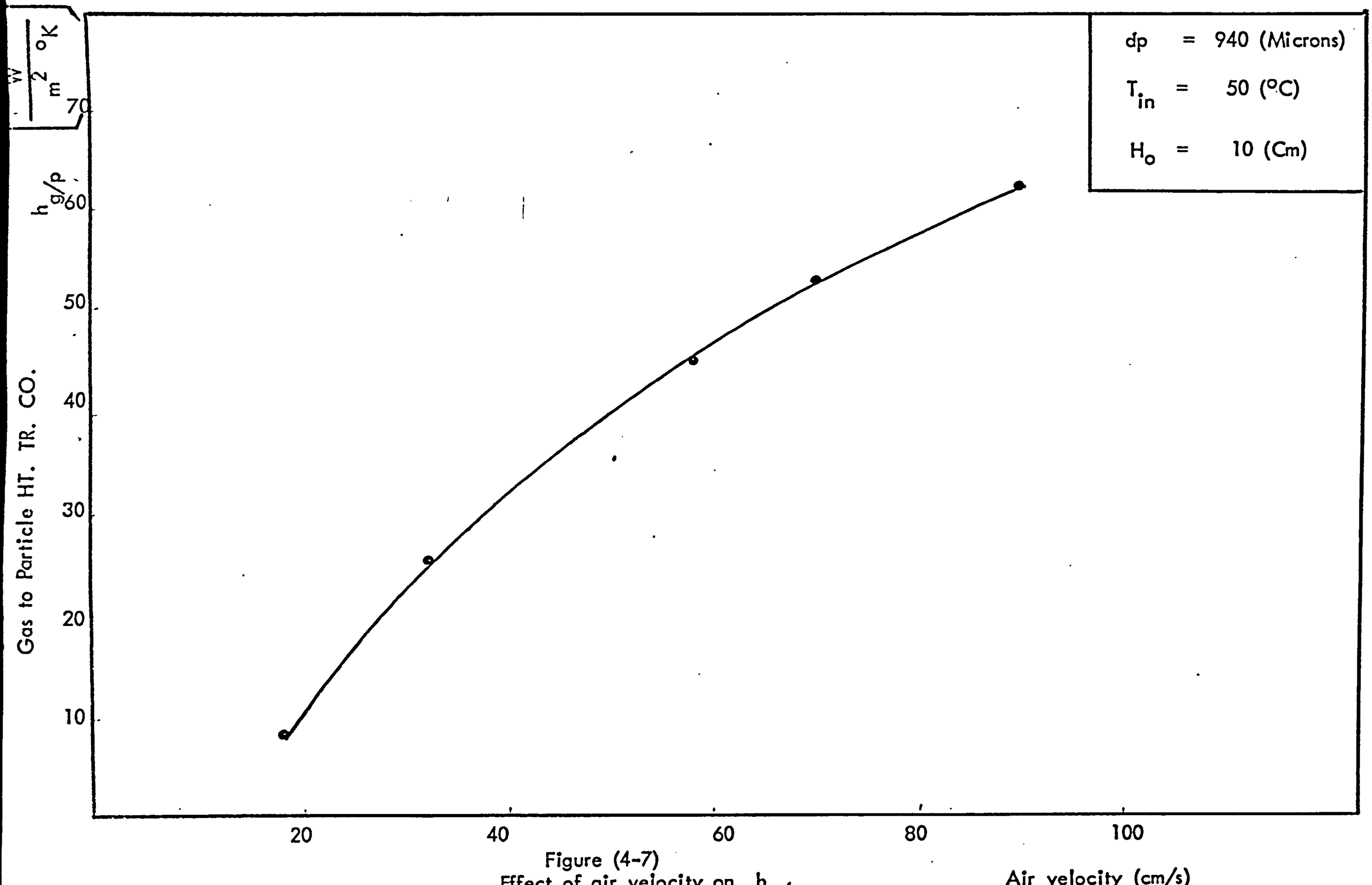


Figure (4-7)
Effect of air velocity on $h_{g/p}$

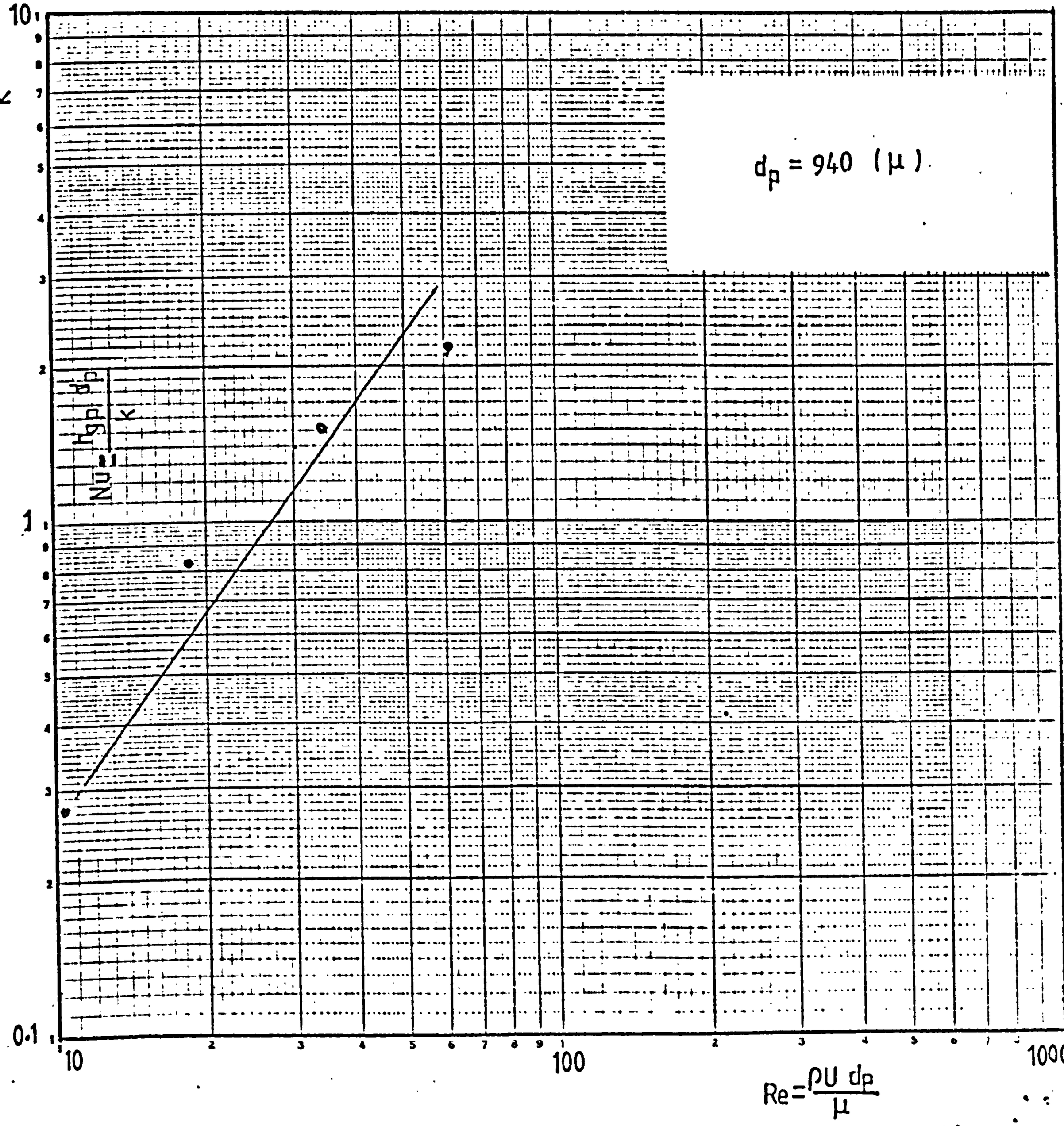


Figure (4-8)

Gas to particle heat transfer

dp = 940 microns

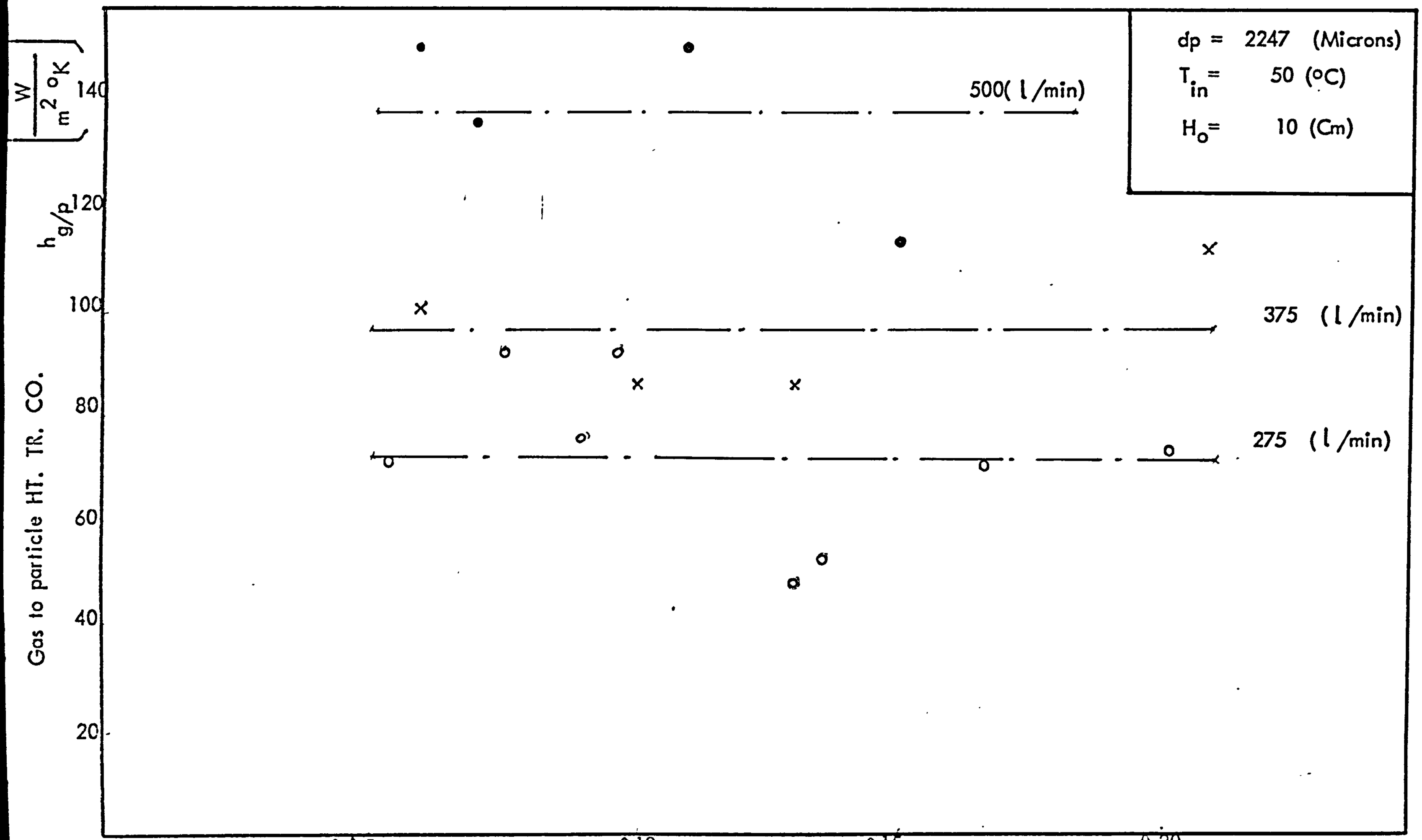


Figure (4-9)
($h_{g/p}$) vs. (X) at different air flowrates

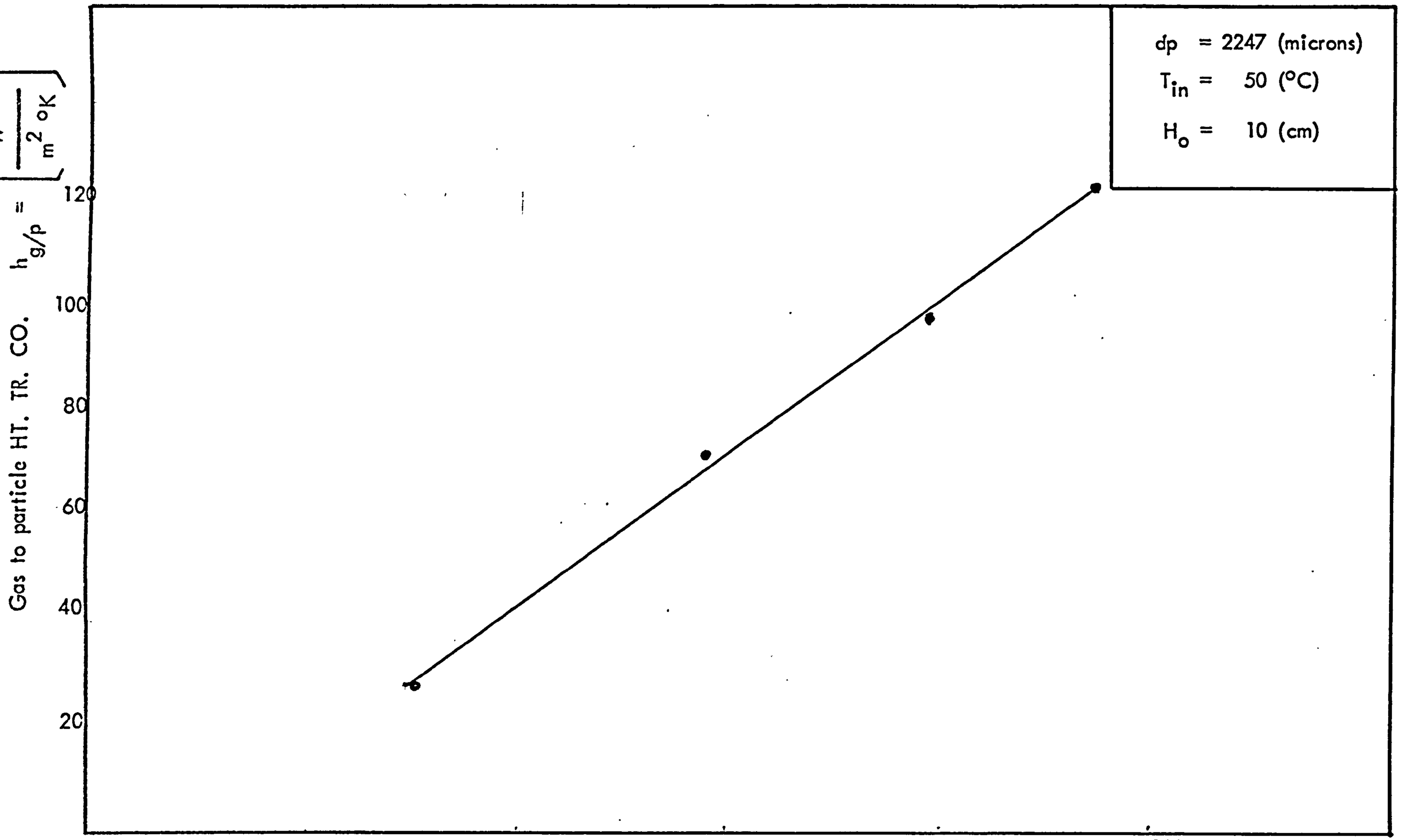


Figure (4-10)
Effect of air velocity on $h_{g/p}$

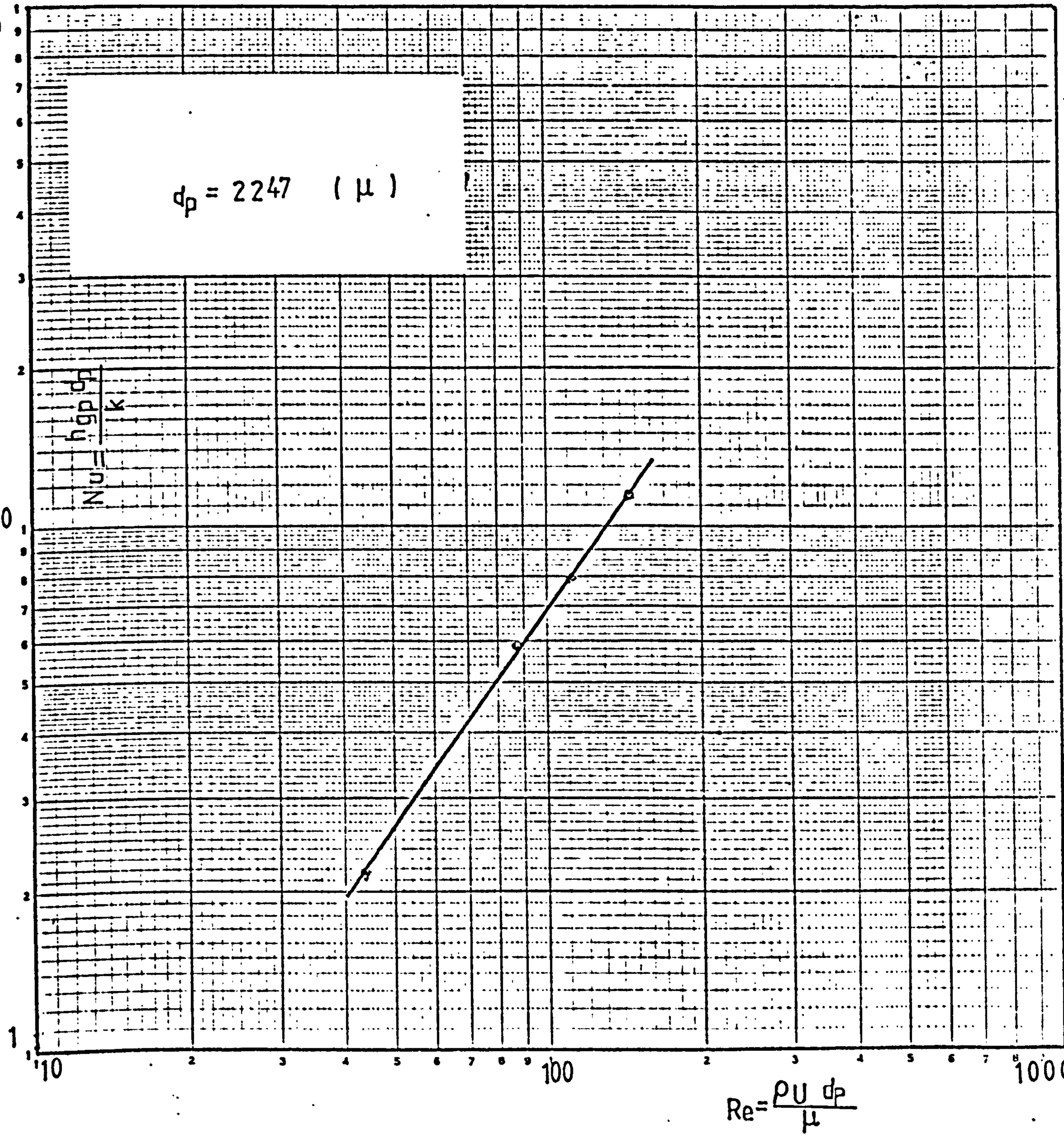


Figure (4-11)

Gas to particle heat transfer

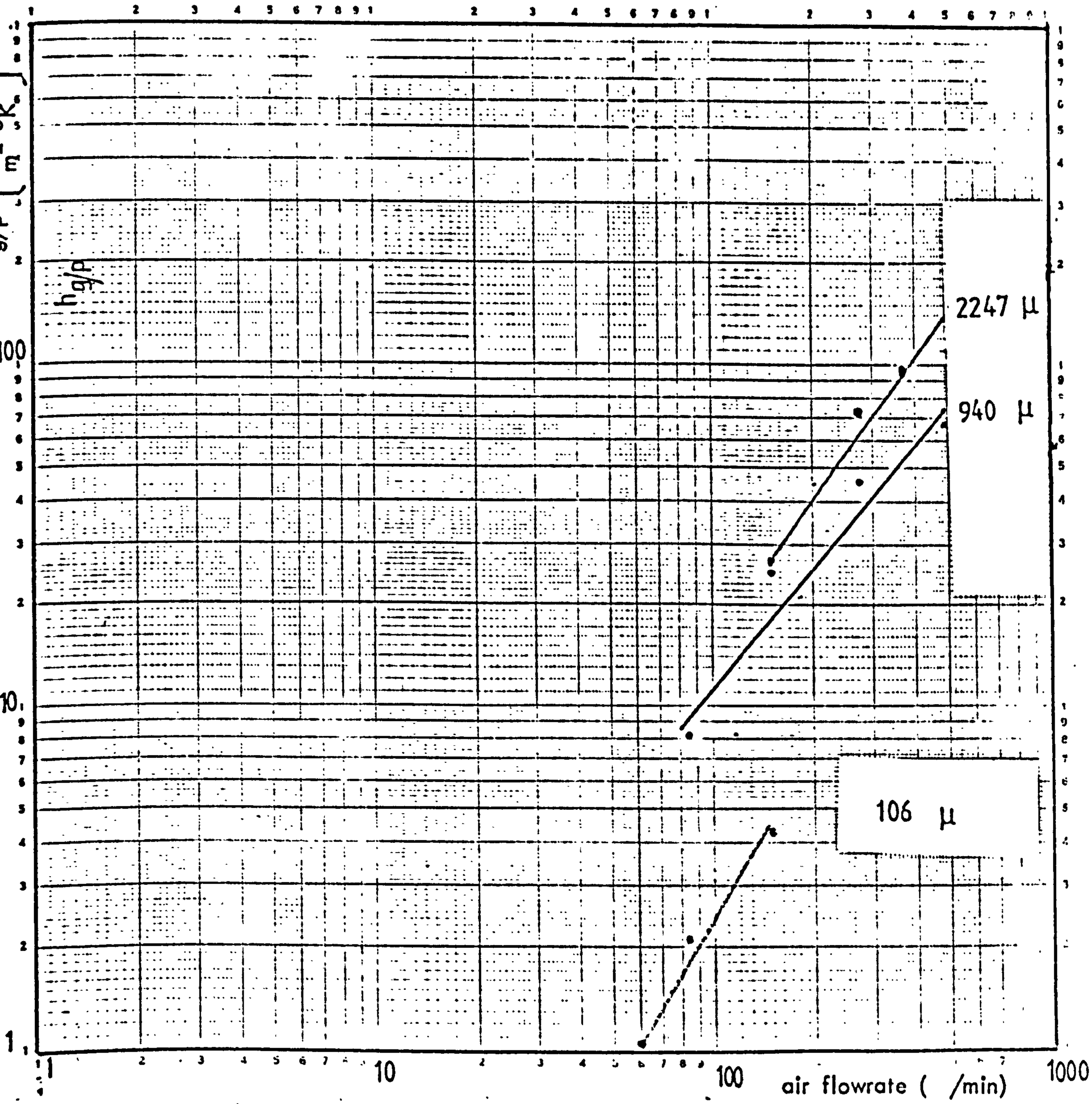


Figure (4-12)

Effect of particle size on $h_{g/p}$

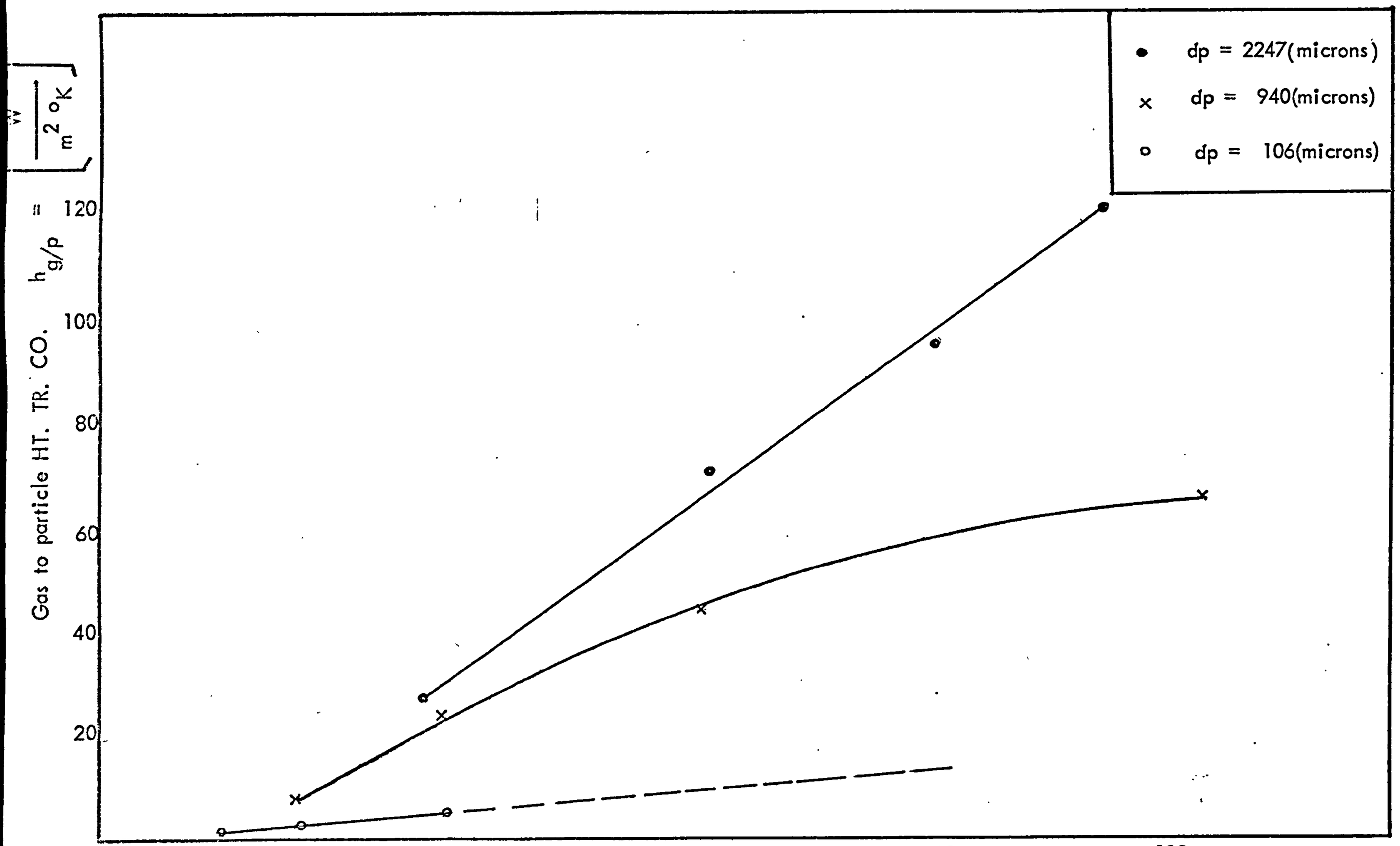
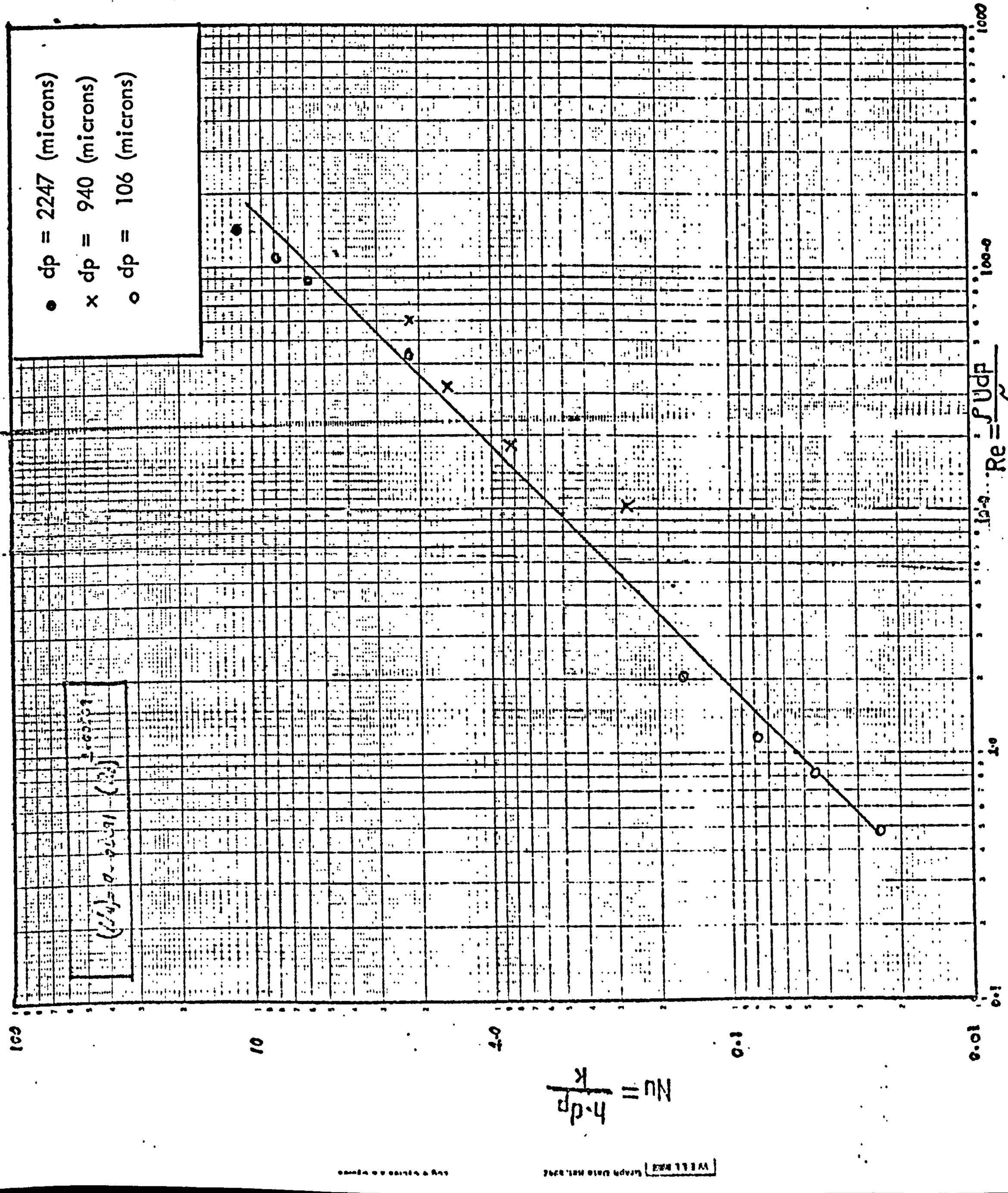


Figure (4-13)
Effect of air velocity on $h_{g/p}$

Figure (4-14)

Gas to particle overall heat transfer correlation



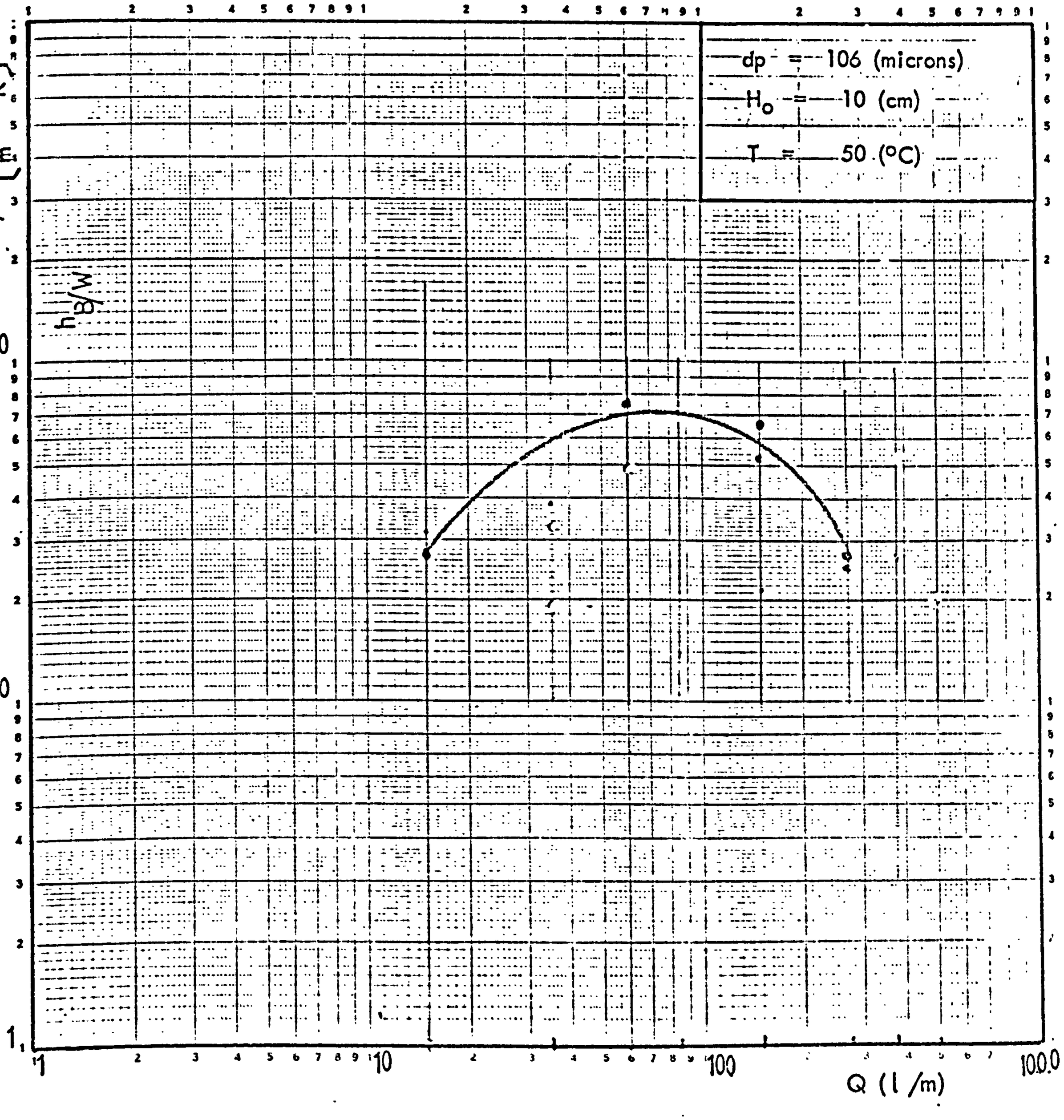


Figure (4-15)

Effect of air flowrate on $h_{B/W}$

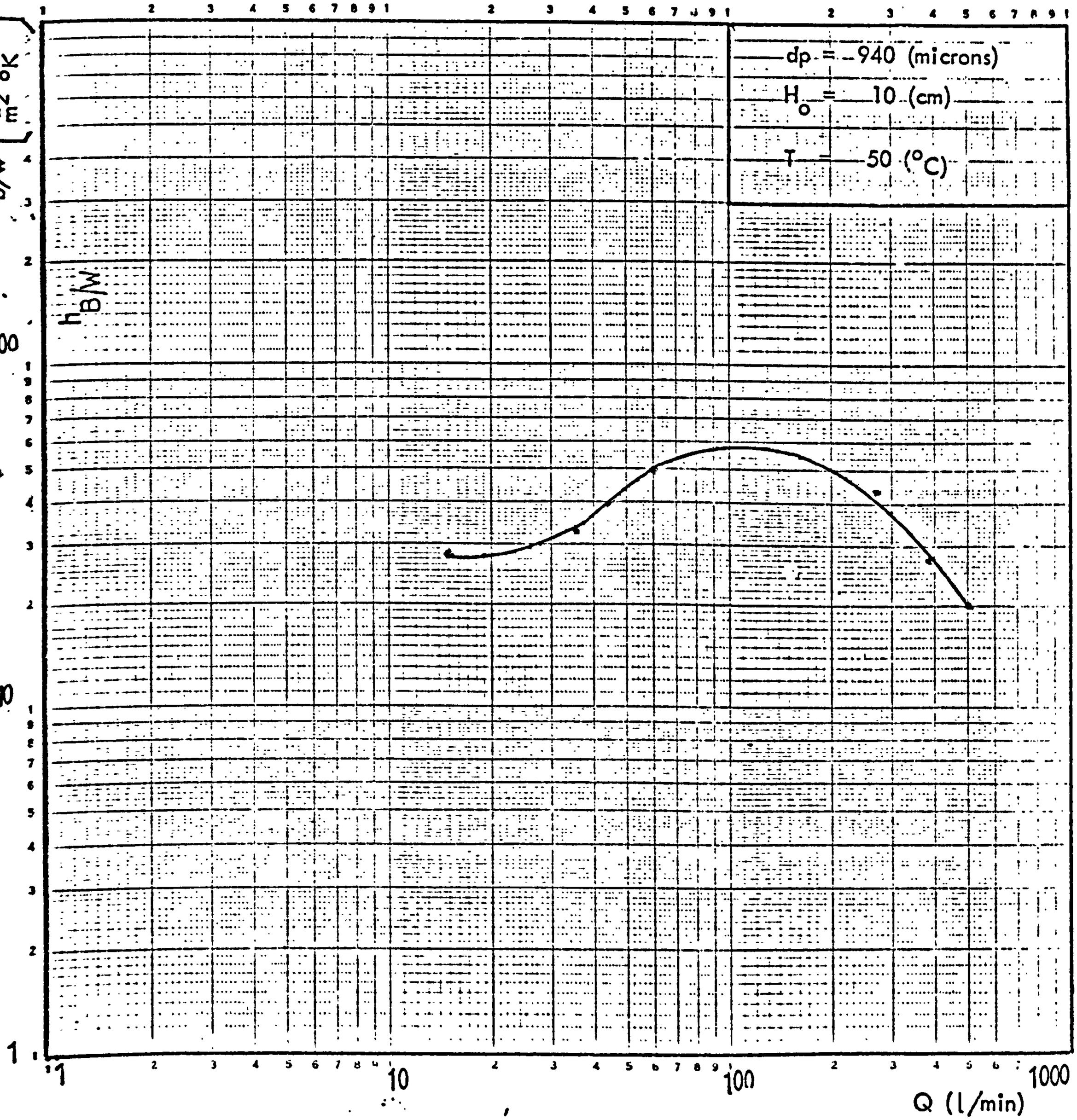


Figure (4-16)

Effect of air flowrate on $h_{B/w}$

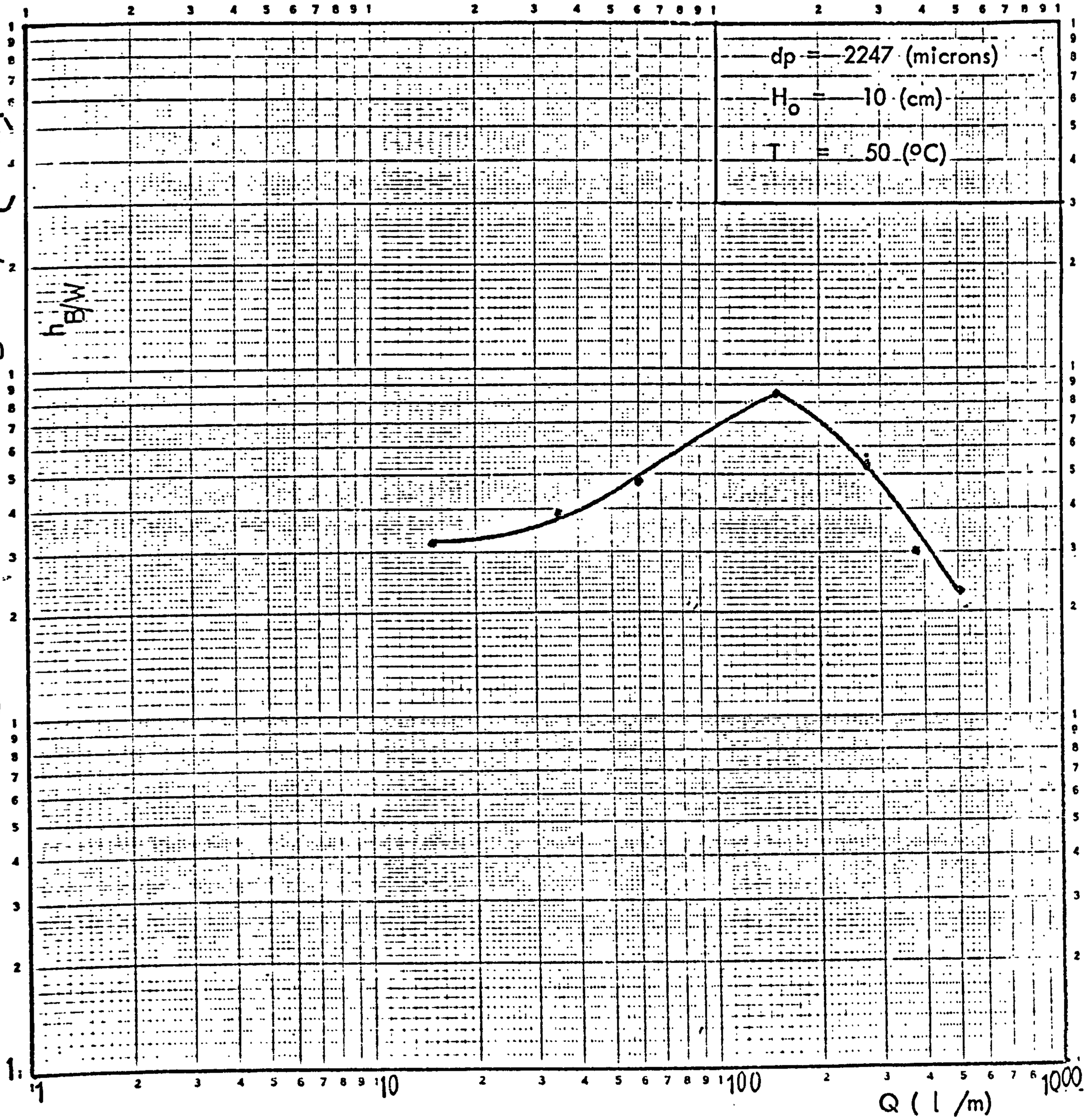


Figure (4-17)

Effect of air flowrate on $h_{B/w}$

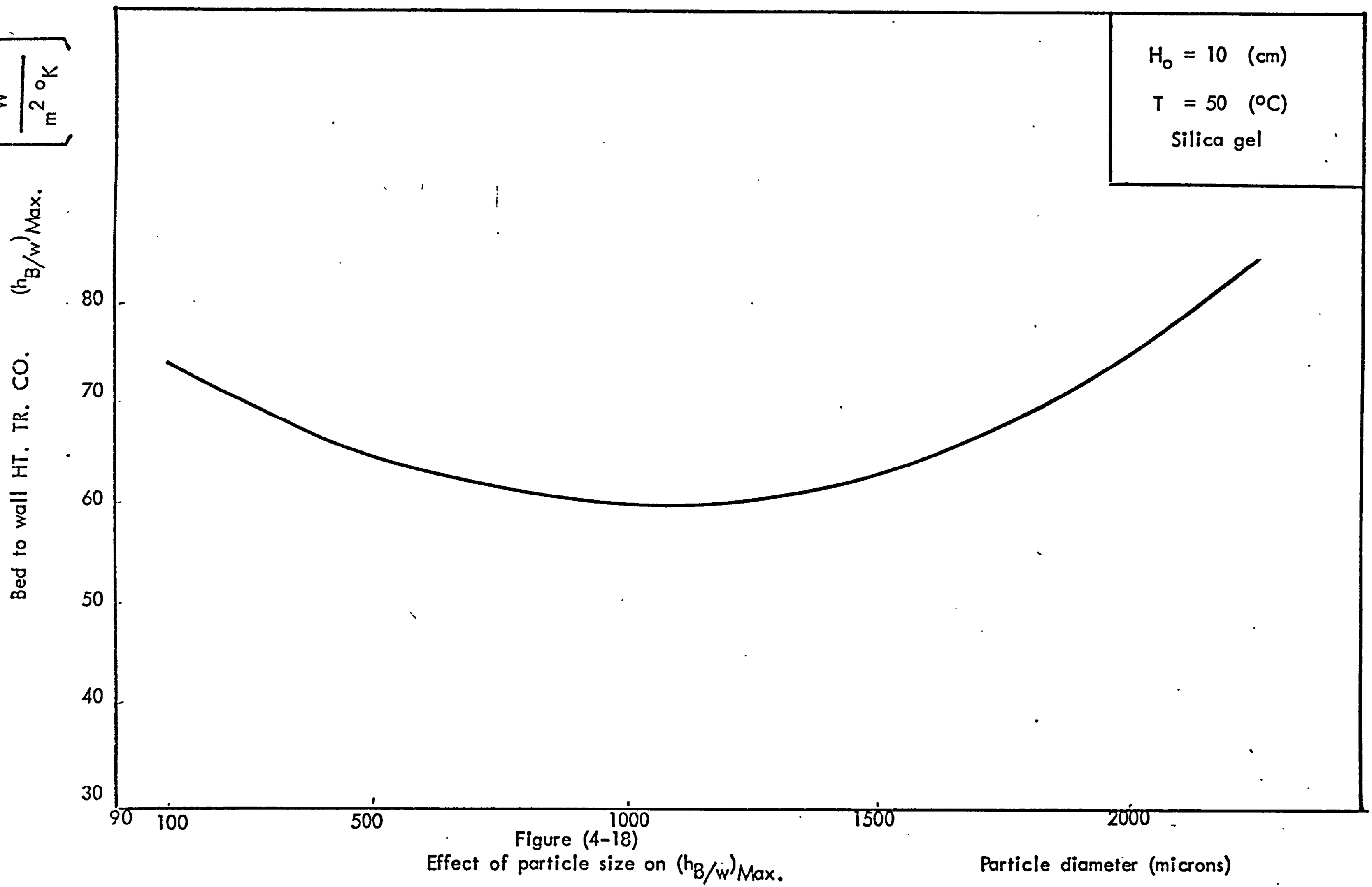


Figure (4-18)
Effect of particle size on $(h_{B/w})_{Max.}$

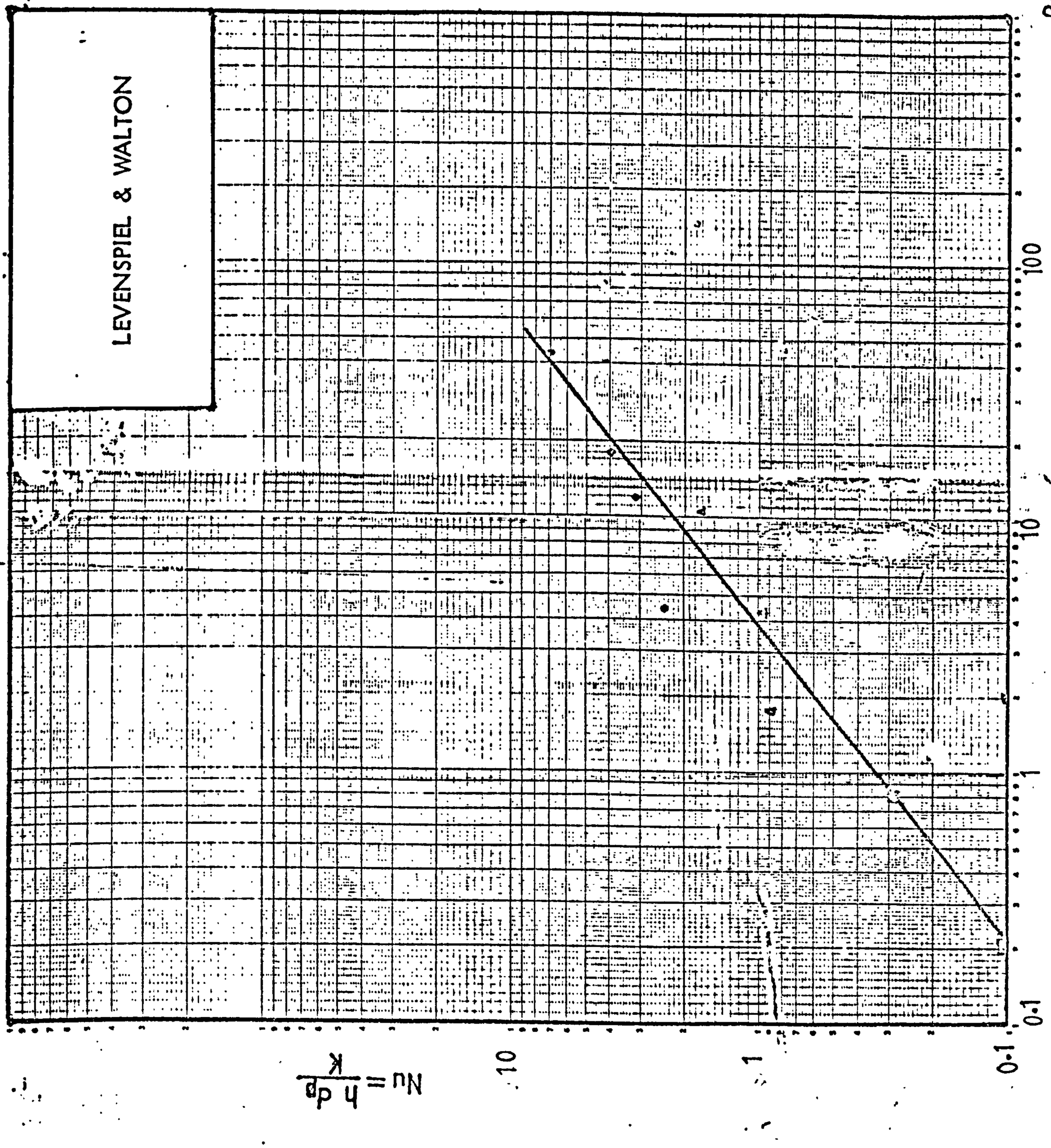
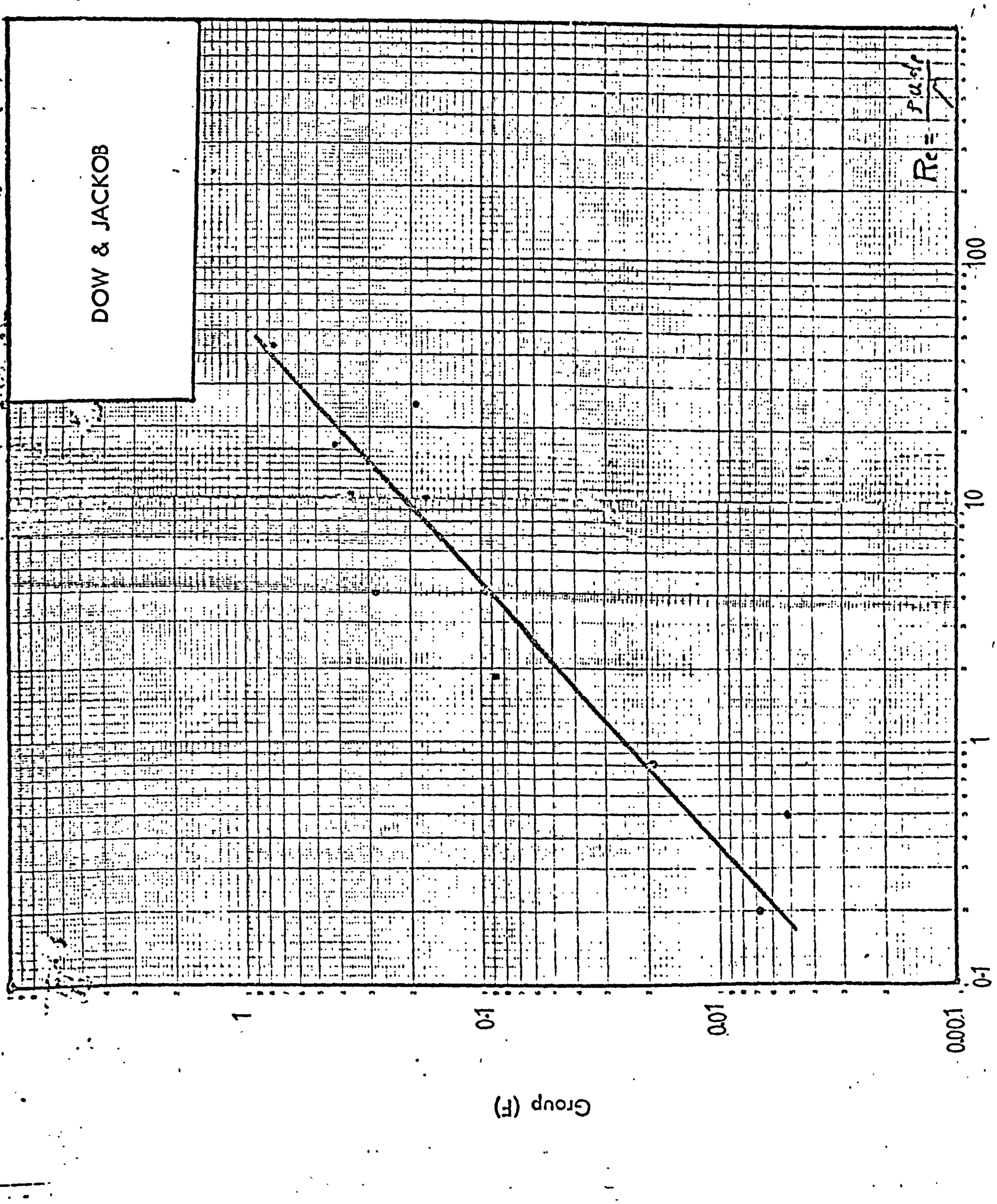


Figure (4-19)

Levenspiel & Walton modified correlation

Figure (4-20)

Dow & Jackob modified correlation



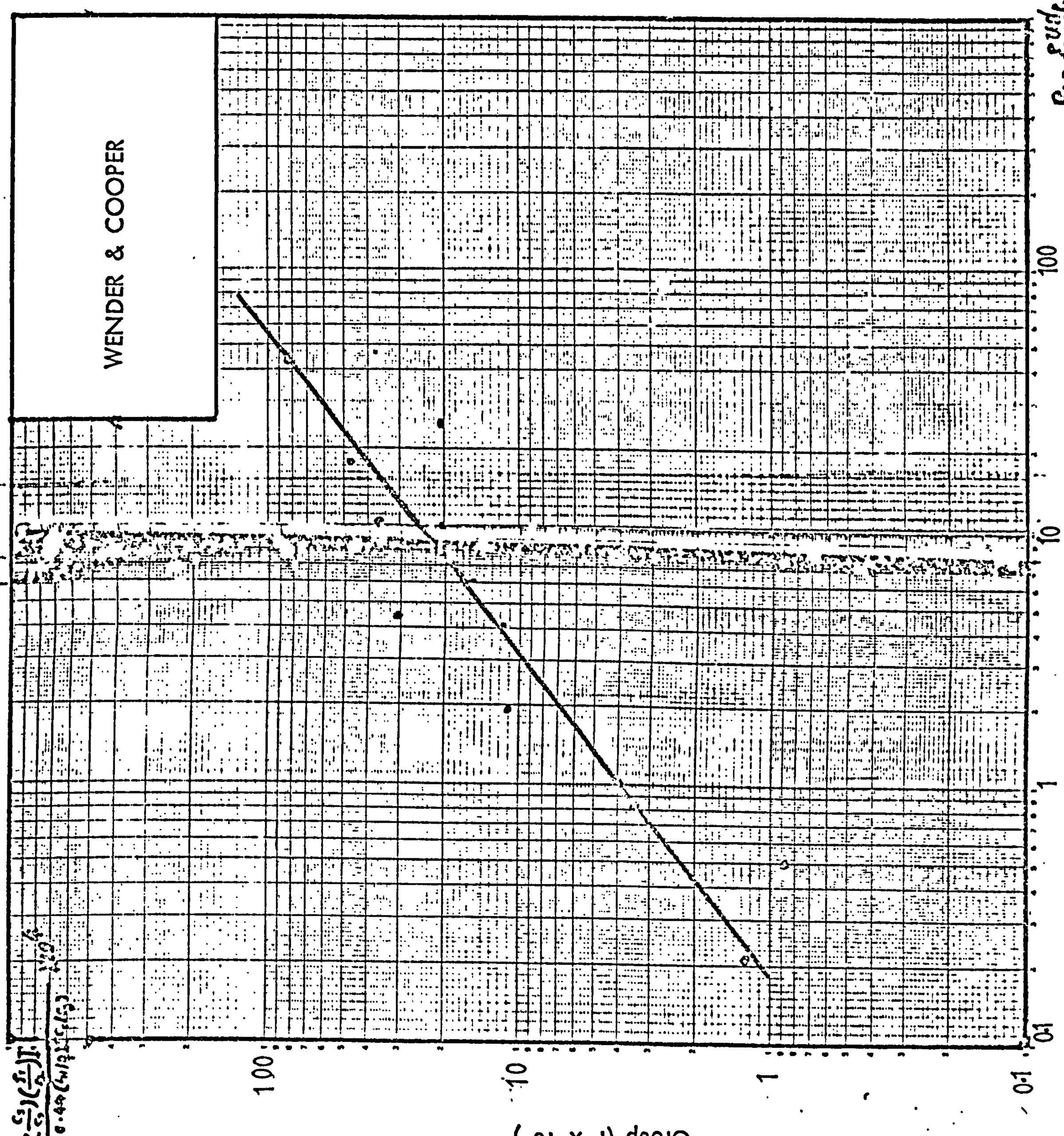


Figure (4-21)

Wender & Cooper modified correlation

FIGURES (5)

MASS TRANSFER

Figure (5-1) Variation of air humidity with bed height - (2247 μ)

Figure (5-2) Variation of air humidity with bed height - (940 μ)

Figure (5-3) Variation of air humidity with bed height - (106 μ)

Figure (5-4) Effect of air velocity on mass transfer

Figure (5-5) Effect of particle size on mass transfer

Figure (5-6) Overall mass transfer correlation

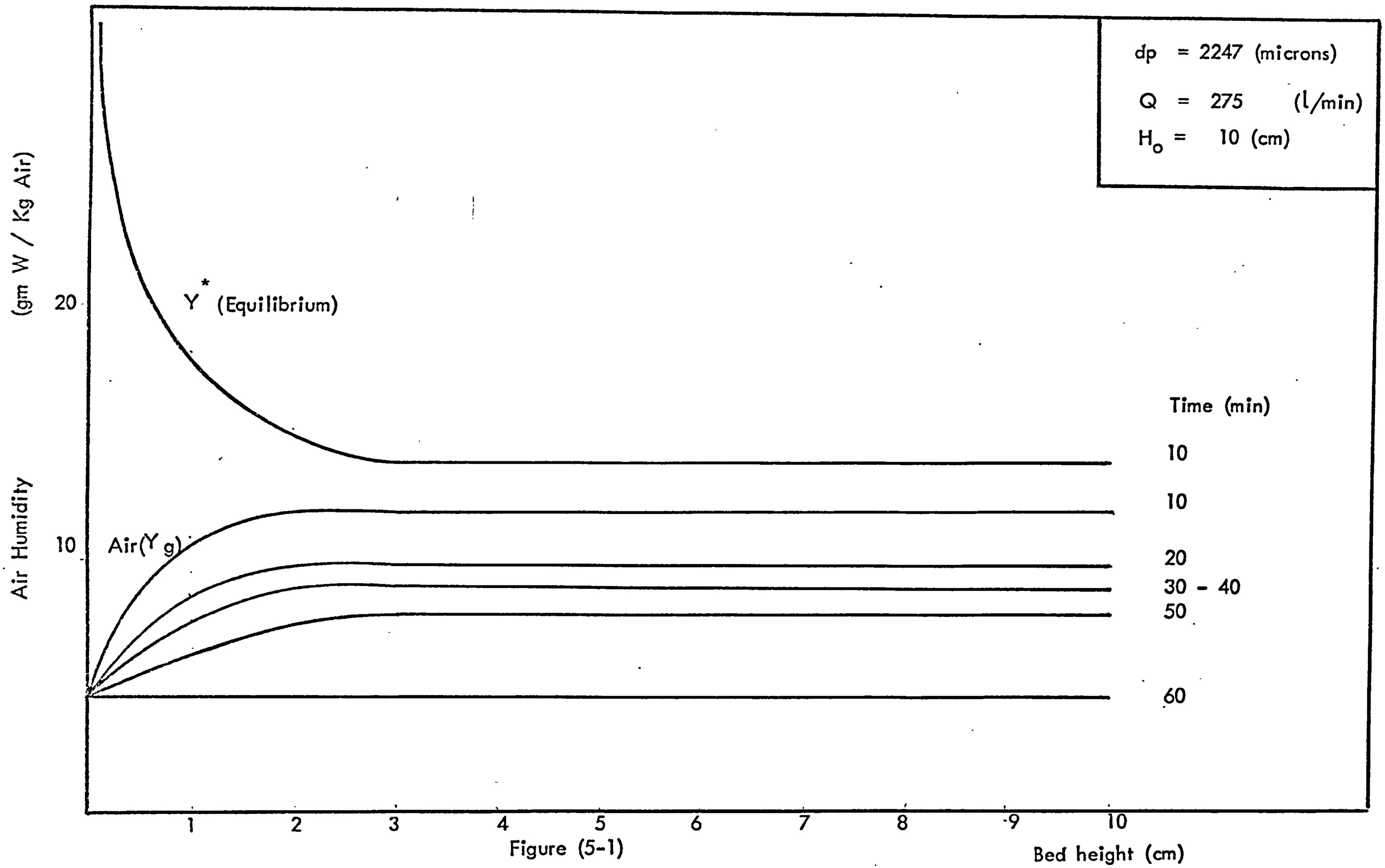


Figure (5-1)

Variation of air humidity with bed height

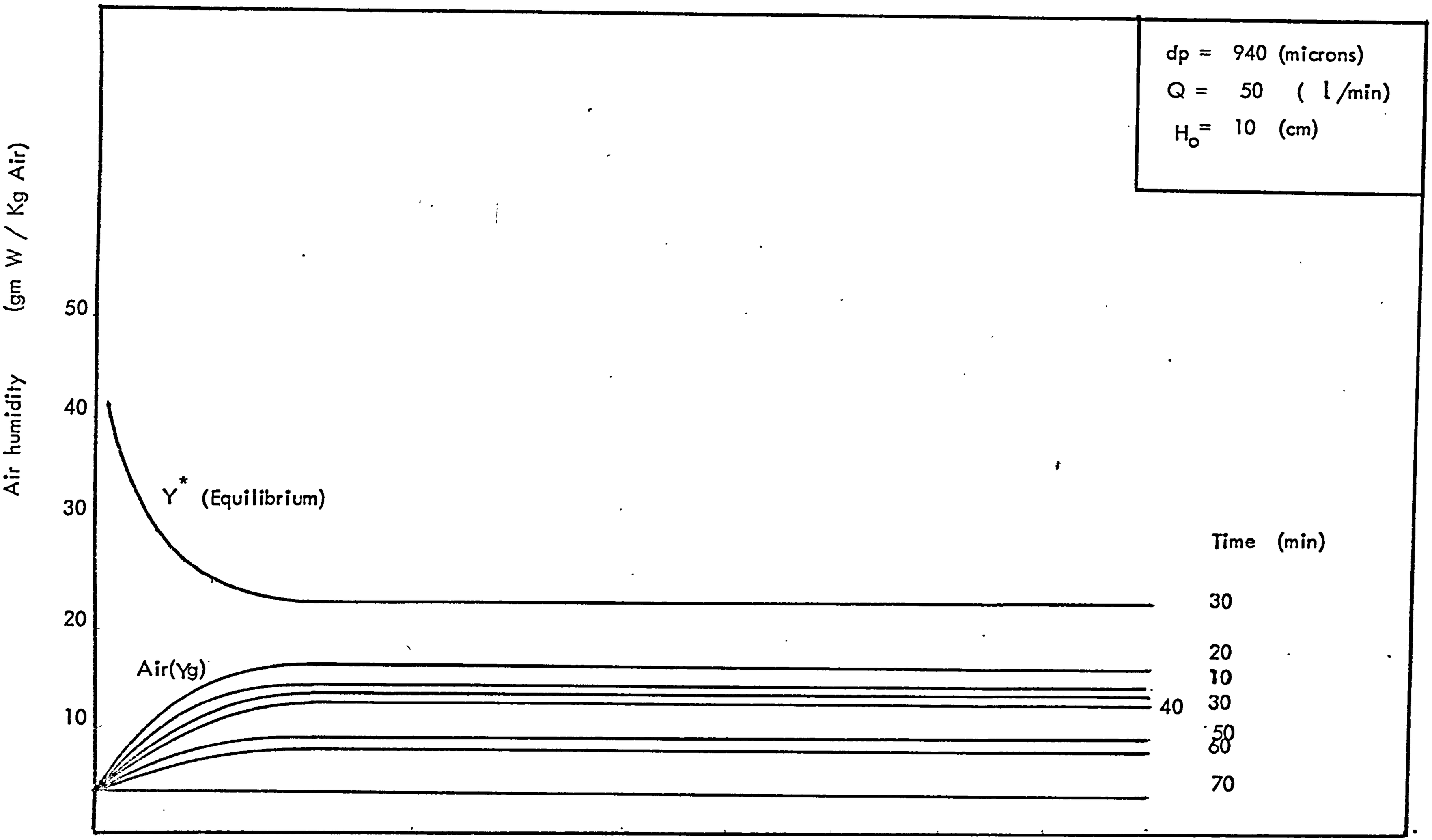


Figure (5-2)
Variation of air humidity with bed height

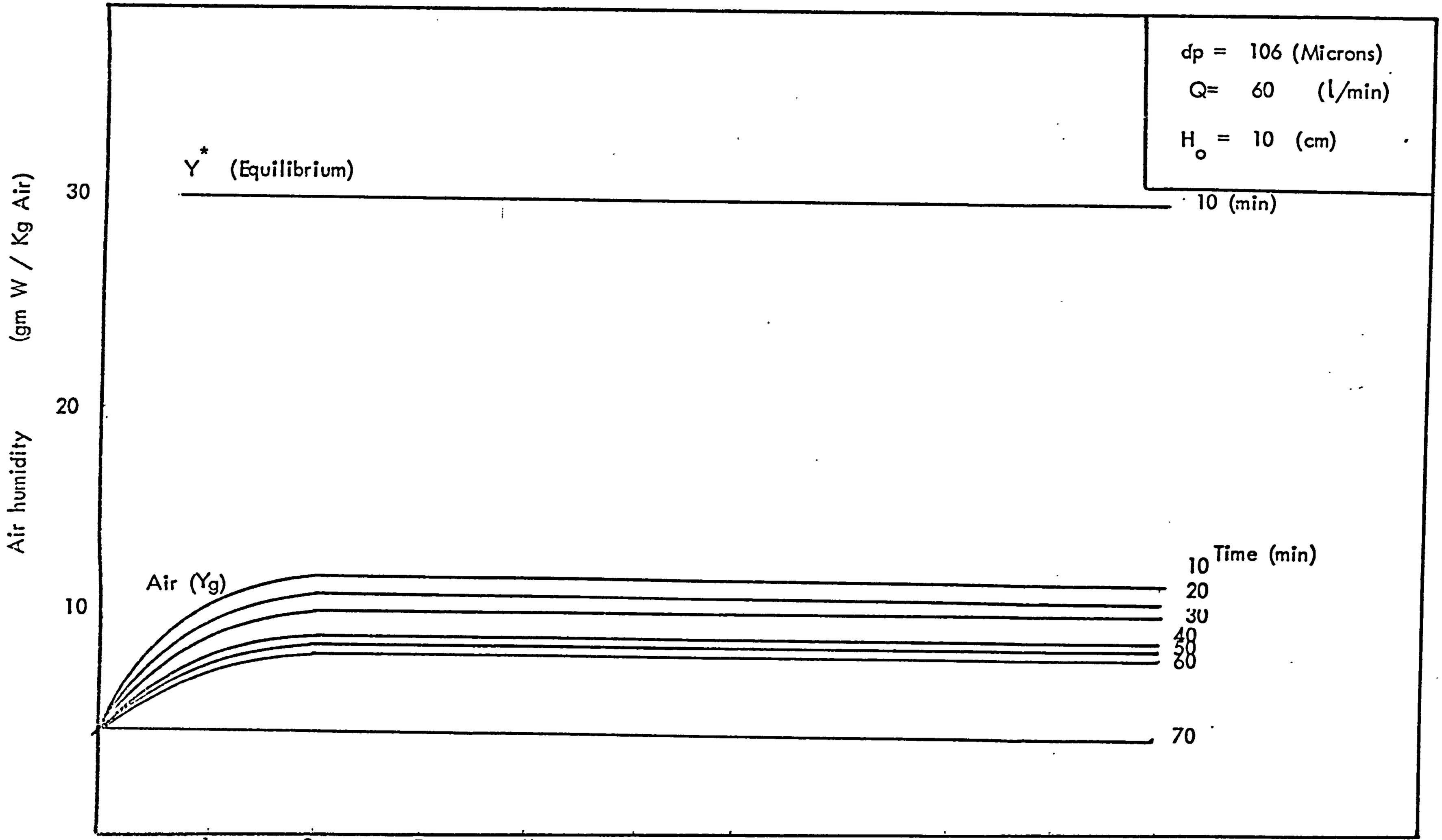
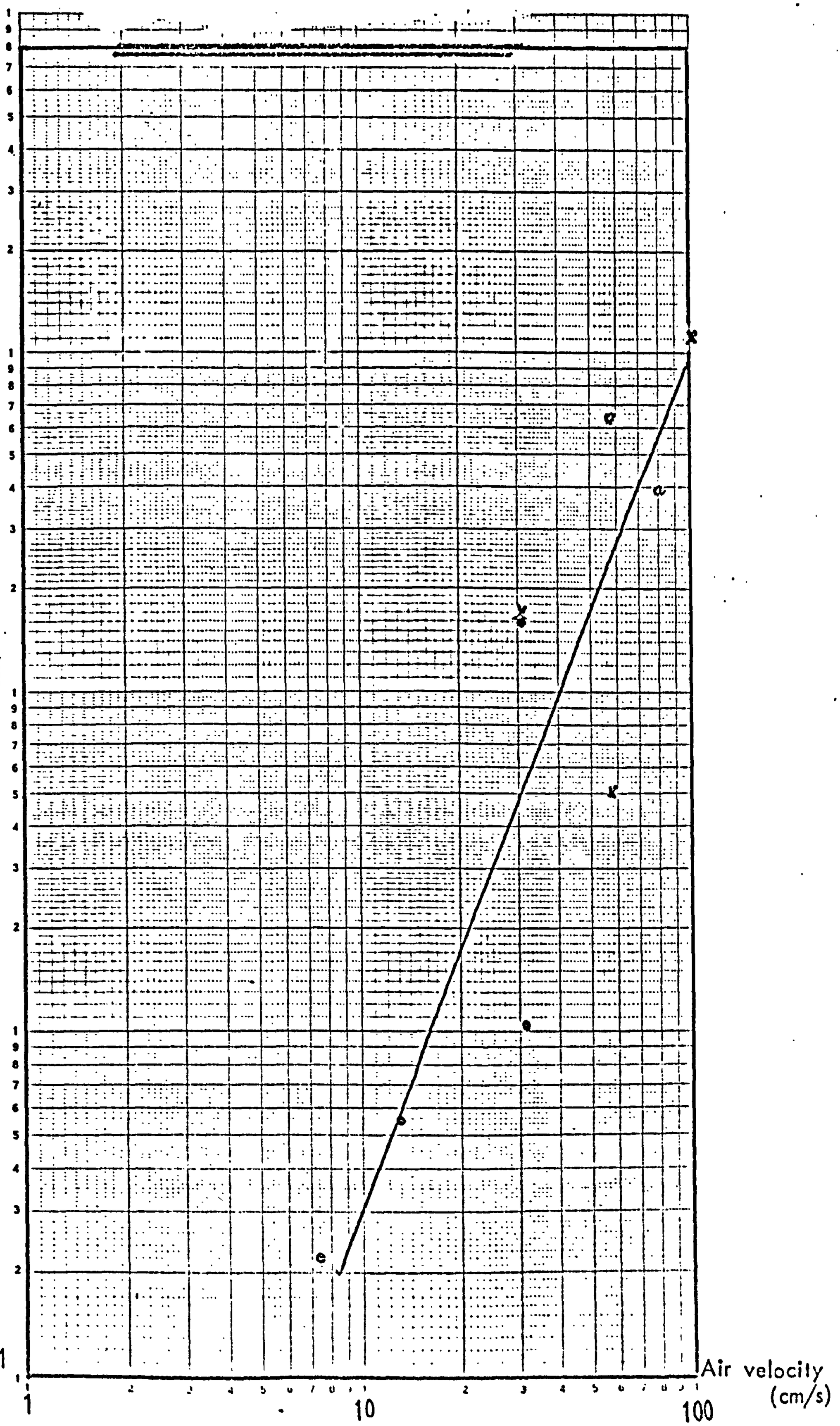


Figure (5-3)
Variation of air humidity with bed height

Figure (5-4)



Effect of air velocity on mass transfer

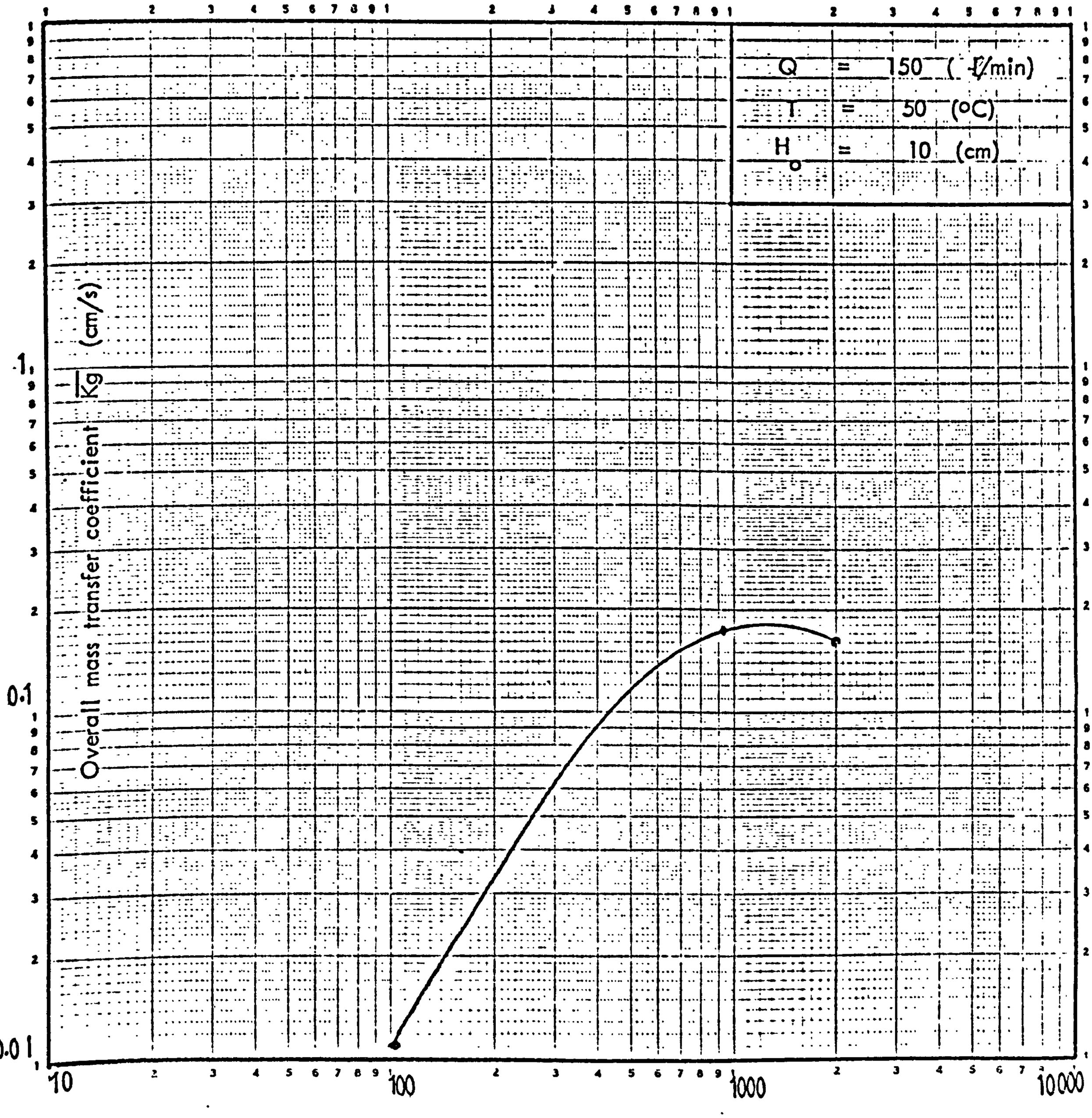


Figure (5-5)

Effect of particle size on mass transfer

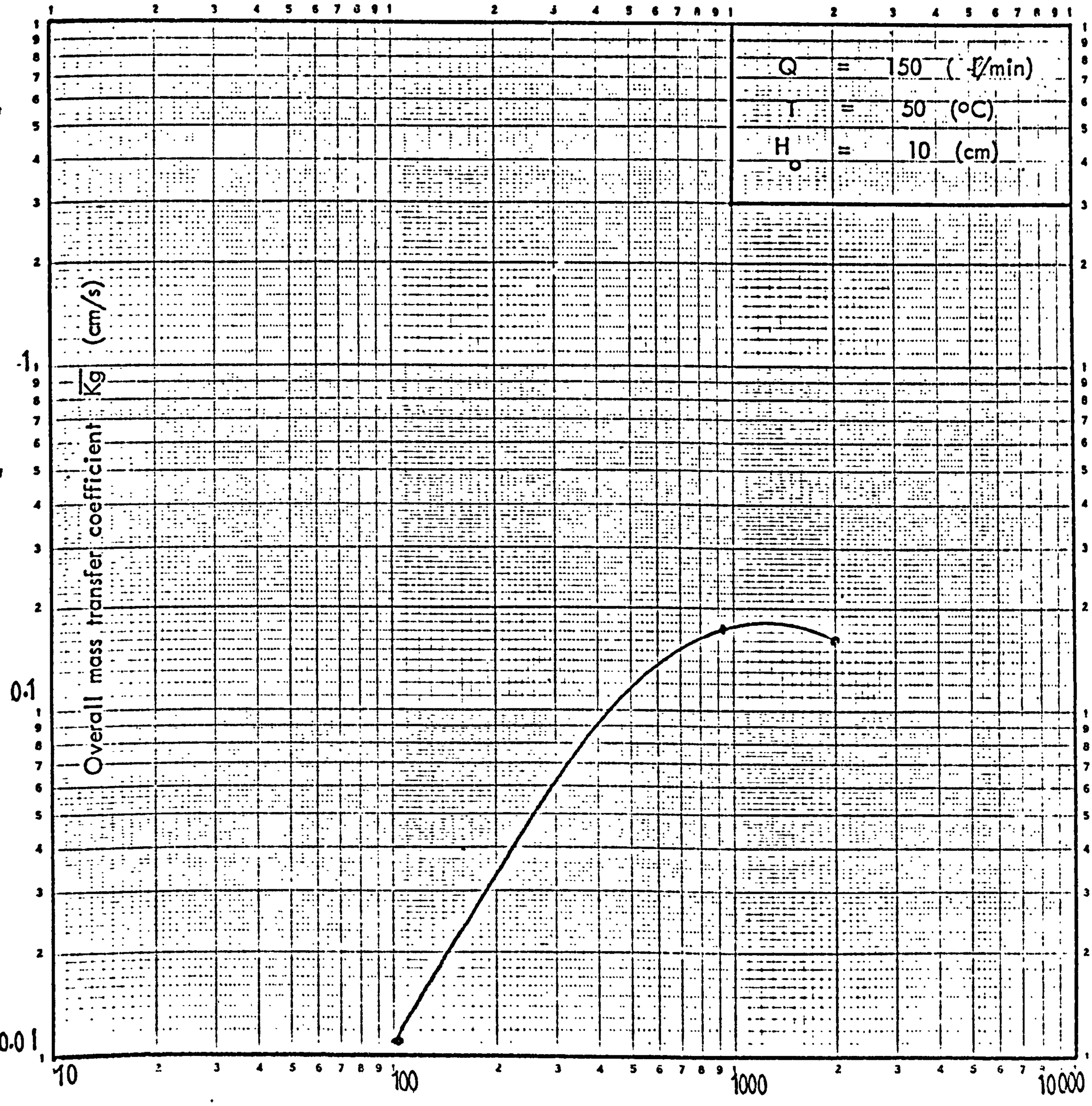


Figure (5-5)

Effect of particle size on mass transfer

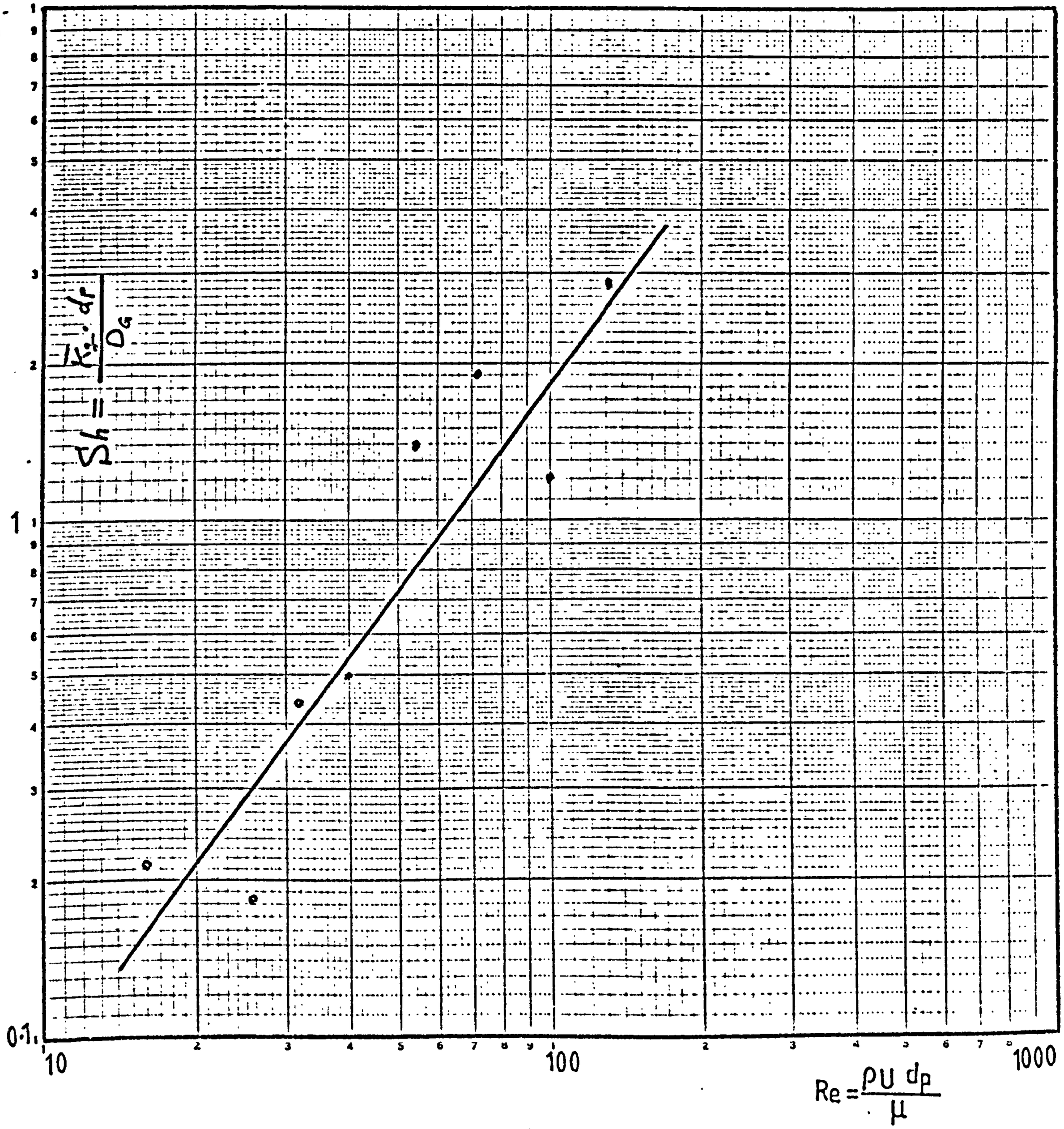


Figure (5-6)

Gas to particle mass transfer correlation

FIGURES (6)

SOLIDS DRYING CURVES

Figure (6-1) Silicagel hygrothermal Equilibrium Curve.

Figure (6-2) Non-Hygroscopic Capillary Porous Solids

Figure (6-3) Hygroscopic Porous Capillary Solids

Figure (6-4) Hygroscopic Non-Porous Solids

Figure (6-5) Effect of Bed Height on Drying Curves

Figure (6-6) Effect of (H_o/D) on Solids Drying Rates

Figure (6-7) Effect of Air Flowrate on Drying Curves - dp = 106 Microns

Figure (6-8) Effect of Air Flowrate on Drying Curves - dp = 940 Microns

Figure (6-9) Effect of Air Flowrate on Drying Curves - dp =2247 Microns

Figure (6-10) Effect of Air Flowrate on Solids Drying Rates

Figure (6-11) Effect of Air Flowrate on Drying Curves - T = 40 °C

Figure (6-12) Effect of Air Flowrate on Drying Curves - T = 60 °C

Figure (6-13) Effect of Air Flowrate on Drying Curves - T = 80 °C

Figure (6-14) Effect of Air Flowrate on Drying Curves - T =100 °C

Figure (6-15) Effect of Air Flowrate on Drying Rates

Figure (6-16) Effect of Particle Size on Drying Curves - Q = 150 l/min

Figure (6-17) Effect of Particle Size on Drying Curves - Q = 275 l/min

Figure (6-18) Effect of Particle Size on Drying Curves - Q = 500 l/min

Figure (6-19) Relationship between Particle Size and Drying Rates

CONT

Figure (6-20) Effect of Temperature on Drying Curves - Q = 150 l/min

Figure (6-21) Effect of Temperature on Drying Curves - Q = 275 l/min

figure (6-22) Effect of Temperature on Drying Curves - Q = 400 l/min

Figure (6-23) Effect of Temperature on Drying Curves - Q = 500 l/min

Figure (6-24) Relationship between Temperature and Drying Rates

Figure (6-25) Effect of Prandtl Number on Drying Rates

Figure (6-26) Effect of $(N.T.U.)_B$ on Drying Rates

Figure (6-27) Solids Drying Rates Correlations

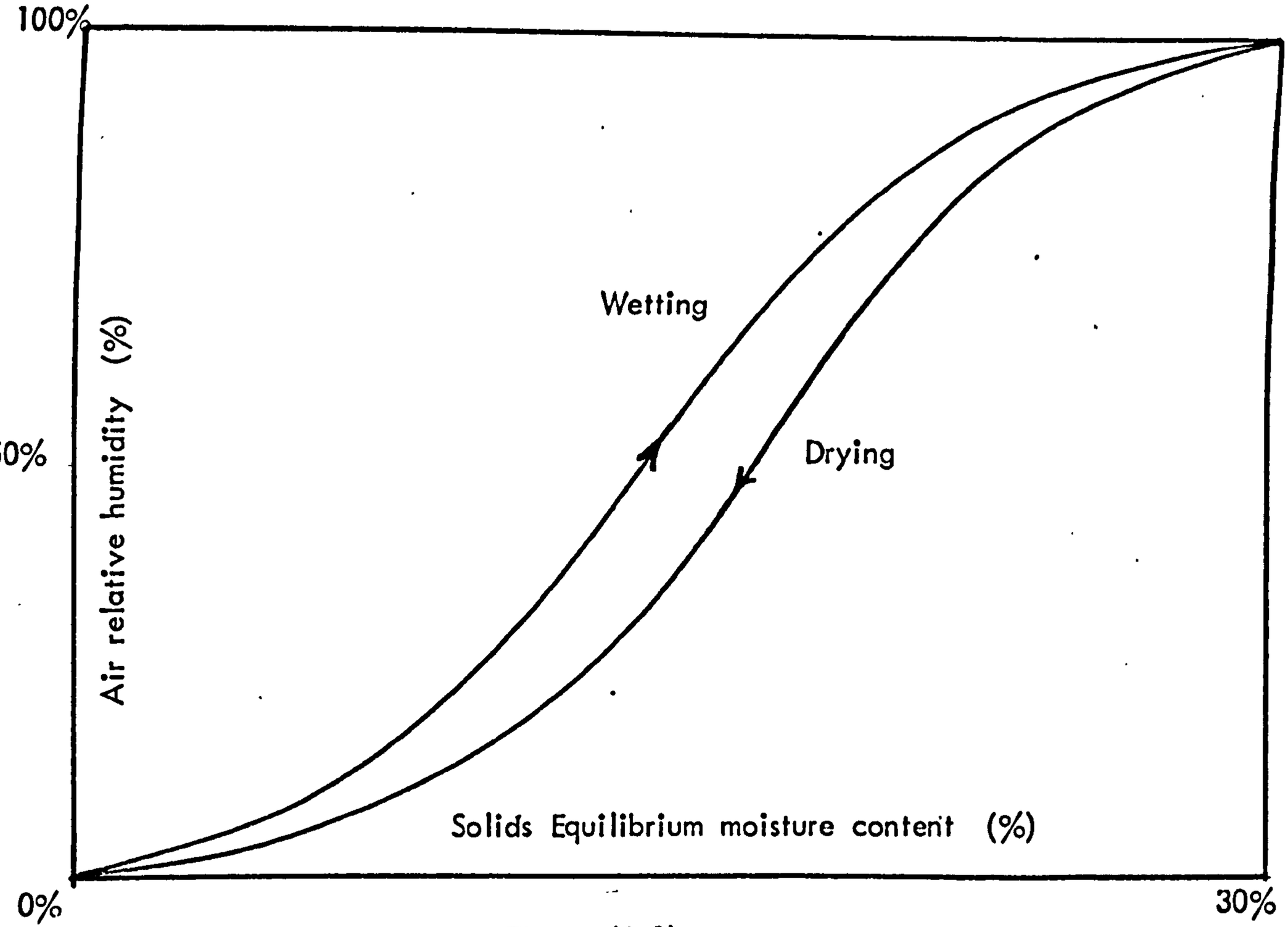


Figure (6-1)

Silica gel hygrothermal equilibrium curve

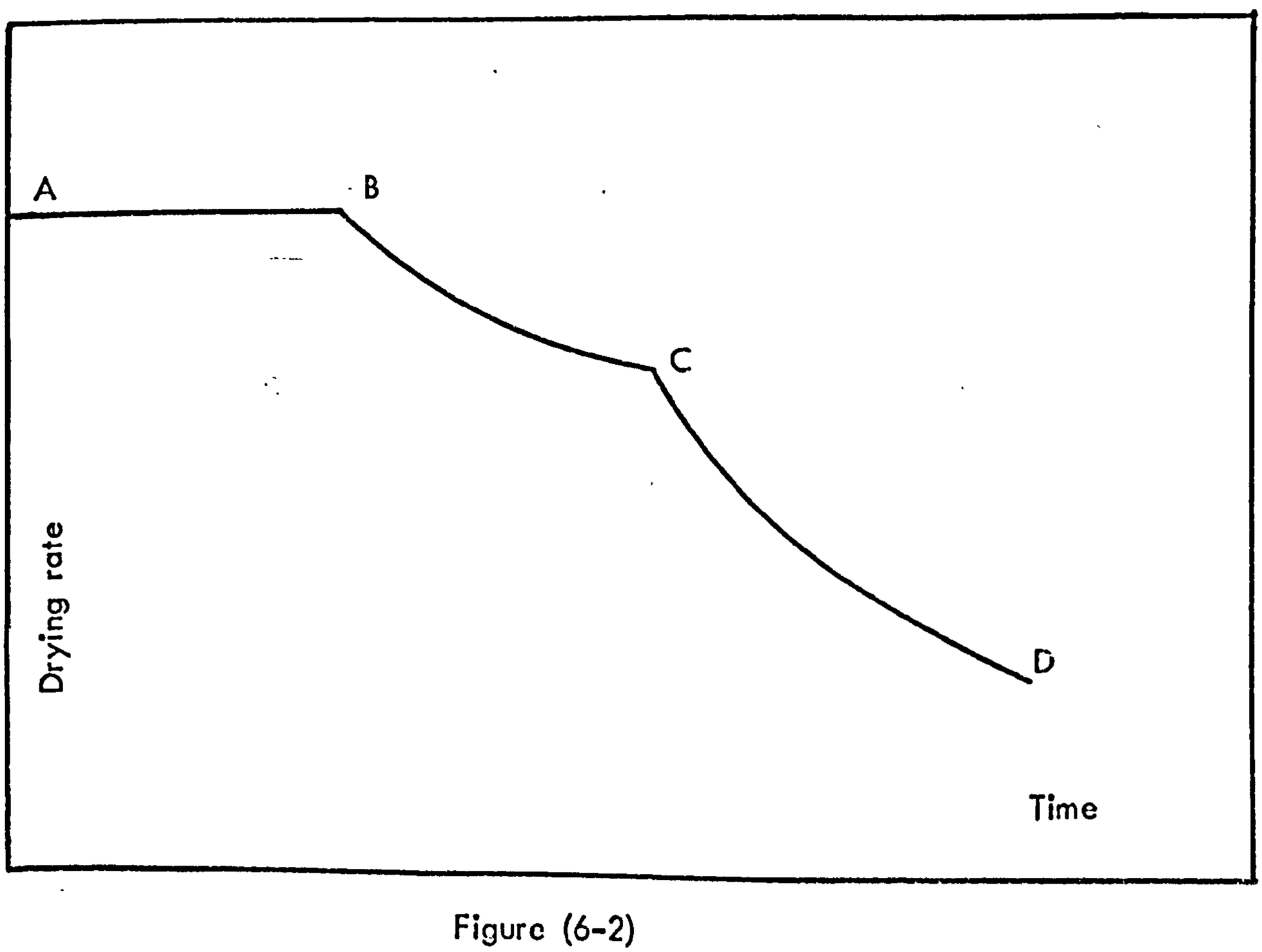


Figure (6-2)
Non-hygroscopic capillary solids

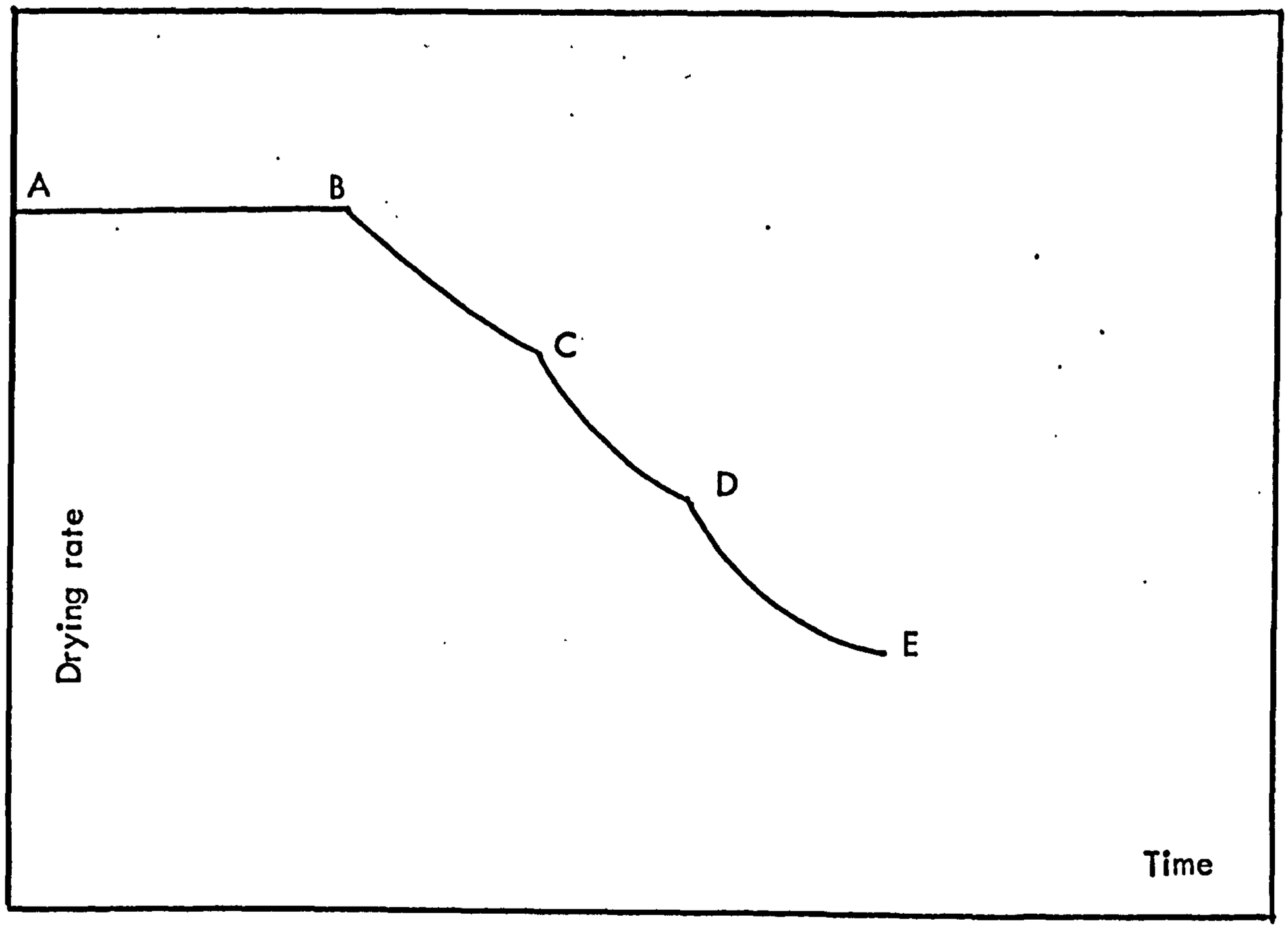


Figure (6-3)

Hygroscopic Porous capillary solids

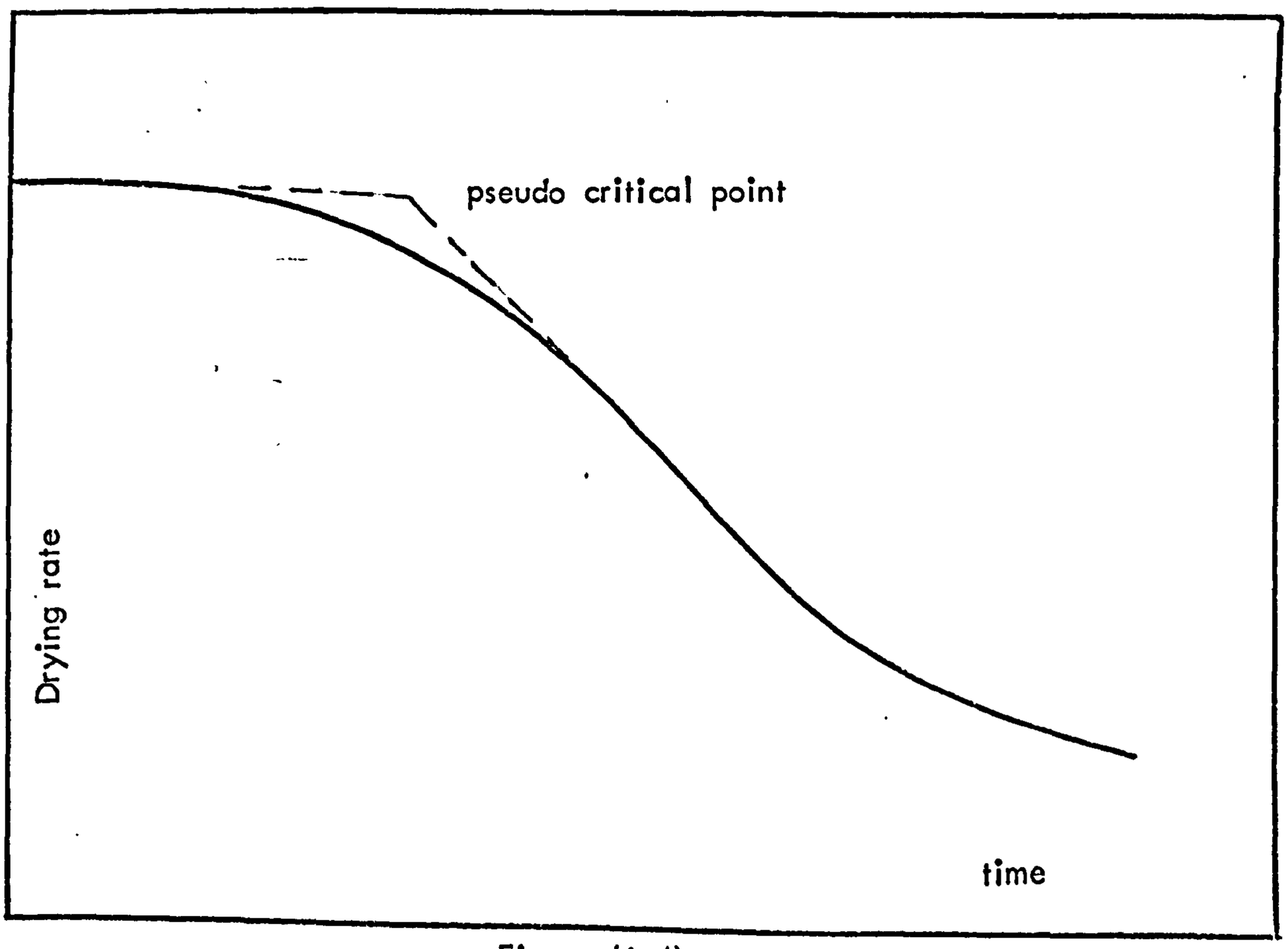


Figure (6-4)

Hygroscopic non-porous solids

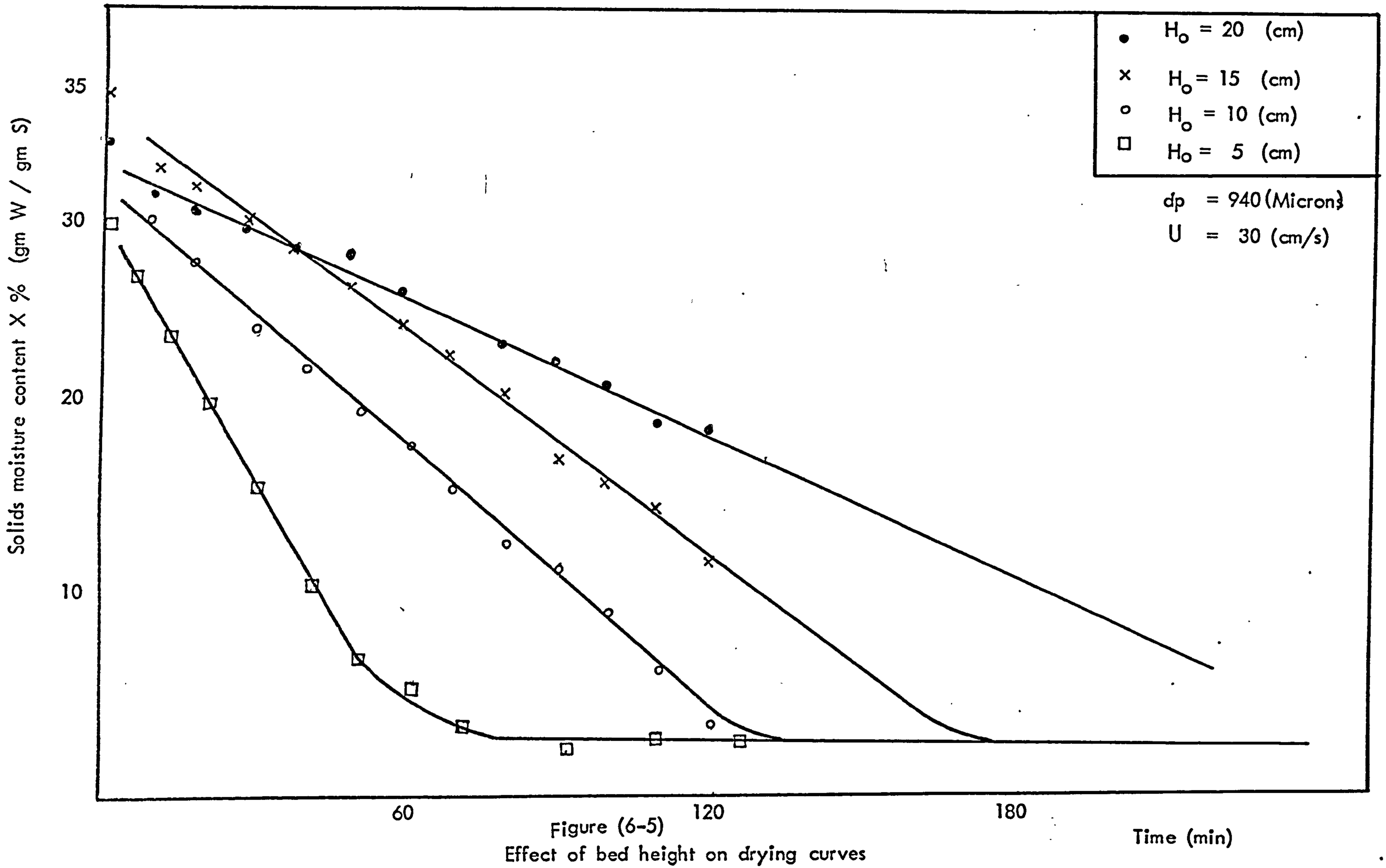


Figure (6-5)
Effect of bed height on drying curves

Drying rate $R \times 10^3 \left[\frac{\text{gm W}}{\text{gm S}}/\text{min}\right]$

Height over diameter ratio (H_o/D)

Effect of (H_o/D) on solids drying rate

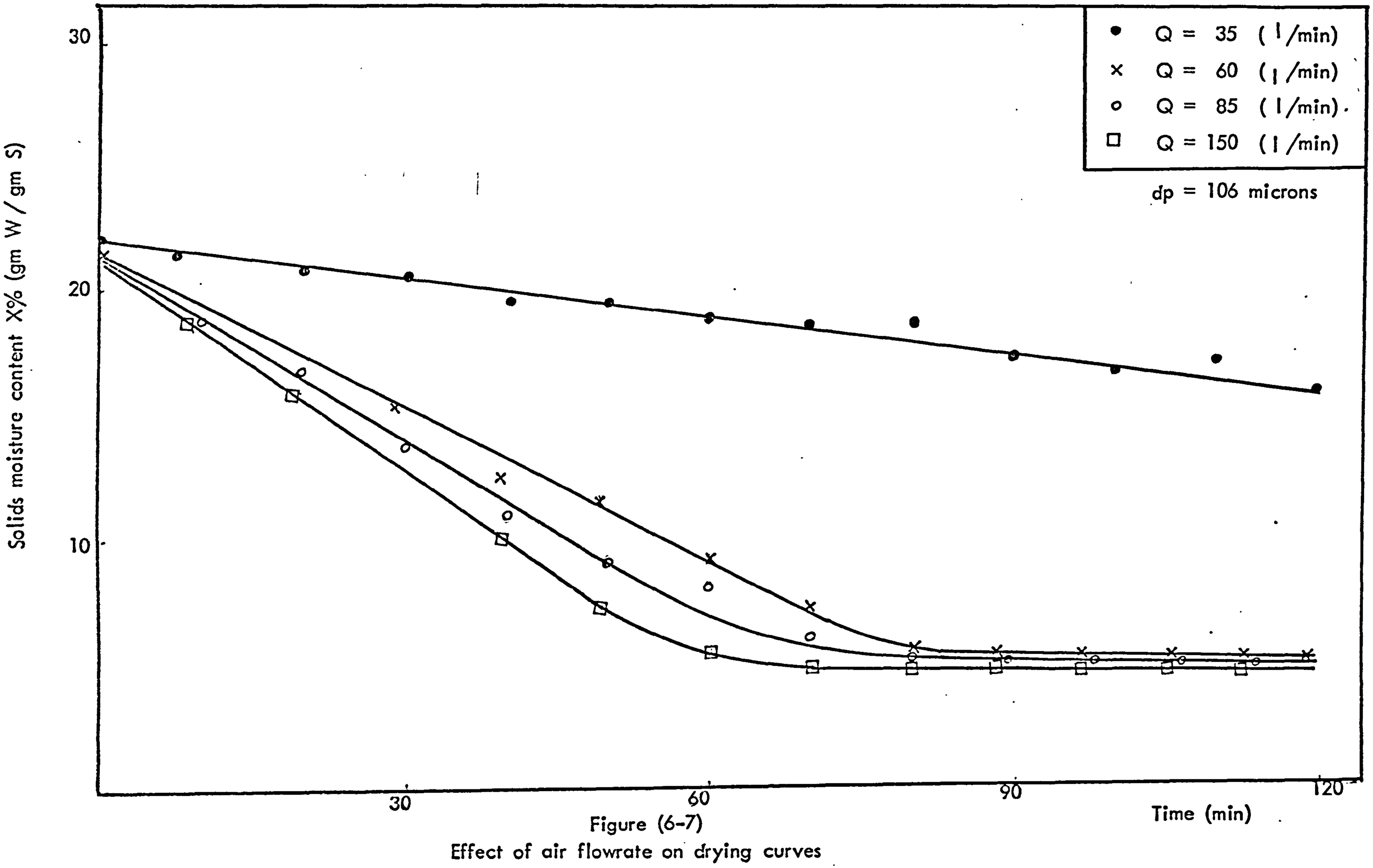


Figure (6-7)
Effect of air flowrate on drying curves

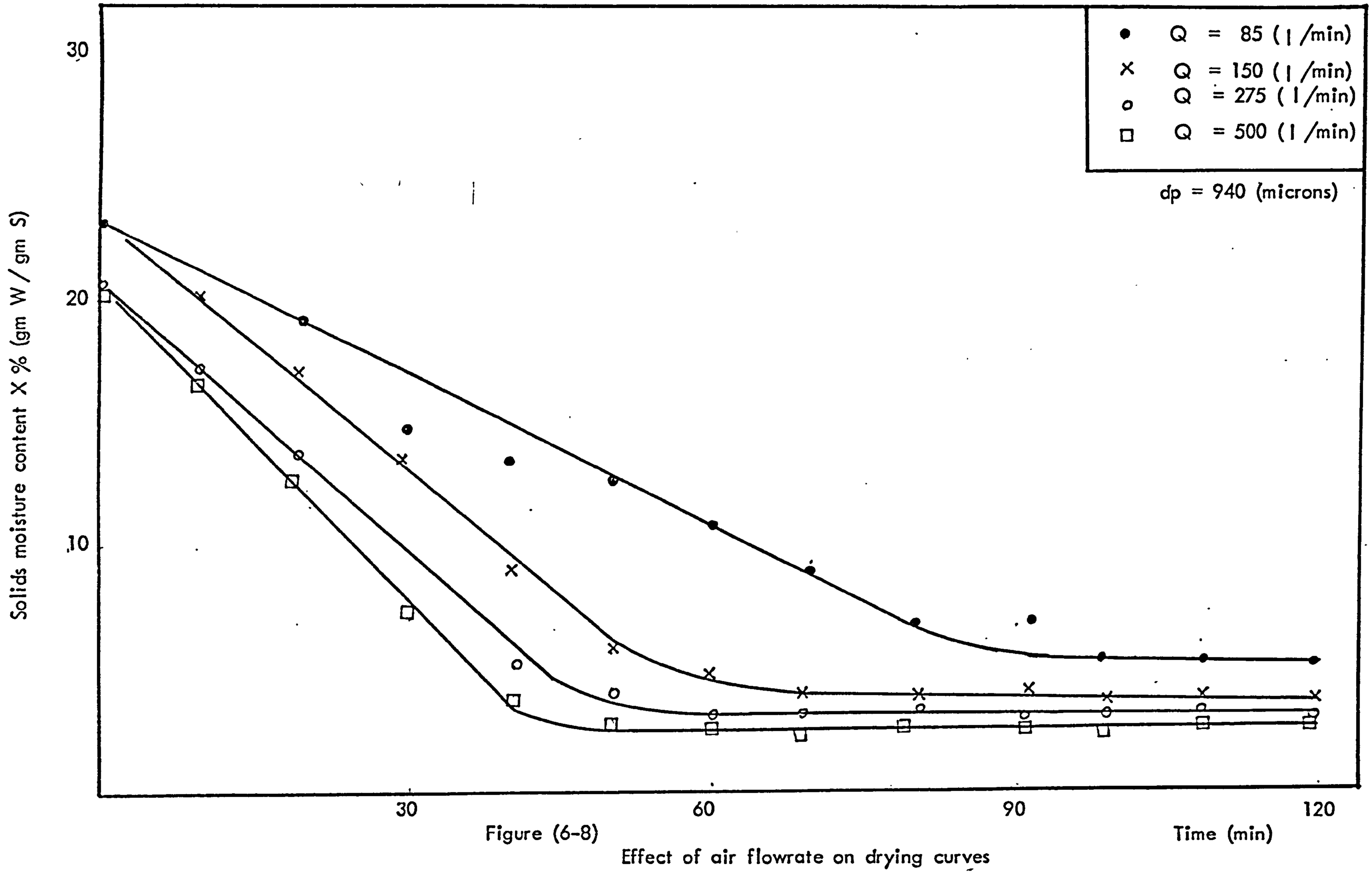


Figure (6-8)

Effect of air flowrate on drying curves

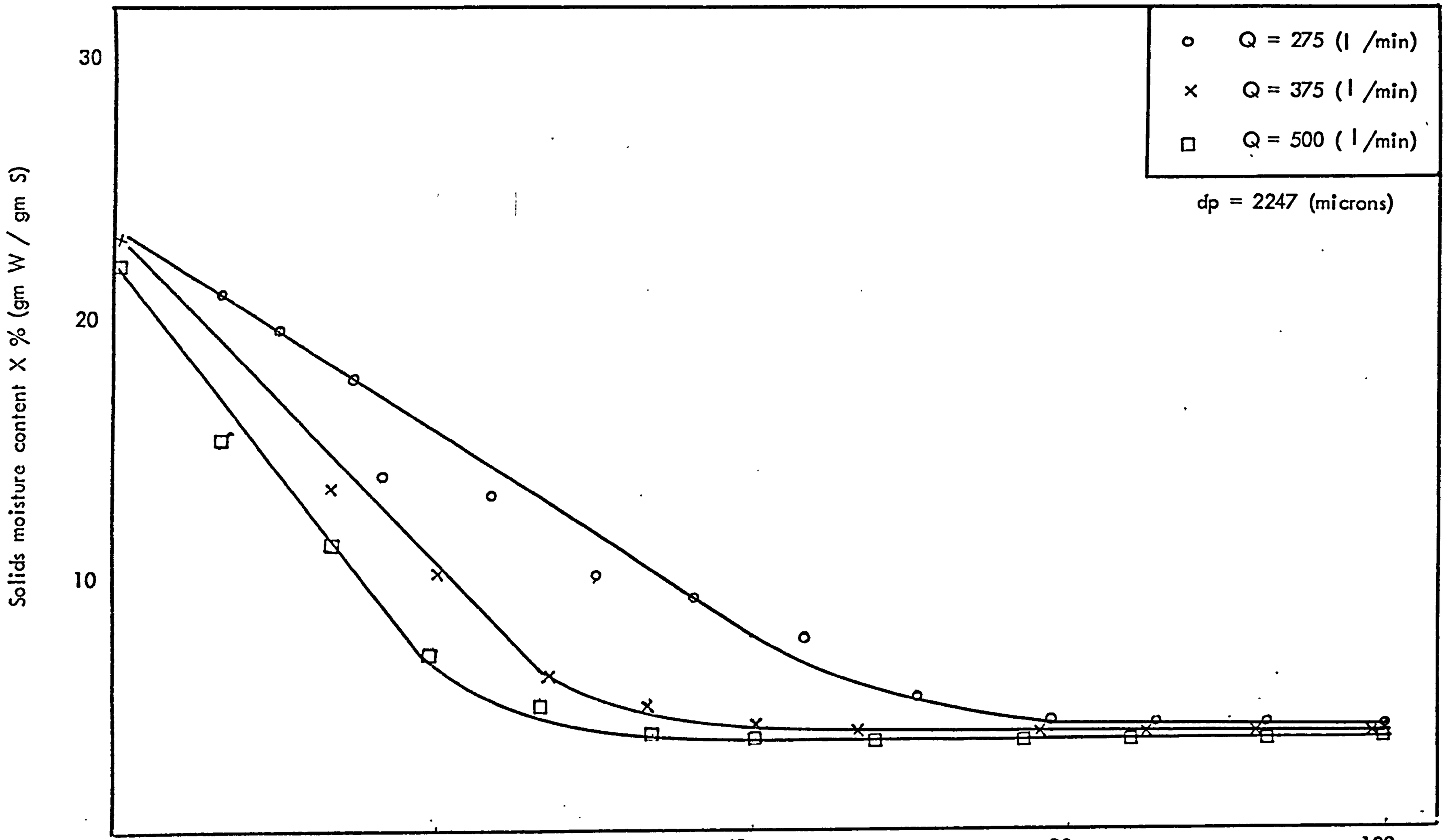
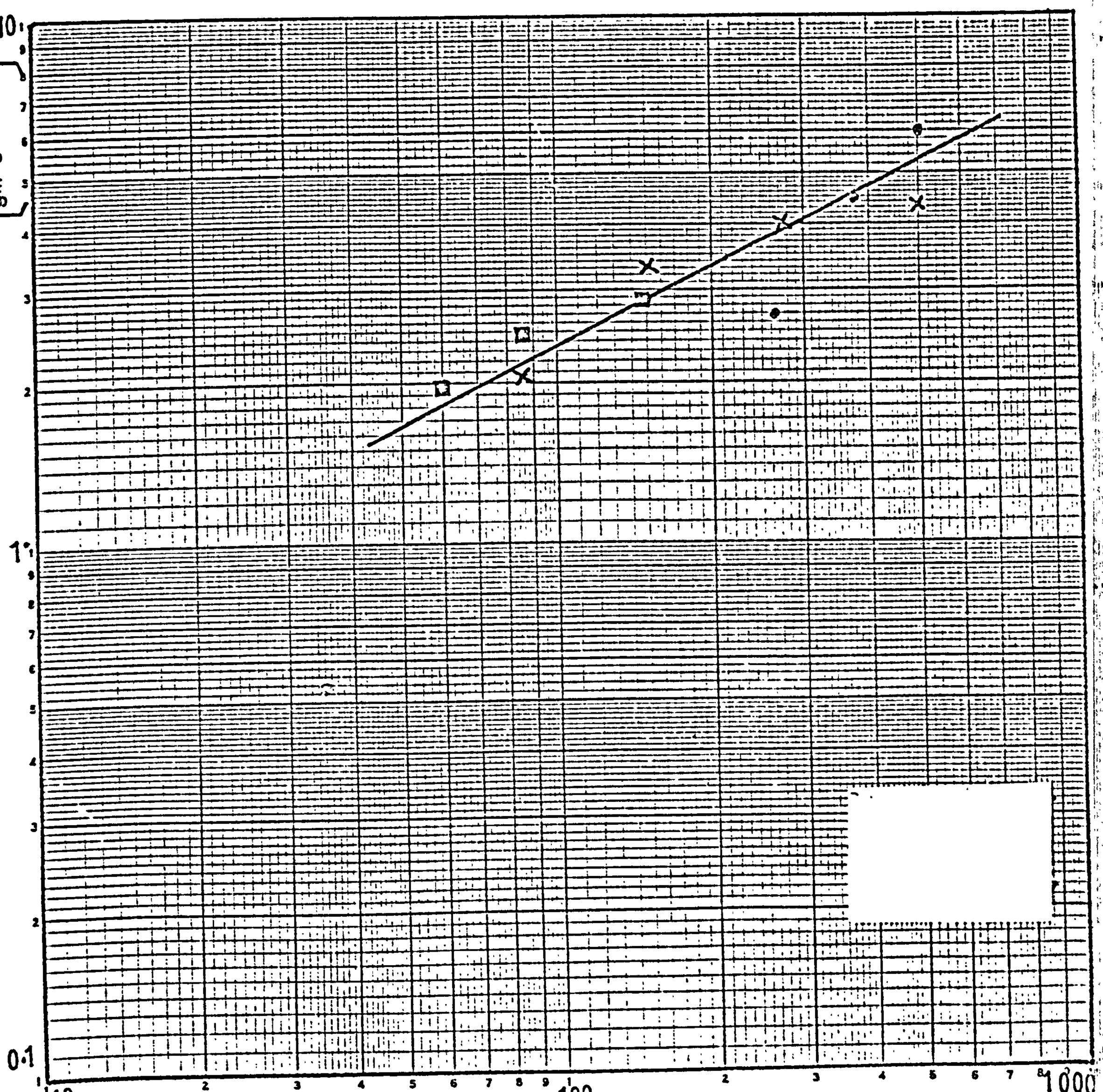


Figure (6-9)
Effect of air flowrate on drying curves

Figure (6-10)

Effect of air flowrate on solids drying rates



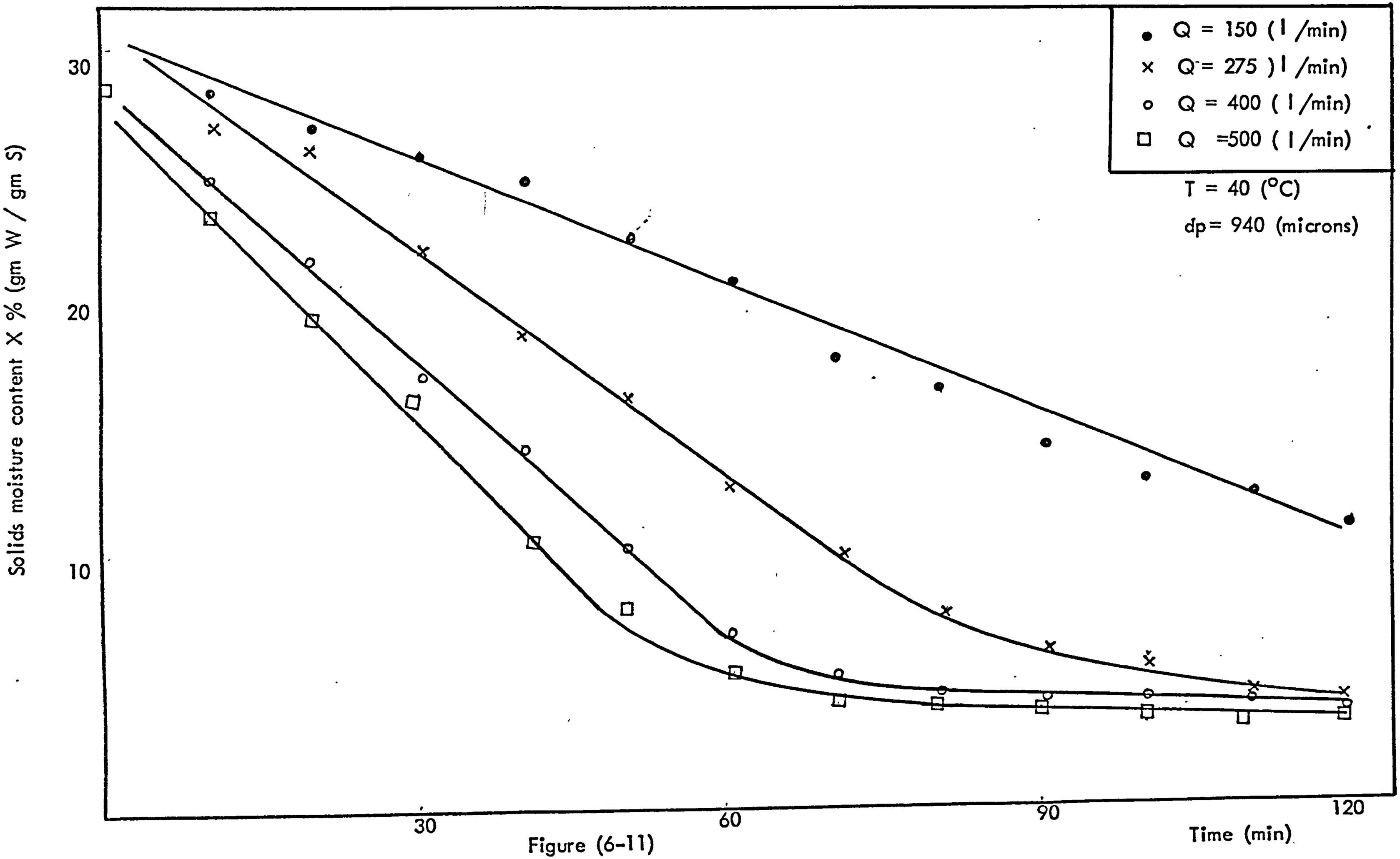


Figure (6-11)

Effect of air flowrate on drying curves

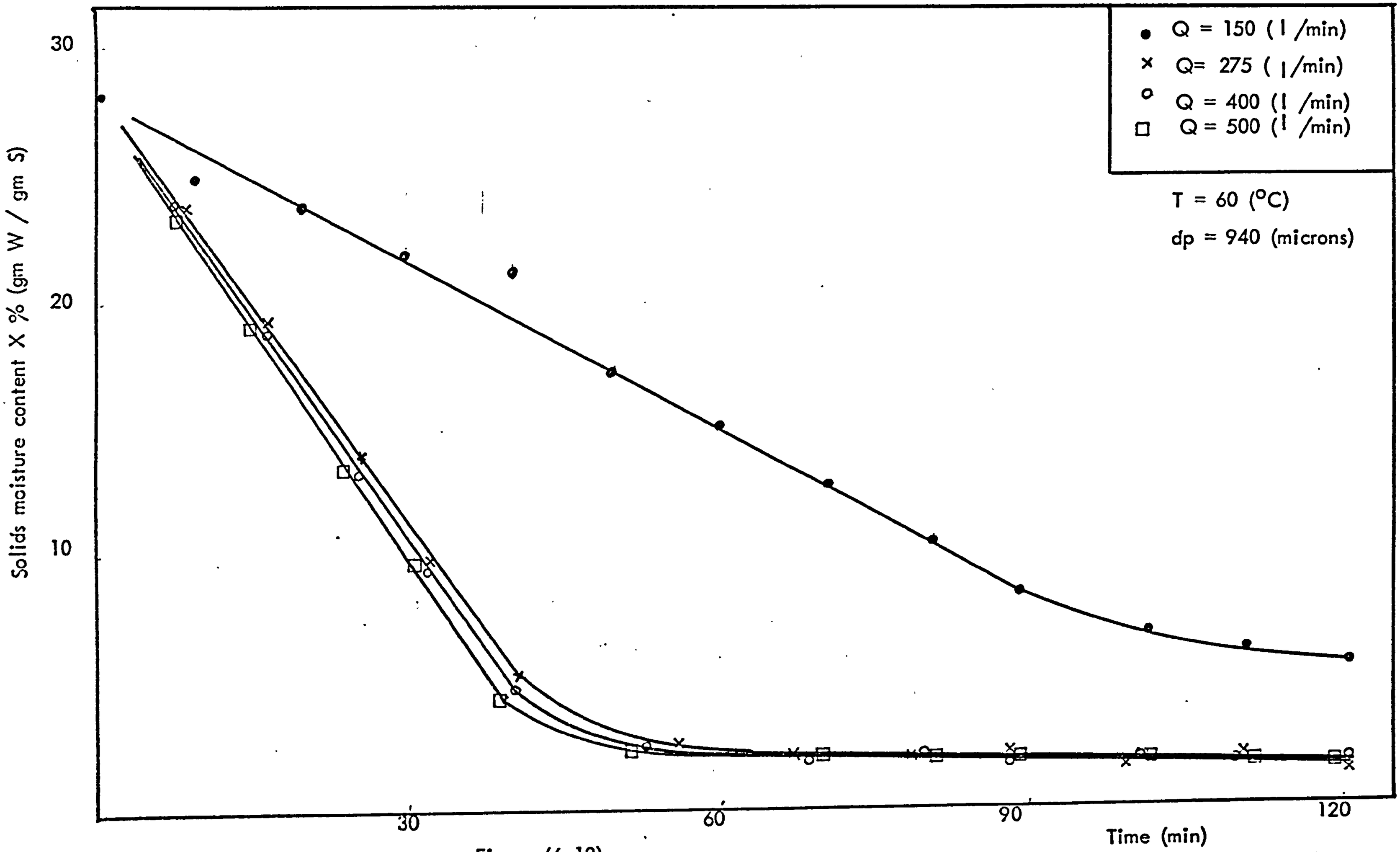


Figure (6-12)

Effect of air flowrate on drying curves

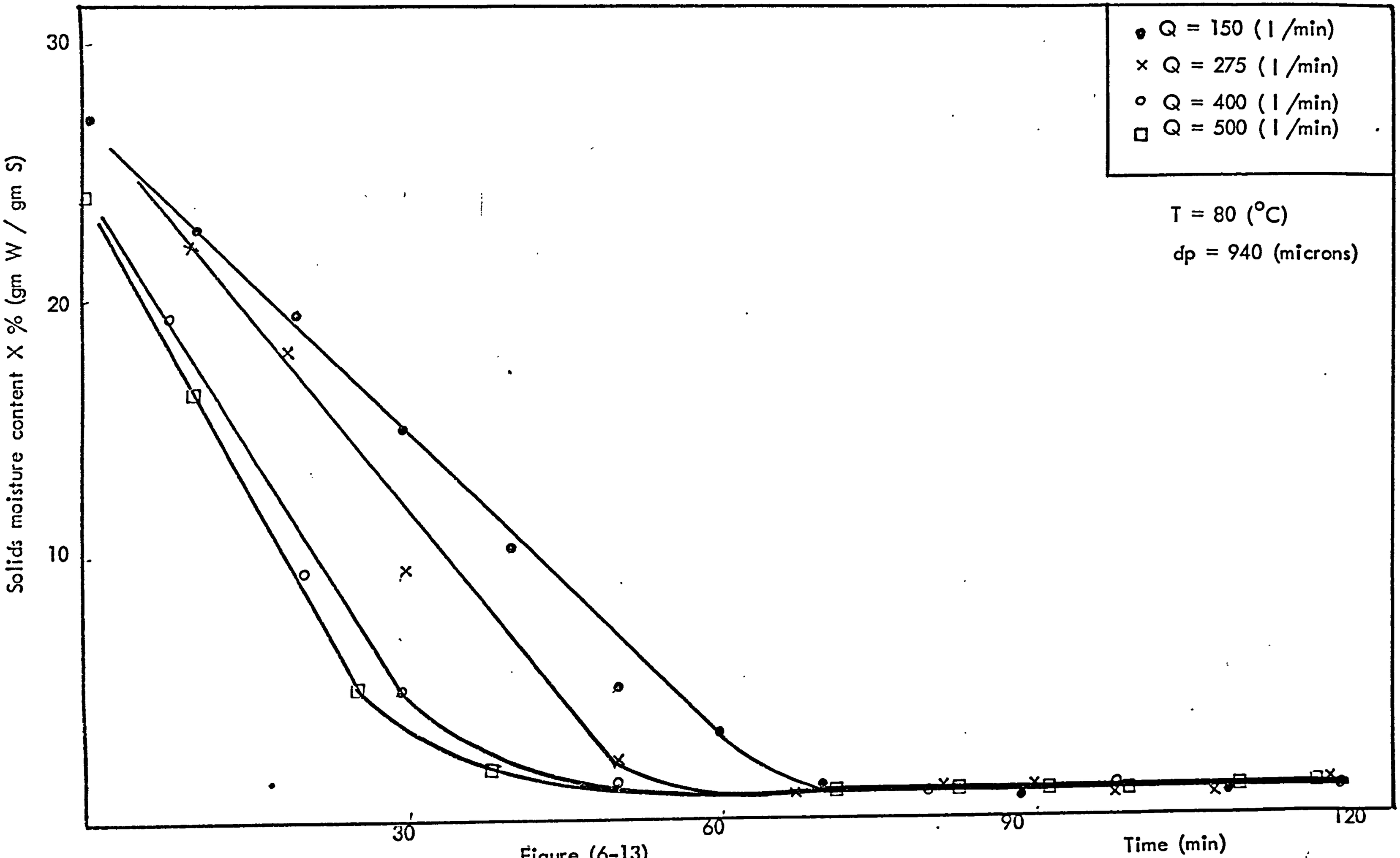


Figure (6-13)
Effect of air flowrate on drying curves

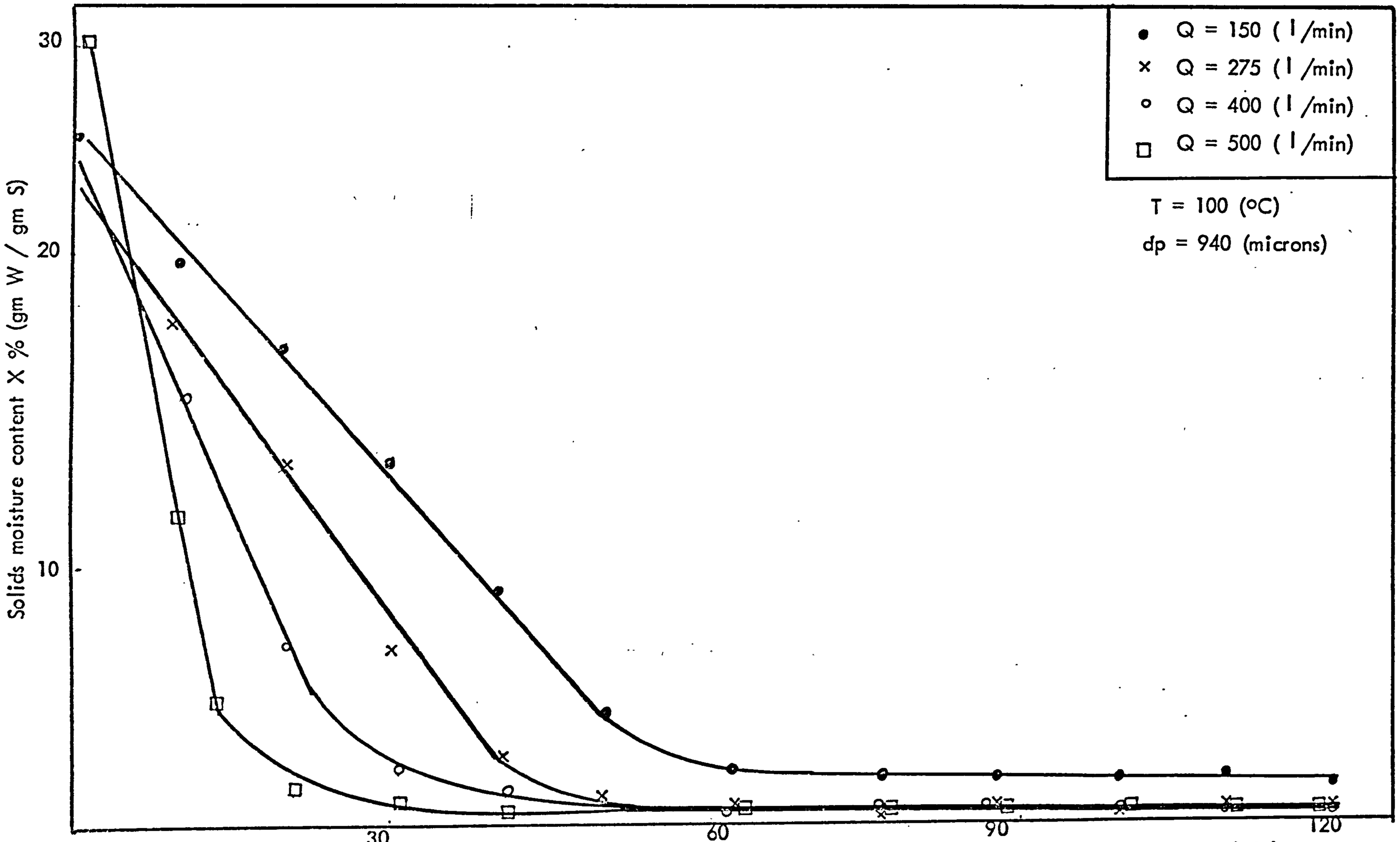


Figure (6-14)
Effect of air flowrate on drying curves

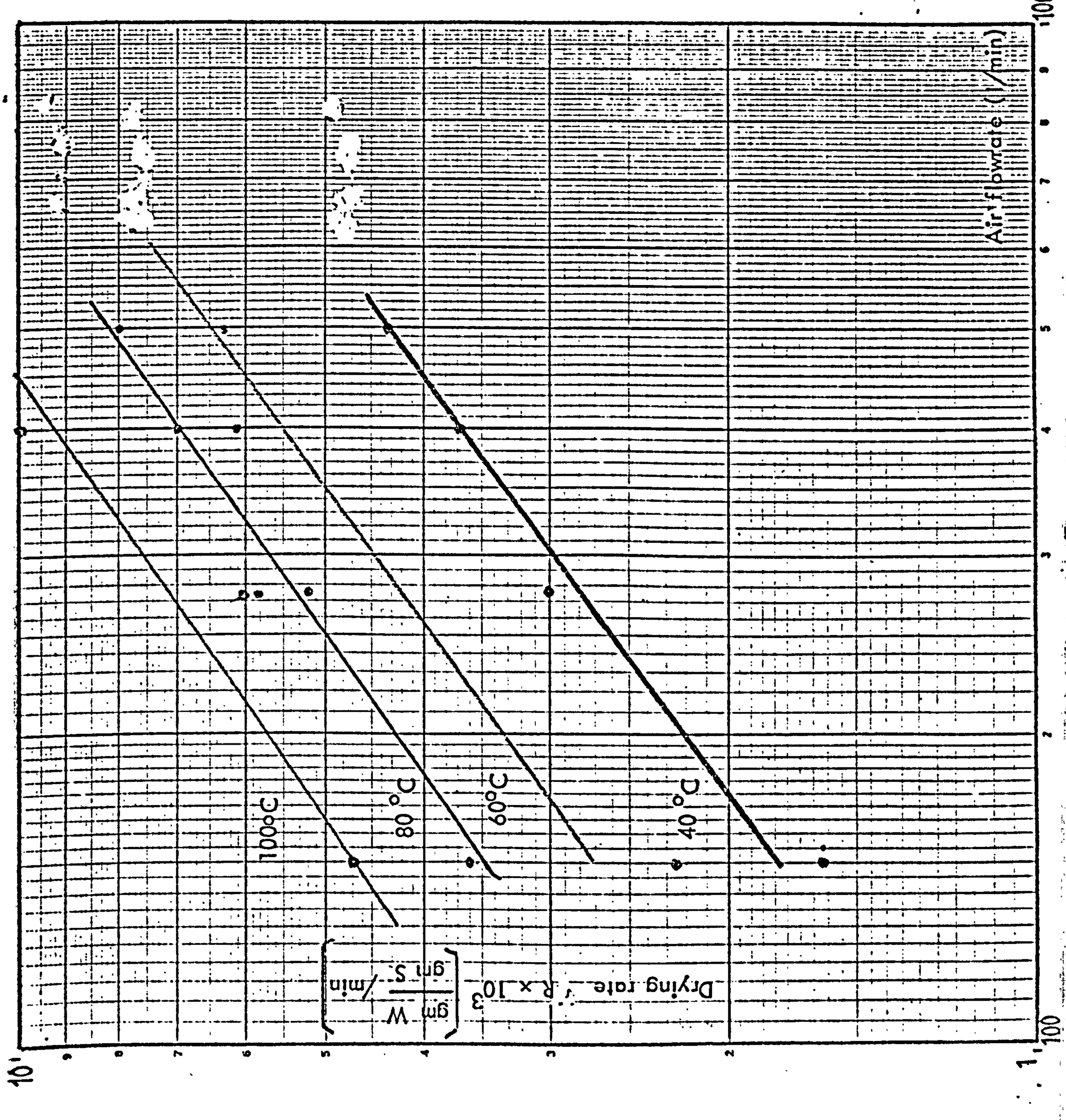


Figure (6-15)

Effect of air flowrate on solids drying rate

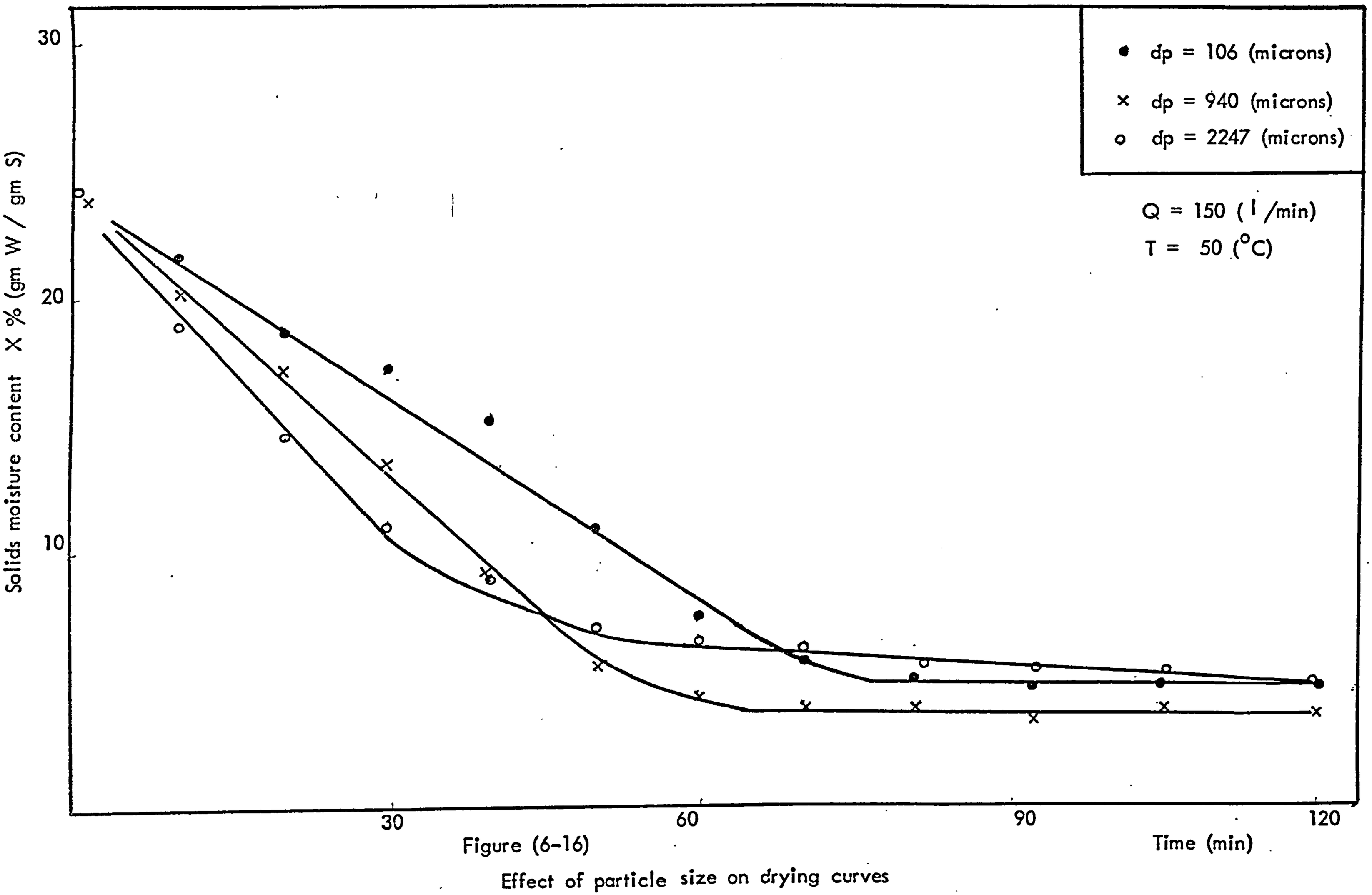


Figure (6-16)

Effect of particle size on drying curves

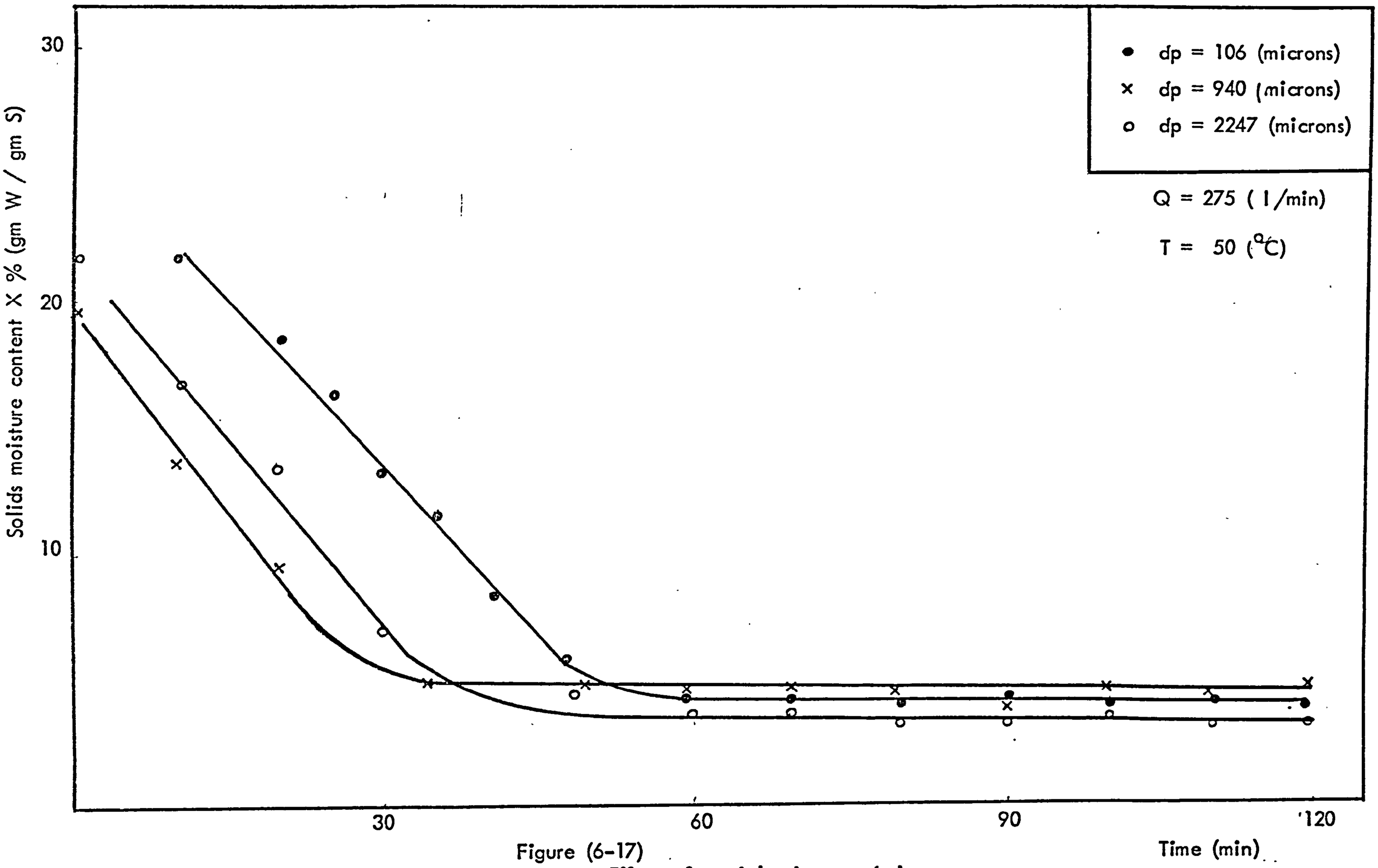


Figure (6-17)
Effect of particle size on drying curves

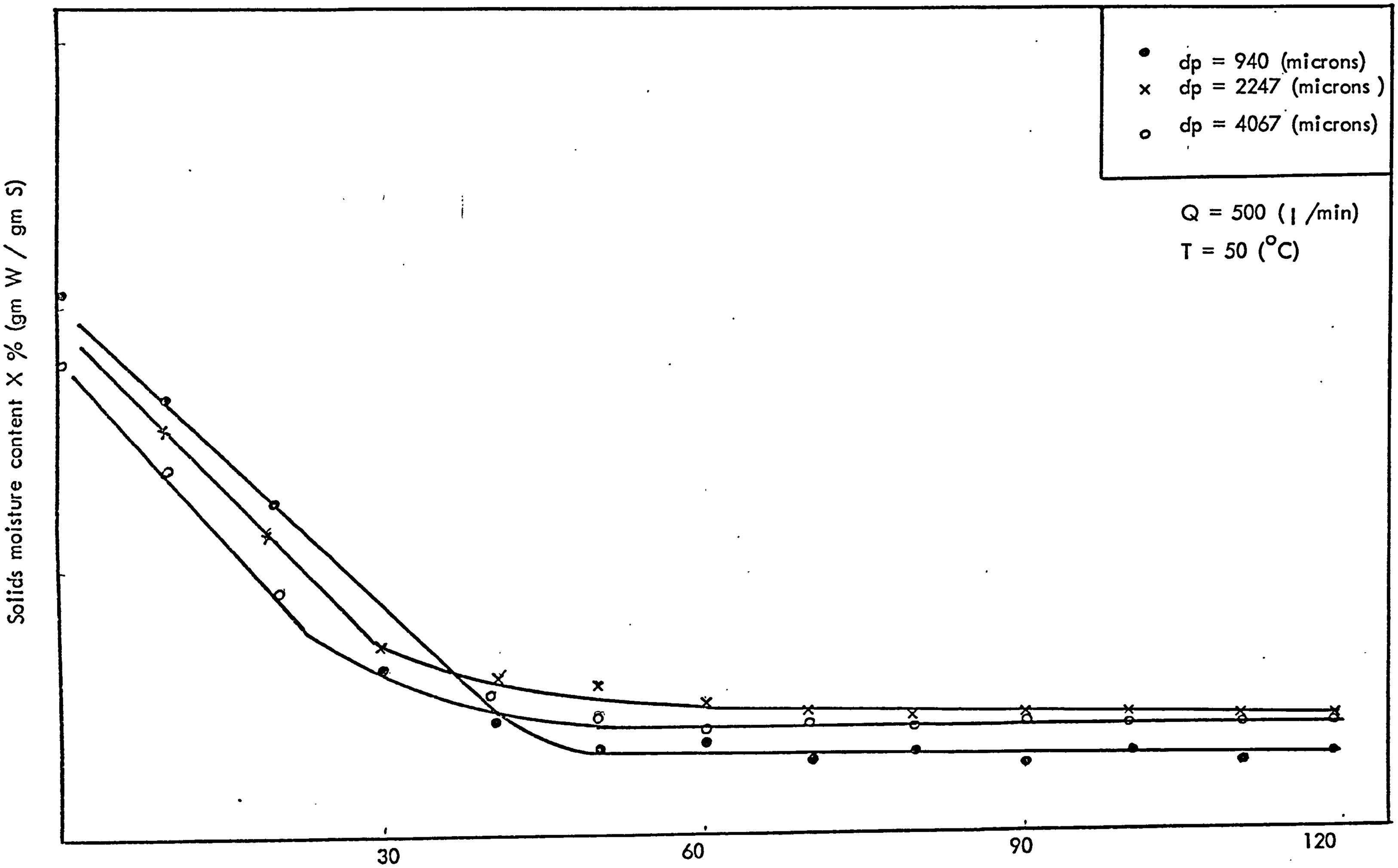
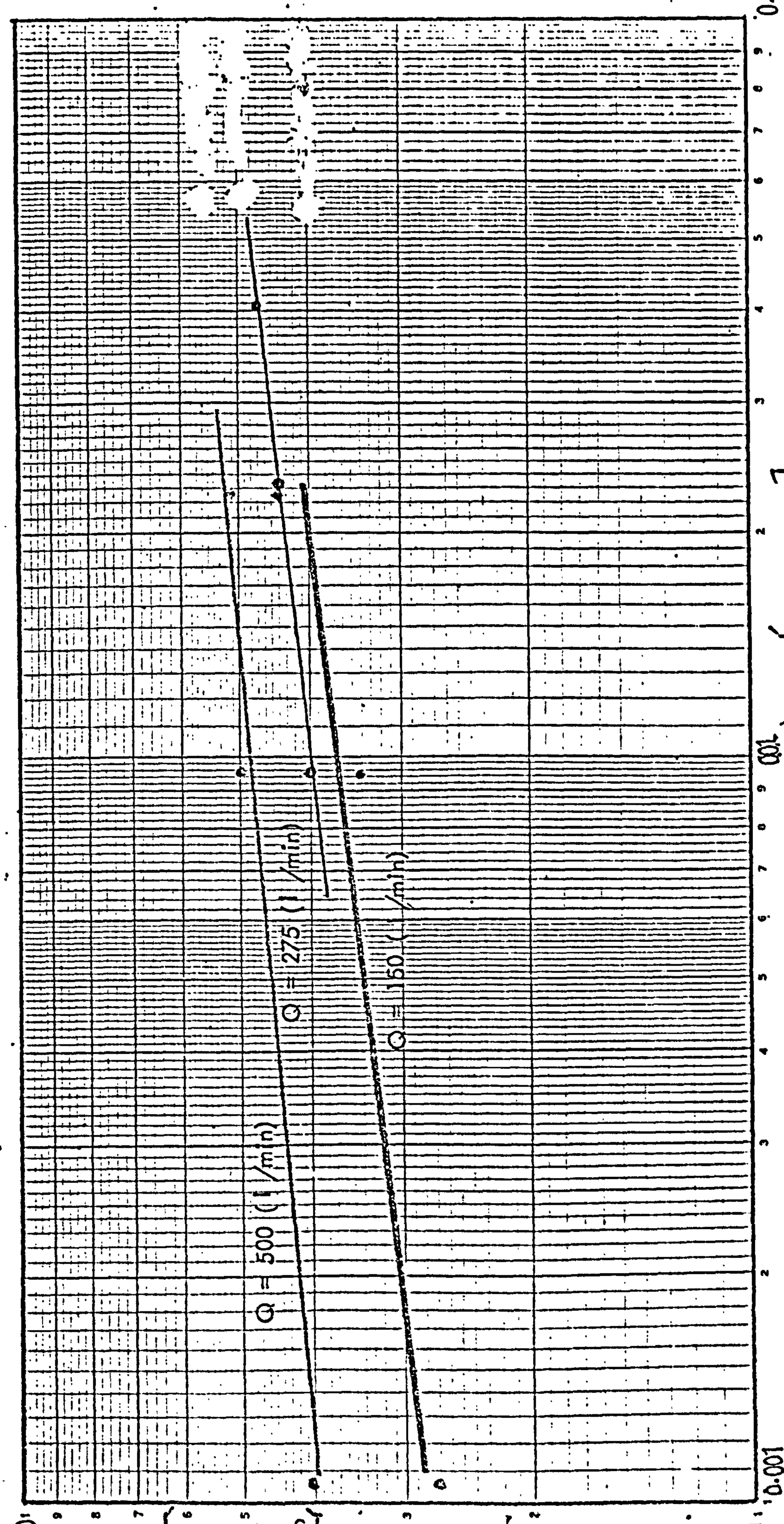


Figure (6-18)
Effect of particle size on drying curves

Figure (6-19)

Relationship between particle size and drying rates



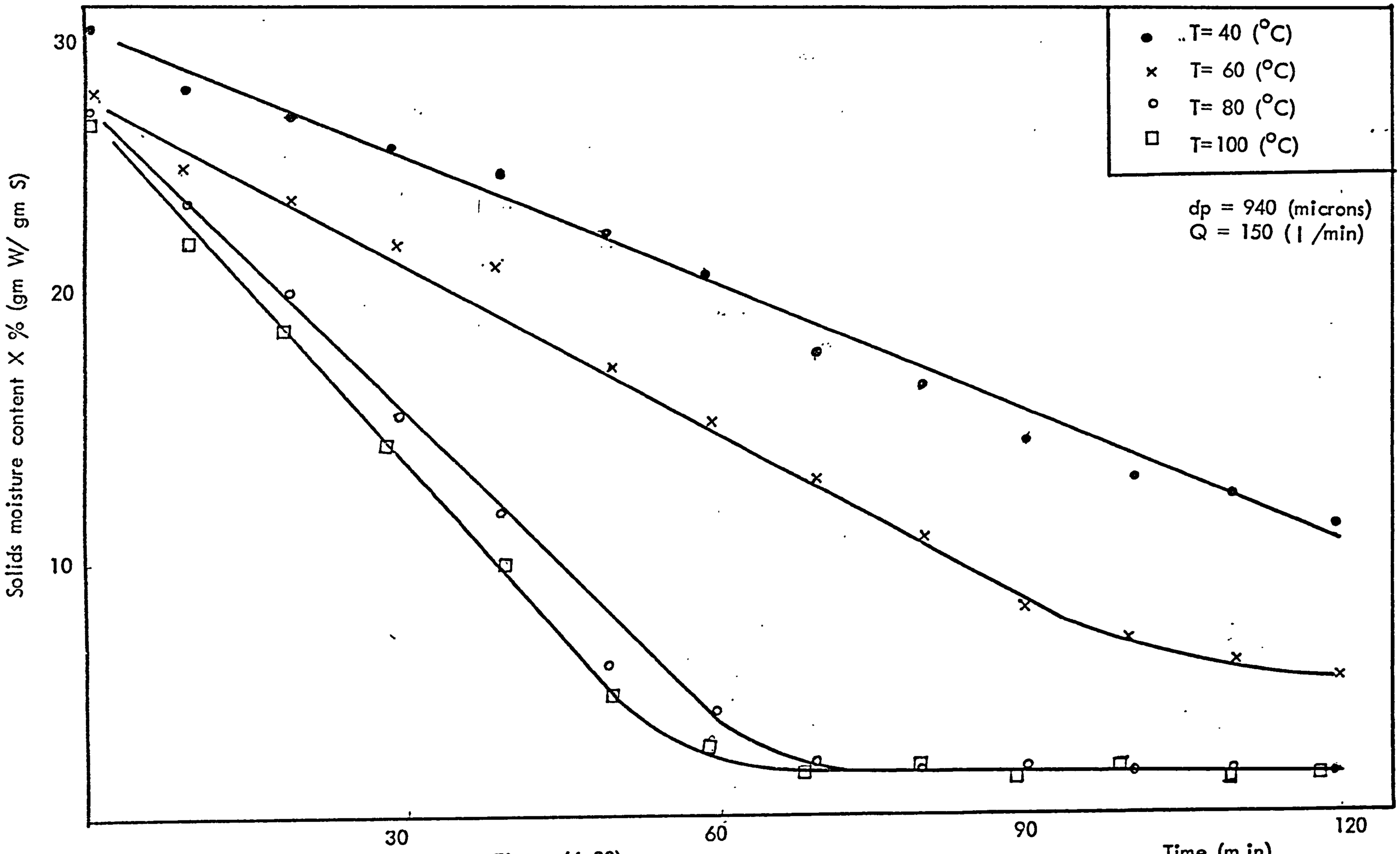


Figure (6-20)

Effect of temperature on drying curves

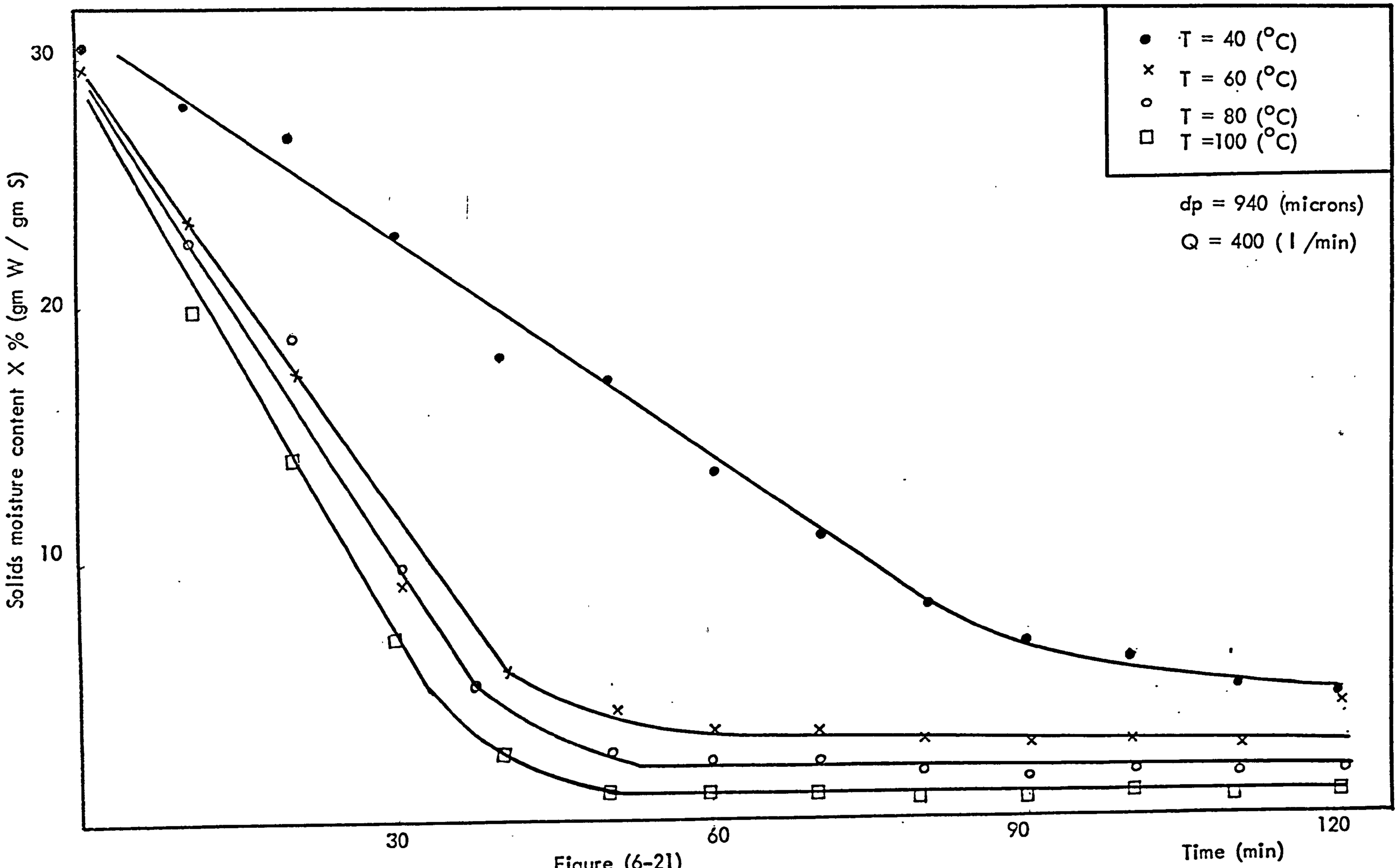


Figure (6-21)
Effect of temperature on drying curves

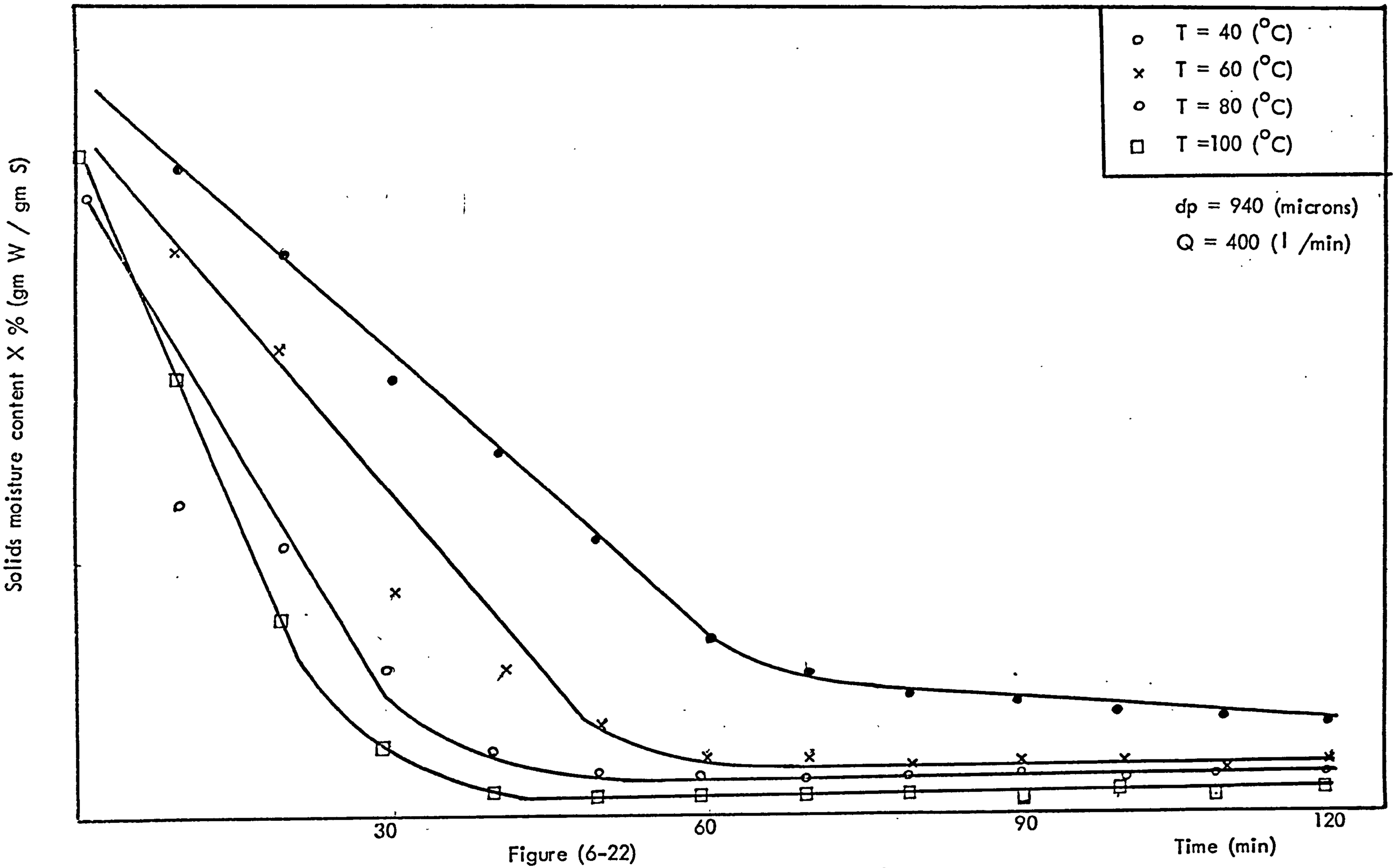


Figure (6-22)
Effect of temperature on drying curves

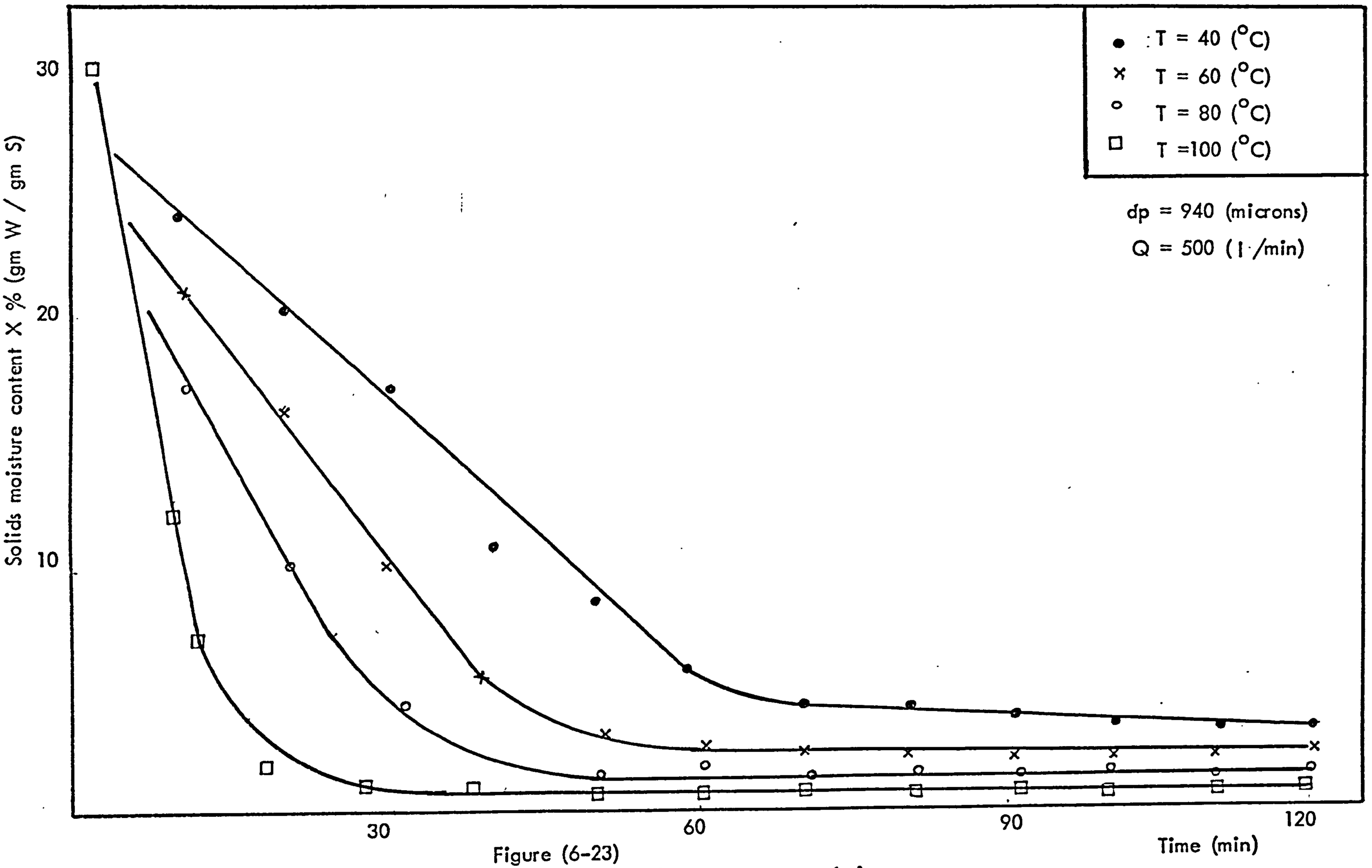


Figure (6-23)
Effect of temperature on drying curves

Figure (6-24)

Relationship between bed temperature and solids drying rate

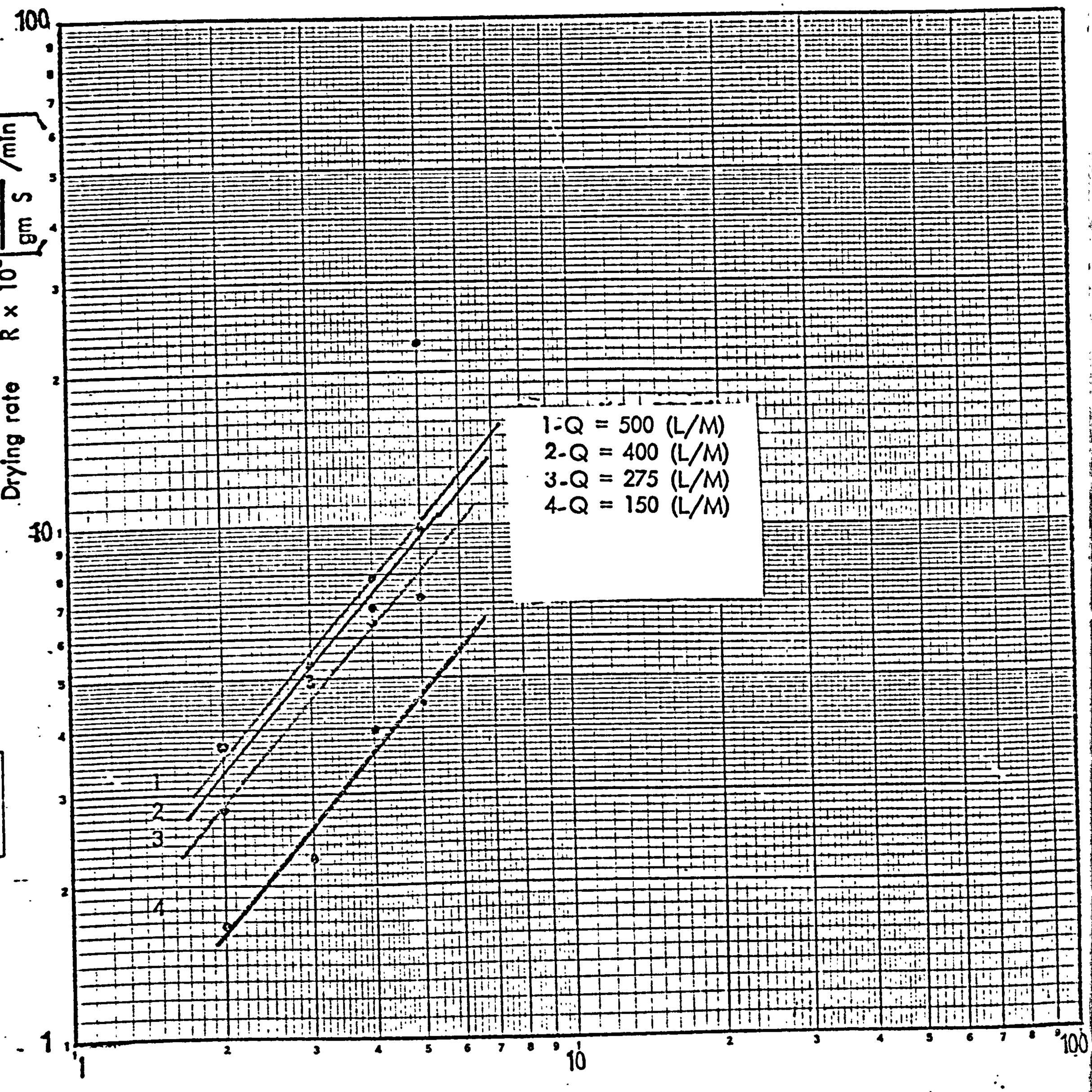
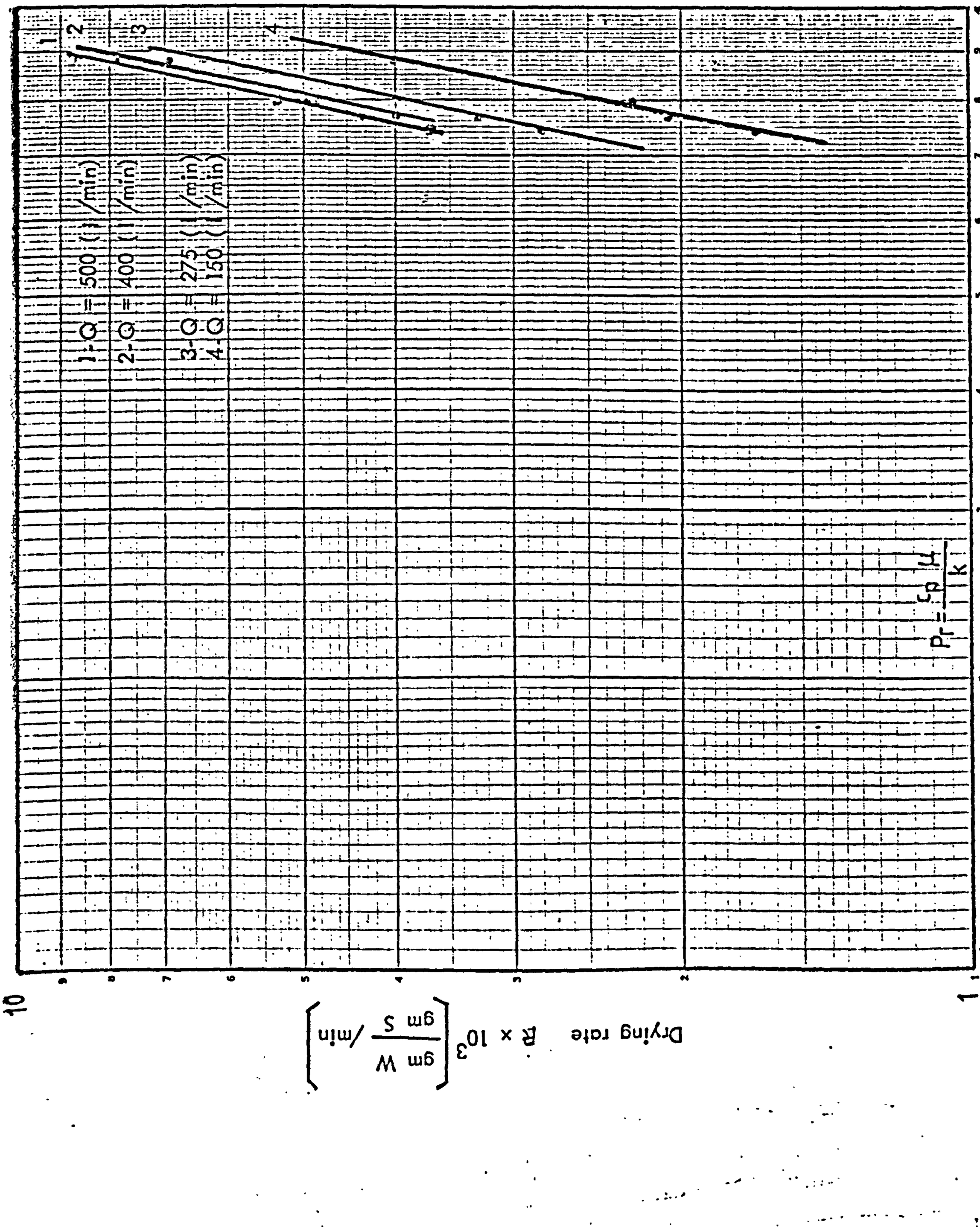


Figure (6-25)

Effect of Prandtl number on solids drying rate



RESULTS OF
EXPERIMENT THREE FLUIDIZED BED DRYING
X(1)= 31.75

NO/	TIME MIN	WET (GM)	DRY(GM)	WATER G	SOLID GM	(X)(%)	RATE M(-1)
2	10.00000	22.01537	19.82624	2.18913	8.74979	25.01923	.67294
3	20.00000	21.48566	19.60136	1.88430	8.52491	22.10346	.29158
4	30.00000	21.37431	19.89862	1.47569	8.82217	16.72706	.53764
5	40.00000	20.89515	19.65542	1.23973	8.57897	14.45080	.22763
6	50.00000	20.33225	19.44635	.88590	8.36990	10.58436	.38664
7	60.00000	18.79205	18.29174	.50031	7.21529	6.93402	.36503
8	70.00000	21.61453	21.05868	.55585	9.98223	5.56840	.13656
9	80.00000	21.08722	20.61115	.47607	9.53470	4.99303	.05754
10	90.00000	20.23100	19.83616	.36482	8.75973	4.16474	.08283
11	100.00000	20.25114	19.92112	.33302	8.84467	3.73129	.04335
12	110.00000	21.37918	21.33831	.34087	9.96186	3.42175	.03095
13	120.00000	20.61433	20.28452	.32981	9.20807	3.58175	-.01600

TABLE (A - 3)

Q = 400 (L/M)

RESULTS OF
EXPERIMENT FOUR FLUIDIZED BED DRYING
X(1)= 29.55

NO/	TIME MIN	WET (GM)	DRY(GM)	WATER G	SOLID GM	(X)(..)	RATE M(-1)
2	10.00000	21.75855	19.73500	2.02355	8.65855	23.37054	.61799
3	20.00000	22.69534	20.78144	1.91390	9.70499	19.72078	.36498
4	30.00000	21.36721	19.86445	1.50276	8.78800	17.10014	.26206
5	40.00000	20.70300	19.78721	.91579	8.71076	10.51332	.65868
6	50.00000	20.66900	19.94600	.72300	8.86955	8.15148	.23618
7	60.00000	21.04000	20.52271	.51729	9.44626	5.47614	.26753
8	70.00000	21.14941	20.73877	.41064	9.66232	4.24991	.12262
9	80.00000	20.51735	20.14100	.37635	9.06455	4.15189	.00980
10	90.00000	20.73100	20.36777	.36323	9.29132	3.90935	.02425
11	100.00000	19.42858	19.13557	.29301	8.05912	3.63576	.02736
12	110.00000	20.07141	19.74500	.32641	8.66855	3.76545	-.01297
13	120.00000	19.60642	19.31871	.28771	8.24226	3.49067	.02748

TABLE (A - 4)

Q= 500 (L/M)

RESULTS OF
EXPERIMENT ONE FLUIDIZED BED DRYING
X(1)= 29.12

NO/	TIME MIN	WET (GM)	DRY(GM)	WATER G	SOLID GM	(X)(.)	RATE M(-1)
2	10.00000	22.67375	20.37118	2.30257	9.29473	24.77286	.43505
3	20.00000	22.03442	19.92945	2.10497	8.85300	23.776 1	.09959
4	30.00000	20.17942	18.52705	1.65237	7.45060	22.17764	.15992
5	40.00000	22.52225	20.64495	1.87730	9.56850	19.61959	.25581
6	50.00000	20.29816	18.92517	1.37299	7.84872	17.49317	.21264
7	60.00000	20.77831	19.50765	1.27066	8.43120	15.07093	.24222
8	70.00000	19.71245	18.72935	.98310	7.65290	12.84611	.22248
9	80.00000	20.65935	19.74400	.91535	8.66755	10.56065	.22855
10	90.00000	20.28300	19.60321	.67979	8.52676	7.97243	.25882
11	100.00000	19.05338	18.54015	.51323	7.46370	6.87635	.10961
12	110.00300	21.73518	21.14930	.61618	10.07255	6.11742	.07589
13	120.00000	21.77235	21.23085	.54150	10.15440	5.33266	.07848

B. TEMP= 60 (°C)

TABLE =(B-1)

Q = 150 (L/M)

RESULTS OF
EXPERIMENT TWO FLUIDIZED BED DRYING
X(1)= 29.24

NO/	TIME MIN	WET (GM)	DRY(GM)	WATER G	SOLID GM	(X)(g/g)	RATE M(-1)
2	10.00000	23.73568	21.38122	2.35446	10.30477	22.8482	.63913
3	20.00000	23.18640	21.41885	1.76755	10.34240	17.09033	.57579
4	30.00000	21.87825	21.02660	.85165	9.95015	8.55917	.85312
5	40.00000	22.60309	22.04545	.55464	10.96900	5.05643	.35027
6	50.00000	20.46910	20.06242	.40668	8.98597	4.52572	.05307
7	60.00000	22.37772	22.05200	.32572	10.97555	2.96769	.15580
8	70.00000	20.87660	20.66691	.20969	7.59046	2.76255	.02051
9	80.00000	20.49616	20.26144	.23472	9.18499	2.55547	.02071
10	90.00000	20.43633	20.21717	.18883	9.14072	2.06581	.04897
11	100.00000	20.00594	19.90000	.10594	8.82355	1.20065	.08652
12	110.00000	21.05045	20.84893	.20155	9.77245	2.06243	-.08618
13	120.00000	20.92436	20.32765	.39673	9.45126	4.19767	-.21352

TABLE(B.2)

Q= 275 (L/M)

FIGURES (7)

(MODELLING)

Figure (7-1)	Bed Performance	- dp = 106 Microns
Figure (7-2)	Bed Performance	- dp = 106 Microns
Figure (7-3)	Bed Performance	- dp = 106 Microns
Figure (7-4)	Bed Performance	- dp = 940 Microns
Figure (7-5)	Bed Performance	- dp = 940 Microns
Figure (7-6)	Bed Performance	- dp = 940 Microns
Figure (7-7)	Bed Performance	- dp =2247 Microns
Figure (7-8)	Bed Performance	- dp =2247 Microns
Figure (7-9)	Bed Performance	- dp =2247 Microns
Figure (7-10)	Air Humidity Gain vs. Time	- dp = 106 Microns
Figure (7-11)	Air Humidity Gain vs. Time	- dp = 106 Microns
Figure (7-12)	Air Humidity Gain vs. Time	- dp = 106 Microns
Figure (7-13)	Air Humidity Gain vs. Time	- dp = 940 Microns
Figure (7-14)	Air Humidity Gain vs. Time	- dp = 940 Microns
Figure (7-15)	Air Humidity Gain vs. Time	- dp = 940 Microns
Figure (7-16)	Air Humidity Gain vs. Time	- dp =2247 Microns
Figure (7-17)	Air Humidity Gain vs. Time	- dp =2247 Microns
Figure (7-18)	Air Humidity Gain vs. Time	- dp =2247 Microns

CONT

Figure (7-19) Effect of Bed Height on Bed Performance

Figure (7-20) Variation of Air Humidity with Bed Height

Figure (7-21) Effect of Air Flowrate on Bed Performance - dp = 106

Figure (7-22) Effect of Air Flowrate on Bed Performance - dp = 940

Figure (7-23) Effect of Air Flowrate on Bed Performance - dp =2247

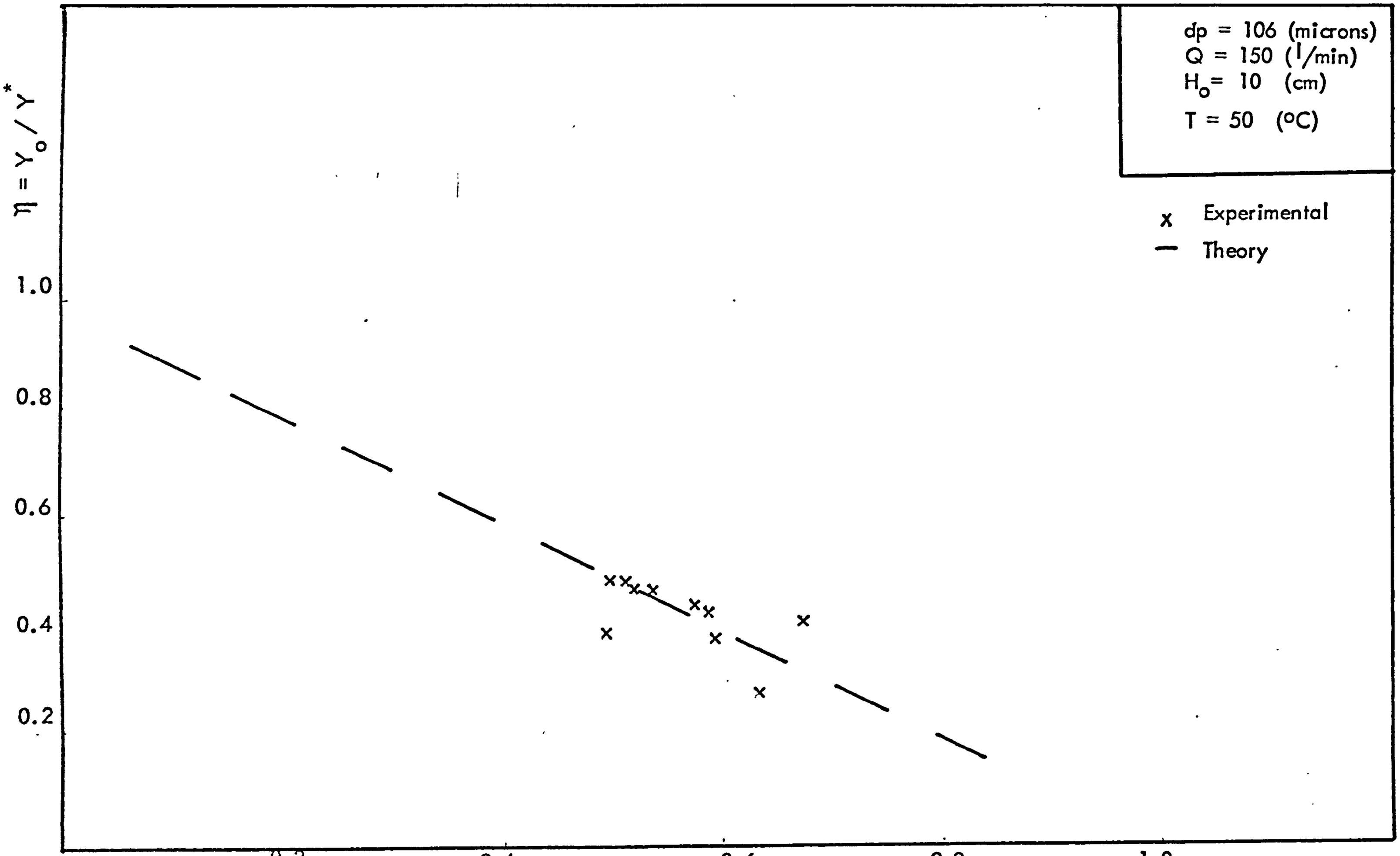


Figure (7-1)

Bed Performance

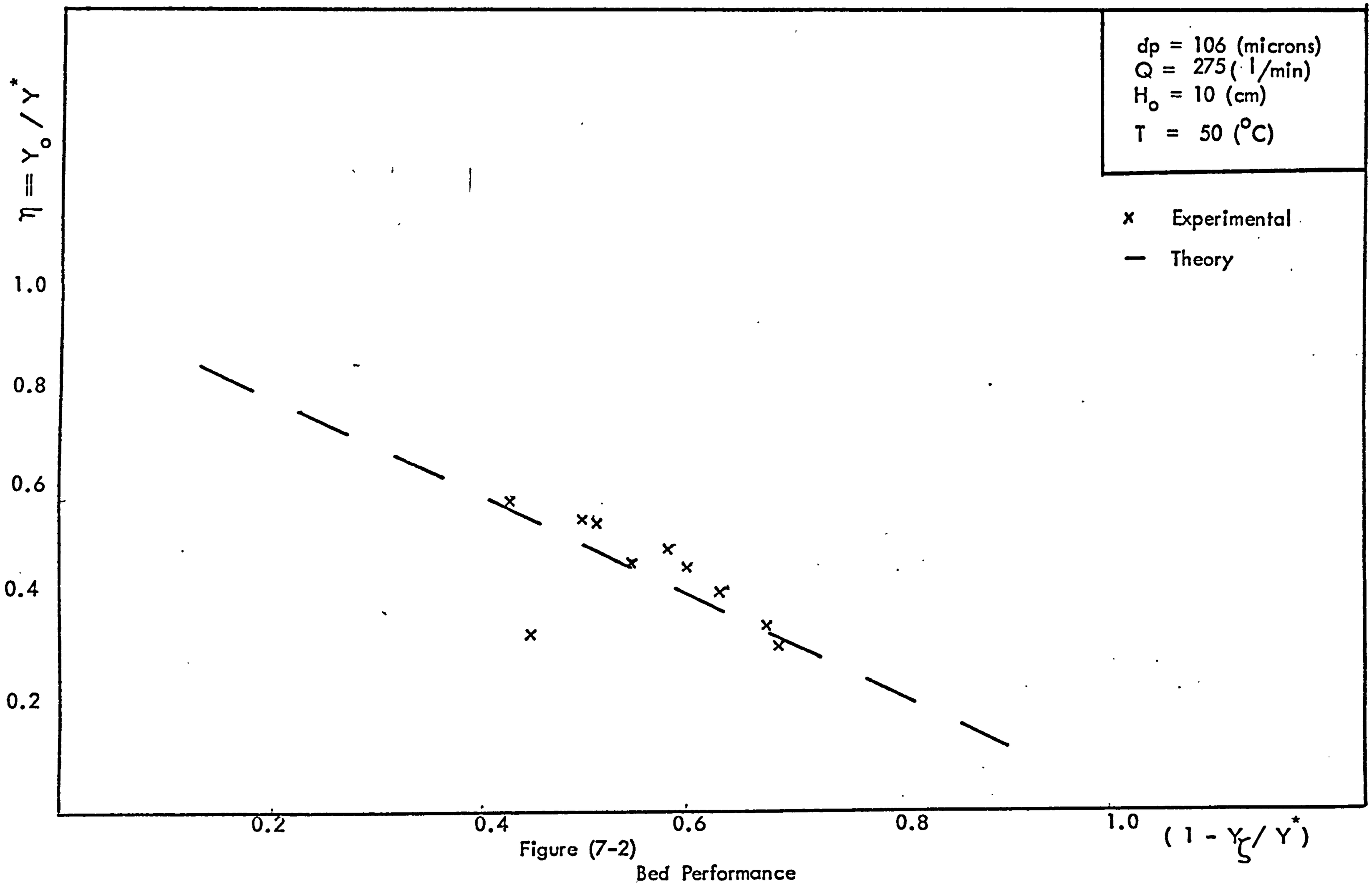


Figure (7-2)
Bed Performance

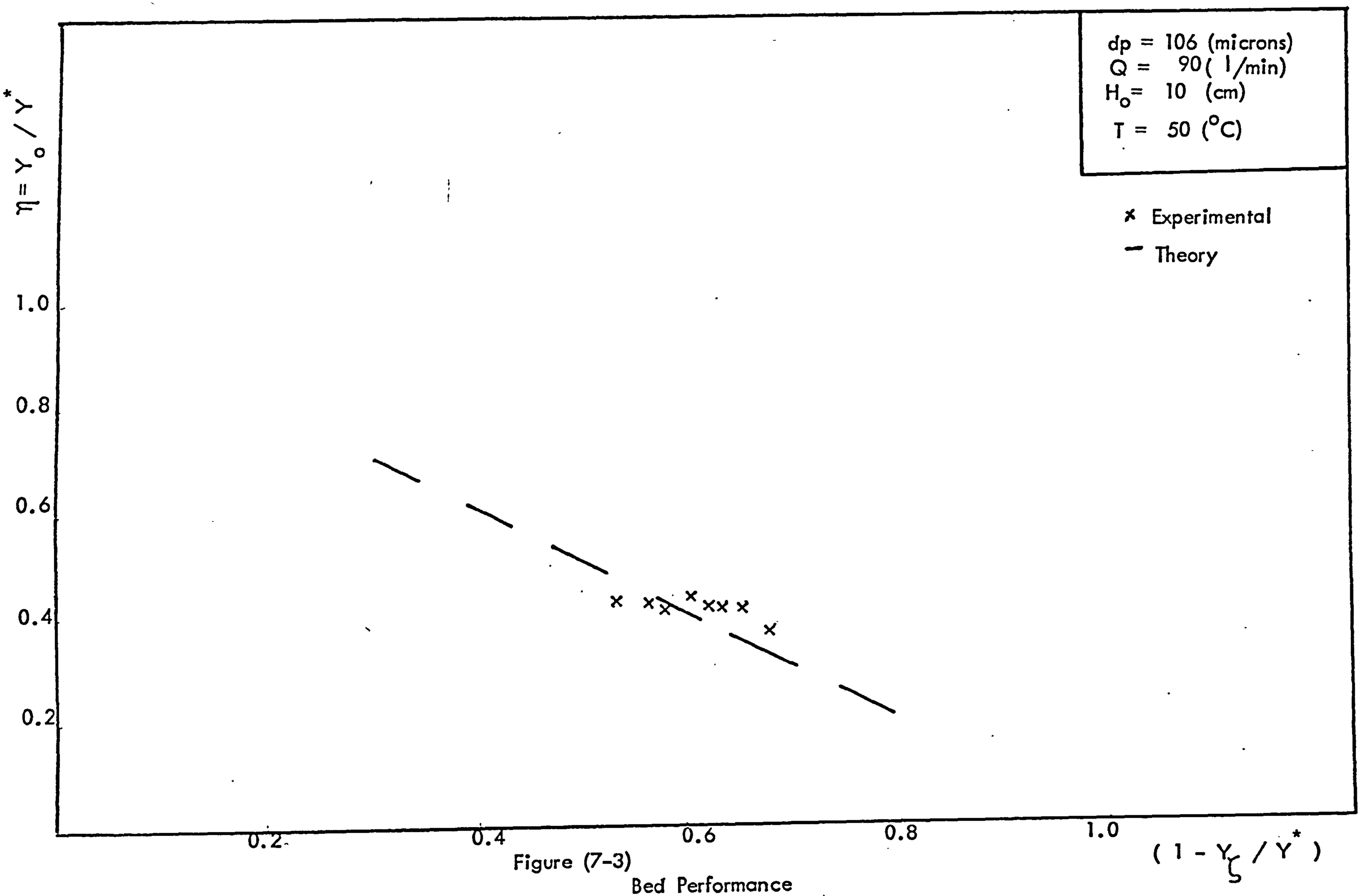


Figure (7-3)
Bed Performance

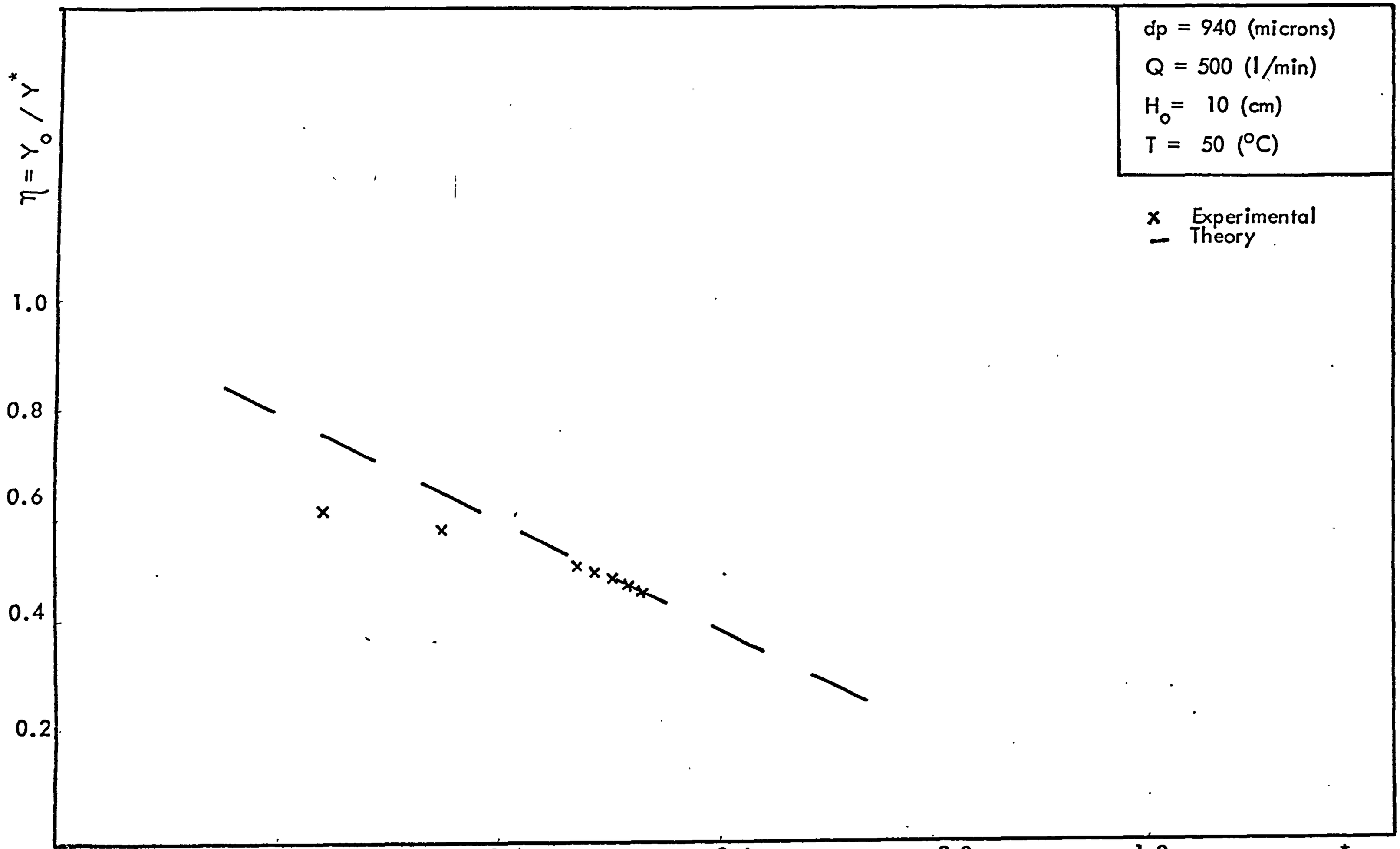


Figure (7-4)

Bed Performance

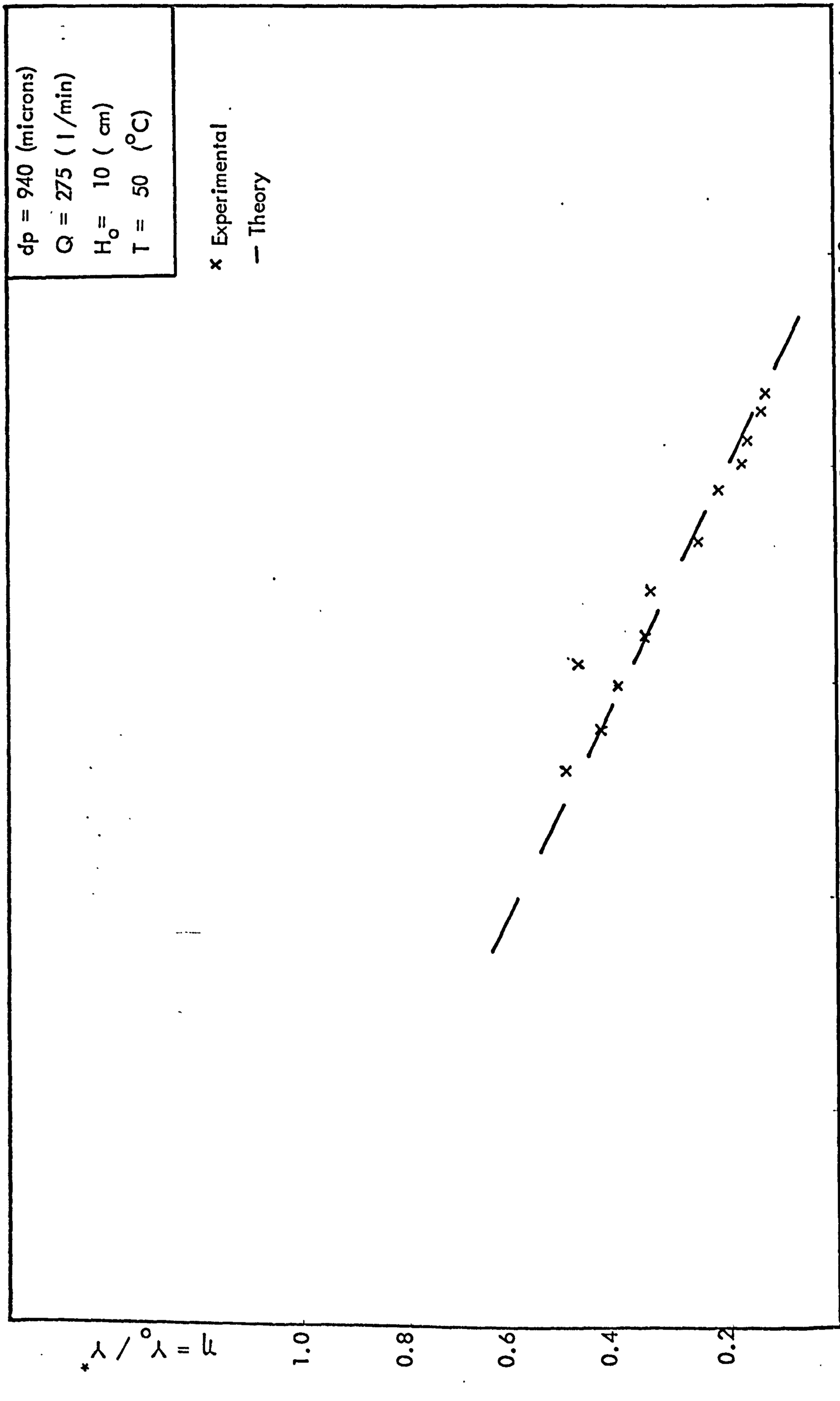

dp = 940 (microns)
Q = 275 (l /min)
H_o = 10 (cm)
T = 50 (^oC)
× Experimental
— Theory
1.0 (1 - Y_ζ / Y^*)
0.8
0.6
0.4
0.2
Bed Performance
$\mu = \lambda / {}^o\lambda$
1.0
0.8
0.6
0.4
0.2

Figure (7-5)

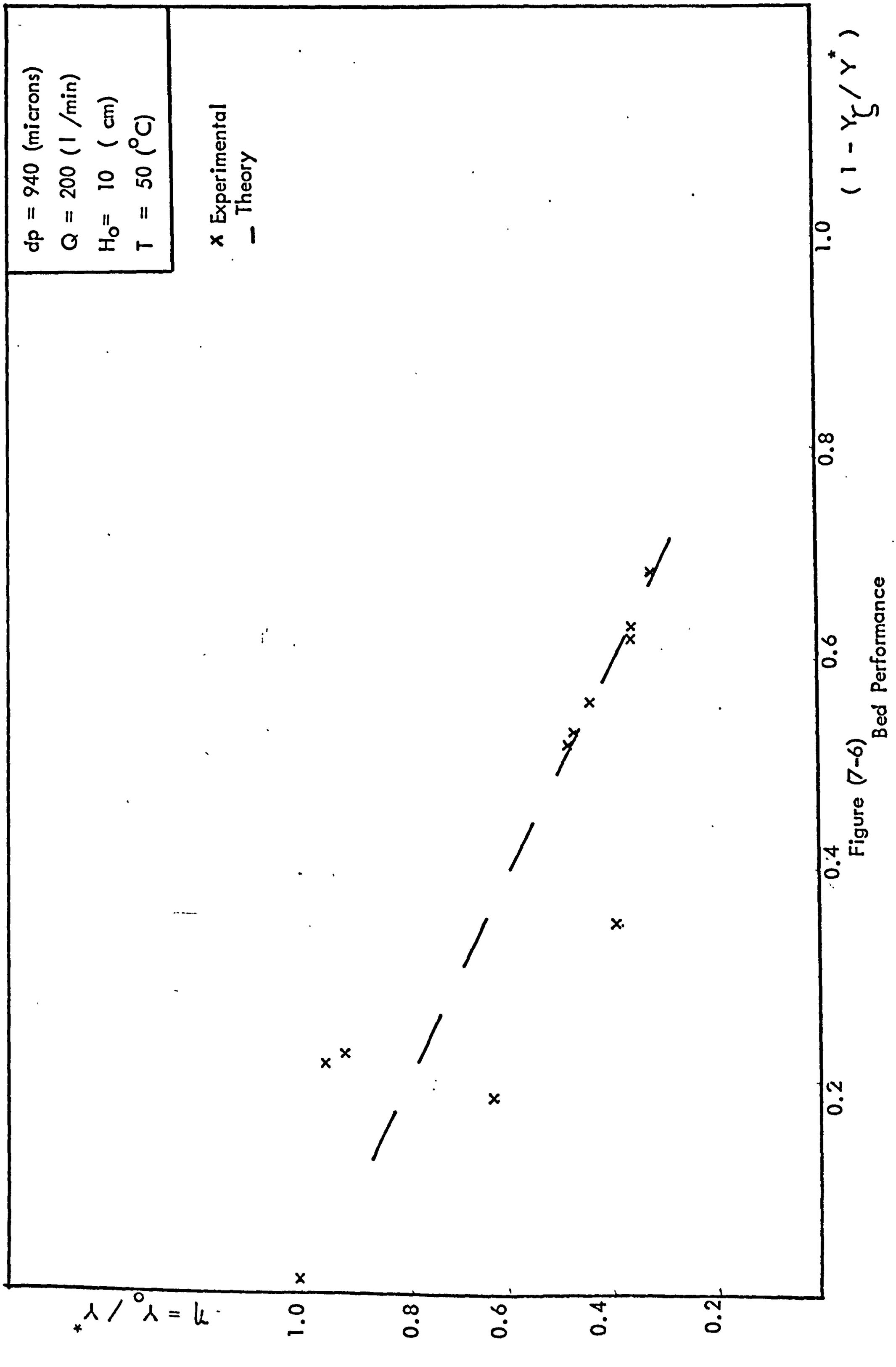

dp = 940 (microns)
Q = 200 (l /min)
H_o= 10 (cm)
T = 50 (^oC)
x Experimental
— Theory
1.0
0.8
0.6
0.4
0.2
$(1 - Y_\zeta / Y^*)$
Bed Performance
$\lambda / {}^o\lambda = \mu^*$

Figure (7-6)

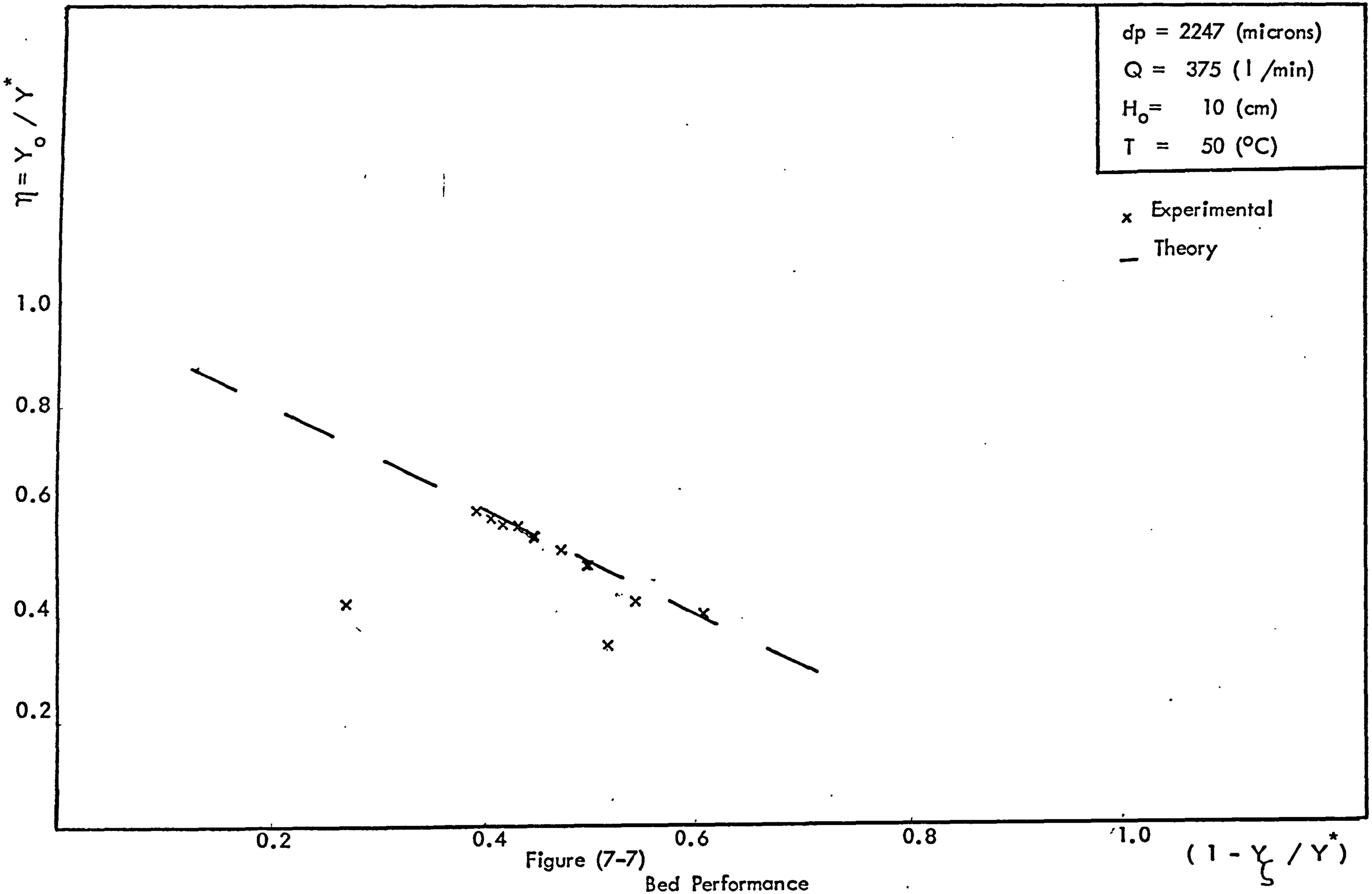


Figure (7-7)
Bed Performance

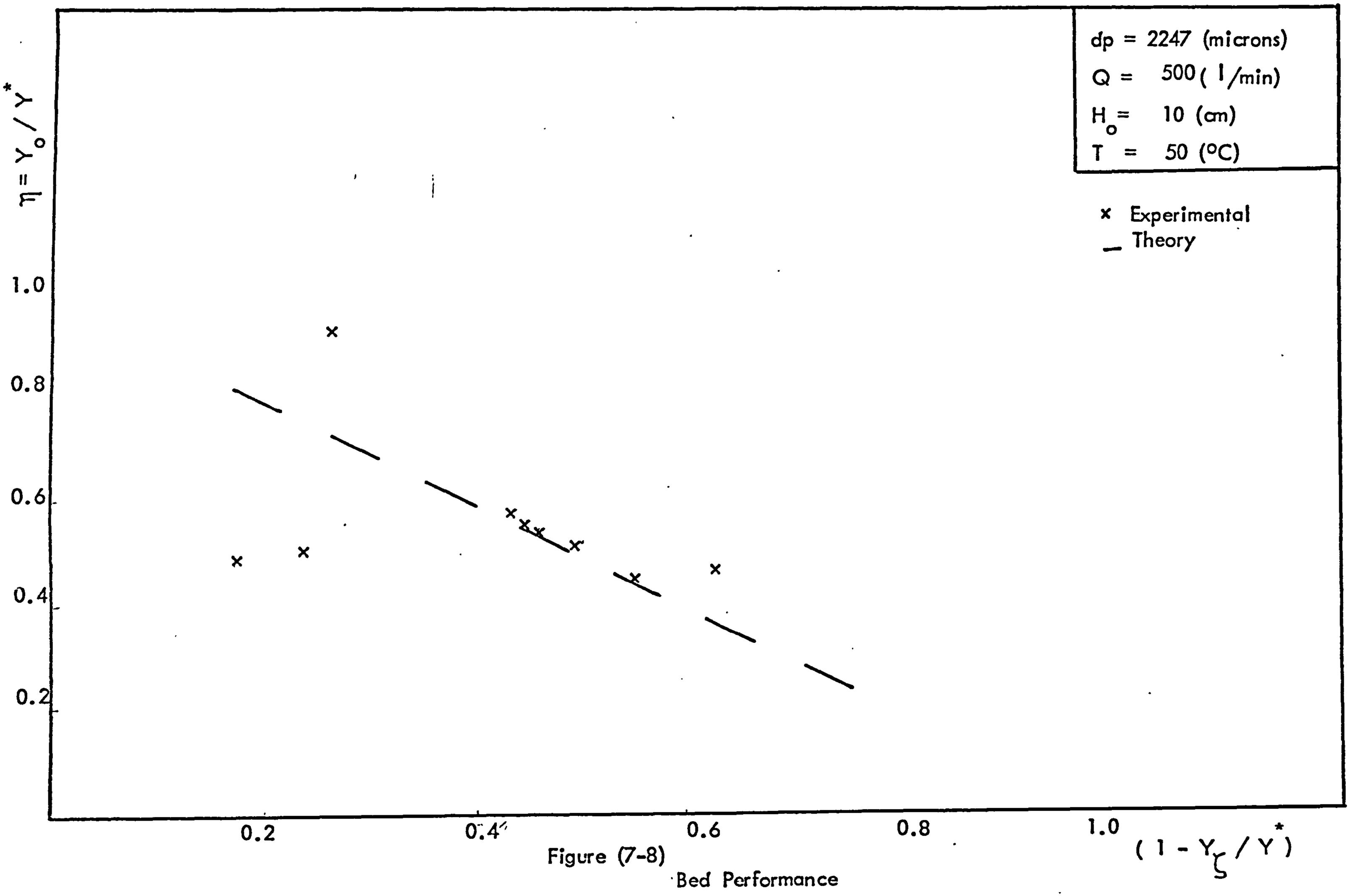


Figure (7-8)
Bed Performance

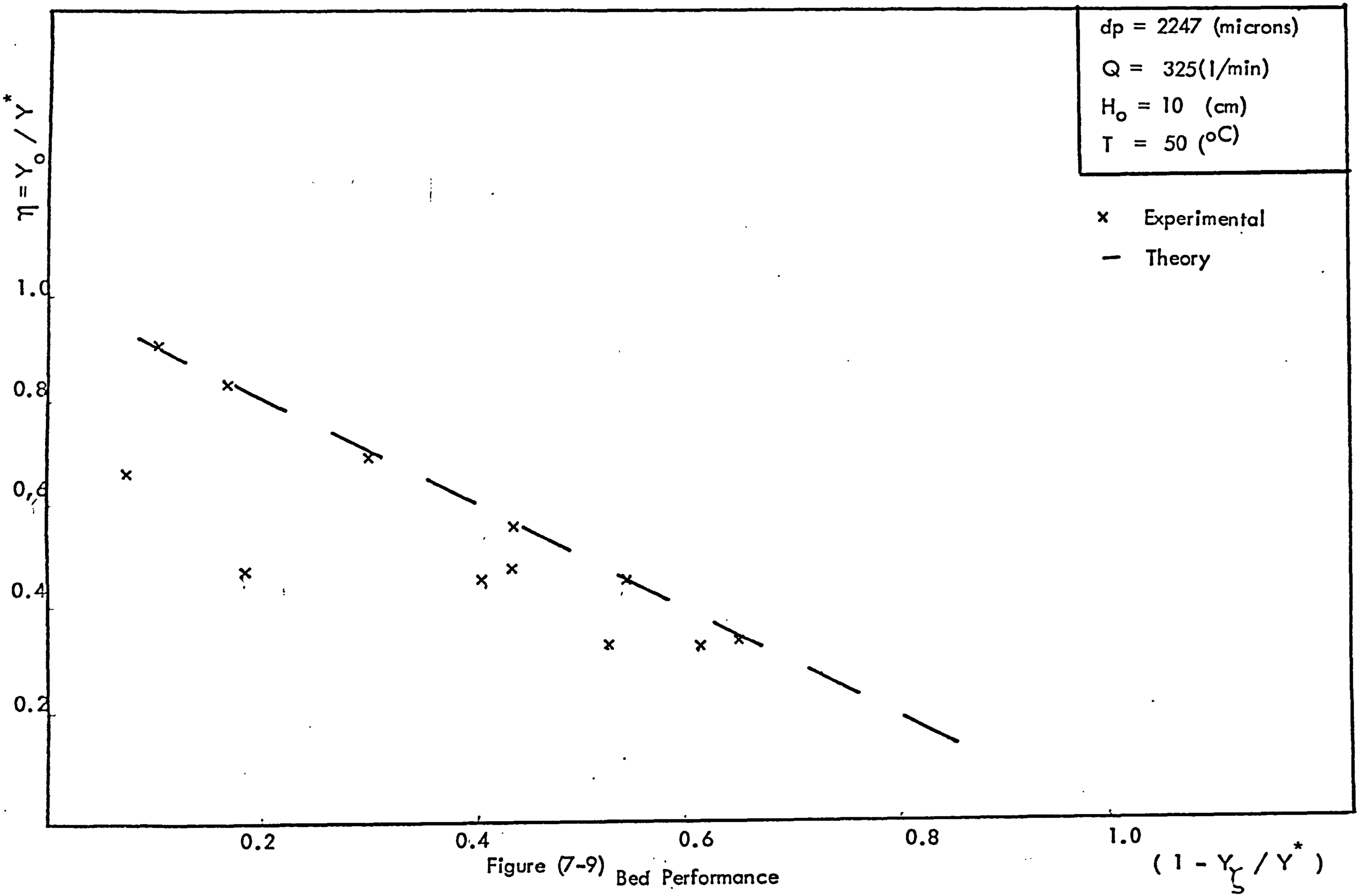


Figure (7-9) Bed Performance

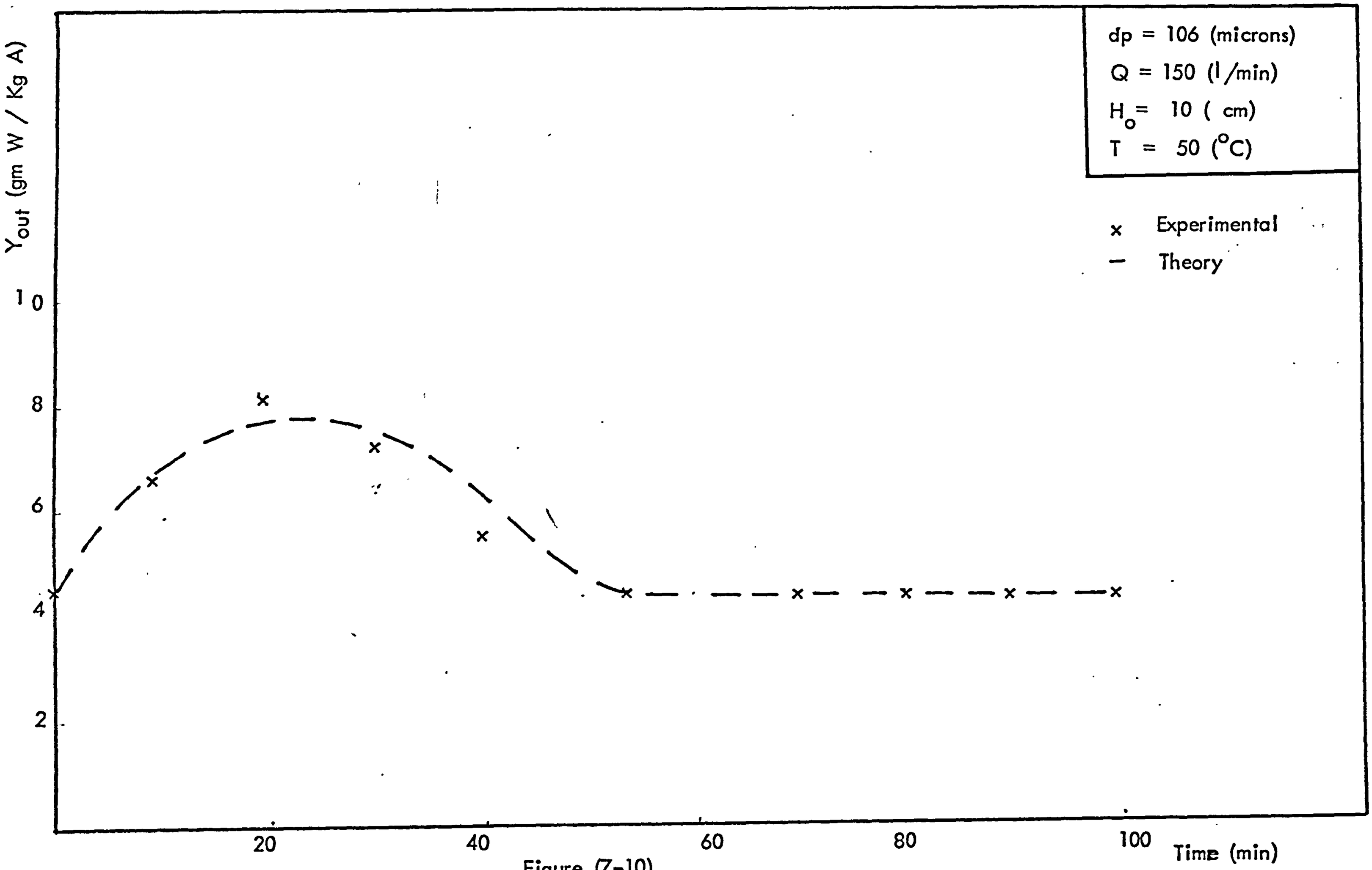


Figure (7-10)
Air humidity gain vs. time

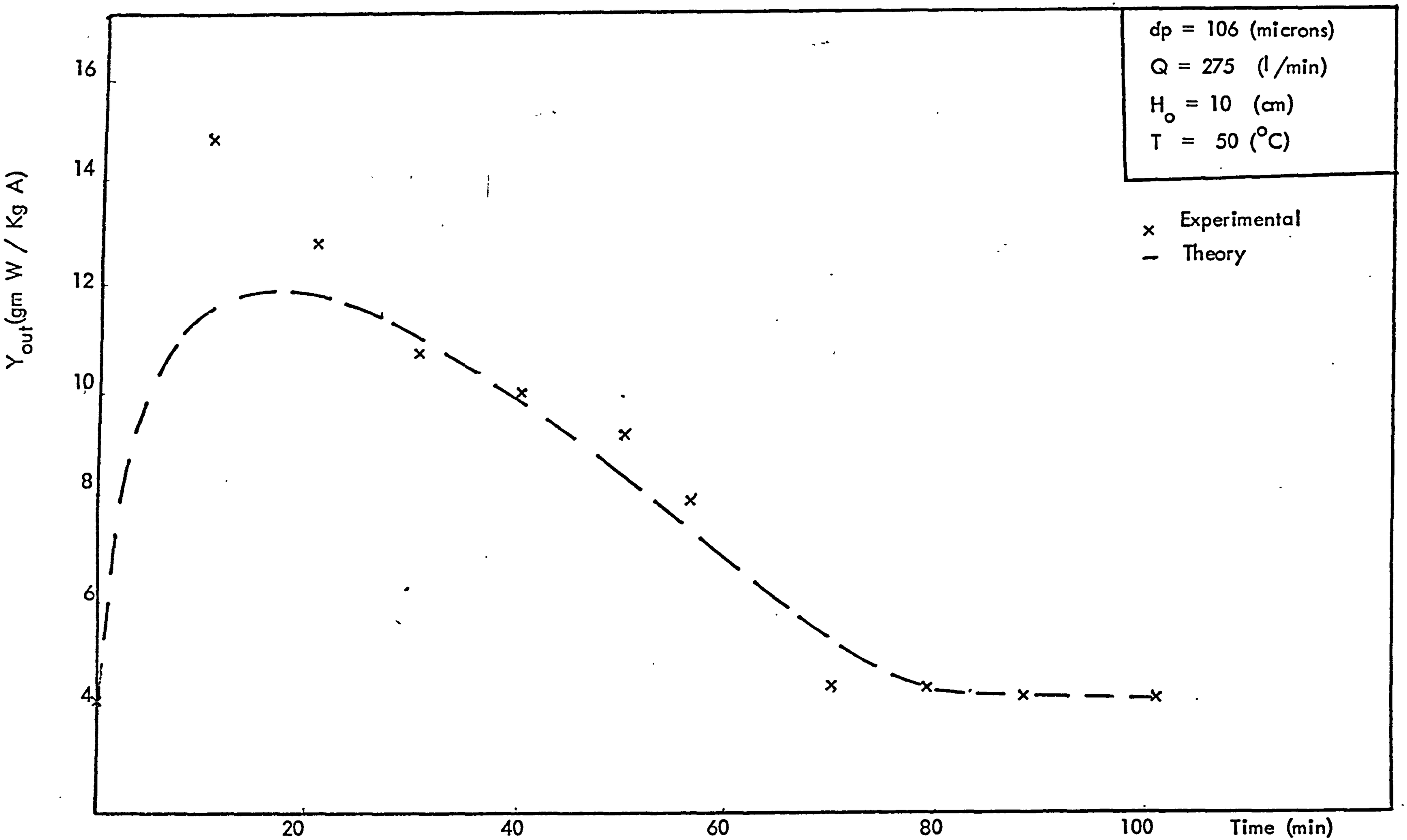


Figure (7-11)
Air Humidity gain vs. time

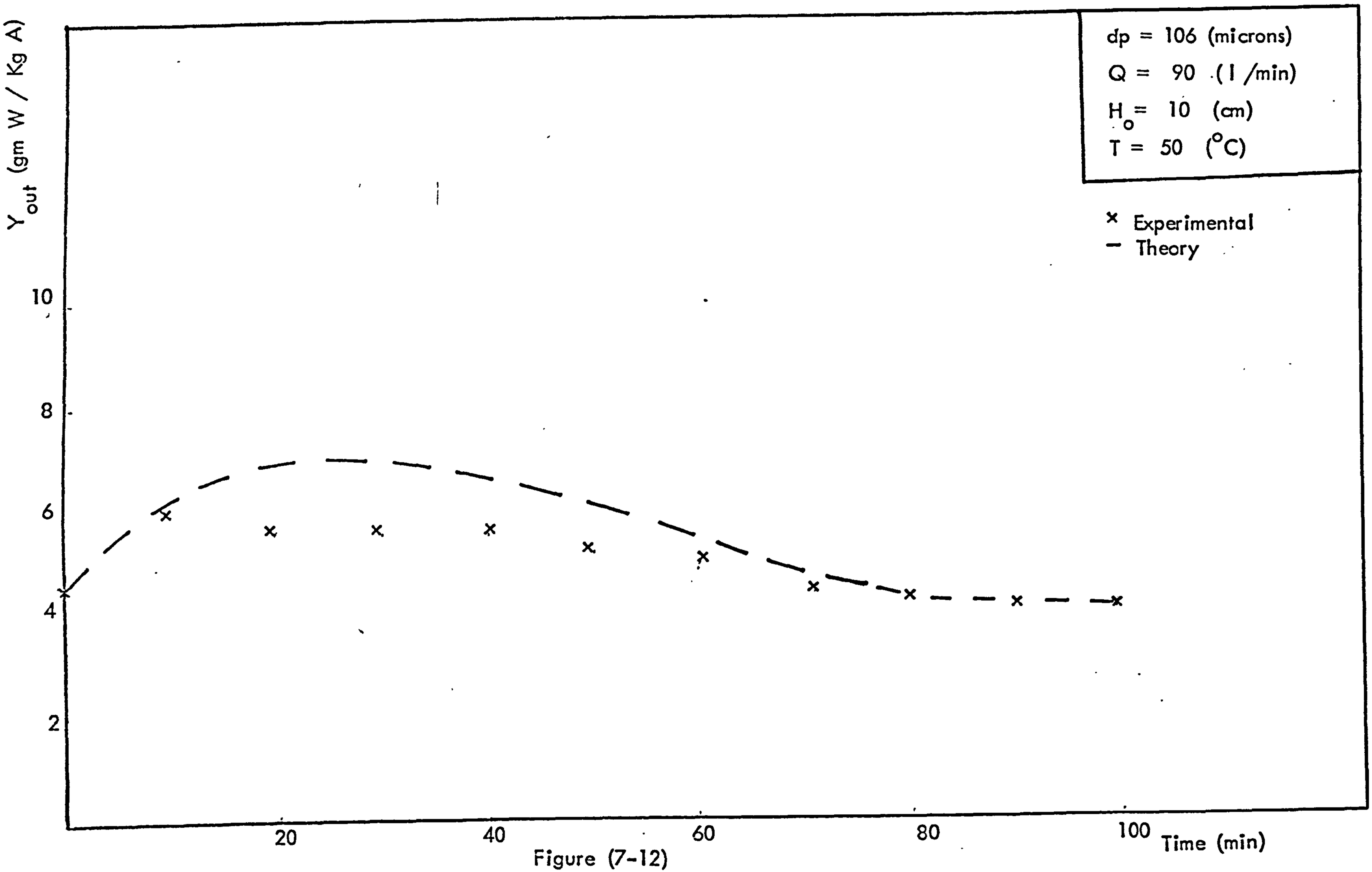


Figure (7-12)

Air humidity gain vs. time

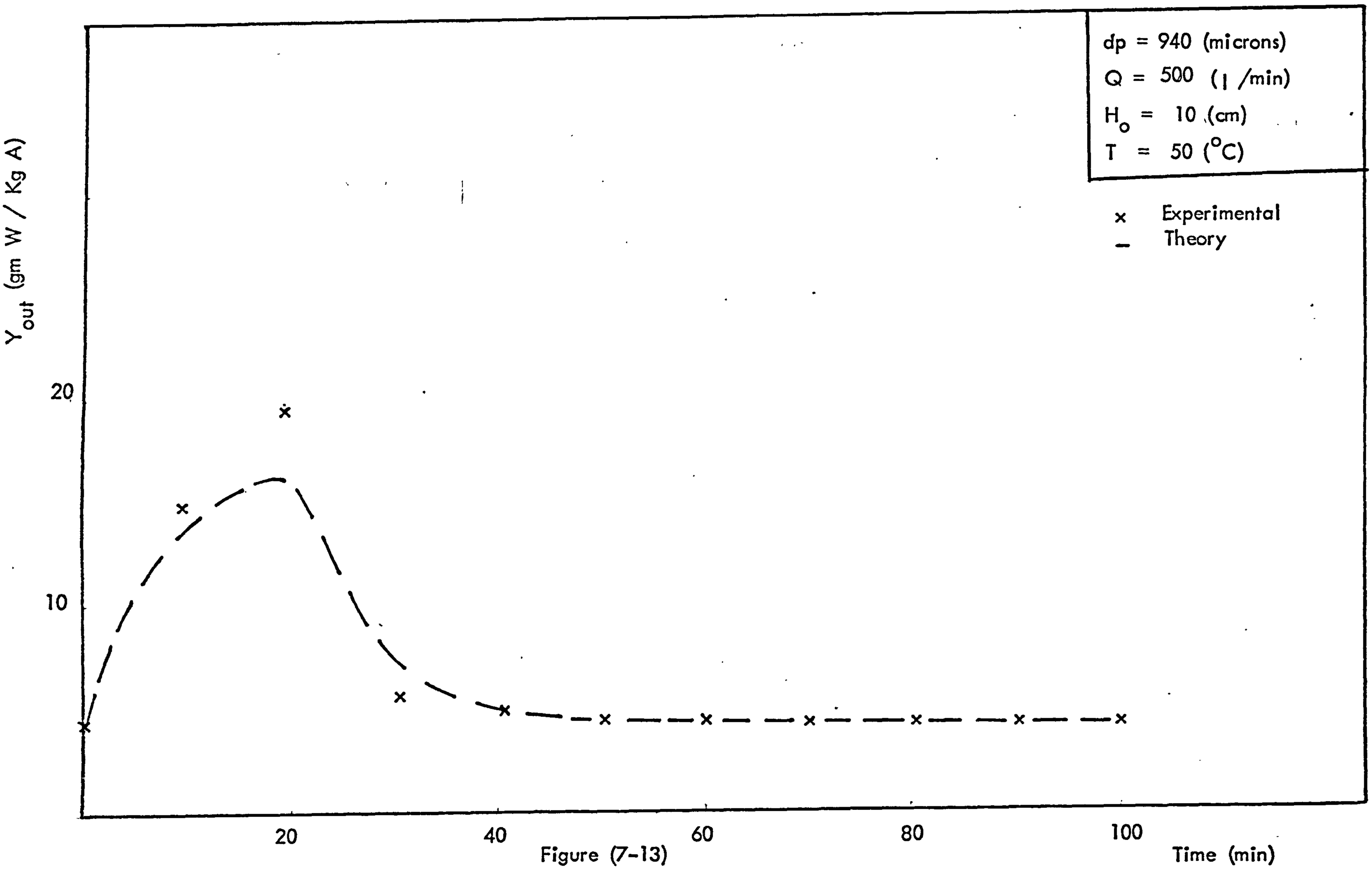


Figure (7-13)
Air Humidity gain vs. time

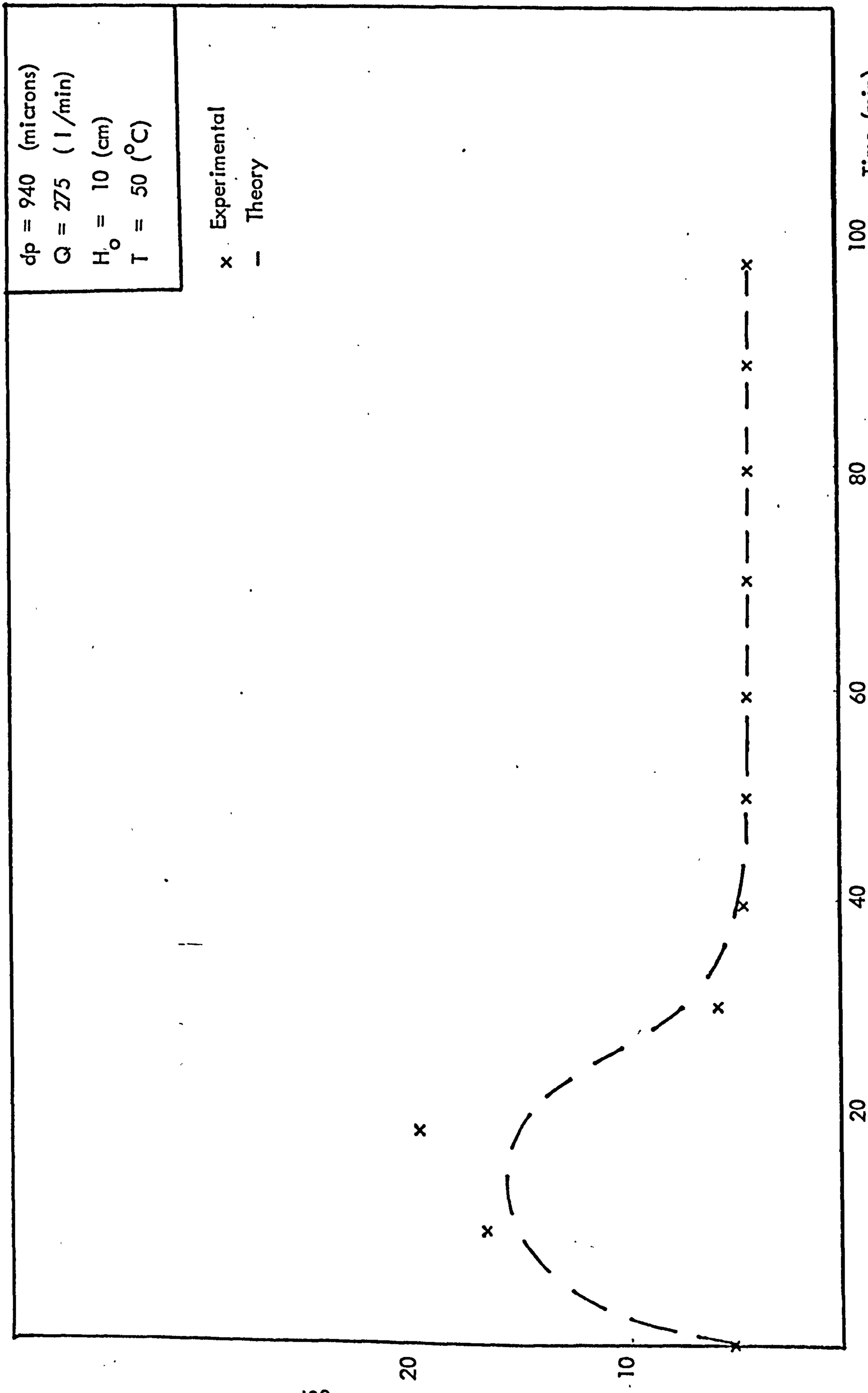


Figure (7-14)
Air humidity gain vs. time

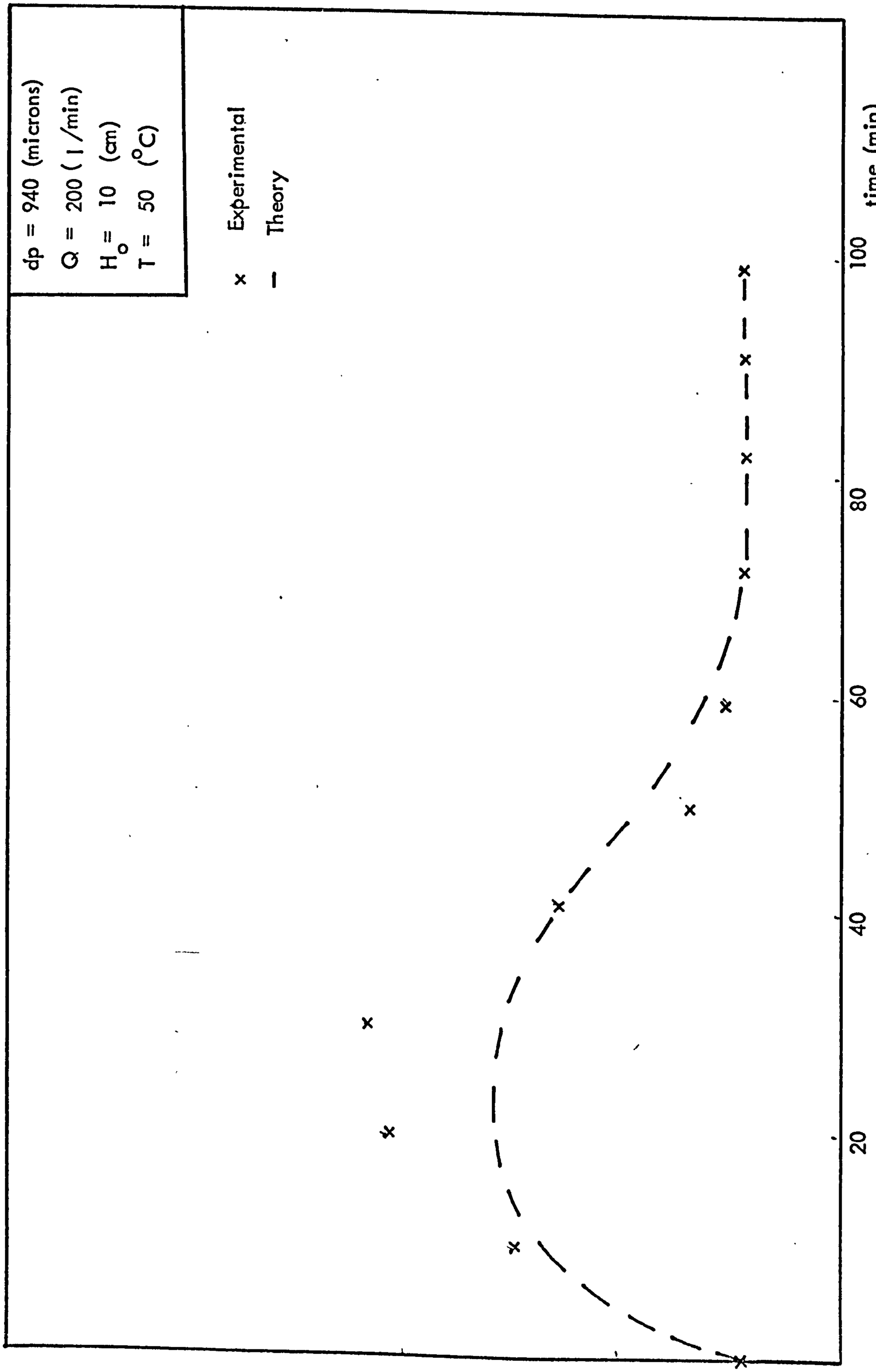


Figure (7-15) Air humidity gain vs. time

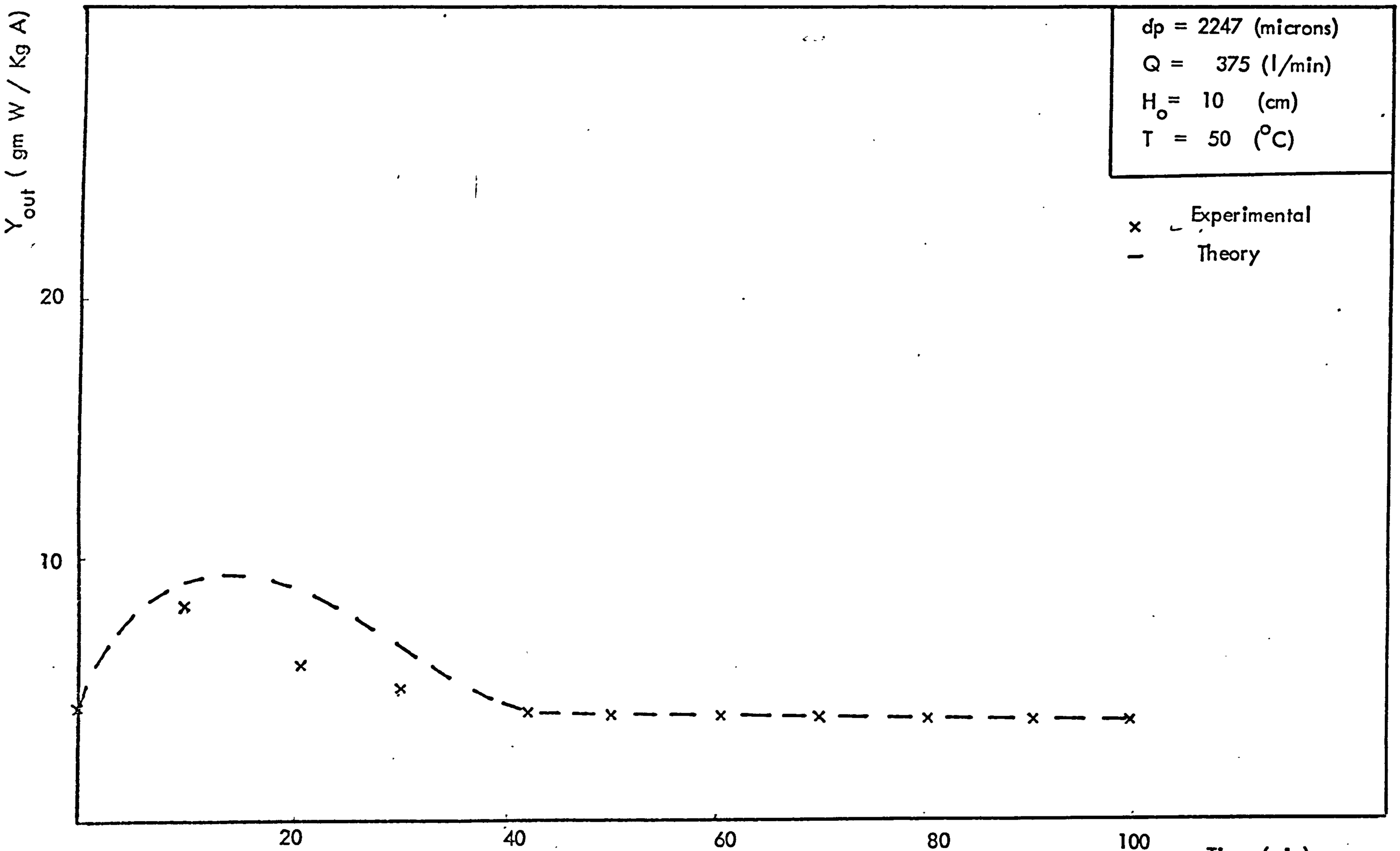


Figure (7-16)
Air humidity gain vs. time

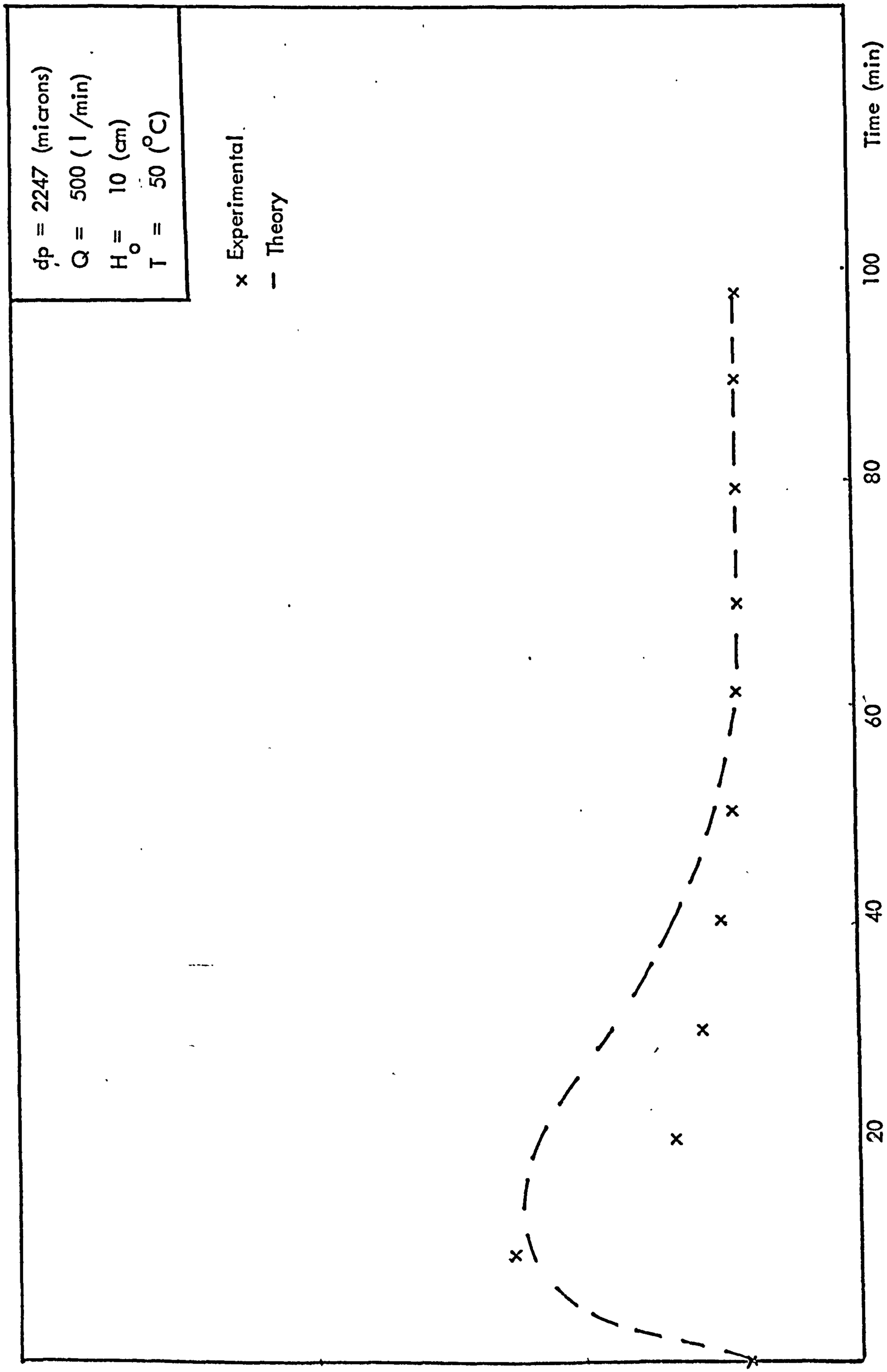


Figure (7-17)
Air humidity gain vs. time

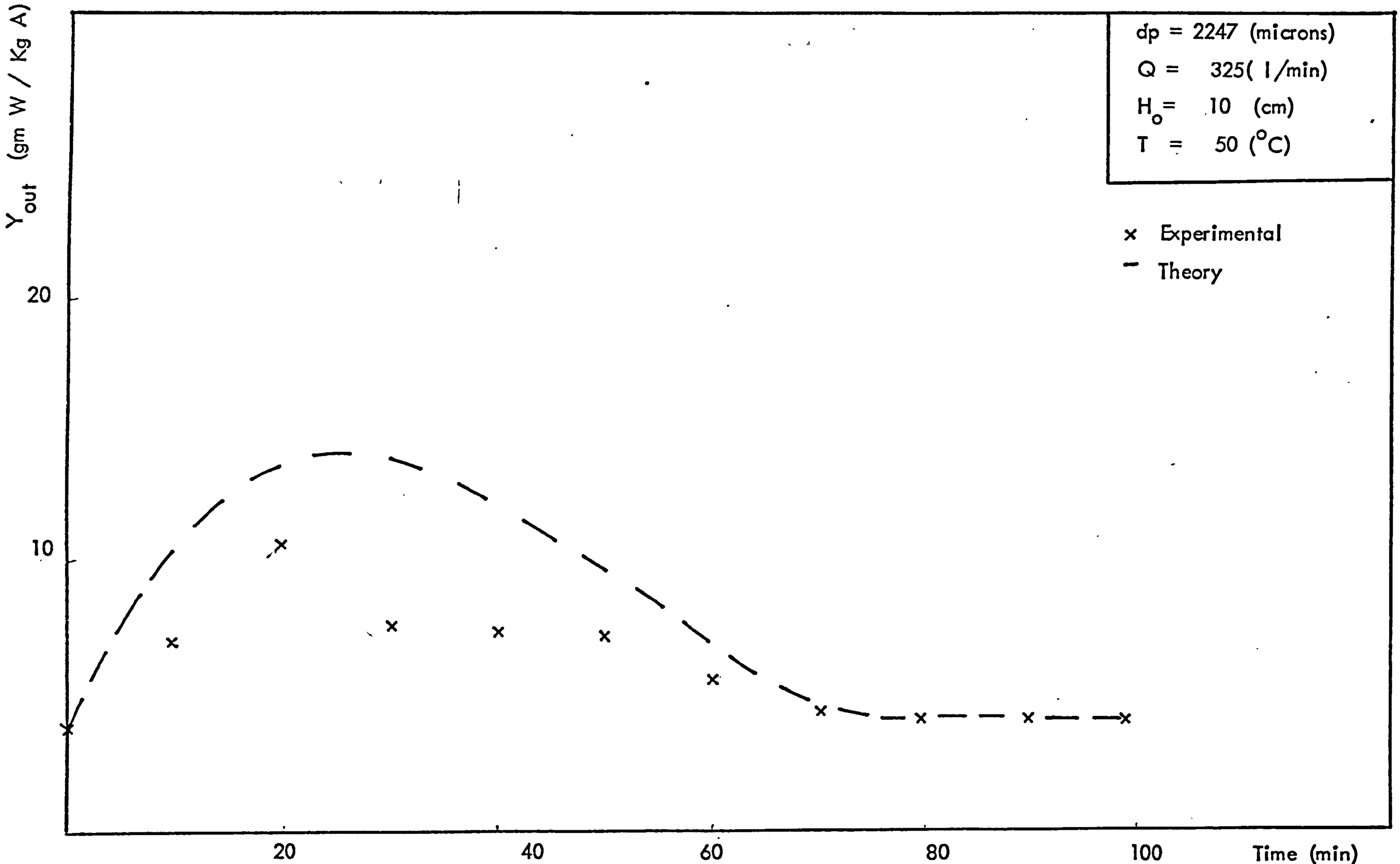


Figure (7-18)
Air humidity gain vs. time

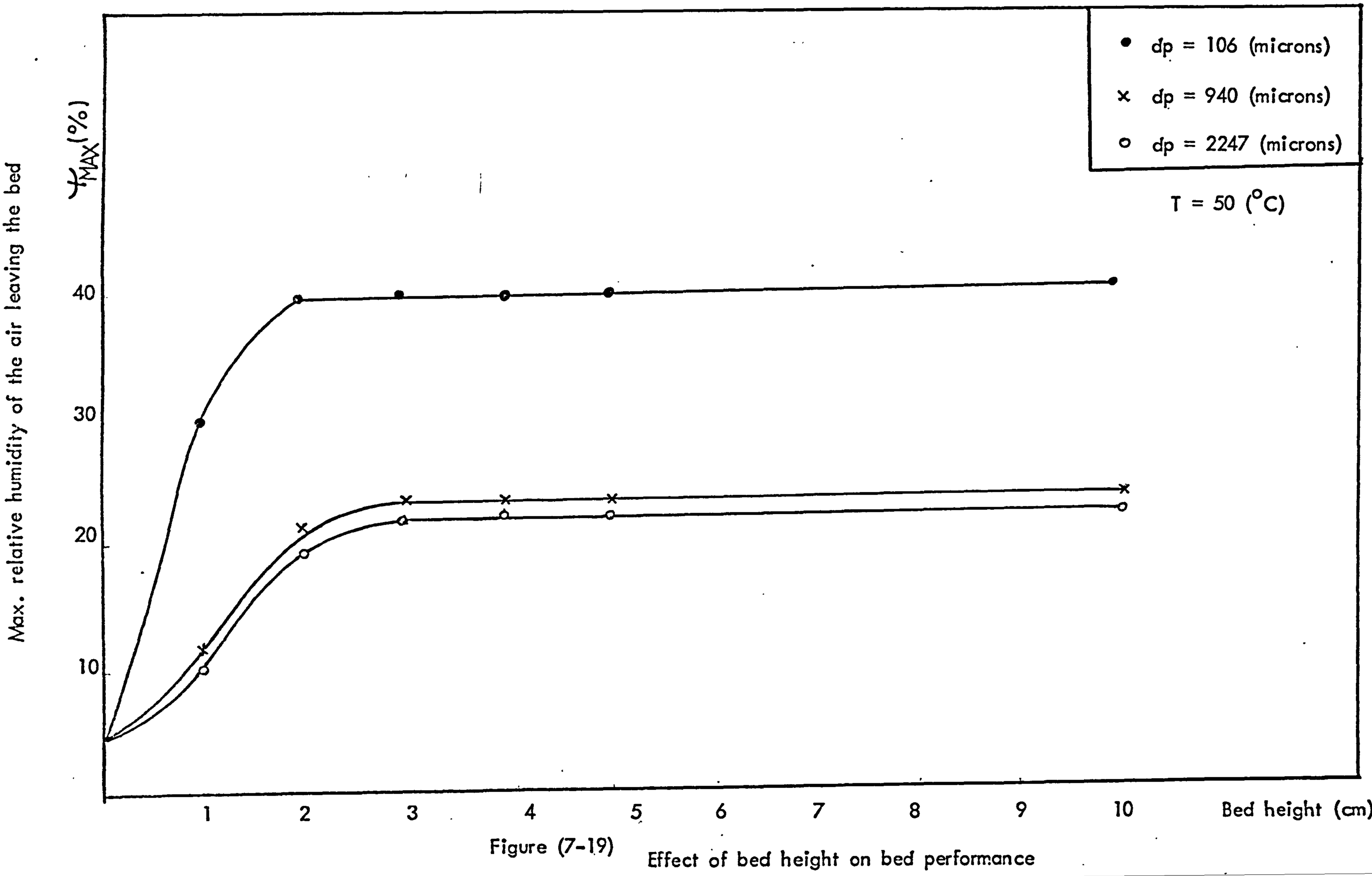


Figure (7-19) Effect of bed height on bed performance

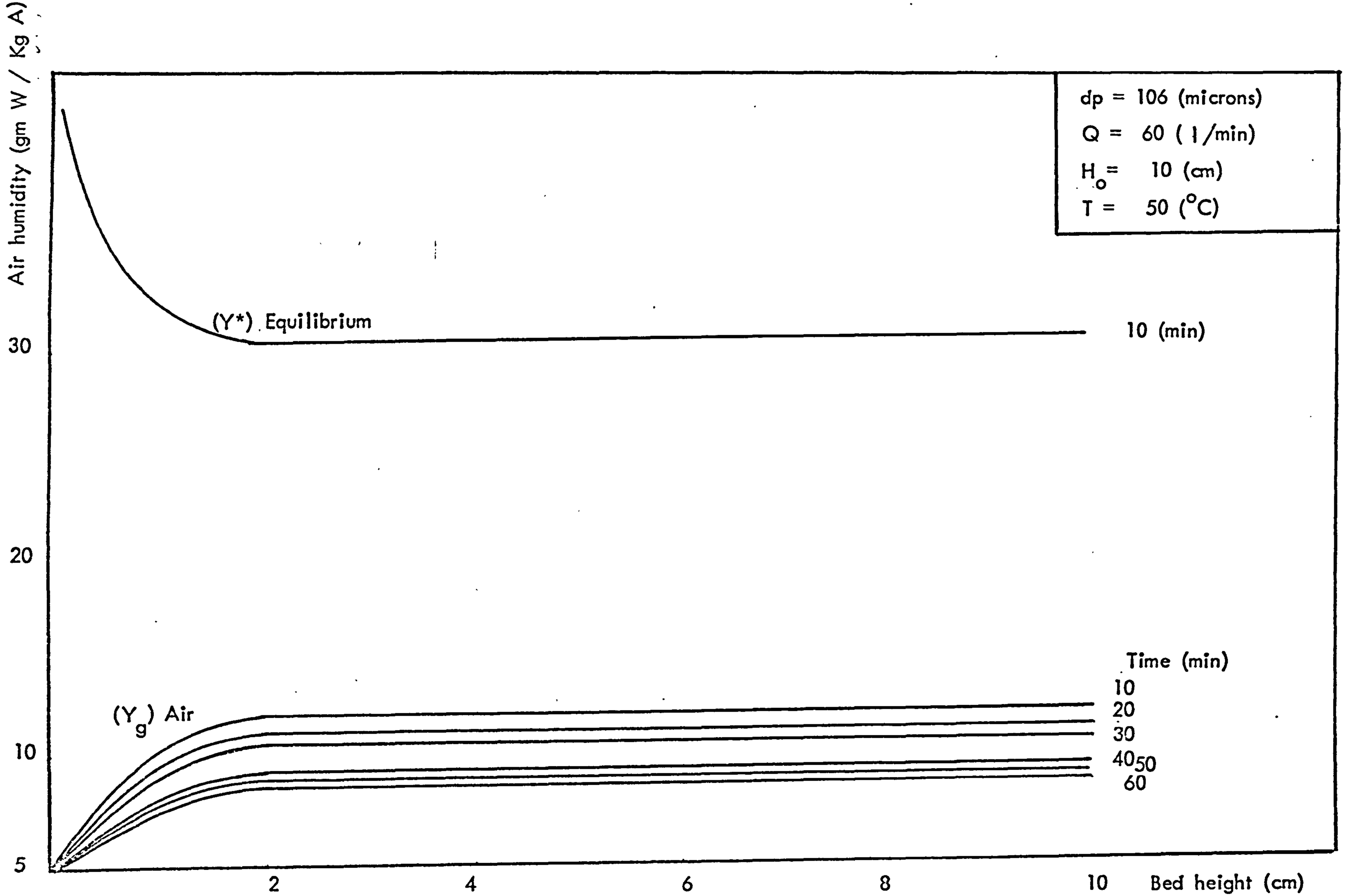


Figure (7-20)
Variation of air humidity with bed height

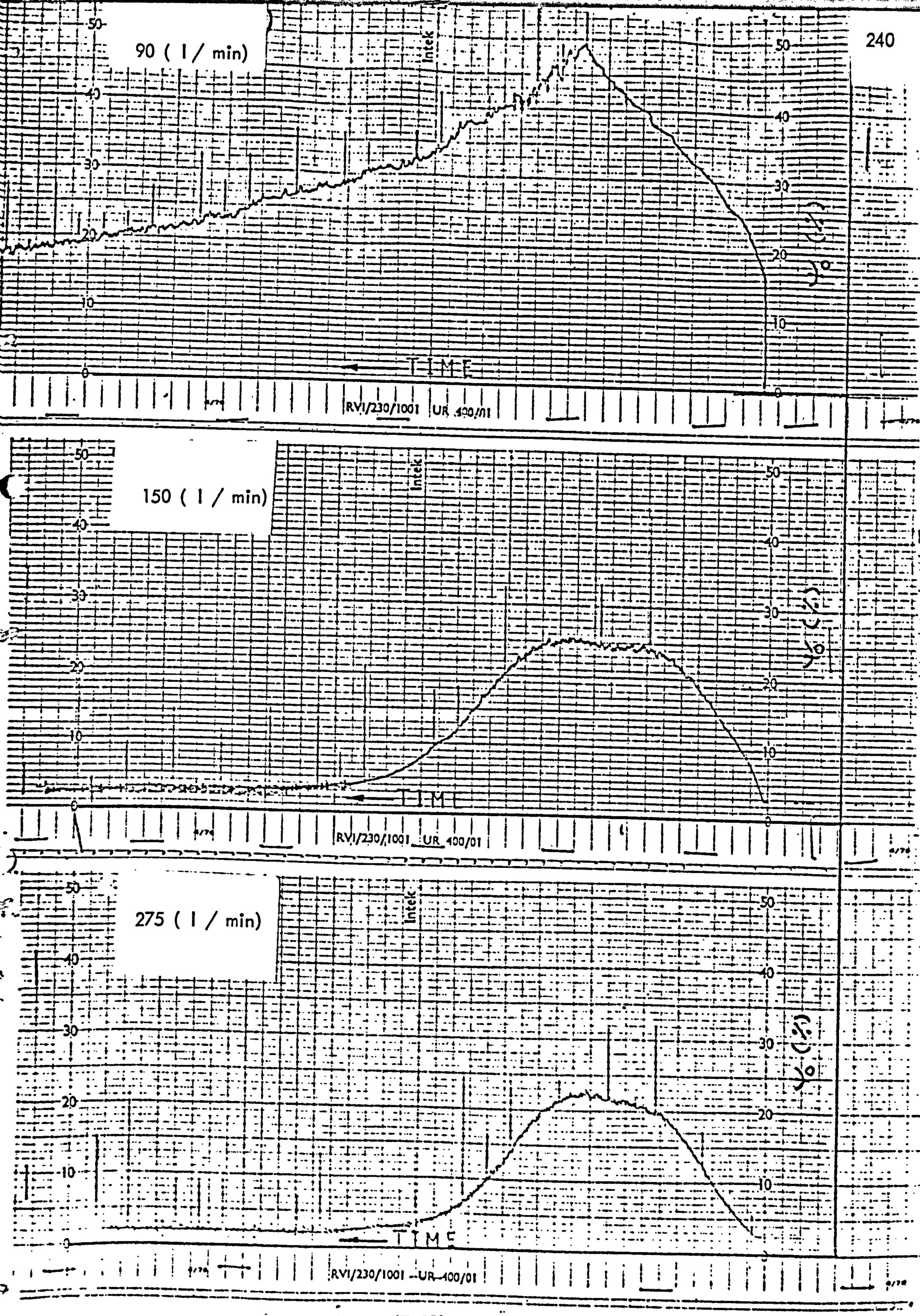


Figure (7-21)
Effect of air flowrate on bed performance (dp = 106)

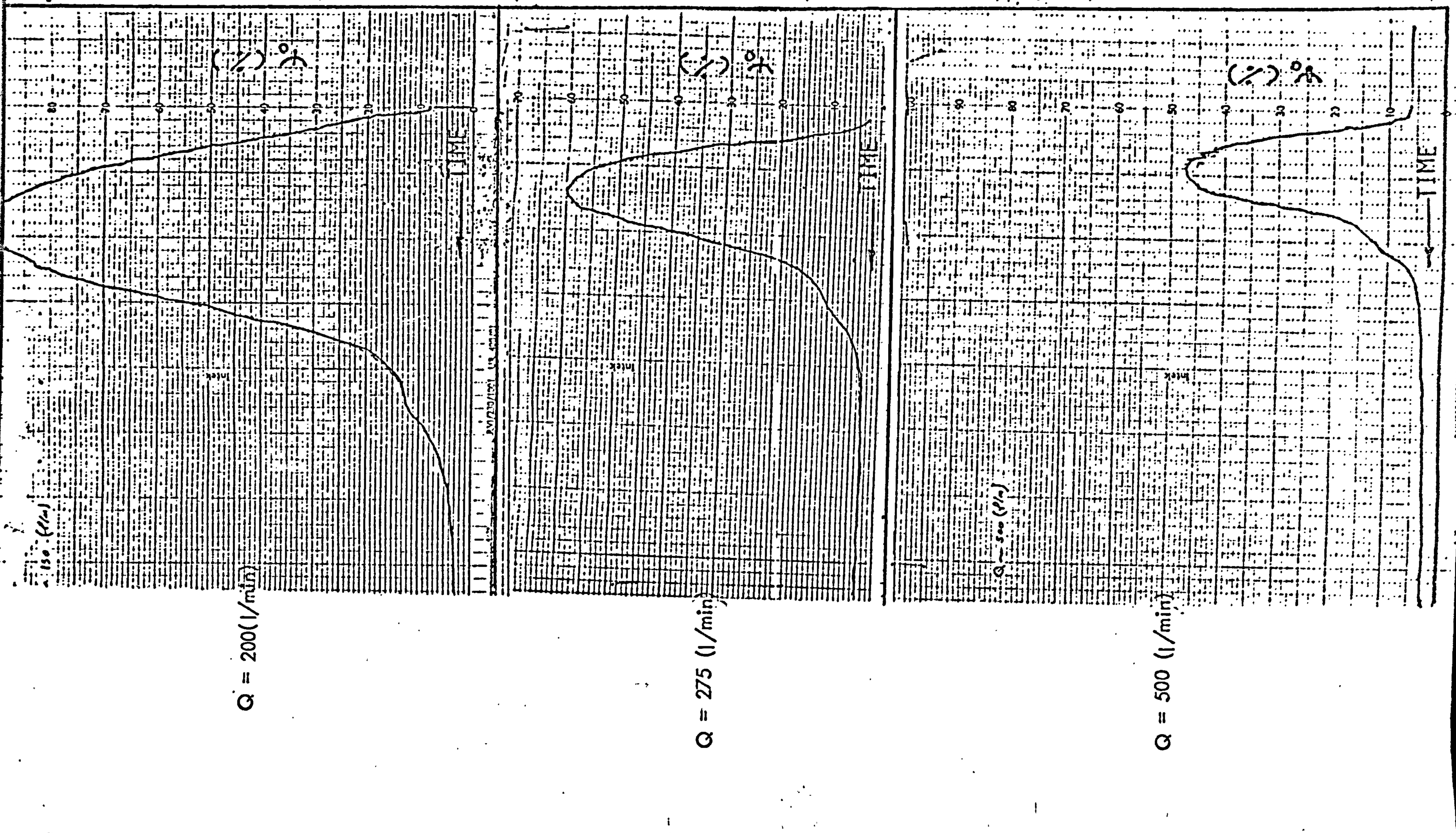
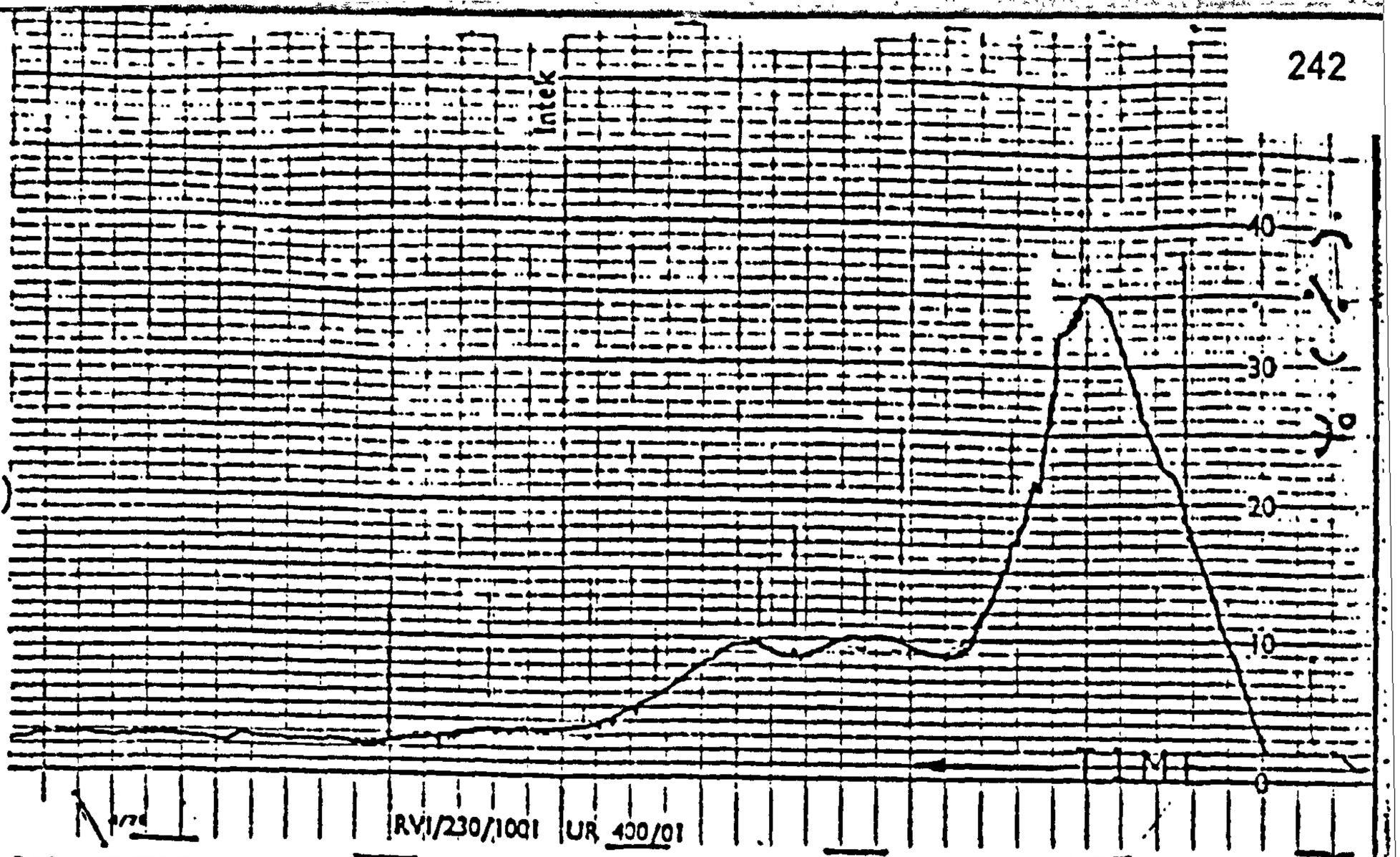


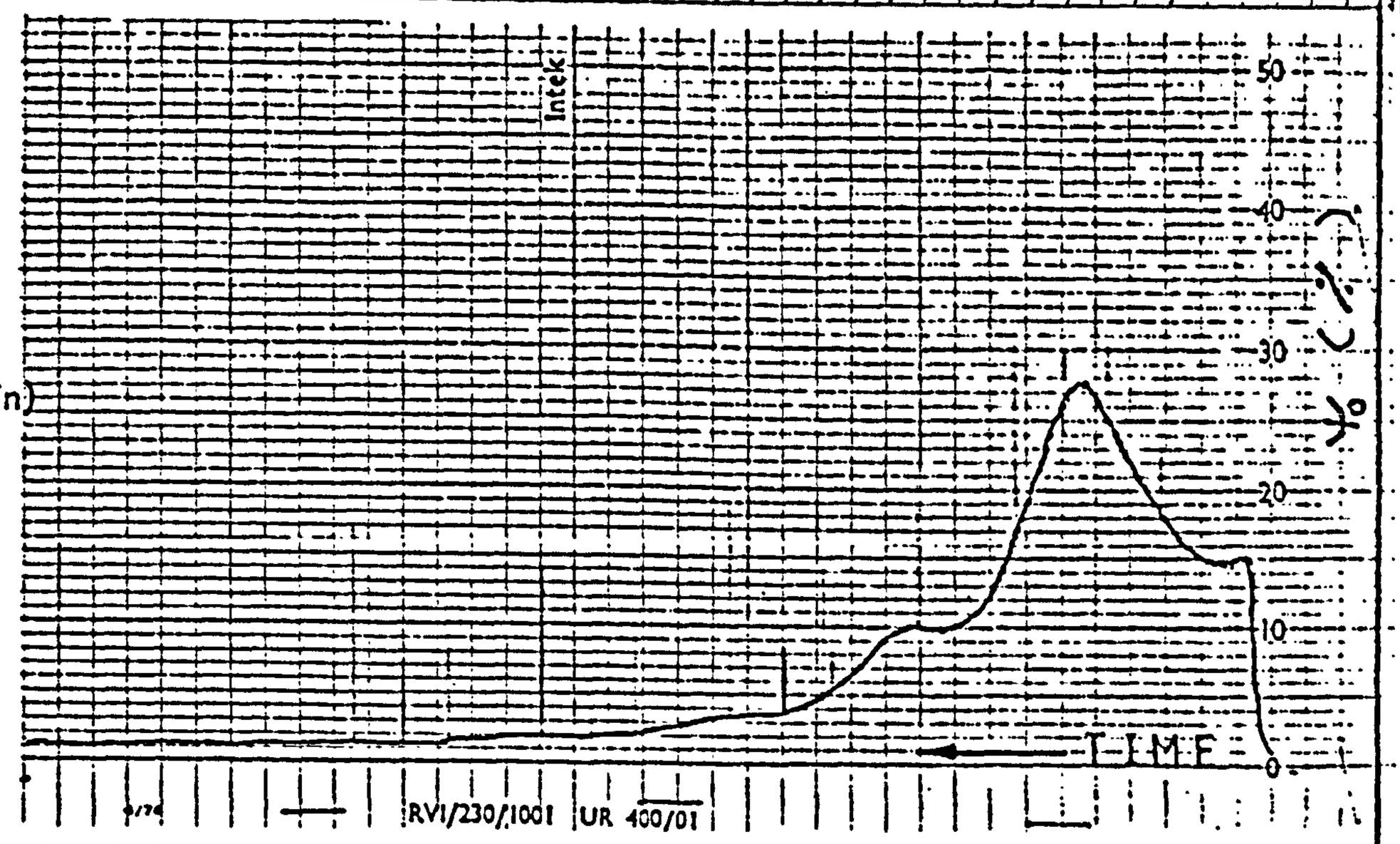
Figure (7-22)

Effect of air flowrate on bed performance (dp = 940)

Q = 325 (l/min)



Q = 375 (l/min)



Q = 500 (l/min)

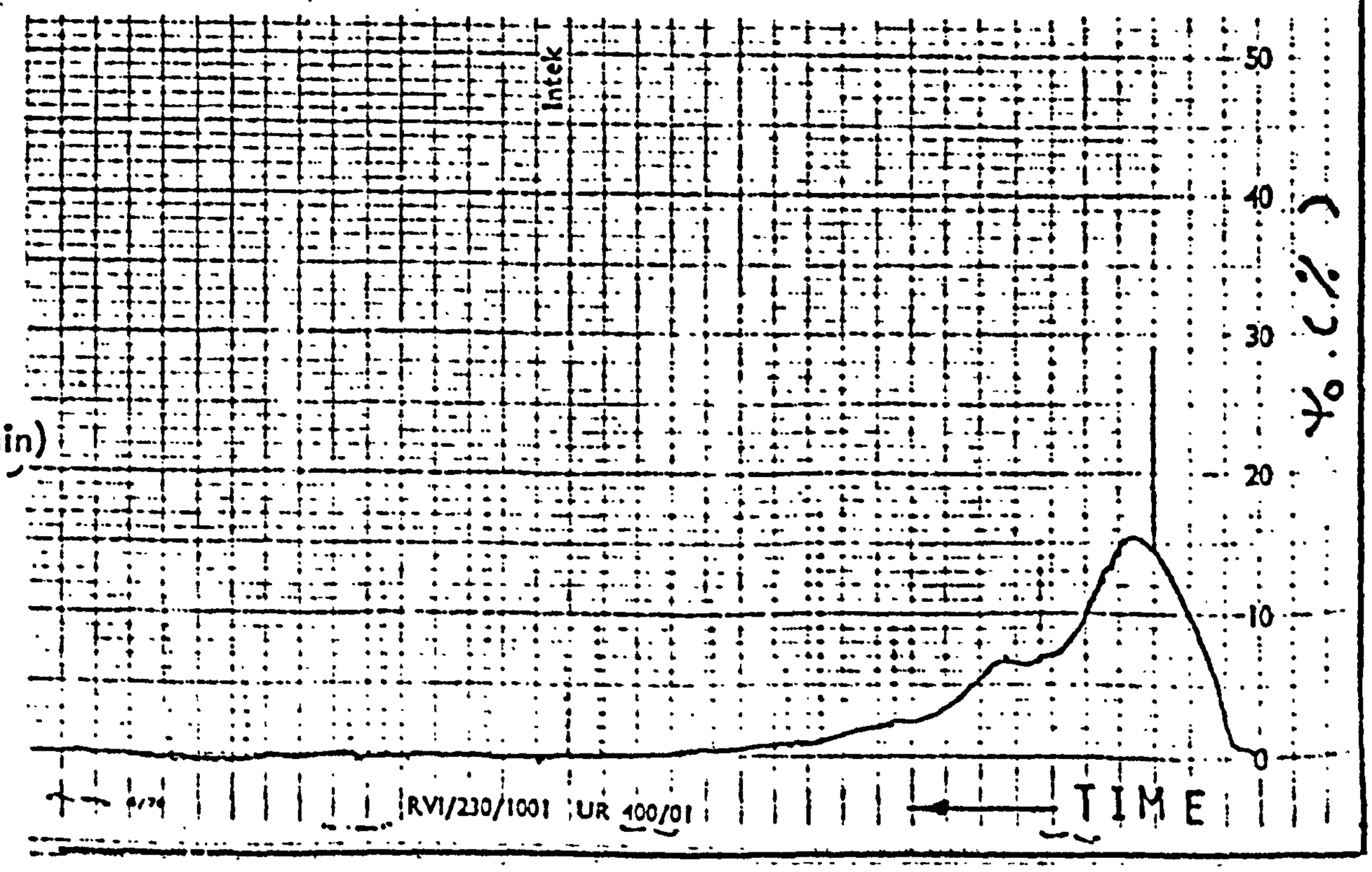


Figure (7-23) Effect of air flowrate on bed performance (dp = 2247)

APPENDIX (1)

(HYGROTHERMAL PROPERTIES OF SATURATED HUMID AIR)

TABLE A

HYGROTHERMAL PROPERTIES OF AIR SATURATED WITH WATER VAPOUR AT ATMOSPHERIC PRESSURE

Temperature (°C)	Humidity (kg/kg dry air)	Moisture vapour pressure (kN/m²)	Moisture concentration (kg/m³)	Enthalpy of vaporization (kJ/kg)	Humid enthalpy (kJ/kg dry air)	Humid volume (m³/kg dry air)	Kinematic viscosity (10^6 m²/s)	Humid heat (kJ/K kg)	Thermal conductivity (W/m K)	Moisture diffusivity (10^6 m²/s)
0	0·003 821	0·610 8	0·004 846	2 500·8	9·55	0·778 1	13·25	1·010 8	0·023 80	22·2
2	0·004 418	0·705 4	0·005 557	2 495·9	13·06	0·784 5	13·43	1·012 0	0·024 13	22·4
4	0·005 100	0·812 9	0·006 358	2 491·3	16·39	0·791 1	13·61	1·013 4	0·024 27	22·6
6	0·005 868	0·934 6	0·007 257	2 486·6	20·77	0·797 7	13·79	1·014 9	0·024 40	22·8
8	0·006 749	1·072 1	0·008 267	2·481·9	25·00	0·804 6	13·97	1·016 7	0·024 54	23·1
10	0·007 733	1·227 1	0·009 396	2 477·2	29·52	0·811 6	14·15	1·018 6	0·024 66	23·3
12	0·008 849	1·401 5	0·010 66	2 472·5	34·37	0·818 7	14·34	1·020 8	0·024 78	23·6
14	0·010 105	1·597 4	0·012 06	2 467·8	39·57	0·826 1	14·52	1·023 3	0·024 90	23·9
16	0·011 513	1·816 8	0·013 63	2 463·1	45·18	0·833 7	14·71	1·026 0	0·025 00	24·2
18	0·013 108	2·062	0·015 36	2 458·4	51·29	0·841 5	14·89	1·029 1	0·025 11	24·5
20	0·014 895	2·337	0·017 29	2·453·1	57·86	0·849 7	15·08	1·032 5	0·025 20	24·8
22	0·016 892	2·642	0·019 42	2 449·0	65·02	0·851 1	15·27	1·036 4	0·025 29	25·2
24	0·019 131	2·982	0·021 77	2 442·0	72·60	0·866 9	15·46	1·040 7	0·025 37	25·5
26	0·021 635	3·360	0·024 37	2 439·5	81·22	0·876 1	15·65	1·045 5	0·025 44	25·9
28	0·024 435	3·778	0·027 23	2 434·8	90·48	0·885 7	15·84	1·050 9	0·025 08	26·3
30	0·027 558	4·241	0·030 36	2 430·0	100·57	0·895 8	16·03	1·056 9	0·025 56	26·6
32	0·031 050	4·753	0·033 80	2 425·3	111·58	0·906 5	16·22	1·063 5	0·025 61	27·0
34	0·034 950	5·318	0·037 58	2 420·5	123·72	0·917 8	16·41	1·071 0	0·025 65	27·4
36	0·039 289	5·940	0·041 71	2 415·8	136·99	0·929 7	16·61	1·079 3	0·025 67	27·8
38	0·044 136	6·624	0·046 22	2 411·0	151·60	0·942 5	16·80	1·088 5	0·025 69	28·3
40	0·049 532	7·375	0·051 14	2 406·2	167·64	0·956 0	17·00	1·098 9	0·025 69	28·7
42	0·055 560	8·198	0·056 50	2 401·4	185·40	0·970 6	17·20	1·110 3	0·025 68	29·1
44	0·062 278	9·010	0·062 33	2 396·6	204·94	0·986 2	17·39	1·123 2	0·026 66	29·6
46	0·069 778	10·085	0·068 67	2 391·8	226·55	1·003 0	16·59	1·137 5	0·025 63	30·0
48	0·078 146	11·161	0·075 53	2 387·0	250·45	1·021 3	17·79	1·153 4	0·025 58	30·5
50	0·087 516	12·335	0·082 98	2 382·1	277·04	1·041 0	17·99	1·171 3	0·025 52	30·9
52	0·098 018	13·613	0·091 03	2 377·3	306·64	1·062 6	18·19	1·191 3	0·025 45	31·4
54	0·109 76	15·002	0·099 74	2 372·4	339·51	1·086 1	18·39	1·213 7	0·025 36	31·9
56	0·122 97	16·509	0·109 1	2 367·6	373·31	1·111 2	18·59	1·238 9	0·025 26	32·4
58	0·137 90	18·146	0·119 3	2 362·7	417·72	1·140 5	18·79	1·267 3	0·025 14	32·9
60	0·154 72	19·92	0·130 2	2 357·9	464·11	1·172 1	18·99	1·299 4	0·025 01	33·4
62	0·173 80	21·84	0·141 9	2 353·0	516·57	1·207 3	19·19	1·335 7	0·024 87	34·0
64	0·195 41	23·91	0·154 5	2 348·1	575·77	1·246 7	19·38	1·377 0	0·024 71	34·5
66	0·220 21	26·14	0·168 0	2 343·1	643·51	1·291 0	19·57	1·424 1	0·024 55	35·1
68	0·248 66	28·55	0·182 6	2 338·2	721·01	1·341 2	19·76	1·478 2	0·024 37	35·7
70	0·281 54	31·16	0·198 1	2 333·3	810·36	1·398 6	19·94	1·541 8	0·024 18	36·3
72	0·319 66	33·96	0·214 6	2 328·3	915 57	1·464 3	20·01	1·613 2	0·023 99	36·9
74	0·364 68	36·96	0·232 4	2 323·3	1 035·60	1·541 1	20·28	1·698 6	0·023 79	37·6
76	0·417 90	40·19	0·251 4	2 318·3	1 179·42	1·630 9	20·44	1·799 4	0·023 60	38·3
78	0·480 48	43·65	0·271 7	2 313·3	1 348·40	1·737 5	20·58	1·919 9	0·023 41	39·0
80	0·559 31	47·36	0·293 3	2 308·3	1 560·80	1·866 3	20·71	2·066 4	0·023 23	39·8
82	0·655 73	51·33	0·316 2	2 303·2	1 820·46	2·024 7	20·81	2·247 7	0·023 07	40·7
84	0·777 81	55·57	0·340 6	2 298·1	2 148·92	2·223 8	20·90	2·476 7	0·022 94	41·5
86	0·937 68	60·50	0·366 6	2 293·0	2 578·73	2·481 0	20·96	2·773 9	0·022 85	42·5
88	1·152 44	64·95	0·394 2	2 287·9	3 155·67	2·823 5	20·99	3·170 8	0·022 81	43·6
90	1·458 73	70·11	0·423 5	2 282·8	3 978·03	3·301 7	20·99	3·739 4	0·022 83	44·7

APPENDIX (2)

(EQUIPMENT)

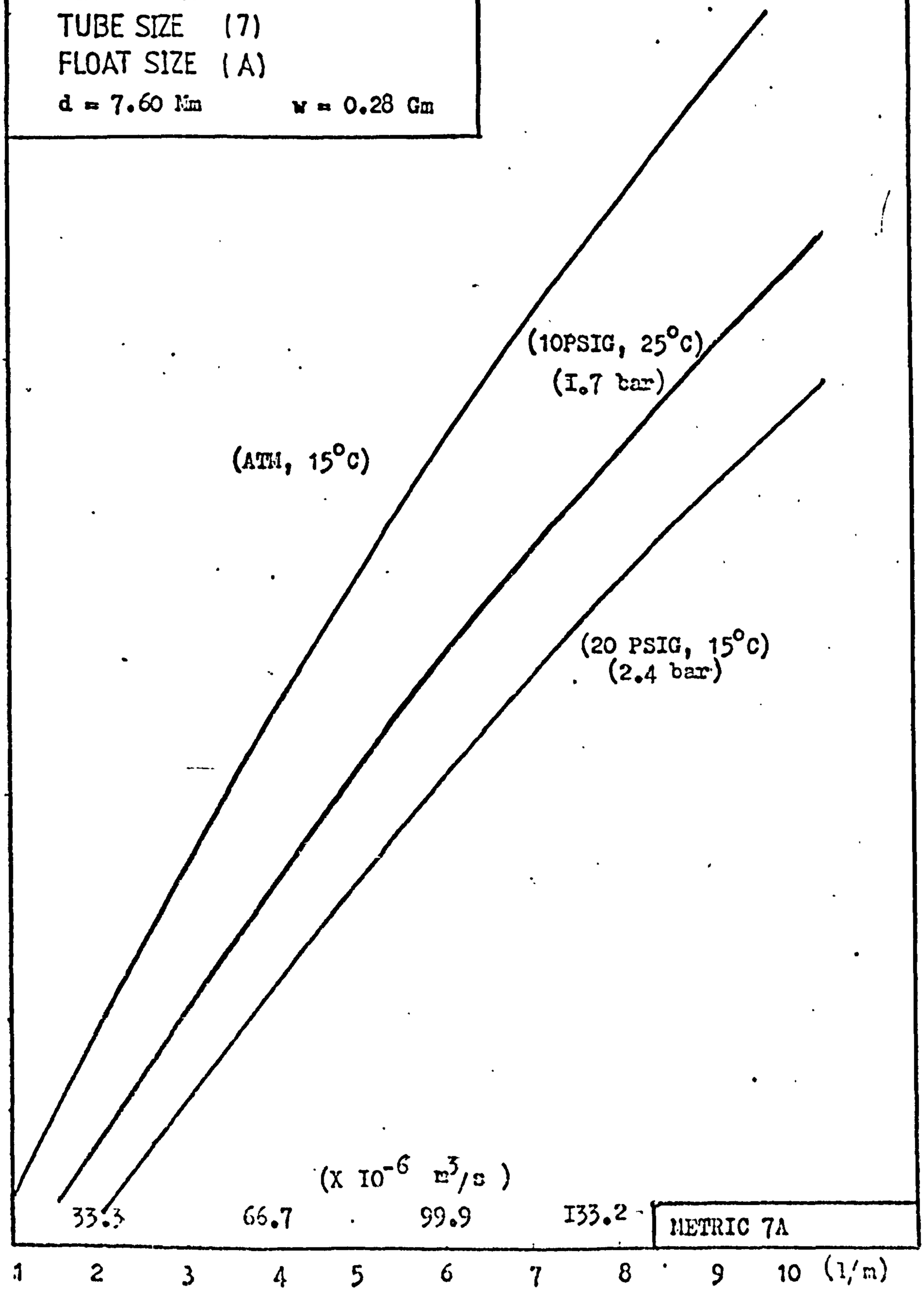
APPENDIX (2.1) ROTOMETERS CALIBRATION

APPENDIX (2.2) THERMO-COUPLES CALIBRATION

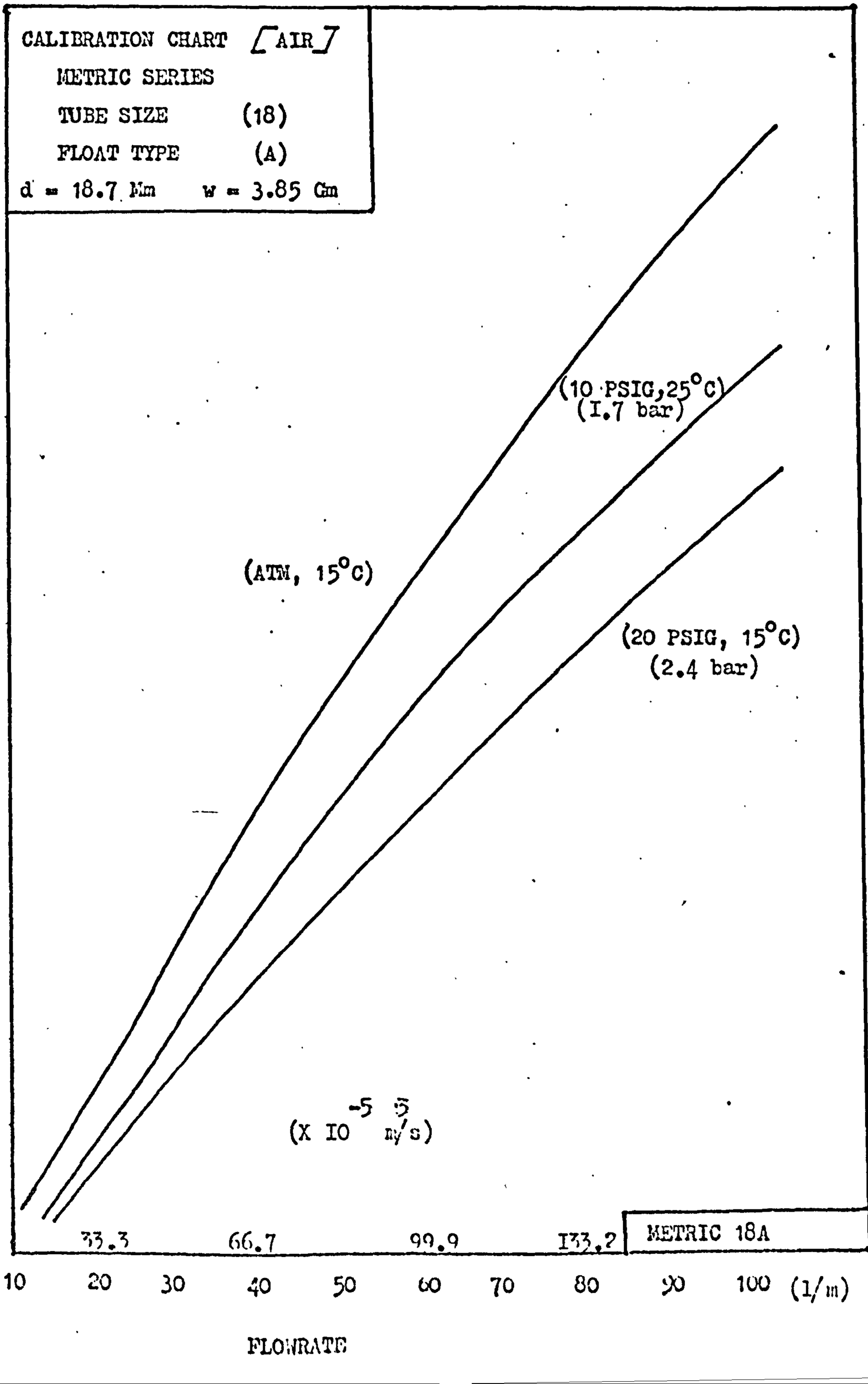
APPENDIX (2.3) HYGROMETER CALIBRATION

APPENDIX (2.1.1)

CALIBRATION CHART FOR AIR
METRIC SERIES
TUBE SIZE (7)
FLOAT SIZE (A)
d = 7.60 Mm w = 0.28 Gm

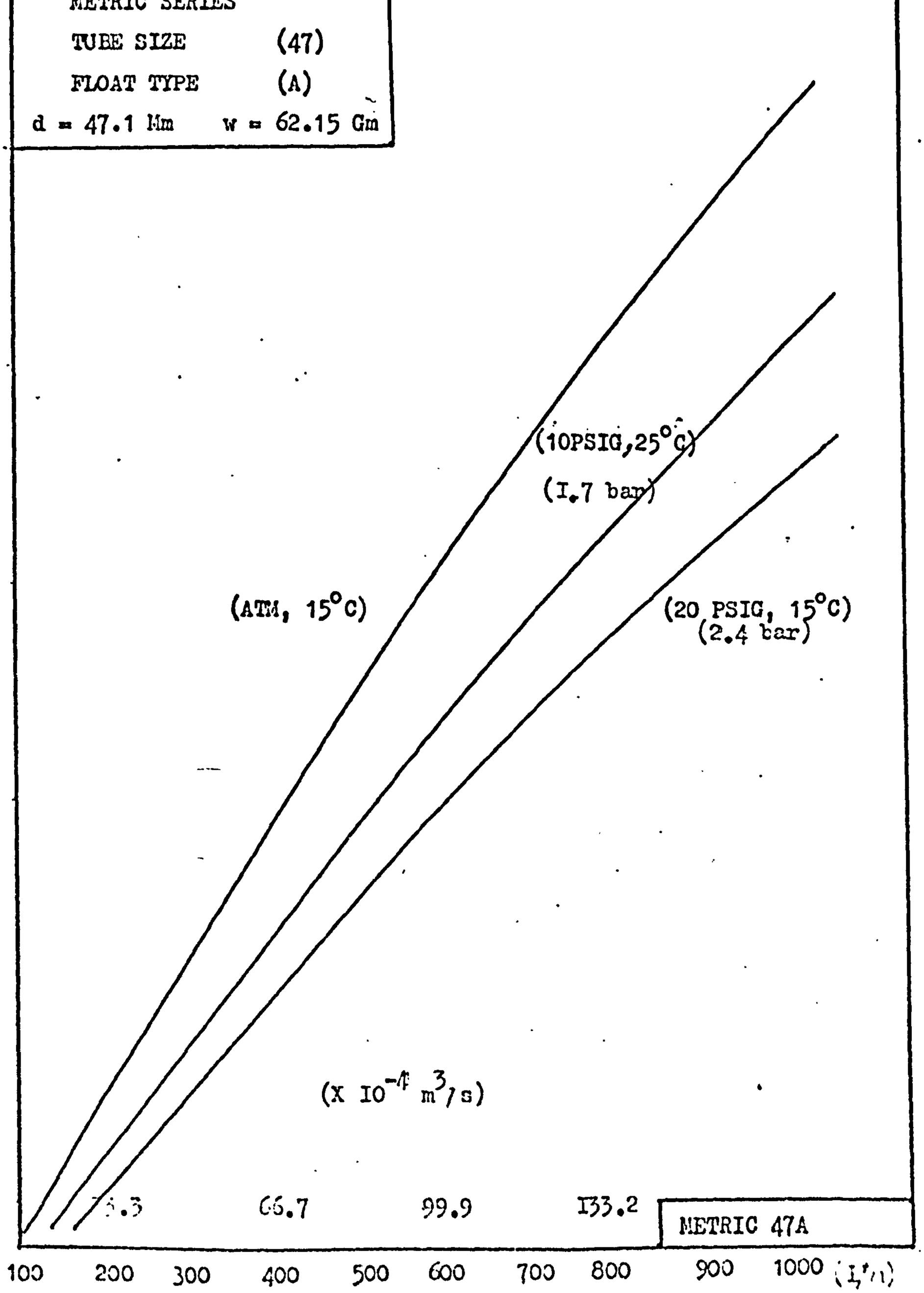


APPENDIX (2.1.2)

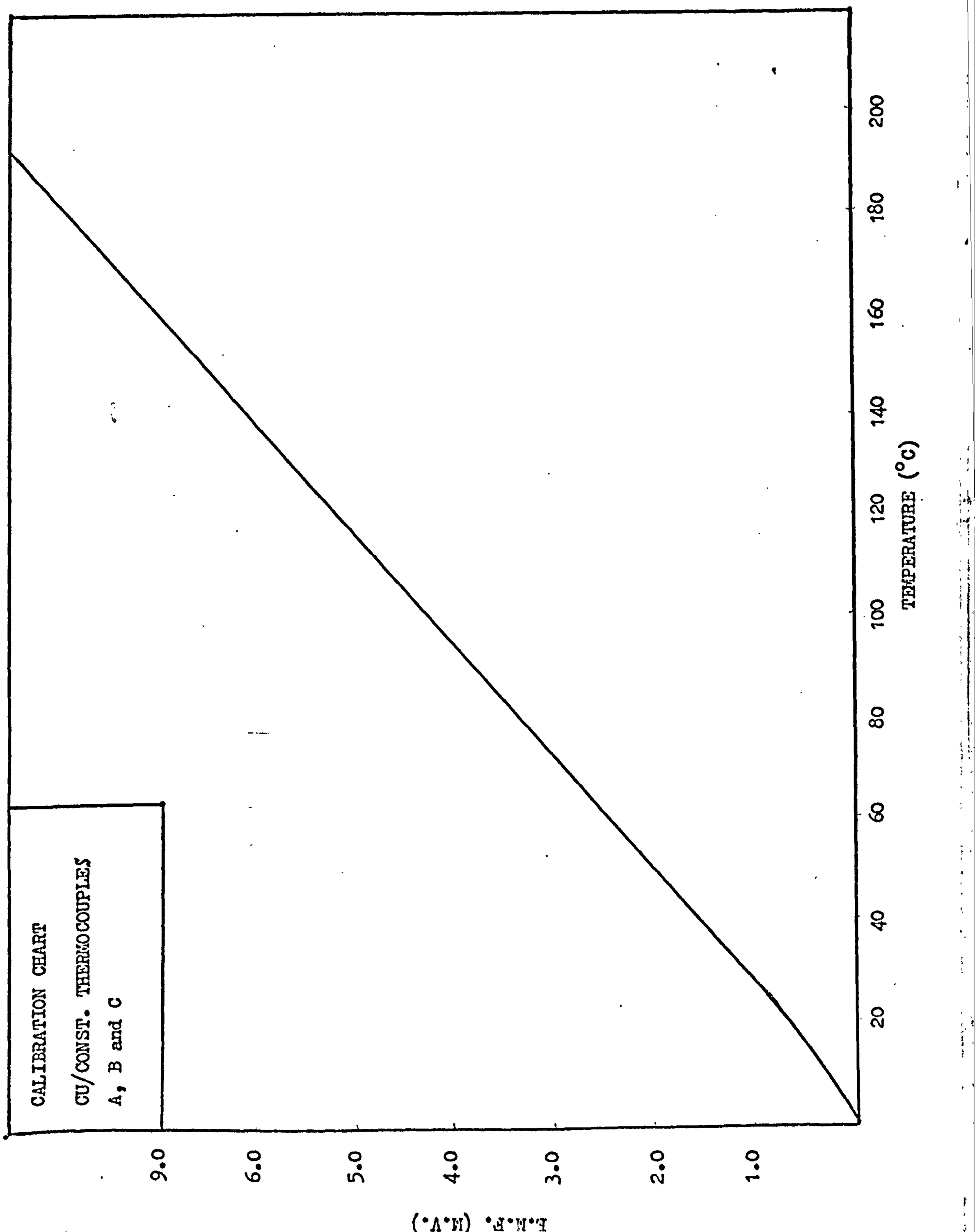


APPENDIX (2.1.3)

CALIBRATION CHART (AIR)
METRIC SERIES
TUBE SIZE (47)
FLOAT TYPE (A)
d = 47.1 Mm w = 62.15 Gm



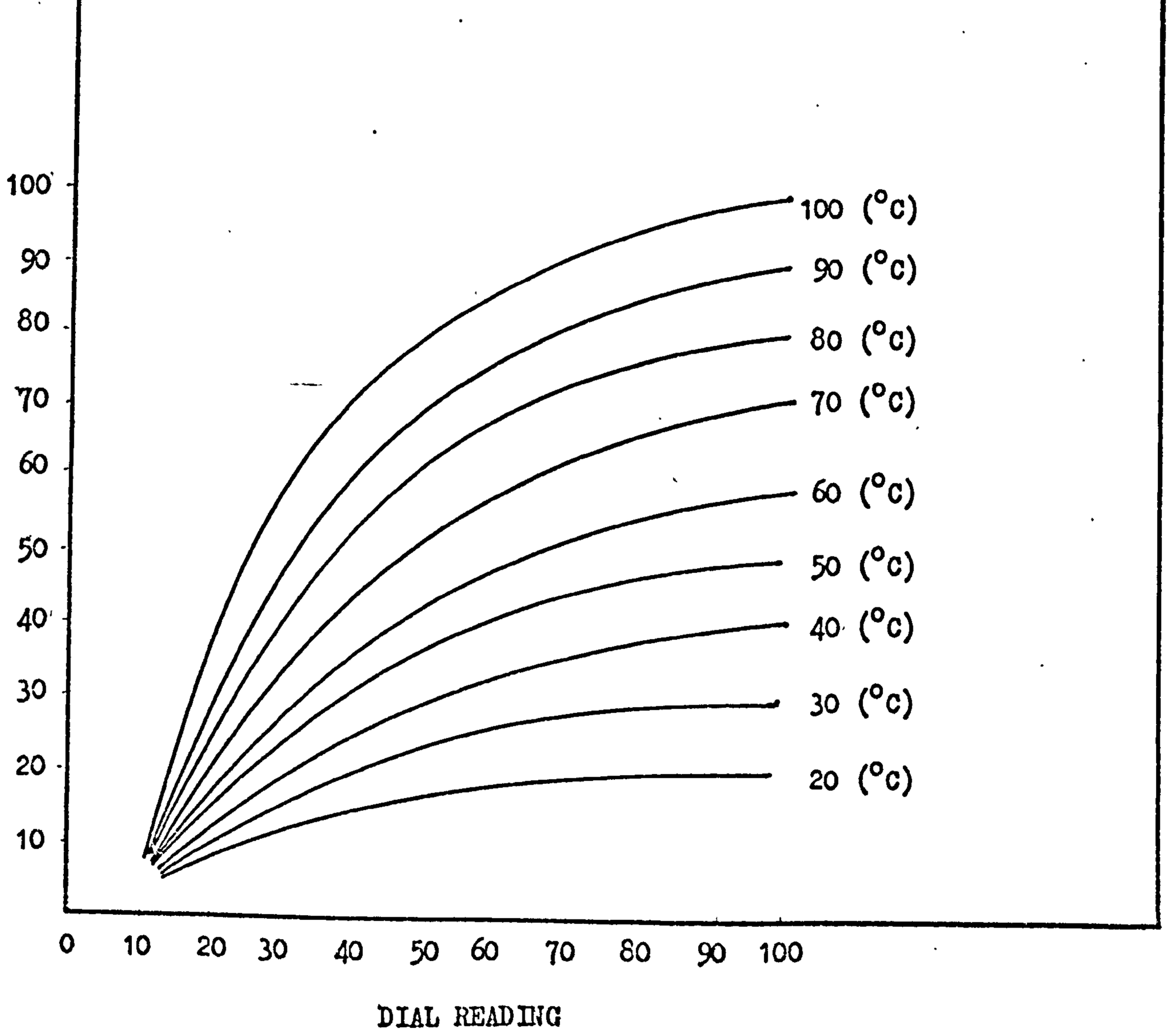
APPENDIX (2.2)


CALIBRATION CHART
CU/CONST. THERMOCOUPLES
A, B and C
E.M.F. (M.V.)
9.0
6.0
5.0
4.0
3.0
2.0
1.0
20
40
60
80
100
120
140
160
180
200
TEMPERATURE (°C)

APPENDIX (2.3.1)

CALIBRATION CHART FOR
SHAW HYGROMETER

ELEMENT : Normal
RANGE : 0/100 °C[D.P.]
OPERATING TEMP. 20/100 °C



APPENDIX (2.3.2)

MOISTURE IN GASES - APPROXIMATE RELATIONSHIPS

Dewpoint °C	Dewpoint °F	Vapour Pressure (Ice in Equilibrium) mm of Mercury	PPM on Volume Basis	Relative Humidity at 70°F %	PPM on Weight Basis in Air	PPM on Weight Basis in CO^2
-90	-130	.000070	.0923	.0003	.057	.035
-88	-126	.00010	.134	.00054	.082	.049
-86	-123	.00014	.184	.00075	.11	.069
-84	-119	.00020	.263	.00107	.16	.099
-82	-116	.00029	.382	.00155	.24	.14
-80	-112	.00040	.526	.00214	.33	.20
-78	-108	.00056	.747	.00300	.46	.28
-76	-105	.00077	1.01	.00412	.63	.38
-74	-101	.00105	1.38	.00562	.82	.52
-72	-98	.00143	1.88	.00765	1.17	.71
-70	-94	.00194	2.55	.0104	1.64	.96
-68	-90	.00261	3.44	.0140	2.13	1.29
-66	-87	.00349	4.60	.0187	2.84	1.72
-64	-83	.00464	6.10	.0248	3.71	2.29
-62	-80	.00614	8.07	.0328	5.01	3.22
-60	-76	.00808	10.6	.0433	6.59	3.90
-58	-72	.0106	14.0	.0567	8.21	5.24
-56	-69	.0138	18.3	.0738	11.6	6.81
-54	-65	.0178	23.4	.0952	14.5	8.80
-52	-62	.0230	31.1	.126	18.8	11.4
-50	-58	.0295	39.4	.160	24.2	14.6
-48	-54	.0378	49.7	.202	30.7	18.7
-46	-51	.0481	63.2	.257	39.3	23.8
-44	-47	.0609	80.0	.325	49.7	30.1
-42	-44	.0768	101.	.410	62.7	38.0
-40	-40	.0966	127.	.516	79.1	47.8
-38	-36	.1209	159.	.646	98.6	59.7
-36	-33	.1507	198.	.804	123.	74.4
-34	-29	.1873	249.	1.01	156.	92.5
-32	-26	.2318	309.	1.24	189.	115.
-30	-22	.2859	376.	1.55	234.	141.
-28	-18	.351	462.	1.88	287.	173.
-26	-15	.430	566.	2.30	351.	212.
-24	-11	.526	691.	2.81	431.	260.
-22	-8	.640	841.	3.42	524.	316.
-20	-4	.776	1,020.	4.14	635.	384.
-18	0	.939	1,230.	5.01	766.	464.
-16	+3	1.132	1,490.	6.06	925.	560.
-14	+7	1.361	1,790.	7.29	1,110.	672.
-12	+10	1.632	2,140.	8.75	1,340.	808.
-10	+14	1.950	2,560.	10.4	1,590.	964.
-8	+18	2.326	3,060.	12.8	1,900.	1,150.
-6	+21	2.765	3,640.	14.8	2,260.	1,370.
-4	+25	3.280	4,320.	17.5	2,680.	1,620.
-2	+28	3.880	5,100.	20.7	3,170.	1,920.
0	+32	4.579	6,020.	24.1	3,800	2,360.
+2	+36	5.303	7,060.	28.2	4,439.	2,824.
+4	+39	6.000	8,130.	32.5	5,100.	3,245.
+6	+42	7.020	9,370.	37.5	5,900.	3,754.
+8	+46	8.100	10,720.	42.9	6,746.	4,293.
+10	+50	9.210	12,280.	49.2	7,729.	4,919.

APPENDIX (3)

(PARTICLE SIZE DETERMINATION)

Example for:

PARTICLE SIZE DETERMINATION
(4/6 Batch - Silica Gel)

Mesh	Size (Microns)	W1 (Total)	W2 (Tray)	W (On Tray)	Xi (WT.Fr.)	Di (Microns)	$(\frac{Xi}{Di})$
115	125	357.65	349.55	8.10	.005733	312.5	.000018
32	500	416.71	403.00	13.71	.009704	550	.000018
28	600	475.00	413.37	61.63	.043621	800	.000055
16	1,000	578.28	433.13	145.15	.102735	1350	.000076
10	1,700	540.10	458.09	82.01	.058045	1850	.000031
7	2,000	788.13	462.22	325.91	.230674	2400	.000096
6	2,800	748.00	493.41	254.59	.180195	3075	.000059
5	3,350	821.56	491.03	330.53	.233944	3675	.000064
4	4,000	689.35	498.12	191.23	.135350	4800	.000028
3	5,600	689.35	498.12	-	-	-	-

$$\bar{d}_p = \frac{1}{\sum^{mil} \left(\frac{X}{D}\right)_i} = \frac{1}{0.000445}$$

$$= 2247 \text{ (Microns)}$$

APPENDIX (4)

(HEAT TRANSFER CALCULATIONS)

APPENDIX (4.1) GAS TO PARTICLE HT. TRANSFER (d_p=106 μ)

APPENDIX (4.2) GAS TO PARTICLE HT. TRANSFER (d_p=940 μ)

APPENDIX (4.3) GAS TO PARTICLE HT. TRANSFER (d_p=2247 μ)

APPENDIX (4.4) BED TO WALL HT. TRANSFER (DOW & JACKOB)

APPENDIX (4.5) BED TO WALL HT. TRANSFER (WENDER & COOPER)

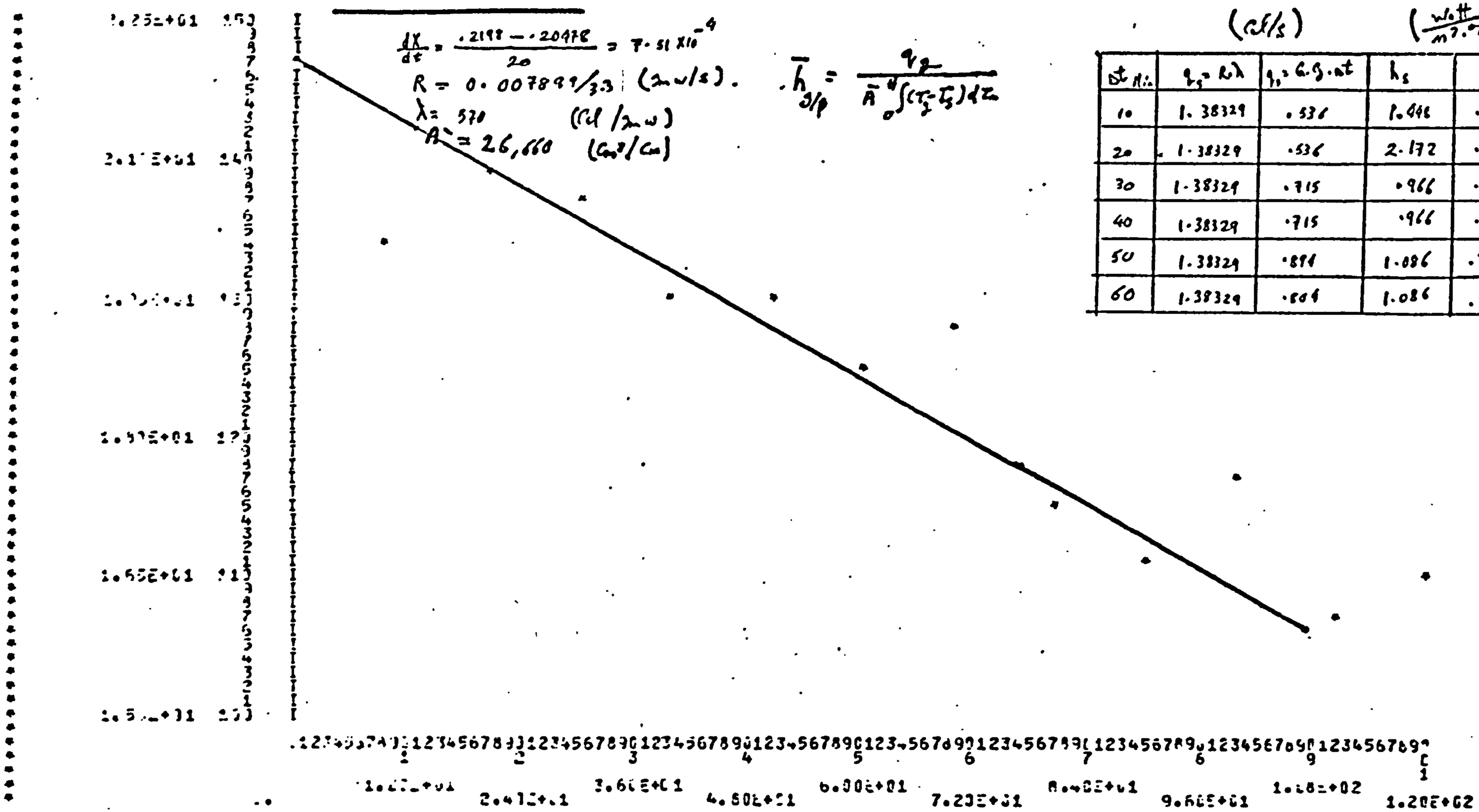
RESULTS OF
EXPERIMENT ONE FLUIDIZED BED DRYING
X(1)= 21.98

NO/	TIME MIN	WET (GM)	DRY(GM)	WATER G	SOLID GM	(X)(%)	RATE M(-1)
2	10.00000	16.84775	17.54375	1.30400	6.46730	20.16297	.18197
3	20.00000	16.56937	17.29625	1.29332	6.21980	20.79359	-.06306
4	30.00000	16.23646	17.01945	1.21701	5.94300	20.47804	.03156
5	40.00000	17.37415	16.34716	1.02697	5.27073	19.48440	.03936
6	50.00000	16.03633	15.97811	.95789	4.90166	19.54216	-.00578
7	60.00000	15.62230	15.74521	.87679	4.66876	18.77993	.07622
8	73.00000	17.34403	16.30111	1.00289	5.22466	19.19532	-.04154
9	93.00000	16.33365	15.60515	.78653	4.53170	17.22312	.19722
10	93.00000	16.21459	17.13424	1.00434	6.05779	16.57931	.06438
11	130.00000	18.03340	17.02340	1.04003	5.94695	17.46947	-.09102
12	110.00000	18.13633	17.21548	.99052	6.12903	15.99796	.14915
13	123.00000	17.19584	16.32758	.86796	5.25113	16.52961	-.05310

TABLE (4.1.1)

Q= 35 (L/M)

X INCREMENT = 1.00E+01
Y INCREMENT = 1.00E+00



II Q ~ 35 (l/m)

$$\frac{dx}{dt} = \frac{.2198 - .2047\text{B}}{20} = 7.51 \times 10^{-4}$$

$R = 0.0078\,99/3.3$ (cm/s).

$\lambda = 570$ (Cl/cm w)

$A = 26,660$ (cm^2/cm)

$$\bar{h}_{s/p} = \frac{q_2}{\bar{A}\int_0^H (T_2 - T_3)\,dz}$$

	(Cl/s)	$\left(\frac{w/\#}{m^2 \cdot ^\circ C}\right)$			($cm \cdot ^\circ C$)
St No.	$q_2 = R\lambda$	$q_1 = C.S.\sigma t$	h_s	h_2	$\int (T_2 - T_3)\,dz$
10	1.38329	.536	1.046	.561	1.5
20	1.38329	.536	2.172	.972	1
30	1.38329	.715	.966	.499	2.25
40	1.38329	.715	.966	.499	2.25
50	1.38329	.894	1.086	.702	2
60	1.38329	.894	1.086	.702	2

$\bar{h} \sim .634$ $\left(\frac{w}{m^2 \cdot ^\circ C}\right)$

CONT. (4.1.1)

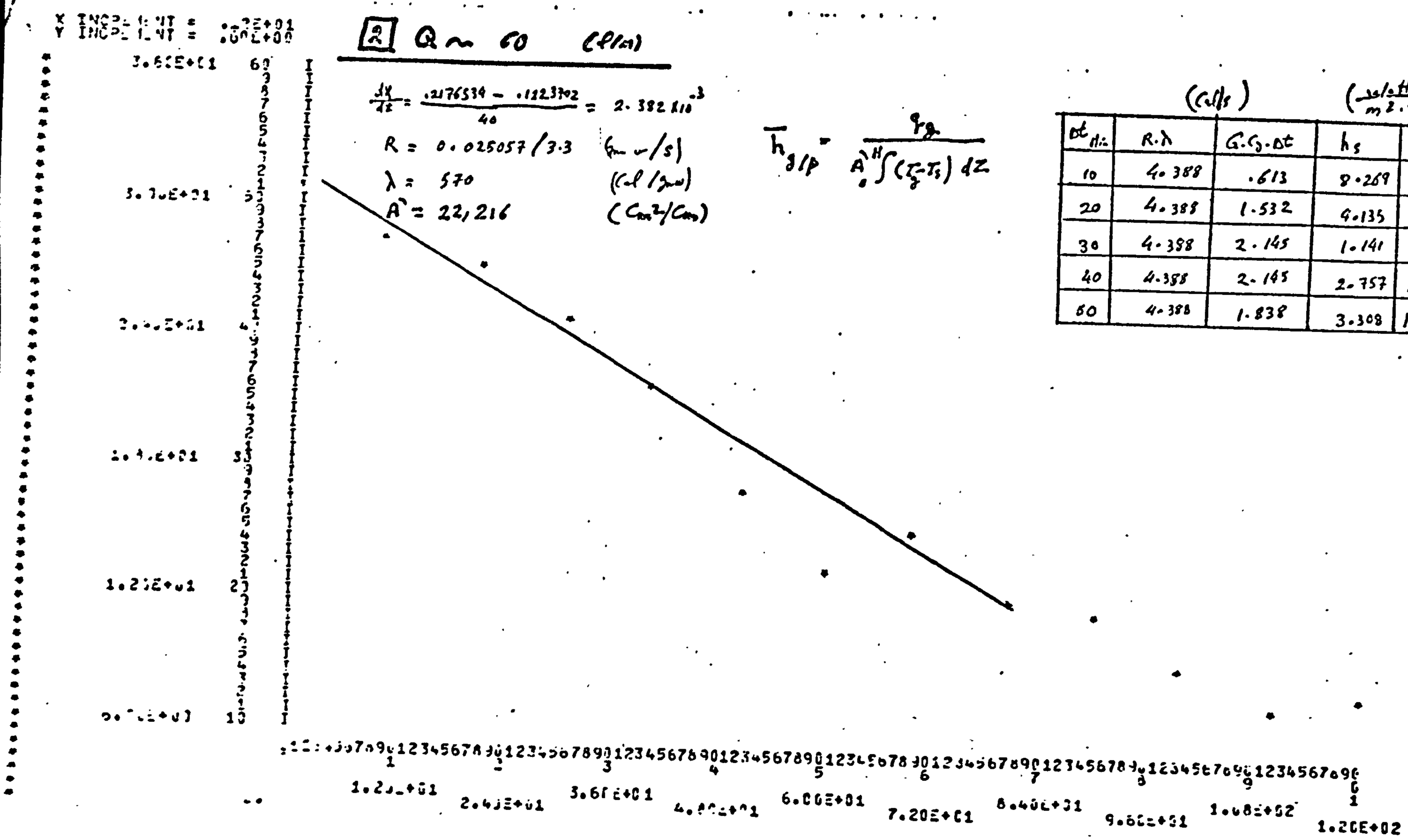
RESULTS OF
EXPERIMENT TWO FLUICIZED RED DRYING
X(1)= 30.84

NO/	TIME MIN	WET (GM)	DRY(GM)	WATER G	SOLID GM	(X)(%)	RATE M(-1)
2	10.00000	18.10307	16.56812	1.53495	5.49167	27.95051	.28919
3	20.00000	18.24963	16.71675	1.53188	5.64036	27.15955	.27910
4	30.00000	18.52119	17.05521	1.46597	5.97876	24.51963	.26399
5	40.00000	18.75158	17.37950	1.37208	6.30305	21.76534	.27543
6	50.00000	17.12314	16.24075	.88239	5.16436	17.08634	.46790
7	60.00000	17.02355	17.05486	-.77469	5.97841	12.95813	.41202
8	70.00000	17.23243	16.41745	.81495	5.34100	15.25839	-.23003
9	80.00000	16.93873	16.25500	.63373	5.17855	12.23702	.30214
10	90.00000	16.81525	16.23700	.59825	5.16055	11.59276	.06443
11	100.00000	16.79611	16.32430	.47181	5.23785	9.00770	.25851
12	110.00000	16.75039	16.34935	.40103	5.47290	7.32756	.16801
13	120.00000	16.68795	16.28895	.39900	5.21250	7.65468	-.03271

TABLE (4.1.2)

Q= 60 (L/M)

X INCREMENT = .20E+01
Y INCREMENT = .00E+00



2 Q ~ 60 (l/hr)

$\frac{dx}{dz} = \frac{.2176534 - .1223702}{40} = 2.382 \times 10^{-3}$

$R = 0.025057 / 3.3$ (gm-w/s)

$\lambda = 570$ (cal/gm)

$A = 22,216$ (Cm^2/Cm)

$\bar{h}_{slp} = \frac{q_g}{A \int_0^H (T_g - T_s)\, dz}$

Δt_{hr}	$R \cdot \lambda$ (cal/s)	$G \cdot C_g \cdot \Delta t$	h_s ($\frac{w/o H}{m^2 \cdot ^oC}$)	h_z	$\int_0^H (T_g - T_{gr})\, dz$ ($G \cdot ^oC$)
10	4.388	.613	8.269	1.155	1
20	4.388	1.532	4.135	1.443	2
30	4.388	2.145	1.141	.558	7.25
40	4.388	2.145	2.757	1.342	3
60	4.388	1.838	3.308	1.386	2.5

$\bar{h} \sim 1.178$ ($\frac{w}{m^2 \cdot ^oC}$)

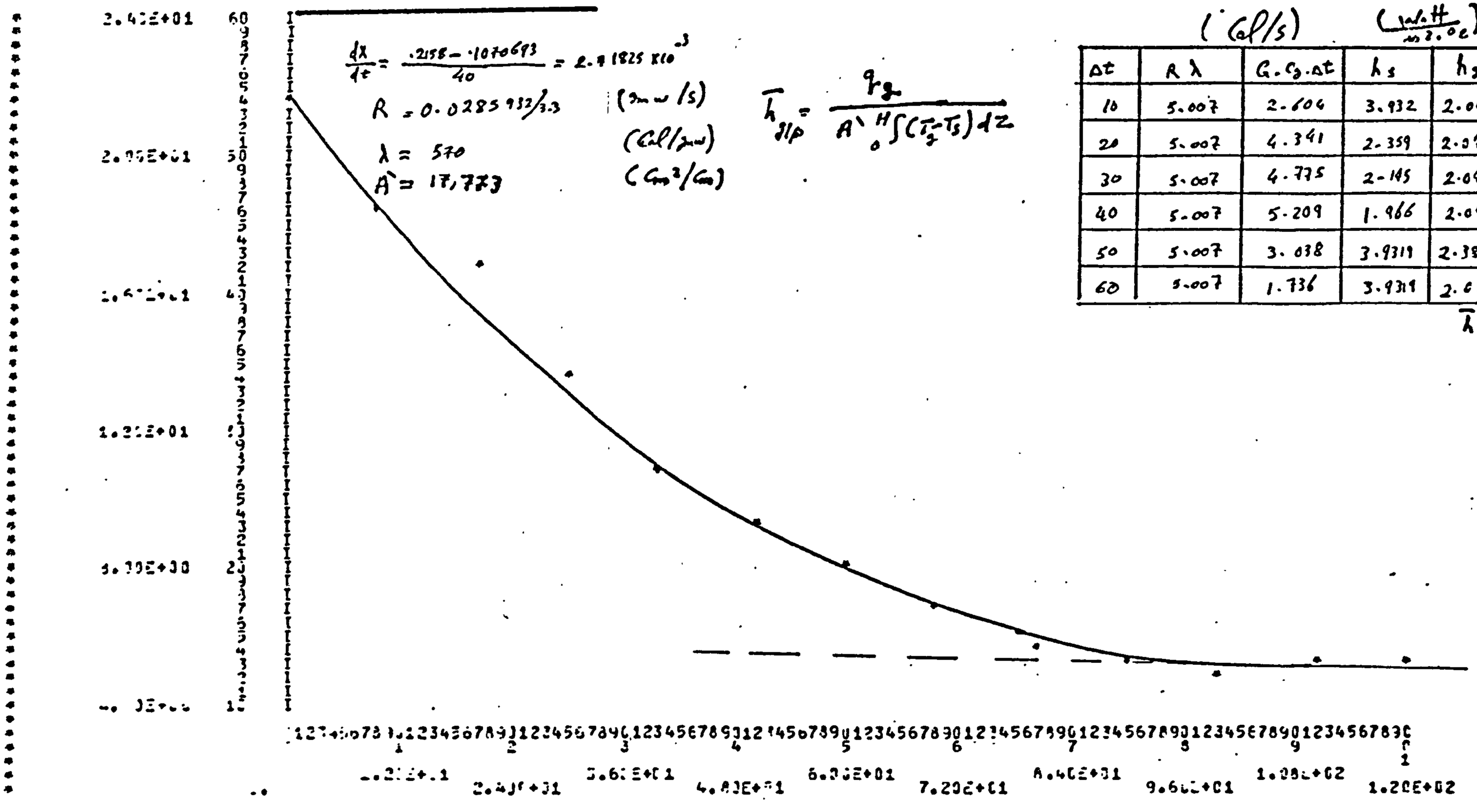
CONT. (4.1.2)

RESULTS OF
EXPERIMENT THREE FLUIDIZED BED DRYING
X(1)= 21.55

NO/	TIME MIN	WET (GM)	DRY(GM)	WATER G	SOLID GM	(X)(%)	RATE M(-1)
2	10.00000	17.99532	16.90609	1.07323	5.82964	18.51281	.30699
3	20.00000	18.90322	17.77765	1.12557	6.70120	16.79654	.17163
4	30.00000	19.09286	18.13541	.95745	7.05896	13.56361	.32329
5	40.00000	17.37433	16.76566	.60814	5.68921	10.68693	.28567
6	50.00000	18.17980	17.58520	.59360	6.50875	9.12003	.15069
7	60.00000	17.39935	17.06900	.48335	5.99255	8.16597	.09541
8	70.00000	17.85835	17.43651	.42184	6.36006	6.63264	.15333
9	80.00000	18.35768	17.96300	.39468	6.88655	5.73117	.09015
10	90.00000	18.33940	18.14698	.19156	7.07045	5.11283	.06183
11	100.00000	18.17533	17.94325	.33175	6.76680	4.90261	.02102
12	110.00000	17.57760	17.26025	.31735	6.18380	5.13190	-.02293
13	120.00000	17.67724	17.35311	.32413	6.27666	5.16405	-.00321

TABLE (4.1.3)
Q= 85 (L/M)

3. Q ~ 85 (l/s)



$\frac{dx}{dt} = \frac{.2158 - .1070693}{40} = 2.71825 \times 10^{-3}$

$R = 0.028593^2/3.3$ (cm ~ l/s)

$\lambda = 570$ (cal/cm)

$A = 17,773$ (Cm^2/Cm)

$\bar{h}_{slp} = \frac{q_2}{A \int_0^H (T_2 - T_s)\, dz}$

(cal/s)		(watt/m².°c)		(Cm.°c)
Δt	Rλ	G.C_p.Δt	h_s	h_2	$\int_0^H (T_2 - T_s)\, dz$
10	5.007	2.606	3.932	2.045	3
20	5.007	4.341	2.359	2.045	5
30	5.007	4.775	2.145	2.045	5.5
40	5.007	5.209	1.966	2.045	6
50	5.007	3.038	3.9319	2.386	3
60	5.007	1.736	3.9319	2.044	3

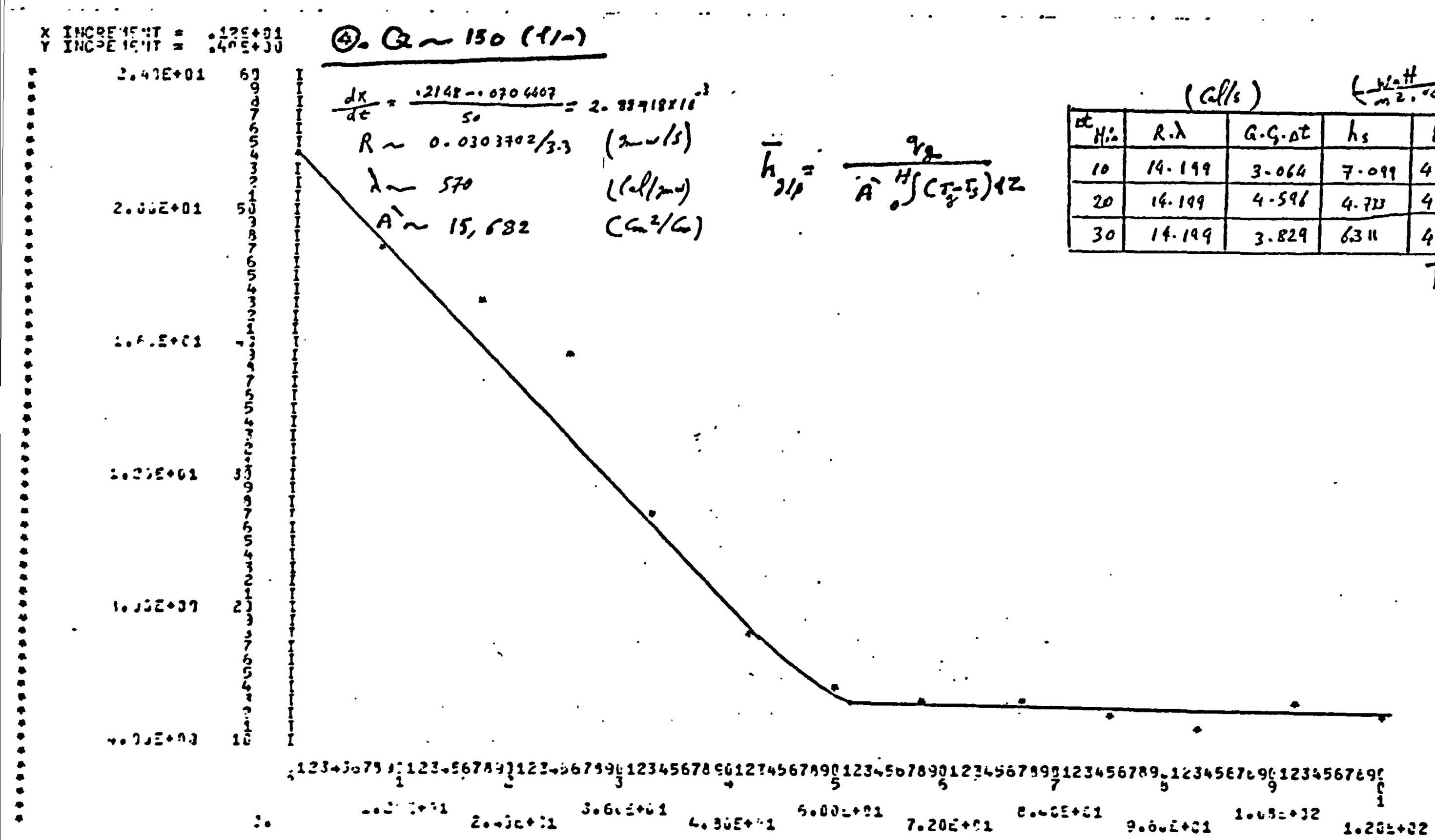
$\bar{h} \sim 2.095$ ($\frac{w}{m^2.°c}$)

CONT. (4.1.3)

RESULTS OF
EXPERIMENT FOUR FLUIDIZED BED DRYING
X(1)= 21.49

NO/	TIME MIN	WET (GM)	DRY(GM)	WATER G	SOLID GM	(X)(%)	RATE M(-1)
2	10.00000	17.34835	16.78356	1.06479	5.70711	18.65725	.28234
3	20.00000	17.97069	16.95106	1.01963	5.87461	17.35656	.13007
4	30.00000	17.27521	16.44000	.83521	5.36355	15.57196	.17846
5	40.00000	15.73619	15.32924	.45695	4.25279	10.74471	.48273
6	50.00000	16.55962	16.20814	.36148	5.13169	7.04447	.37006
7	60.00000	16.54830	16.25211	.29639	5.17566	5.72661	.13175
8	70.00000	16.94649	16.64920	.29828	5.57175	5.35343	.03732
9	80.00000	17.31547	16.72409	.29138	5.64764	5.15932	.01941
10	90.00000	16.13205	15.89971	.23234	4.82326	4.81707	.03422
11	100.00000	16.94733	16.70447	.24253	5.62932	4.30933	.05677
12	110.00000	17.15803	16.86447	.29353	5.78802	5.07134	-.07620
13	120.00000	17.32035	17.02325	.27710	5.94680	4.65965	.04117

TABLE (4.1.4)
Q = 150 (L/M)



④. Q ~ 150 (l/s)

$\frac{dx}{dt} = \frac{.2148 - .0704407}{50} = 2.887185 \times 10^{-3}$

$R \sim 0.0303702/3.3$ (m/s)

$\lambda \sim 570$ (cal/m·s·°C)

$A \sim 15,682$ (cm²/cm)

$$\bar{h}_{2\phi} = \frac{q_R}{A \int_0^H (T_g - T_s)\,dz}$$

α_{H_2O}	R.λ (cal/s)	G.Cp.Δt	h_s	h_g	$\int_0^H (T_g - T_s)\,dz$ (cm·°C)
10	14.199	3.064	7.099	4.0902	2
20	14.199	4.598	4.733	4.0902	3
30	14.199	3.829	6.311	4.543	2.25

$\bar{h} \sim 4.241$ $\left(\frac{W}{m^2 \cdot °C}\right)$

CONT.(4.1.4)

GAS TO PARTICLES HEAT TRANSFER

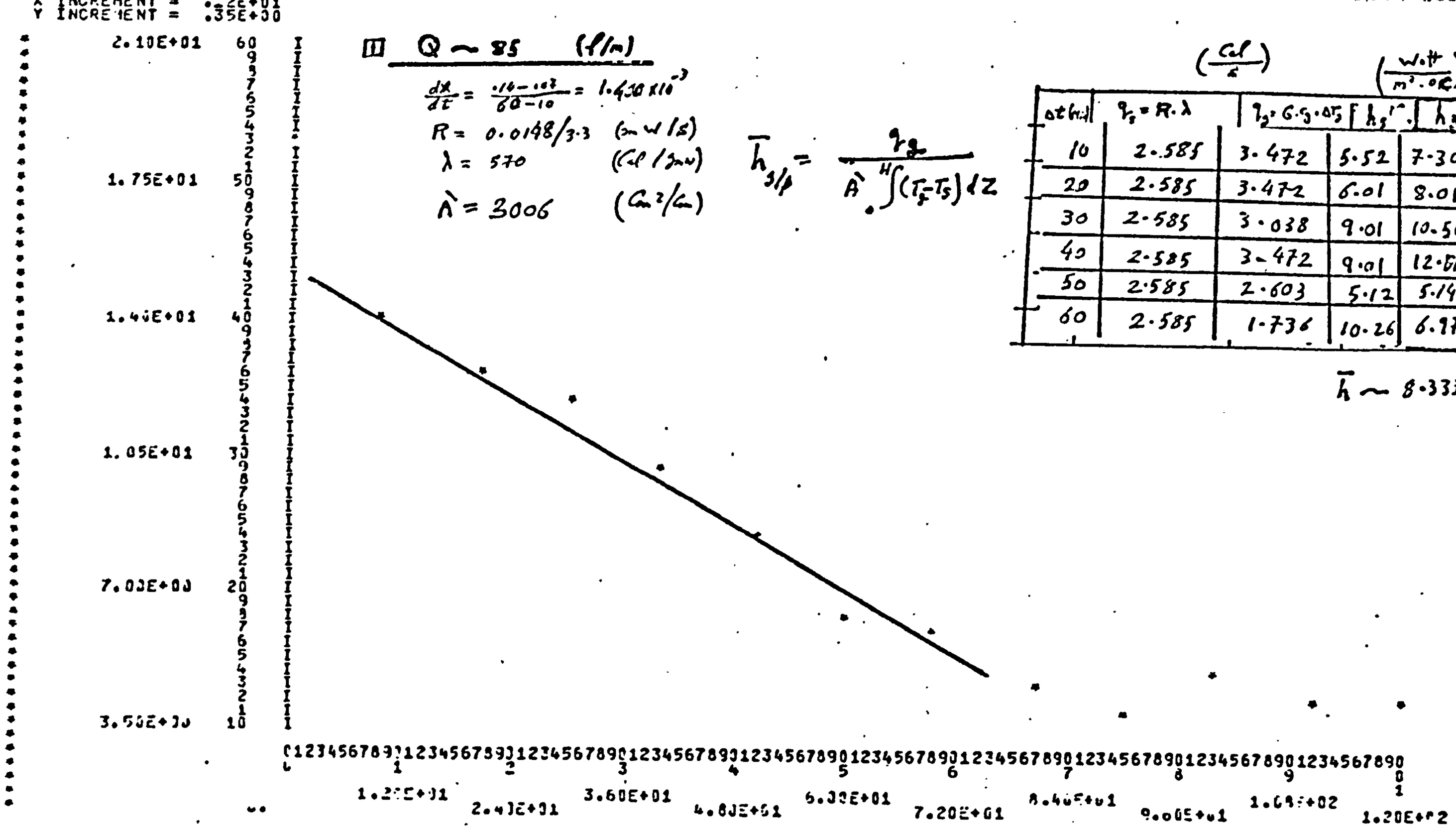
$d_p = 940\ (1/\mu)$

RESULTS OF EXPERIMENT ONE FLUIDIZED BED DRYING
X(1)= 18.56

NO/	TIME MIN	WET (GM)	DRY(GM)	WATER G	SOLID GM	(X)(%)	RATE M(-1)
2	10.00000	20.16885	19.05535	1.11350	7.97890	13 95556	.46054
3	20.00000	18.69300	17.84015	.85285	6.76370	12.60922	.13463
4	30.00000	20.21309	19.24561	.96748	8.16916	11.84308	.07661
5	40.00000	18.07900	17.42847	.65053	6.35202	10.24131	.16018
6	50.00000	19.59164	18.92265	.65899	7.84620	8.39884	.18425
7	60.00000	18.44945	18.01965	.42980	6.94320	6.19023	.22086
8	70.00000	18.13060	17.74034	.39026	6.66389	5.85634	.03339
9	80.00000	18.83700	18.46077	.34623	7.38432	4.68872	.11676
10	90.00000	17.97270	17.70630	.26670	6.62955	4.02290	.06658
11	100.00000	17.99910	17.68527	.31373	6.60882	4.74714	-.07242
12	110.00000	19.27720	18.95320	.32400	7.87675	4.11337	.06338
13	120.00000	19.23165	18.90368	.32797	7.82723	4.19012	-.00767

TABLE (4.2.1)

Q = 85 (L/M)



III $Q \sim 85$ (l/m)

$\frac{dx}{dt} = \frac{.16-.102}{60-10} = 1.430 \times 10^{-3}$

$R = 0.0148/3.3$ (gm w/s)

$\lambda = 570$ (Cal/gm)

$\hat{A} = 3006$ (cm²/cm)

$$\bar{h}_{s/p} = \frac{q_s}{\hat{A}\int_0^H (T_s - T_s)\,dz}$$

$\left(\frac{Cal}{s}\right)$			$\left(\frac{w.th}{m^2.^oC}\right)$		$(C_m.^oC)$
at h=1	$q_s = R.\lambda$	$q_s = 6.3.0.5$	h_s	h_s	$\int_0^H (T_s - T_s)\,dz$
10	2.585	3.472	5.52	7.30	6.5
20	2.585	3.472	6.01	8.01	6
30	2.585	3.038	9.01	10.51	4
40	2.585	3.472	9.01	12.61	4
50	2.585	2.603	5.12	5.14	7.0
60	2.585	1.736	10.26	6.77	3.5

$\bar{h} \sim 8.333$ $\left(\frac{W}{m^2.^oC}\right)$

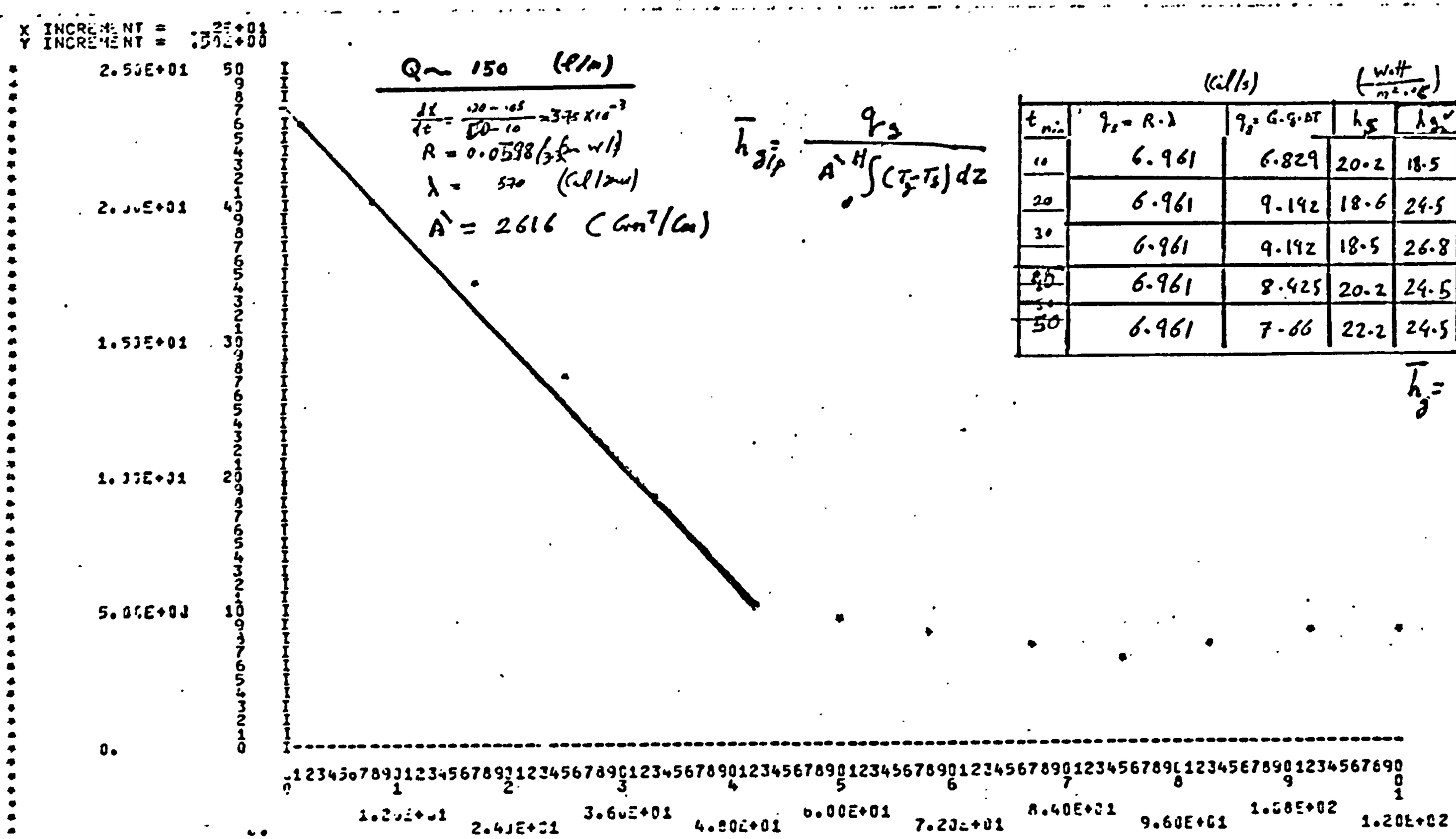
CONT. (4.2-1)

RESULTS OF
EXPERIMENT TWO FLUIDIZED BED DRYING
X(1)= 23.36

NO/	TIME MIN	WET (GM)	DRY(GM)	WATER G	SOLID GM	(X)(./.)	RATE M(-1)
2	10.00000	19.75246	18.29270	1.45976	7.21625	20.22879	.31292
3	20.00000	20.17128	18.85100	1.32028	7.77455	16.98268	.32467
4	30.00000	19.19400	18.23000	.96400	7.15355	13.47583	.35062
5	40.00000	18.76475	18.14117	.62358	7.06472	8.82668	.46491
6	50.00000	17.46932	17.15575	.31357	6.07930	5.15900	.36687
7	60.00000	19.95575	19.58526	.37049	8.50881	4.35419	.08038
8	70.00000	18.79325	18.50664	.28661	7.43019	3.85737	.04968
9	80.00000	18.55415	18.30200	.25215	7.22555	3.48970	.03677
10	90.00000	17.66543	17.47500	.19143	6.39855	2.99177	.04979
11	100.00000	16.84425	16.64020	.20405	5.56375	3.66749	-.06757
12	110.00000	16.13925	17.87732	.26093	6.80087	3.83672	-.01692
13	120.00000	18.56300	18.26631	.29669	7.18986	4.12651	-.02898

TABLE (4.2.2)

Q= 150 (L/M)



$Q \sim 150 \quad (l/m)$

$\frac{dx}{dt} = \frac{120 - 105}{100 - 10} = 3.75 \times 10^{-3}$

$R = 0.0598 \left(\frac{3}{4}\text{in wall}\right)$

$\lambda = 570 \quad (Cal/sec)$

$A' = 2616 \quad (Cm^2/Cm)$

$$\bar{h}_{air} \quad \frac{q_s}{A' \int_0^H (T_s - T_s)\, dz}$$

	$q_s = R \cdot \lambda$ (Cal/s)	$q_s = G \cdot S \cdot \Delta T$	h_s $\left(\frac{Watt}{m^2 \cdot ^\circ C}\right)$	h_s'	$\int_0^H (T_s - T_s)\, dz$ $(Cm \cdot ^\circ C)$
10	6.961	6.829	20.2	18.5	5.5
20	6.961	9.192	18.6	24.5	6
30	6.961	9.192	18.5	26.8	5.5
40	6.961	8.425	20.2	24.5	5.5
50	6.961	7.66	22.2	24.5	5

$\bar{h}_s = 25.00 \left(\frac{W}{m^2 \cdot ^\circ C}\right)$

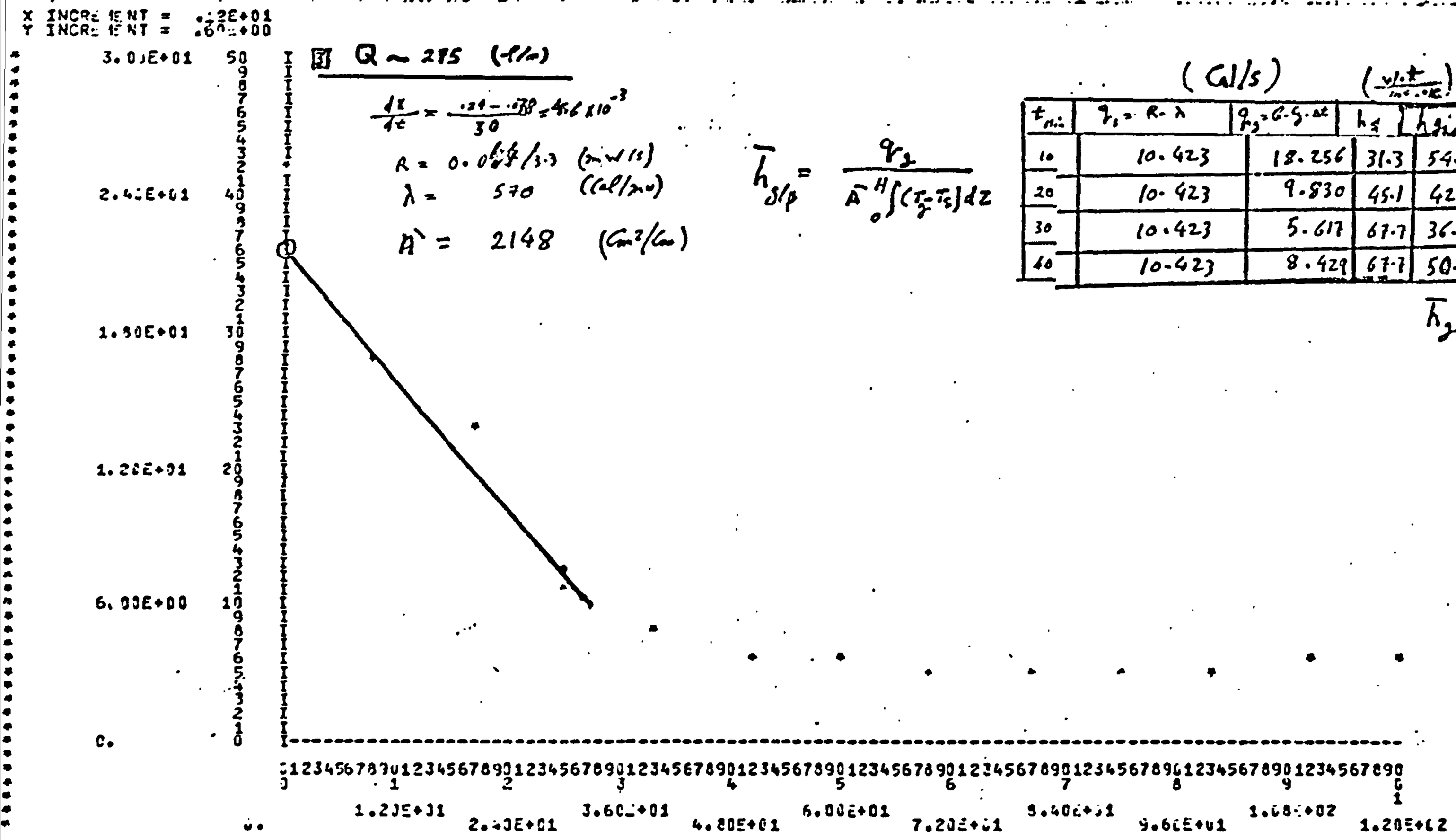
CONT. (4.2.2)

RESULTS OF
EXPERIMENT THREE FLUIDIZED BED DRYING
X(1)= 25.27

NO/	TIME MIN	WET (GM)	DRY(GM)	WATER G	SOLID GM	(X)(g/g)	RATE M(-1)
2	10.00000	19.77730	18.52455	1.25245	7.44810	16.81570	.84513
3	20.00000	20.03434	18.96725	1.06709	7.89080	13.52322	.32925
4	30.00000	18.40572	17.95975	.44597	6.88330	6.47901	.70442
5	40.00000	17.13125	16.86100	.27025	5.78455	4.67193	.18071
6	50.00000	18.51920	18.24525	.27395	7.16800	3.82142	.08505
7	60.00000	18.52625	18.28500	.24125	7.20855	3.34672	.04747
8	70.00000	18.49435	18.27024	.22411	7.19379	3.11533	.02314
9	80.00000	18.86164	18.63045	.23119	7.55400	3.06050	.00548
10	90.00000	19.13780	18.90461	.23319	7.82816	2.97886	.00816
11	100.00000	19.44435	19.20317	.24118	8.12672	2.96774	.00111
12	110.00000	19.41841	19.14535	.27306	8.06890	3.38410	-.04164
13	120.00000	18.40873	18.17066	.23807	7.09421	3.35584	.00283

TABLE (4.2.3)

Q= 275 (L/M)



3 $Q \sim 275$ (l/m)

$\frac{dx}{dt} = \frac{.124 - .078}{30} = 4.6 \times 10^{-3}$

$R = 0.0\frac{1}{3}/3.3$ (cm w/s)

$\lambda = 570$ (cal/cm)

$A' = 2148$ (cm²/cm)

$$\bar{h}_{s/p} = \frac{q_2}{\bar{A}' \int_0^H (T_2 - T_s)\,dz}$$

t_{min}	$q_1 = R \cdot \lambda$ (Cal/s)	$q_2 = C \cdot \rho \cdot \Delta t$ (Cal/s)	h_s $\left(\frac{w}{m^2 \cdot °C}\right)$	h_{fin} $\left(\frac{w}{m^2 \cdot °C}\right)$	$\int_0^H (T_2 - T_s)\,dz$ (cm·°C)
10	10.423	18.256	31.3	54.8	6.5
20	10.423	9.830	45.1	42.6	4.5
30	10.423	5.617	67.7	36.5	3
40	10.423	8.429	67.7	50.8	3

$\bar{h}_2 = 45.830 \left(\frac{w}{m^2 \cdot °C}\right)$

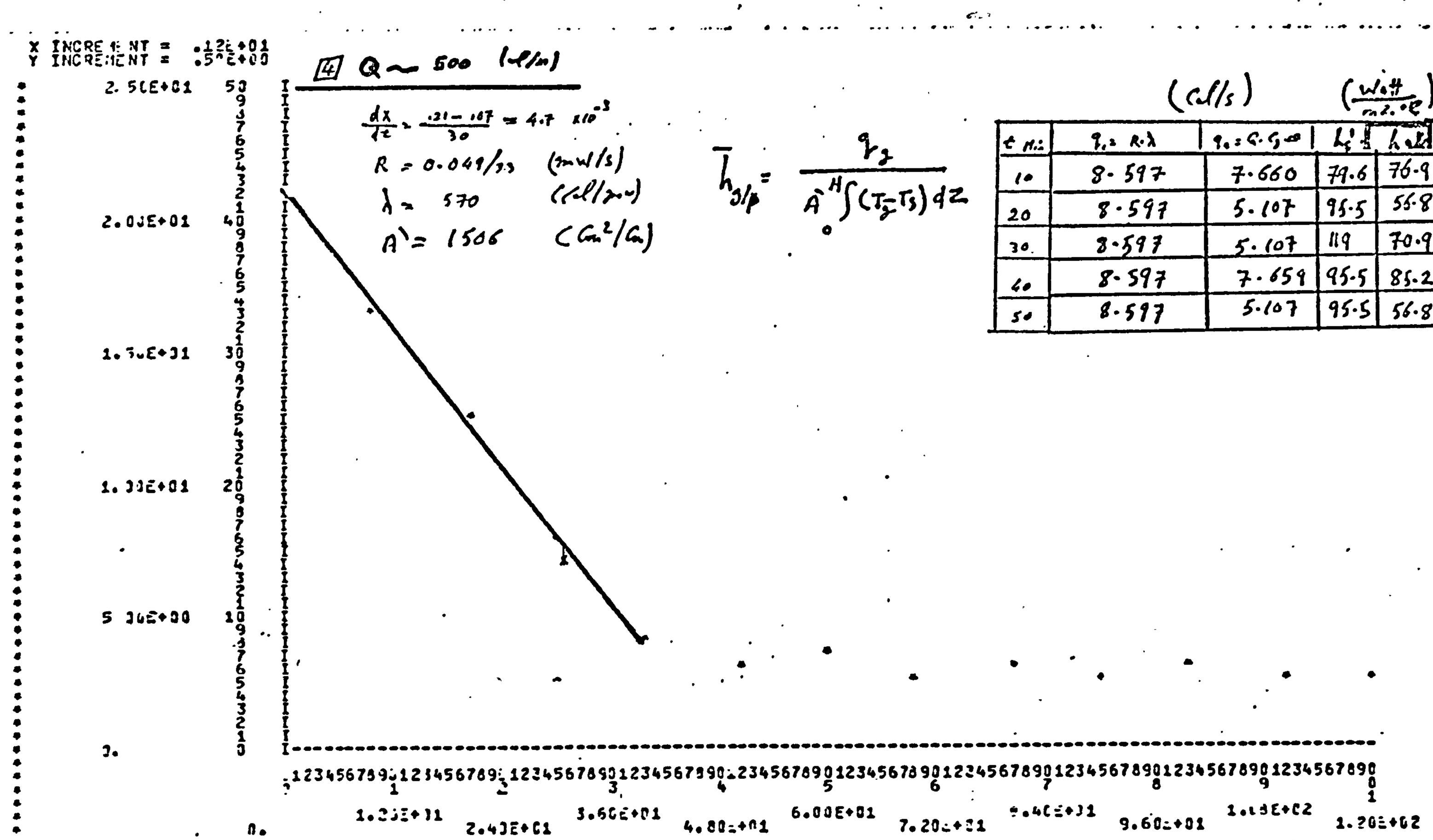
CONT. (4.2.3)

RESULTS OF
EXPERIMENT FOUR FLUIDIZED BED DRYING
X(1)= 21.07

NO/	TIME MIN	WET (GM)	DRY(GM)	WATER G	SOLID GM	(X)(G/G)	RATE M(-1)
2	13.00000	18.13768	17.13853	.99915	6.06208	16.48197	.45838
3	23.00000	20.33234	19.32018	1.01216	8.24373	12.27796	.42040
4	33.00000	18.17185	18.00000	.17185	6.92355	2.48215	.97958
5	43.00000	18.75519	18.46151	.29368	7.38506	3.97668	-.14945
6	53.00000	17.97350	17.68500	.28850	6.60855	2.85237	.11243
7	63.00000	18.59367	18.32605	.26762	7.24960	3.69151	-.08391
8	73.00000	18.52683	18.34300	.18380	7.26655	2.52940	.11621
9	83.00000	19.74396	19.50144	.23952	8.42499	2.84297	-.03136
10	93.00000	19.21742	19.02890	.18852	7.95245	2.37059	.04724
11	103.00000	17.64326	17.45110	.19216	6.37465	3.01444	-.06438
12	113.00000	18.54027	18.36800	.17227	7.29155	2.36260	.06518
13	123.00000	19.05225	18.84990	.20235	7.77345	2.60309	-.02405

TABLE (4.2.4)
Q= 500 (L/M)

X INCREMENT = .12E+01
Y INCREMENT = .5?E+00



④ $Q \sim 500$ (cl/m)

$\frac{dx}{dz} = \frac{.21 - .107}{30} = 4.7 \times 10^{-3}$

$R = 0.049/3.3$ (mW/s)

$\lambda = 570$ (cal/gm)

$A = 1506$ (Cm^2/Cm)

$$\bar{h}_{s/p} = \frac{q_z}{A \int_0^H (T_z - T_s)\, dz}$$

(cal/s) ($\frac{W \cdot H}{m^2 \cdot ^oC}$) ($Cm \cdot ^oC$)

t N.:	$q_z = R \cdot \lambda$	$q_z = Q \cdot \rho$	h_s	h_{sl}	$\int_0^H (T_z - T_s)\, dz$
10	8.597	7.660	79.6	76.9	3
20	8.597	5.107	95.5	56.8	2.5
30	8.597	5.107	119	70.9	2
40	8.597	7.659	95.5	85.2	2.5
50	8.597	5.107	95.5	56.8	2.5

$\bar{h}_s = 66.6 \left(\frac{W}{m^2 \cdot ^oC}\right)$

CONT. (4.2.4)

$d_p = 2247\ (\mu)$

EXPERIMENT ONE FLUIDIZED BED DRYING
X(1)= 22.02

NO/	TIME MIN	WET (GM)	DRY(GM)	WATER G	SOLID GM	(X)(%)	RATE M(-1)
2	10.00000	19.89325	18.10586	1.79239	7.02941	25 49844	-.34819
3	20.00000	20.42561	18.50770	1.91791	7.43125	25.80871	-.03103
4	30.00000	20.08325	18.20085	1.88240	7.12446	26.42187	-.06132
5	40.00000	20.07149	18.21577	1.85572	7.13932	25.99295	.04289
6	50.00000	20.53646	18.63938	1.89708	7.61293	24.26241	.17305
7	60.00000	20.37860	18.90942	1.46918	7.83297	18.75635	.55060
8	70.00000	19.81716	18.69815	1.11901	7.62176	14.68195	.40745
9	80.00000	19.20380	18.38300	.82080	7.30655	11.23376	.34481
10	90.00000	19.79428	19.03830	.75598	7.96185	9.49503	.17307
11	100.00000	19.70318	19.13800	.56518	8.06155	7.01081	.24842
12	110.00000	18.95500	18.35880	.49620	7.28235	6.81373	.01971
13	120.00000	19.53042	19.11655	.41387	8.04010	5.14757	.16662

TABLE (4.3.1)

Q = 150 (L/M)

RESULTS OF
EXPERIMENT TWO FLUIDIZED BED DRYING
X(1)= 19.20

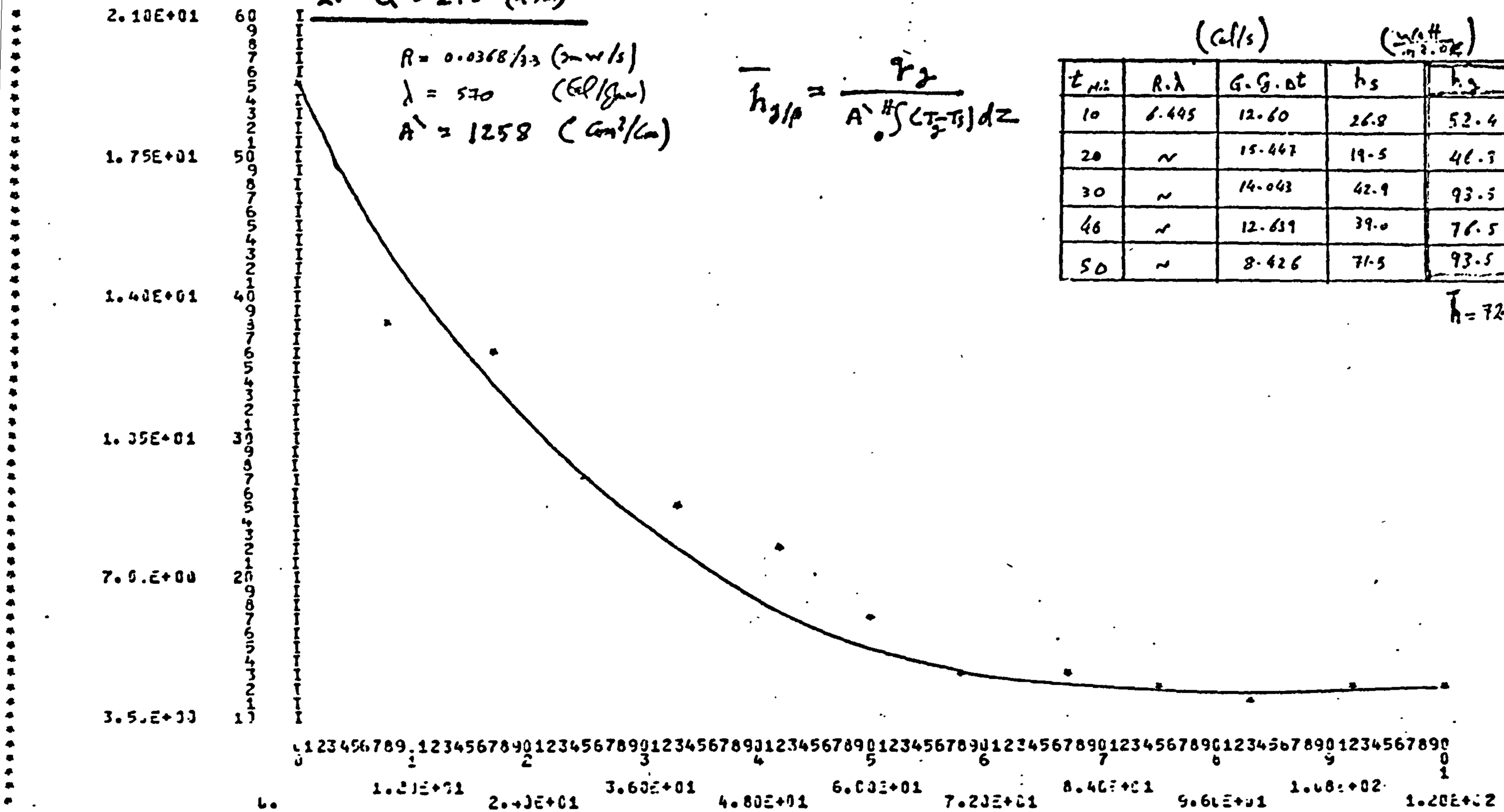
NO/	TIME MIN	WET (GM)	DRY(GM)	WATER G	SOLID GM	(X)(%)	RATE M(-1)
2	10 00000	19.28964	18.31700	.97264	7.24055	13.43323	.57620
3	20.00000	19.66815	18.69515	.97300	7.61870	12.77121	.06620
4	30.00000	19.25645	18 53985	71660	7.46340	9.60152	.31697
5	40 00000	19.11500	18.46500	.65000	7.38835	8.79743	.08041
6	50.00000	18.91677	18 36717	54960	7.29072	7 53835	.12590
7	60 00000	19.83068	19.40490	.48578	9.32845	5.83278	.17056
8	70.00000	18.62851	18.30354	32497	7.22709	4 49655	13362
9	80 00000	18.41200	18.10322	.30878	7.02677	-.39434	.01022
10	90.00000	18.05236	17.78881	.29355	6.71236	4 37328	.00211
11	100.00000	18.70231	18.42701	.27530	7.35056	3.74529	.00280
12	110.00000	18.55019	18.25342	.30477	7.17697	4.24650	-.05012
13	120.00000	18.76631	18.44855	.31776	7.37210	4.31031	-.00638

TABLE (4.3.2)

Q= 275 (L/M)

X INCREMENT = .12E+01
Y INCREMENT = .35E+00

2. Q ~ 275 (l/m)



$R = 0.0368/33$ (m w/s)

$\lambda = 570$ (Cal/Gm)

$A' = 1258$ (Cm^2/Cm)

$$\overline{h}_{g/p} = \frac{\dot{q}_2}{A' \int_0^{H} (T_2 - T_s)\, dz}$$

	(Cal/s)			(Watt/m²·°K)	(Cm·°C)
t_{Hr}	R.λ	G.G.Δt	h_s	h_2	$\int_0^H (T_2 - T_s)\, dz$
10	8.445	12.60	26.8	52.4	8
20	~	15.447	19.5	46.3	11
30	~	14.043	42.9	93.5	5
40	~	12.639	39.0	76.5	5.5
50	~	8.426	71.5	93.5	3

$\overline{h} = 72.54$ $\left(\frac{W}{m^2 \cdot °C}\right)$

CONT.(4.3.2)

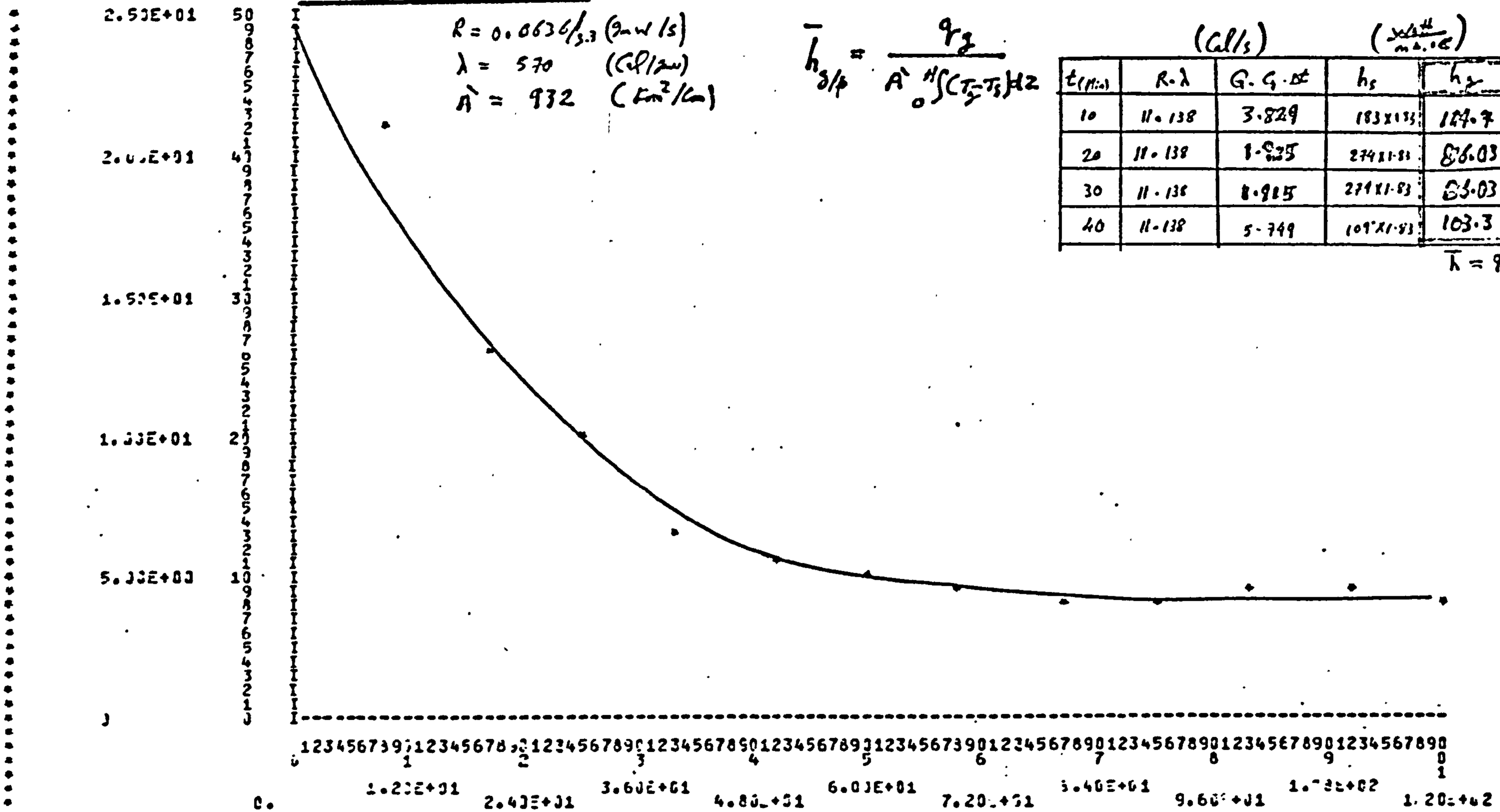
RESULTS OF
EXPERIMENT THREE FLUIDIZED BED DRYING
X(1)= 24.58

NO/	TIME MIN	WET (GM)	DRY(GM)	WATER G	SOLID GM	(X)(%)	RATE M(-1)
2	13.00000	18.15745	16.93290	1.22455	5.85645	20.90942	.36754
3	23.00000	19.80200	18.81165	.99035	7.73520	12.80316	.81063
4	33.00000	18.92378	18.22540	.69838	7.14895	9.76899	.30342
5	43.00000	19.38828	18.89717	.49111	7.82072	6.27964	.34694
6	53.00000	17.73918	17.38917	.35001	6.31272	5.54452	.07351
7	63.00000	18.58960	18.21900	.37060	7.14255	5.18946	.03551
8	73.00000	18.53190	18.21074	.32116	7.13429	4.50164	.06878
9	83.00000	19.80075	19.46150	.33925	8.38505	4.04589	.04557
10	93.00000	19.28510	18.96965	.31545	7.89320	3.99648	.00494
11	103.00000	19.23476	18.88700	.34776	7.81055	4.45244	-.04560
12	113.00000	19.73521	19.31673	.38848	8.24028	4.71440	-.02620
13	123.00000	19.58920	19.25600	.33320	8.17955	4.07357	.06408

TABLE (4.3.3)

Q= 375 (L/M)

X INCREMENT = .12E+01
Y INCREMENT = .50E+00



3. Q — 375 (l/m)

$R = 0.0636\ kg/s.m\ (gm/ls)$

$\lambda = 570\ (Cal/cm)$

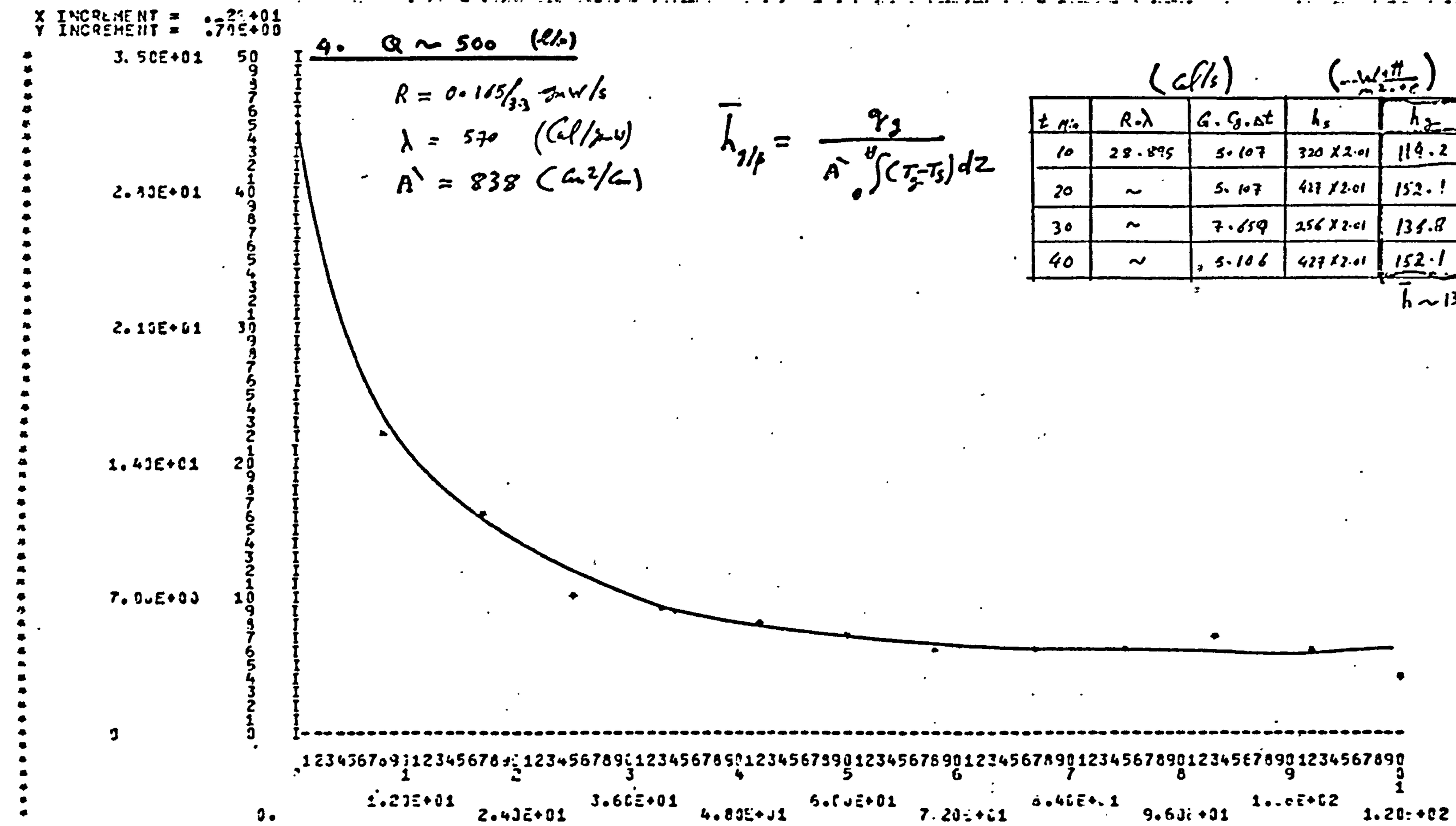
$A' = 932\ (cm^2/cm)$

$$\bar{h}_{s/p} = \frac{q_z}{A' \int_0^H (T_z - T_s) dz}$$

$t_{(min)}$	$R \cdot \lambda$ (Cal/s)	$G \cdot C_p \cdot \Delta t$ (Cal/s)	h_s $(\frac{Cal}{m^2 \cdot ^oC})$	h_x	$\int_0^H (T_z - T_s) dz$ (Cm. °C)
10	11.138	3.829	183 x 13	184.7	1.5
20	11.138	3.825	274 x 1.83	86.03	1
30	11.138	3.825	274 x 1.83	83.03	1
40	11.138	5.749	109 x 1.83	103.3	2.5

$\bar{h} = 97.498\ (C \frac{w}{m^2 \cdot ^oC})$

CONT. (4.3.3)



4. $Q \sim 500$ (l/s)

$R = 0.165/3.3$ m W/s

$\lambda = 570$ (Cal/m-W)

$A' = 838$ (cm²/cm)

$$\bar{h}_{g/p} = \frac{q_z}{A' \int_0^H (T_z - T_s)\,dz}$$

	(cal/s)				($\frac{W}{m^2 \cdot °C}$)	($cm \cdot °C$)
t min	R.λ	G.C_g.Δt	h_s	h_z		$\int_0^H (T_z - T_s)\,dz$
10	28.895	5.107	320 X2.01	114.2		2
20	~	5.107	427 X2.01	152.1		1.5
30	~	7.659	256 X2.01	134.8		2.5
40	~	5.106	427 X2.01	152.1		1.5

$\bar{h} \sim 138.5$ ($\frac{W}{m^2 \cdot °C}$)

CONT. (4.3.4)

RESULTS OF
EXPERIMENT FOUR FLUIDIZED BED DRYING
X(1)= 31.53

NO/	TIME MIN	WET (GM)	DRY(GM)	WATER G	SOLID GM	(X) (g/g)	RATE M(-1)
2	13.00000	19.19480	18.11780	1.07700	7.04135	15.29536	1.62390
3	23.00000	19.90362	19.02245	.88117	7.94600	11 08948	.42059
4	33.00000	19.73940	19.14740	.59200	8.07095	7.33495	.37545
5	43.00000	18.56330	18.21090	.45240	7.13445	6.34106	.09939
6	53.00000	18.86939	18.45820	.41119	7.38175	5.57036	.07707
7	63.00000	18.29730	17.95536	.33394	6.86191	4.92509	.06453
8	73.00000	18.51673	18.19515	.32158	7.11870	4.51740	.04077
9	83.00000	19.09151	18.76790	.32361	7.69145	4.20740	.03100
10	93.00000	19.24775	18.89505	.35273	7.81860	4.51142	-.03040
11	103.00000	18.74276	18.39905	.34371	7.32260	4.69382	-.01824
12	113.00000	19.62343	19.28397	.33943	8.20752	4.13560	.05582
13	123.00000	18.75385	18.53200	.22685	7.45555	3.04273	.10929

TABLE (4.3.4)

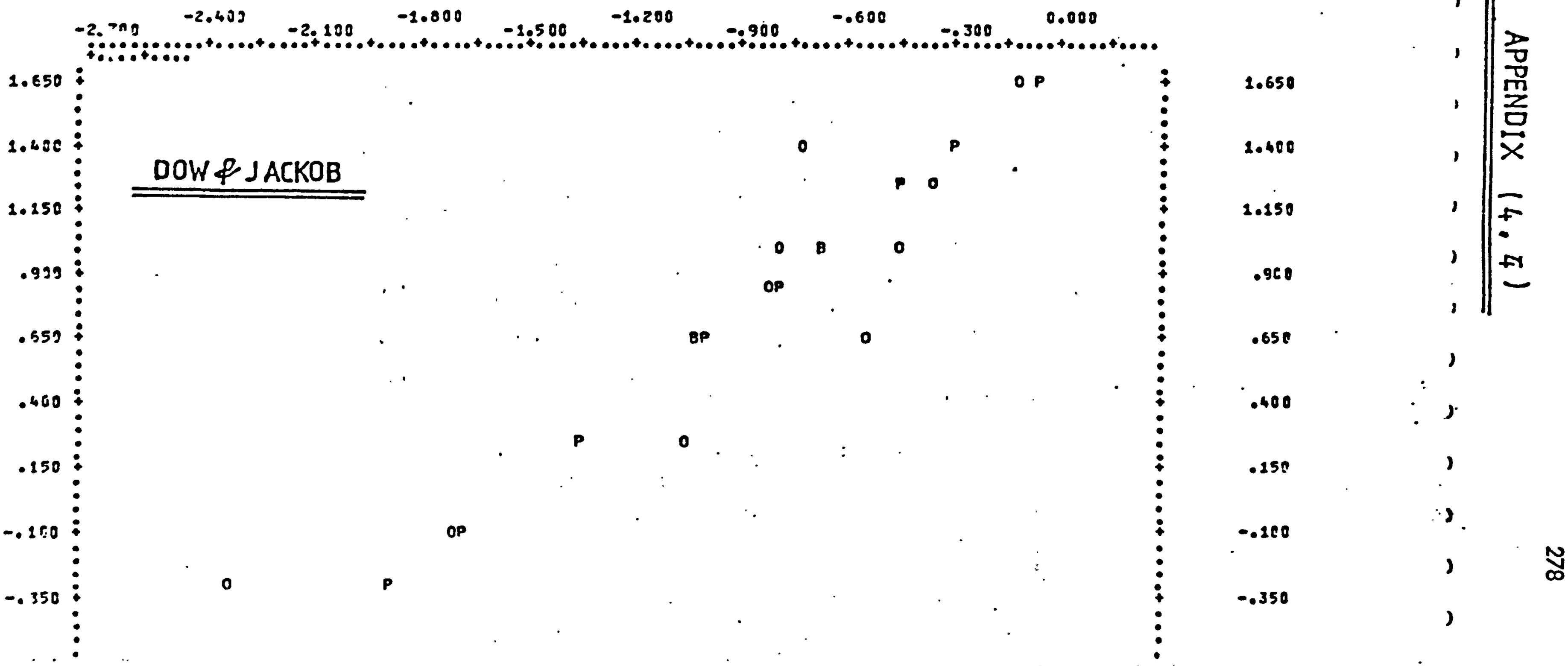
Q= 500 (L/M)

TABLE OF RESIDUALS

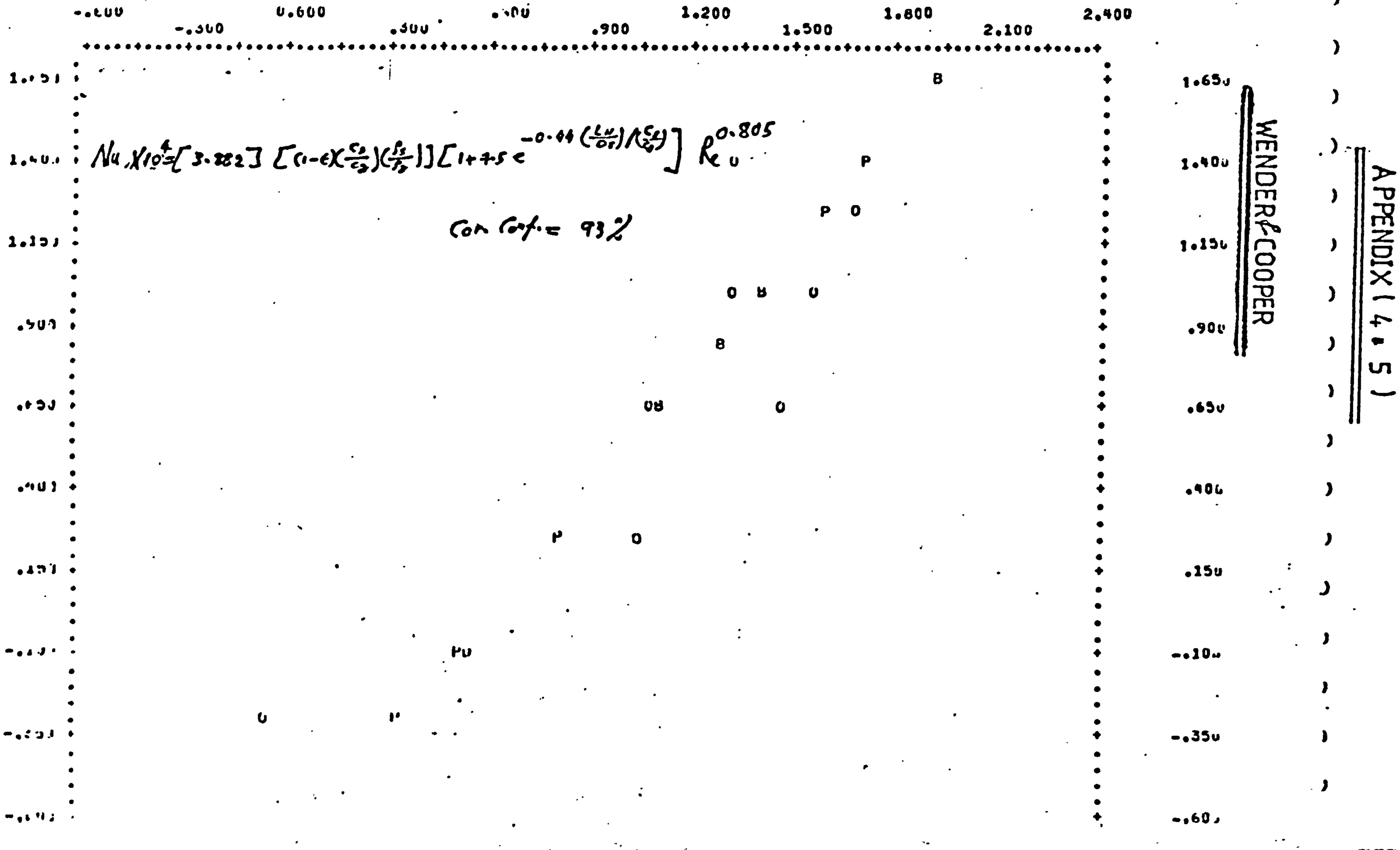
NO.	X VALUE	Y VALUE	Y PREDICTED	RESIDUAL
1	-.6803	-2.1670	-2.2250	.0580
2	-.3161	-2.3280	-1.8879	-.4401
3	-.0815	-1.7210	-1.6709	-.0501
4	.2676	-1.0510	-1.3478	.2968
5	.6316	-1.0270	-1.0110	-.0160
6	.8657	-.8070	-.7939	-.0131
7	1.0202	-.7790	-.6515	-.1275
8	.6461	-.5450	-.9976	.4526
9	1.0101	-.4590	-.6608	.2018
10	1.2448	-.3580	-.4436	.0856
11	1.3335	-.7170	-.3013	-.4157
12	1.6434	-.1070	-.0748	-.0322

$$Nu = 0.025 \left(\frac{D_t}{L}\right)^{0.65} \left(\frac{D_t}{D_p}\right)^{0.17} \left[(1-\epsilon)\left(\frac{\rho_s}{\rho_f}\right)\left(\frac{c_s}{c_f}\right)\right]^{0.35} Re^{0.92536}$$

Corr. Coff. = 93%



11	1.5960	1.5120	1.7150	-.4030
12	1.4464	1.4220	1.4121	.0099



APPENDIX (5)

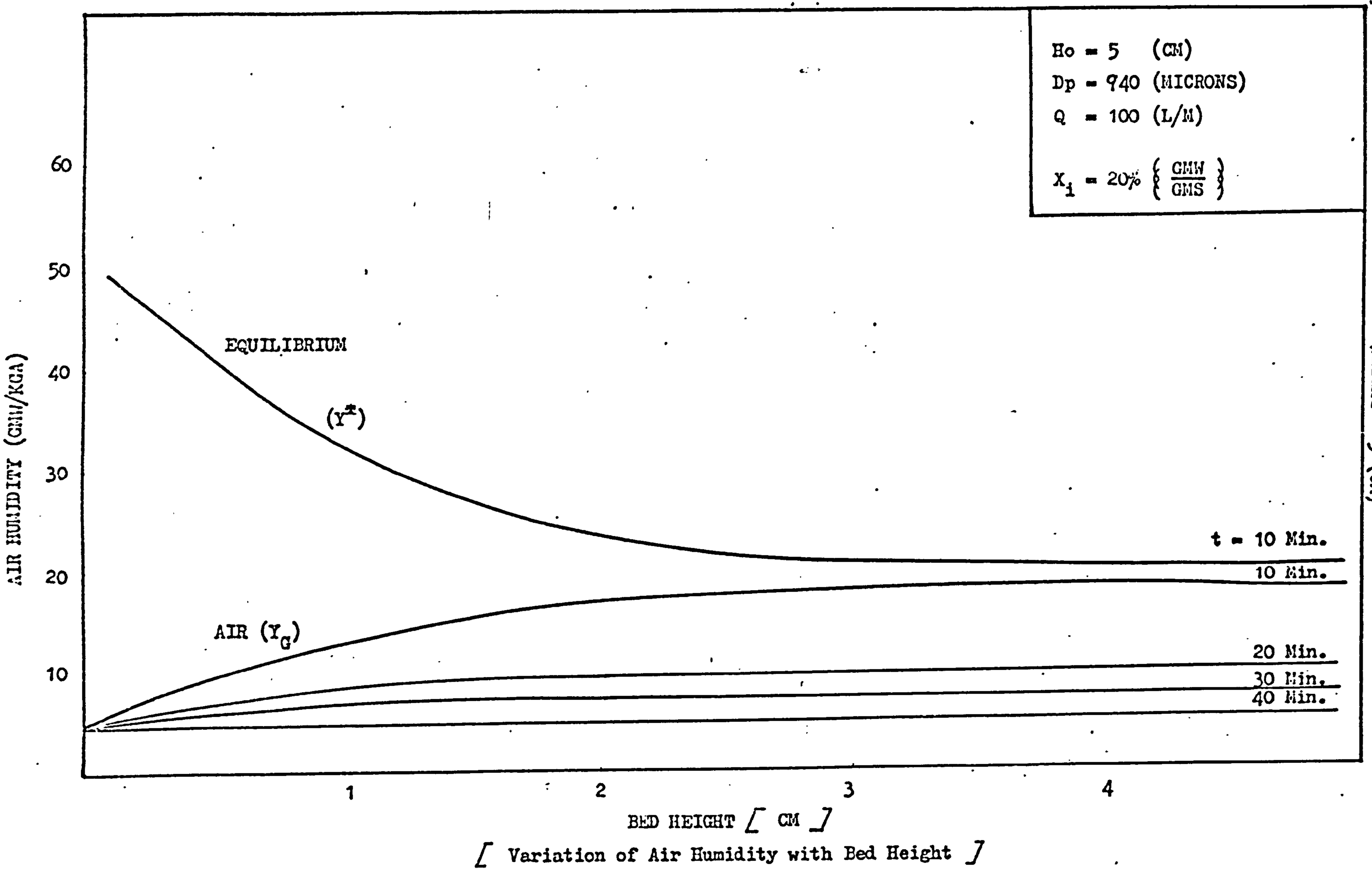
(AIR HUMIDITY CALCULATIONS)

APPENDIX (5.1) BED HEIGHT = 5 (CM)

APPENDIX (5.2) BED HEIGHT =10 (CM)

APPENDIX (5.3) BED HEIGHT =15 (CM)

BED HEIGHT = 5 (CM)



[Variation of Air Humidity with Bed Height]

GAS ANALYSIS
SHALLOW BED MODEL(1)
ING MASS BALANCE

$Z = 5\ (M_M)$

NO/	(X)(•/•)	(Y IN)(GM/KGM)	(Y OUT)(GM/KGM)	(Y M.B.)(GM/KGM)	Z=(Y OUT/YM.B.	HT.TR.COEF
2	16.41233	4.43900	18.00300	5.75174	3.12949	-4.47701
3	12.65263	4.43900	10.81300	5.08639	2.12587	1.71381
4	7.48479	4.43900	7.23700	4.79416	1.50954	4.23143
5	5.13841	4.43900	5.50300	4.83978	1.13642	4.20891
6	3.94545	4.43900	5.10300	4.99266	1.02150	3.39411
7	2.88916	4.43900	4.76900	4.92980	.96738	4.43918
8	5.04246	4.43900	4.43900	4.43900	1.00000	6.17047
9	2.89796	4.43900	4.43900	4.43900	1.00000	34.52893
10	2.30374	4.43900	4.43900	4.43900	1.00000	32.49782
11	2.21143	4.43900	4.43900	4.43900	1.00000	30.46671
12	2.07913	4.43900	4.43900	4.43900	1.00000	28.40448
13	2.01249	4.43900	4.43900	4.43900	1.00000	28.31114

CONT. (5.1)

GAS ANALYSIS
SHALLOW GEO MODEL(3)
EQM CURVE

$Z = 5\ (M_m)$

NO/	XA/(•/•)	TEMP(OC)	P(MM HG)	(R.H.)(•/•)	Y EQM(GM/KGM)	Y OUT(GM/KGM)	Z=YOUT/YEQM
2	-3.47126	57.00000	129.82000	.42872	49.38728	18.00000	.36447
3	-4.53251	61.00000	156.43000	.32238	44.41908	10.81300	.24343
4	-4.06874	66.00000	196.06000	.22943	39.31893	7.23700	.18406
5	-4.31160	69.00000	223.73000	.15389	29.65855	5.50000	.18544
6	-4.34193	70.00000	233.70000	.13177	26.39488	5.10000	.19322
7	-4.41731	72.00000	254.60000	.11772	25.65871	4.76900	.18586
8	-4.46581	70.00000	233.70000	.12457	24.89493	4.43900	.17831
9	-4.47021	73.00000	265.70000	.12463	28.47209	4.43900	.15591
10	-4.59935	74.00000	277.20000	.10749	25.50382	4.43900	.17405
11	-4.25608	74.00000	277.20000	.10320	24.44594	4.43900	.18158
12	-4.14528	75.00000	289.10000	.10192	25.18170	4.43900	.17628
13	-4.34581	75.00000	289.10000	.10057	24.86196	4.43900	.17855

CONT.(5.1)

GAS ANALYSIS
SHALLOW BED MODEL(1)
INS MASS BALANCE

$Z = 1$ (CM)

NO/	(X)(%)	(Y IN)(GM/KGM)	(Y OUT)(GM/KGM)	(Y M.B.)(GM/KGM)	Z=(Y OUT/YM.B.	HT.TR.COEF
2	16.41233	4.43900	18.00000	11.75878	1.53077	-4.47701
3	12.65269	4.43900	10.81300	7.75407	1.39449	1.71381
4	7.48479	4.43900	7.23700	6.41837	1.12754	4.23143
5	5.13841	4.43900	5.56000	5.32703	1.03247	4.20891
6	3.94545	4.43900	5.10000	4.72662	1.07899	3.39411
7	2.98316	4.43900	4.76900	4.96407	.96070	4.43918
8	5.04246	4.43900	4.43900	4.43900	1.00000	6.17047
9	2.89796	4.43900	4.43900	4.43900	1.00000	34.52893
10	2.33074	4.43900	4.43900	4.43900	1.00000	32.49782
11	2.21143	4.43900	4.43900	4.43900	1.00000	30.46671
12	2.07913	4.43900	4.43900	4.43900	1.00000	28.40448
13	2.01249	4.43900	4.43900	4.43900	1.00000	28.31114

CONT.(5.1)

GAS ANALYSIS
SHALLOW BED MODEL(3)
EQN CURVE

Z = 1 (CM)

NO/	XAV(%)	TEMP(DC)	P(MM HG)	(R.H.)(%)	Y EQM(GM/KGM)	Y OUT(GM/KGM)	Z=YOUT/YEQM
2	18.47126	49.00000	88.02000	.42872	32.65452	18.00000	.55123
3	14.53251	52.00000	102.09000	.32238	28.29052	10.81300	.38221
4	10.06874	56.00000	123.80000	.22943	24.26491	7.23700	.29825
5	6.31160	62.00000	163.77000	.15389	21.43738	5.50000	.25656
6	4.54193	65.00000	187.54000	.13177	21.00618	5.10000	.24279
7	3.41731	67.00000	204.96000	.11772	20.49194	4.76900	.23273
8	2.96581	66.00000	196.06000	.12457	20.75219	4.43900	.21391
9	2.97021	66.00000	196.06000	.12463	20.76165	4.43900	.21381
10	2.53935	69.00000	223.73000	.10749	20.42354	4.43900	.21735
11	2.25609	71.00000	243.94000	.10120	21.40866	4.43900	.20735
12	2.14528	72.00000	254.60000	.10182	22.07050	4.43900	.20113
13	2.04581	73.00000	265.74000	.10057	22.77627	4.43900	.19490

CONT.(5.1)

GAS ANALYSIS
SHALLOW BED MODEL(1)
INS MASS BALANCE

$Z = 2\ (CM)$

NO/	(X)(%)	(Y IN)(GM/KGM)	(Y OUT)(GM/KGM)	(Y M.B.)(GM/KGM)	Z=(Y OUT/YM.B.	HT.TR.COEF
2	16.41233	4.43900	18.00000	15.72158	1.14492	-4.47701
3	12.65269	4.43900	10.81300	9.17520	1.17850	1.71381
4	7.48479	4.43900	7.23700	6.80386	1.06366	4.23143
5	5.13841	4.43900	5.50300	4.85119	1.13374	4.20891
6	3.94545	4.43900	5.10300	4.16858	1.22344	3.39411
7	2.88916	4.43900	4.76900	4.31894	1.10421	4.43918
8	5.04246	4.43900	4.43900	4.43900	1.00000	8.17047
9	2.89796	4.43900	4.43900	4.43900	1.00000	34.52893
10	2.30374	4.43900	4.43900	4.43900	1.00300	32.49782
11	2.21143	4.43900	4.43900	4.43900	1.00000	30.48571
12	2.07913	4.43900	4.43900	4.43900	1.00000	28.40448
13	2.01243	4.43900	4.43900	4.43900	1.00000	20.31114

CONT.(5.1)

GAS ANALYSIS
SHALLOW BED MODEL(3)
EQM CURVE

Z = 2 (CM)

NO/	XA/(•/•)	TEMP(OC)	P(MM HG)	(R.H.)(•/•)	Y EQM(GM/KGM)	Y OUT(GM/KGM)	Z=YOUT/YEQM
2	4.47126	42.50000	63.13000	.42872	23.07960	18.00000	.77991
3	4.53251	47.00000	79.60000	.32238	21.84045	10.81300	.49509
4	4.06874	52.00000	102.09000	.22943	19.87442	7.23700	.36414
5	4.31160	59.00000	142.60000	.15389	18.58384	5.51000	.29596
6	4.54193	63.00000	171.38000	.13177	19.14068	5.10000	.26645
7	4.41731	65.00000	187.54000	.11772	18.69818	4.76900	.25505
8	4.96581	65.00000	187.54000	.12457	19.82178	4.43900	.22395
9	3.97021	69.00000	214.17000	.12463	22.74920	4.43900	.19513
10	3.53935	71.00000	233.72000	.10749	21.36478	4.43900	.20777
11	3.25608	72.00000	254.63000	.10320	22.38150	4.43900	.19833
12	3.14528	73.00000	265.70000	.10182	23.06824	4.43900	.19243
13	3.04991	74.00000	277.20300	.10057	23.79961	4.43900	.18652

CONT.(5.1)

GAS ANALYSIS
SHALLOW BED MODEL(1)
INS MASS BALANC

$Z = 5$ (CM)

NO/	(X)(•/•)	(Y IN)(GM/KGM)	(Y OUT)(GM/KGM)	(Y M.B.)(GM/KGM)	Z=(Y OUT/YM.B.	HT.TR.COEF
2	16.41233	4.43900	18.00000	18.00000	1.00000	-4.47701
3	12.65269	4.43900	10.81300	10.81300	1.00000	1.71361
4	7.48479	4.43900	7.23700	7.23700	1.00000	4.23143
5	5.13841	4.43900	5.50000	5.50000	1.00000	4.20891
6	3.94545	4.43900	5.10300	5.10000	1.00000	3.39411
7	2.88916	4.43900	4.76900	4.76900	1.00000	4.43918
8	5.04246	4.43900	4.43900	4.43900	1.00000	8.17047
9	2.89796	4.43900	4.43900	4.43900	1.00000	34.52893
10	2.39374	4.43900	4.43900	4.43900	1.00000	32.49782
11	2.21143	4.43900	4.43900	4.43900	1.00000	39.48671
12	2.07913	4.43900	4.43900	4.43900	1.00000	26.40448
13	2.01249	4.43900	4.43900	4.43900	1.00000	20.31114

CONT.(5.1)

GAS ANALYSIS
SHALLOW BED MODEL(3)
EQM CURVE

Z = 5 (CM)

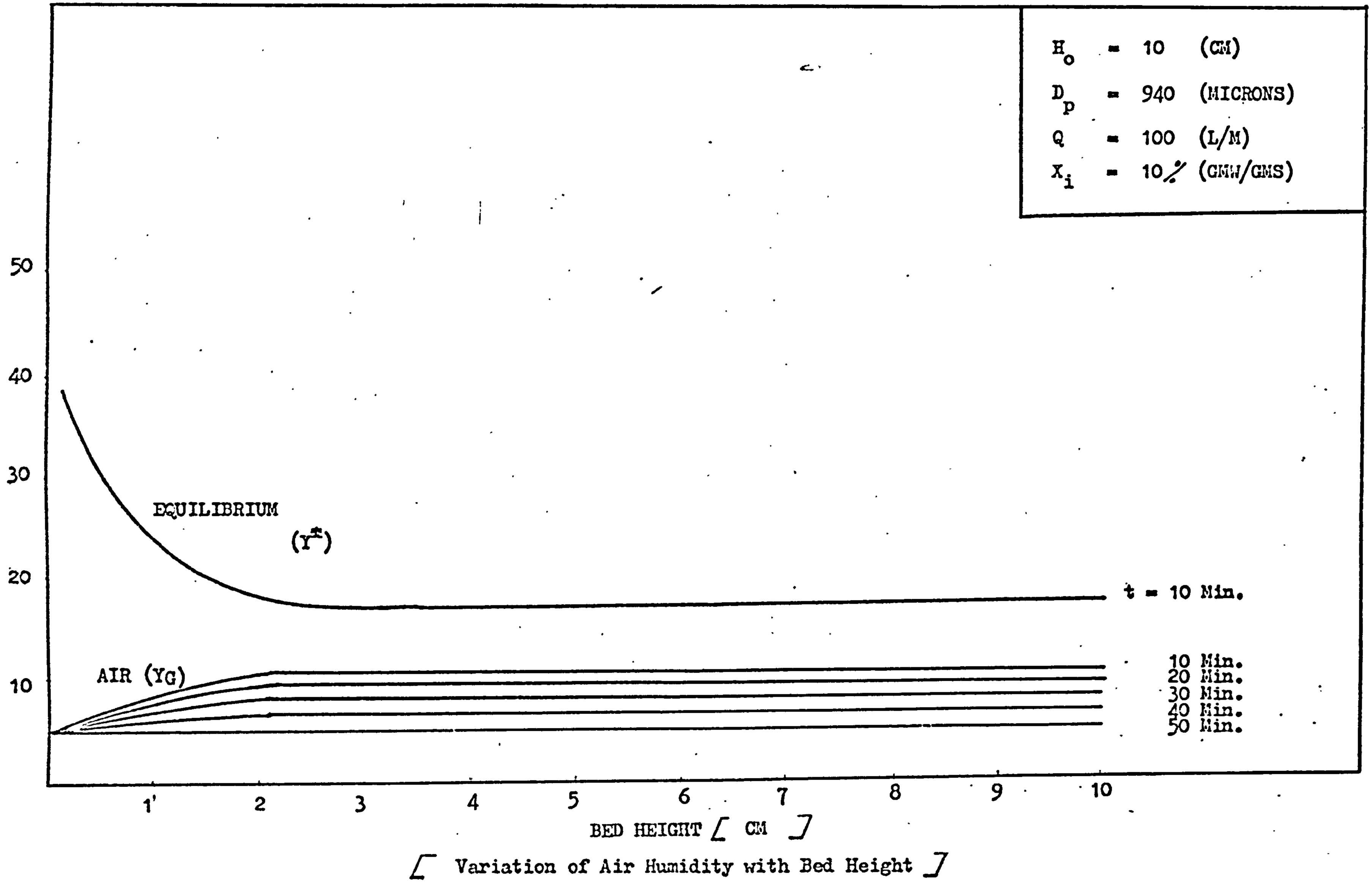
NO/	XA/(o/o)	TEMP(OC)	P(MM HG)	(R.H.)(o/o)	Y EQM(GM/KGM)	Y OUT(GM/KGM)	Z=YOUT/YEQM
2	3.47126	39.50000	53.86703	.42872	19.58703	18.00000	.91898
3	4.53251	41.50000	59.93000	.32238	16.29430	10.81300	.66361
4	1?.06874	47.00000	79.60000	.22943	15.38837	7.23700	.47029
5	6.31160	52.00000	102.09300	.15389	13.19308	5.50000	.41689

C5AD3A C5AD=A *** IMPERIAL COLLEGE COMPUTER CENTRE *** 76/09/27. 17.22.22.

.24237

9	3.97021	58.00000	136.08000	.12463	14.26514	4.43900	.31118
10	?.59975	59.00000	142.63000	.10749	12.86502	4.43900	.34504
11	2.25608	60.00000	149.38000	.10320	12.94026	4.43900	.34304
12	?.14528	62.00000	163.77000	.10182	14.02010	4.43900	.31662
13	?.04581	65.00000	187.54000	.10057	15.90575	4.43900	.27908

CONT.(5.1)



[Variation of Air Humidity with Bed Height]

GAS ANALYSIS
SHALLOW BED MODEL(1)
ING MASS BALANCE

$Z = 5$ (Mm)

NC/	(X)(./.)	(Y IN)(GM/KGM)	(Y OUT)(GM/KGM)	(Y M.B.)(GM/KGP)	Z=(Y CUT/YM.B.	HT.TR.COEF
2	16.21015	4.43900	10.10600	5.04244	2.00419	2.12275
3	13.92394	4.43900	9.48000	4.95566	1.91296	2.56391
4	11.72501	4.43900	7.72900	4.91862	1.57138	2.86553
5	9.92629	4.43900	6.74600	4.85990	1.38809	3.32120
6	7.10969	4.43900	5.10000	4.79688	1.06319	5.00322
7	5.82273	4.43900	4.70000	4.76766	.98581	5.78154
8	4.55732	4.43900	4.43900	4.43900	1.00000	5.85898
9	3.78959	4.43900	4.43900	4.43900	1.00000	3.42915
10	3.78959	4.43900	4.43900	4.43900	1.00000	2.90159
11	3.78959	4.43900	4.43900	4.43900	1.00000	2.90159
12	3.78959	4.43900	4.43900	4.43900	1.00000	2.63781
13	3.78959	4.43900	4.43900	4.43900	1.00000	1.94647

CONT. (5.2)

GAS ANALYSIS
SHALLOW RED MODEL(3)
EQ1 CURVE

$Z = 5\,(M_n)$

NO/	XAV(•/•)	TEMP(DC)	P(MM HG)	(R.H.)(•/•)	Y EQM(GM/KGM)	Y OUT(GM/KGM)	Z=YOUT/YEQM
2	27.44321	54.00000	112.51000	.40097	39.44045	10.10600	.25623
3	25.36704	57.00000	129.82000	.33681	38.15283	9.48000	.24847
4	22.82447	58.00000	136.09000	.28675	33.82623	7.72900	.22849
5	20.82565	61.00000	156.43000	.24517	33.21609	6.74600	.20309
6	8.51799	63.00000	171.38000	.19717	29.08231	5.10000	.17536
7	6.46621	65.00000	187.54000	.15583	24.99391	4.70000	.18805
8	5.19003	67.00000	204.96000	.13988	24.50057	4.44900	.18118
9	4.17345	68.00000	214.17000	.12717	23.23019	4.43900	.19109
10	3.78959	70.00000	233.70000	.12237	24.43751	4.43900	.18165
11	3.78959	70.00000	233.70000	.12237	24.43751	4.43900	.18165
12	3.78959	70.00000	233.70000	.12237	24.43751	4.43900	.18165
13	3.78959	71.00000	243.90000	.12237	25.54770	4.43900	.17375

CONT.(5.2)

GAS ANALYSIS
SMALLOW BED MODEL(1)
INS PASS BALANCE

$Z = 1$ (CM)

NO/	(X)(•/•)	(Y IN)(GM/KGM)	(Y OUT)(GM/KGM)	(Y M.B.)(GM/KGM)	Z=(Y OUT/YM.B.	HT.TR.COEF
2	16.21015	4.43900	10.10600	8.89517	1.13612	2.12275
3	13.92394	4.43900	9.48000	7.34508	1.29066	2.55567
4	11.72531	4.43900	7.72900	6.26855	1.23298	2.62253
5	9.92629	4.43900	6.74600	5.42372	1.24380	3.82120
6	7.11969	4.43900	5.10000	5.93395	.85946	5.00322
7	5.82273	4.43900	4.70600	4.59989	1.02176	5.78054
8	4.55732	4.43900	4.43900	4.43900	1.00000	5.85898
9	3.78959	4.43900	4.43900	4.43900	1.00000	3.42915
10	3.78959	4.43900	4.43900	4.43900	1.00000	2.90159
11	3.78959	4.43900	4.43900	4.43900	1.00000	2.90159
12	3.78959	4.43900	4.43900	4.43900	1.00000	2.63781
13	3.78959	4.43900	4.43900	4.43900	1.00000	1.94647

CONT.(5.2)

GAS ANALYSIS
SHALLOW BED MODEL(3)
EQM CURVE

$Z = 1$ (CM)

NO/	XAV(%)	TEMP(DC)	P(MM HG)	(R.H.)(%)	Y EQM(GM/KGM)	Y OUT(GM/KGM)	Z=YOUT/YEQM
2	17.44321	42.50000	63.30000	.40097	21.59384	10.10600	.46800
3	15.06704	48.00000	83.71000	.33661	24.07946	9.48000	.39370
4	12.52447	51.00000	97.20000	.28675	23.79366	7.72900	.32483
5	10.82565	54.00000	112.51000	.24517	23.53895	6.74600	.28659
6	9.51799	55.00000	118.08000	.19717	19.75174	5.10000	.25821
7	8.46621	59.00000	142.63000	.15583	19.32425	4.76000	.24968
8	8.19603	62.00000	163.77000	.13968	19.42376	4.43900	.22853
9	8.17345	64.00000	179.31000	.12717	19.33210	4.43900	.22962
10	7.78959	66.00000	196.06000	.12237	20.37328	4.43900	.21788
11	7.78959	66.00000	196.06000	.12237	20.37328	4.43900	.21788
12	7.78959	66.00000	196.06000	.12237	20.37328	4.43900	.21788
13	7.78959	69.00000	214.17000	.12237	22.32236	4.43900	.19886

CONT.(5.2)

GAS ANALYSIS
SHALLOW BED MODEL(1)
INS MASS BALANCE

$Z = 2(CM)$

NO/	(X)(%)	(Y IN)(GM/KGM)	(Y OUT)(GM/KGM)	(Y M.B.)(GM/KGM)	Z=(Y OUT/YM.B.	MT.TR.COEF
2	16.21015	4.43900	10.10600	10.52179	.96048	2.12275
3	13.92394	4.43900	9.48000	8.90085	1.06507	2.55567
4	11.72501	4.43900	7.72900	6.87812	1.12371	2.62253
5	9.92629	4.43900	6.74600	5.86205	1.15079	3.49716
6	7.10969	4.43900	5.10300	5.06947	1.03602	5.00322
7	5.82273	4.43900	4.70000	4.78388	.98247	5.78054
8	4.55732	4.43900	4.43900	4.43900	1.00000	5.85898
9	3.78959	4.43900	4.43900	4.43900	1.00000	3.42915
10	3.78959	4.43900	4.43900	4.43900	1.00000	2.98159
11	3.78959	4.43900	4.43900	4.43900	1.00000	2.98159
12	3.78959	4.43900	4.43900	4.43900	1.00000	2.63781
13	3.78959	4.43900	4.43900	4.43900	1.00000	1.84847

CONT.(5.2)

GAS ANALYSIS
SHALLOW PEC MODEL(3)
EQM CURVE

$Z = 2$ (CM)

NO/	XA/(•/•)	TEMP(DC)	P(MM HG)	(R.H.)(•/•)	Y EQM(GM/KGM)	Y OUT(GM/KGM)	Z=YOUT/YEQM
2	27.44721	38.00000	49.69200	.40097	16.82670	10.10600	.60059
3	25.06704	43.00000	64.80000	.33681	18.47911	9.48000	.51301
4	22.92447	47.00000	79.60000	.28675	19.35194	7.72900	.39939
5	21.02565	50.00000	92.51000	.24517	19.22591	6.74600	.35088
6	19.52799	54.00000	112.51000	.19717	18.79200	5.10000	.27139
7	18.46621	55.00000	118.04000	.15583	15.50174	4.70000	.30319
8	18.19007	60.00000	149.38000	.13988	17.66880	4.43900	.25123
9	18.17345	61.00000	156.43000	.12717	16.79902	4.43900	.26424
10	18.78959	64.00000	179.31000	.12237	18.58098	4.43900	.23890
11	18.78959	64.00000	179.31000	.12237	18.58098	4.43960	.23890
12	18.78959	64.00000	179.31000	.12237	18.58098	4.43960	.23890
13	18.78959	68.00000	214.17000	.12237	22.32236	4.43900	.19886

CONT.(5.2)

GAS ANALYSIS
SHALLOW BED MODEL(1)
INS MASS BALANC

$Z = 10$ (CM)

NO/	(X)(*/*)	(Y IN)(GM/KGM)	(Y OLT)(GM/KGM)	(Y M.B.)(GM/KGM)	Z=(Y OUT/YM.B.	HT.TR.COEF
2	16.21015	4.43900	10.10600	10.10600	1.00000	2.12275
3	13.92394	4.43900	9.48000	9.48000	1.00000	1.92869
4	11.72501	4.43900	7.72900	7.72900	1.00000	1.99402
5	9.92629	4.43900	6.74600	6.74600	1.00000	2.36295
6	7.10969	4.43900	5.10000	5.10000	1.00000	3.30722
7	5.82273	4.43900	4.70000	4.70000	1.00000	4.21541
8	4.55732	4.43900	4.43900	4.43900	1.00000	3.95672
9	3.78959	4.43900	4.43900	4.43900	1.00000	3.42915
10	3.78959	4.43900	4.43900	4.43900	1.00000	2.90159
11	3.78959	4.43900	4.43900	4.43900	1.00000	2.90159
12	3.78959	4.43900	4.43900	4.43900	1.00000	2.63781
13	3.78959	4.43900	4.43900	4.43900	1.00000	1.84647

CONT.(5.2)

NO/	XAV(-/-)	TEMP(DC)	P(MM HG)	(R.H.)(-/-)	Y EQM(GM/KGM)	Y OUT(GM/KGM)	Z=YOUT/YEQM
2	17.44321	39.00000	52.44200	.40097	17.78440	10.10600	.56825
3	15.06704	41.00000	58.40000	.33681	16.60552	9.48000	.57089
4	12.82447	42.00000	61.50000	.28675	14.84703	7.72900	.52058
5	10.82569	44.00000	68.26000	.24517	14.07267	6.74600	.47937
6	8.51799	49.00000	88.02000	.19717	14.60597	5.10000	.34917
7	6.46621	52.00000	102.09000	.15583	13.36230	4.70000	.35174
8	5.19003	56.00000	123.80000	.13988	14.47263	4.43900	.30681
9	4.17345	58.00000	136.08000	.12717	14.56271	4.43900	.30482
10	3.78959	60.00000	149.38000	.12237	15.40305	4.43900	.28819
11	3.78959	60.00000	149.38000	.12237	15.40305	4.43900	.28819
12	3.78959	60.00000	149.38000	.12237	15.40305	4.43900	.28819
13	3.78959	64.00000	179.31000	.12237	18.58098	4.43900	.23890

X INCREMENT = .12E+01
Y INCREMENT = .35E+00

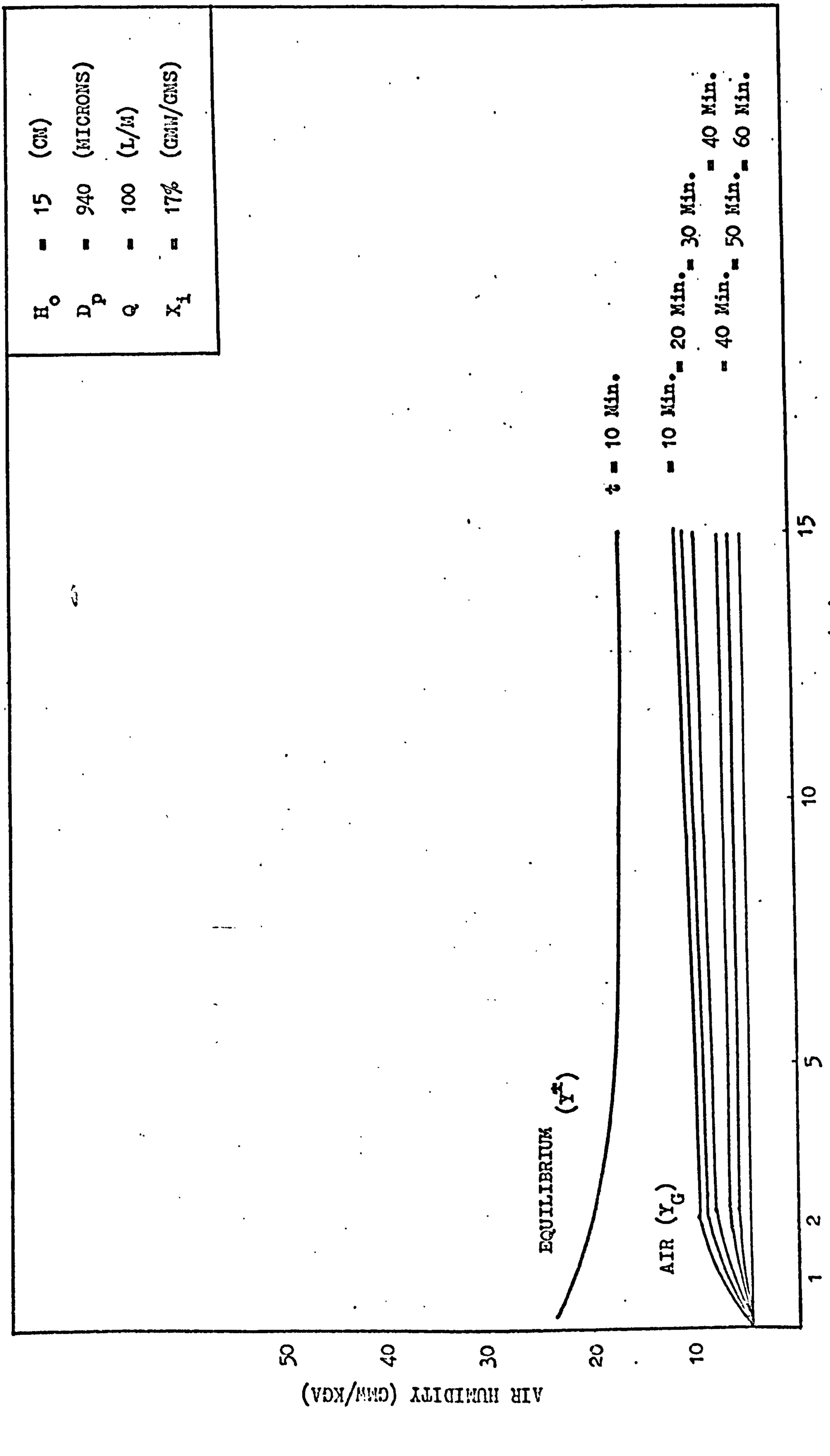
```
*****************
* EXCESS OUTPUT *
* LIMIT = 400   *
*****************
```

CONT.(5.2)

APPENDIX (5.3)

BED HEIGHT = 15 (CM)

H_o = 15 (CM)
D_p = 940 (MICRONS)
Q = 100 (L/M)
X_i = 17% (GMW/GMS)



GAS ANALYSIS
SHALLOW BED MODEL(1)
INS MASS BALANCE

$Z = 5\ (M_m)$

NO/	(X)(./.)	(Y IN)(GM/KGM)	(Y OUT)(GM/KGM)	(Y M.B.)(GM/KGM)	Z=(Y OUT/YM.B.	HT.TR.COEF
2	13.75103	4.43900	10.81300	5.42242	1.99413	-3.95591
3	12.90299	4.43900	10.81300	5.39178	2.00546	-3.15764
4	11.79226	4.43900	8.85400	5.26212	1.68259	.20671
5	9.97073	4.43900	6.74600	5.17119	1.30454	2.77437
6	7.64933	4.43900	5.90000	5.09765	1.15740	4.50528
7	6.26513	4.43900	5.10000	4.28974	1.18888	4.16639
8	6.72396	4.43900	4.76900	4.21275	1.13204	4.42089
9	5.30393	4.43900	4.76900	6.19967	.76923	8.29209
10	4.65619	4.43900	4.50300	5.46787	.82299	5.33684
11	3.69377	4.43900	4.43300	4.43900	1.00000	7.10590
12	3.59702	4.43900	4.43900	4.43900	1.00000	2.30481
13	2.39.14	4.43900	4.43900	4.43900	1.00000	1.95985

CONT.(5.3)

GAS ANALYSIS
SHALLOW BED MODEL(3)
EQM CURVE

$Z = 5\ (M_w)$

NO/	XAV(•/•)	TEMP(DC)	P(MM HG)	(R.H.)(•/•)	Y EQM(GM/KGM)	Y OUT(GM/KGM)	Z=YOUT/YEQM
2	15.22342	47.00000	79.60000	.34103	23.15109	10.81300	.46706
3	13.32701	48.00000	83.71000	.29720	21.15192	10.81300	.51121
4	12.34762	51.00000	97.20000	.27683	22.94045	8.85400	.38596
5	10.88149	52.00000	102.09000	.24634	21.38896	6.74600	.31540
6	9.81953	56.00000	123.80000	.20324	21.40000	5.90000	.27570
7	9.32673	57.00000	129.82000	.16158	17.74035	5.10000	.28748
8	9.46454	59.00000	149.38000	.15581	19.74482	4.76900	.24153
9	9.01394	61.00000	156.43000	.15017	19.93508	4.76900	.23923
10	8.98036	64.00000	179.31000	.13725	20.91614	4.50000	.21514
11	8.27348	65.00000	187.54000	.12842	20.45375	4.43900	.21703
12	8.73889	66.00000	196.09000	.12174	20.26755	4.43900	.21902
13	8.93052	63.00000	214.17000	.11236	20.43617	4.43900	.21721

CONT. (5.3)

GAS ANALYSIS
SHALLOW SED MODEL (1)
INS MASS BALANCE

$Z = 1$ (CM)

NO/	(X) (o/o)	(Y IN) (GM/KGM)	(Y OUT) (GM/KGM)	(Y M.B.) (GM/KGM)	Z=(Y OUT/YM.B.	MT.TR.COEF
2	13.75103	4.43900	10.81300	8.01610	1.34891	-3.95591
3	12.99293	4.43900	10.81300	7.67329	1.40916	-3.15764
4	11.79226	4.43900	8.85400	6.84805	1.29292	.29871
5	9.97073	4.43900	6.74600	5.86175	1.15085	2.77437
6	7.64833	4.43900	5.90000	5.28517	1.11633	4.50526
7	6.20513	4.43900	5.10300	4.79615	1.06335	4.16639
8	6.72396	4.43900	4.76930	4.85501	.98228	4.42689
9	5.30393	4.43900	4.76900	6.00825	.79374	8.29209
10	4.65619	4.43900	4.50000	5.30100	.84888	5.33684
11	3.49077	4.43900	4.43900	4.43900	1.00000	7.10890
12	3.58702	4.43900	4.43900	4.43900	1.00000	2.30481
13	2.79014	4.43900	4.43900	4.43900	1.00000	1.95985

CONT.(5.3)

GAS ANALYSIS
SHALLOW DEC MODEL(3)
EQM CURVE

$Z = 1$ (CM)

NO/	XAV(o/o)	TEMP(DC)	P(MM HG)	(R.H.)(o/o)	Y EQM(GM/KGM)	Y OUT(GM/KGM)	Z=YOUT/YEQM
2	15.22342	44.00000	68.26000	.34103	19.74872	10.81300	.54753
3	13.32701	45.00000	71.88000	.29720	18.07625	10.81300	.59819
4	12.34762	47.00000	79.60000	.27683	18.66259	8.85400	.47443
5	10.88149	48.00000	83.71000	.24634	17.43076	6.74600	.38702
6	9.30953	52.00000	102.09000	.20324	17.54189	5.90600	.33634
7	6.92673	52.50000	107.20000	.16158	14.57716	5.10000	.34986
8	6.46454	55.00000	118.04000	.15561	15.49961	4.76900	.30769
9	6.01394	56.00000	123.80000	.15017	15.67252	4.76900	.30429
10	4.98006	60.00000	149.38000	.13725	17.32808	4.50000	.25969
11	4.27348	62.00000	163.77000	.12842	17.78753	4.43900	.24956
12	3.73869	64.00000	179.31000	.12174	18.48191	4.43900	.24018
13	2.98858	65.00000	187.54000	.11236	17.82266	4.43900	.24906

CONT.(5.3)

GAS ANALYSIS
SHALLOW BED MODEL(1)
INS MASS BALANCE

$Z = 2$ (CM)

NO/	(X)(%)	(Y IN)(GM/KGM)	(Y OUT)(GM/KGM)	(Y M.B.)(GM/KGM)	Z=(Y OUT/YM.B.	HT.TR.COEF
2	13.75103	4.43900	10.81300	8.82592	1.22514	-3.95591
3	12.90299	4.43900	10.81300	8.40059	1.28717	-3.15764
4	11.79226	4.43900	8.85400	7.41884	1.19345	.20671
5	9.97073	4.43900	6.74600	5.70959	1.18152	2.77437
6	7.64833	4.43900	5.90000	5.19447	1.13582	4.50528
7	6.20513	4.43900	5.10000	4.25776	1.19781	4.16639
8	6.72396	4.43900	4.76900	3.83688	1.24294	4.42089
9	5.33393	4.43900	4.76900	4.31935	1.10410	8.29209
10	4.65619	4.43900	4.50000	3.93545	1.14345	5.33684
11	3.89077	4.43900	4.43900	4.43900	1.00000	7.10990
12	3.59702	4.43900	4.43900	4.43900	1.00000	2.30481
13	2.39114	4.43900	4.43900	4.43900	1.00000	1.95985

CONT.(5.3)

GAS ANALYSIS
SHALLOW BED MODEL(3)
EQM CURVE

$Z = 2$ (CM)

NO/	XAV(•/•)	TEMP(OC)	P(MM HG)	(R.H.)(•/•)	Y EQM(GM/KGM)	Y OUT(GM/KGM)	Z=YOUT/YEQM
2	16.22342	44.00000	68.26000	.34103	19.74872	10.81300	.54753
3	13.32701	45.00000	71.88000	.29720	18.07625	10.81300	.59819
4	12.34762	45.50000	73.74000	.27683	17.25076	8.85400	.51325
5	10.88149	47.00000	79.60000	.24634	16.55227	6.74600	.40756
6	8.80953	50.00000	92.51000	.20324	15.85403	5.90000	.37215
7	6.92673	52.00000	102.09000	.16158	13.86688	5.10000	.36778
8	6.46454	55.00000	118.04000	.15581	15.49961	4.76900	.30769
9	6.01394	57.00000	129.82000	.15017	16.45468	4.76900	.28983
10	4.34036	61.00000	149.38000	.13725	17.32808	4.50000	.25969
11	4.27348	62.00000	163.77000	.12842	17.78753	4.43900	.24956
12	3.73889	64.00000	179.31000	.12174	18.48191	4.43900	.24018
13	3.91858	65.00000	187.54000	.11236	17.82266	4.43900	.24906

CONT.(5.3)

GAS ANALYSIS
SHALLOW BED MODEL(1) $Z = 15$ (CM)
INS MASS BALANCE

NO/	(X)(%)	(Y IN)(GM/KGM)	(Y OUT)(GM/KGM)	(Y M.B.)(GM/KGM)	Z=(Y OUT/YM.B.	HT.TR.COEF
2	13.75103	4.43900	10.81300	10.81300	1.00000	-1.66430
3	12.90299	4.43900	10.81300	10.81300	1.00000	-1.15806
4	11.79226	4.43900	8.85400	8.85400	1.00000	.09511
5	9.97073	4.43900	6.74600	6.74600	1.00000	1.07133
6	7.64833	4.43900	5.90000	5.90000	1.00000	1.98438
7	6.26513	4.43900	5.10000	5.10000	1.00000	1.73023
8	6.72396	4.43900	4.76900	4.76900	1.00000	1.72103
9	5.30393	4.43900	4.76900	5.60058	.85152	2.27104
10	4.65619	4.43900	4.90000	5.53158	.88483	2.07929
11	3.89077	4.43900	4.43900	4.43900	1.00000	2.59686
12	3.56702	4.43900	4.43900	4.43900	1.00000	2.30481
13	2.39014	4.43900	4.43900	4.43900	1.00000	1.95985

CONT.(5.3)

GAS ANALYSIS
SHALLOW BED MODEL(3)
EQM CURVE

Z = 15 (CM)

NO/	X1V(%)	TEMP(DC)	P(MM HG)	(R.H.)(%)	Y EQM(GM/KGM)	Y OUT(GM/KGM)	Z=YOUT/YEQM
2	15.22342	43.00000	55.32400	.34103	15.91085	10.81300	.67960
3	11.32701	40.50000	56.81000	.29720	14.20037	10.81300	.76146
4	12.34762	42.00000	61.50000	.27683	14.32172	8.85400	.61822
5	10.88149	43.50000	63.13000	.24634	13.05591	6.74600	.51670
6	8.85953	47.00000	79.60000	.20324	13.59344	5.90000	.43403
7	6.92673	49.00000	88.02000	.16158	11.91930	5.10000	.42788
8	6.46454	50.50000	92.51000	.15581	12.08251	4.76900	.39470
9	6.01394	53.00000	107.20000	.15017	13.52555	4.76900	.35259
10	4.99006	55.00000	113.04000	.13725	13.61345	4.50000	.33056
11	4.27348	57.00000	129.81000	.12542	14.01532	4.43900	.31670
12	3.73889	59.00000	142.60000	.12174	14.60568	4.43900	.30394
13	3.33859	60.00000	144.38000	.11238	13.63154	4.43900	.32564

CONT(5.3)

APPENDIX (6)

(DRYING CURVES)

APPENDIX (6.1) EFFECT OF (HO) ON DRYING RATES

APPENDIX (6.2) EFFECT OF (Q) ON DRYING RATES

APPENDIX (6.3) EFFECT OF (d_p) ON DRYING RATES

APPENDIX (6.4) EFFECT OF (T_{IN}) ON DRYING RATES

EFFECT OF (H_o) ON DRYING RATES

X(1)= 28.43

NO/	TIME MIN	WET (GM)	DRY(GM)	WATER G	SOLID GM	(X)(•/•)	RATE M(-1)
2	10.00000	19.08057	17.50100	1.57957	6.42455	24.58647	.38460
3	20.00000	21.67400	20.11031	1.76369	9.03386	19.52311	.50634
4	30.00000	18.97400	17.92940	1.04460	6.85295	15.24307	.42800
5	40.00000	21.29000	20.37976	.91024	9.30331	9.78404	.54590
6	50.00000	21.89687	21.21095	.68592	10.13450	6.76817	.30159
7	60.00000	19.66962	19.23382	.43580	8.15737	5.34241	.14258
8	70.00000	17.56736	17.33715	.23021	6.26070	3.67706	.16653
9	80.00000	19.25468	19.03675	.21793	7.96030	2.73771	.09394
10	90.00000	19.18330	18.99320	.19010	7.91675	2.40124	.03365
11	100.00000	19.18330	18.98000	.20330	7.90355	2.57226	-.01710
12	110.00000	19.18330	18.97000	.21330	7.89355	2.70221	-.01299
13	120.00000	19.18330	18.96000	.22330	7.88355	2.83248	-.01303

TABLE (6.1.1)

H_o= 5 (CM.)

X(1)= 35.57

NO/	TIME MIN	WET (GM)	DRY(GM)	WATER G	SOLID GM	(X)(%)	RATE M(-1)
2	10.00000	22.22885	19.77755	2.45130	8.70110	28.17230	.73988
3	20.00000	23.09462	20.58315	2.51147	9.50670	26.41789	.17544
4	30.00000	22.01785	19.97540	2.04245	8.89895	22.95158	.34663
5	40.00000	21.10458	19.36152	1.74306	8.28507	21.03857	.19130
6	50.00000	21.10015	19.46400	1.63615	8.38755	19.50689	.15317
7	60.00000	20.08360	18.74695	1.33665	7.67050	17.42585	.20810
8	70.00000	21.73960	20.35000	1.38960	9.27355	14.98455	.24413
9	80.00000	22.13245	20.92585	1.20660	9.84940	12.25049	.27341
10	90.00000	20.66513	19.71615	.94898	8.63970	10.98395	.12665
11	100.00000	20.86188	20.07555	.78633	8.99910	8.73787	.22461
12	110.00000	22.90208	22.16822	.73386	11.09177	6.61626	.21216
13	120.00000	22.37020	21.75949	.61071	10.68304	5.71663	.08996

TABLE (6.1.2)

$H_0 = 10$ (CM)

X(1)= 38.64

NO/	TIME MIN	WET (GM)	DRY(GM)	WATER G	SOLID GM	(X)(./.)	RATE M(-1)
2	10.00000	23.11652	20.42531	2.69121	9.34086	28.78650	.98522
3	20.00000	21.75015	19.28300	2.46715	8.20655	30.06318	-.12767
4	30.00000	20.31170	18.27950	2.03220	7.20305	28.21305	.18501
5	40.00000	21.25117	19.08740	2.16377	8.01095	27.01015	.12029
6	50.00000	20.42650	18.54432	1.88218	7.46787	25.20371	.18064
7	60.00000	20.21166	18.48745	1.72421	7.41100	23.26555	.19382
8	70.00000	19.85760	18.27446	1.58314	7.19801	21.99413	.12714
9	80.00000	21.08983	19.45700	1.63283	8.38055	19.48357	.25106
10	90.00000	22.59409	20.95660	1.63749	9.80015	16.57353	.29100
11	100.00000	21.80300	20.37023	1.43277	9.29378	15.41644	.11571
12	110.00000	20.43840	19.26335	1.17505	8.18690	14.35281	.10636
13	120.00000	22.73075	21.54868	1.18207	10.47223	11.28766	.30651

TABLE (6.1.3)

H_b= 15 (CM)

X(1)= 32.45

NO/	TIME MIN	WET (GM)	DRY(GM)	WATER G	SOLID GM	(X)(%)	RATE M(-1)
2	10.00000	24.49800	21.43430	3.06370	10.35785	29.57853	.28718
3	20.00000	21.71270	19.31500	2.39770	8.23855	29.10342	.04751
4	30.00000	23.78955	20.99100	2.79855	9.91455	28.22670	.08767
5	40.00000	24.66257	21.81357	2.84900	10.73712	26.53412	.16926
6	50.00000	24.17479	21.42817	2.74662	10.35172	26.53298	.00011
7	60.00000	23.67735	21.18029	2.49706	10.10384	24.71397	.18190
8	70.00000	23.14415	20.08272	3.06143	9.00627	33.99215	-.92782
9	80.00000	22.54050	20.45113	2.08937	9.37468	22.28737	1.17048
10	90.00000	22.24038	20.27155	1.96883	9.19510	21.41173	.08756
11	100.00000	22.56895	20.63539	1.93356	9.55894	20.22777	.11840
12	110.00000	23.60075	21.63500	1.96575	10.55855	18.61761	.16102
13	120.00000	22.76116	20.91825	1.84291	9.84180	18.72533	-.01077

TABLE (6.1.4)

H_o= 20 (CM)

RESULTS OF
EXPERIMENT ONE FLUIDIZED BED DRYING
X(1)= 30.83

NO/	TIME MIN	WET (GM)	DRY(GM)	WATER G	SOLID GM	(X)(...)	RATE M(-1)
2	10.00300	20.08835	18.11535	1.97300	7.03890	28.02995	.28008
3	20.00000	20.45900	18.46432	1.99468	7.38787	26.99939	.10306
4	30.00000	20.67916	18.68690	1.99226	7.61045	26.17795	.08214
5	40.00300	18.93950	17.35700	1.58250	6.28055	25.19684	.09811
6	50.00300	20.03030	18.37055	1.65945	7.29410	22.75058	.24463
7	60.00000	20.84411	19.14721	1.69691	8.07075	21.02543	.17251
8	70.00000	21.30315	19.76954	1.53361	8.69309	17.64171	.33837
9	80.00000	20.93285	19.54919	1.38366	8.47274	16.33073	.13110
10	90.00000	21.43858	20.14701	1.29157	9.07056	14.23914	.20916
11	100.00000	19.52237	18.56671	.95566	7.49026	12.75870	.14804
12	110.00000	19.57580	18.62900	.94680	7.55255	12.53616	.02225
13	120.00000	20.20210	19.27017	.93183	8.19372	11.37249	.11637

TABLE (A-1)

Q= 150 (L/M)

RESULTS OF
EXPERIMENT TWO FLUIDIZED BED DRYING
X(1)= 31.17

NO/	TIME MIN	WET (GM)	DRY(GM)	WATER G	SOLID GM	(X)(. .)	RATE M(-1)
2	10.00000	20.31800	18.34589	1.97211	7.26944	27.12977	.40385
3	20.00000	21.05762	18.98000	2.07762	7.90355	26.28717	.08416
4	30.00000	20.10037	18.45251	1.64786	7.37606	22.34065	.39465
5	40.00000	20.07961	18.64081	1.43880	7.56436	19.02078	.33199
6	50.00000	21.84200	20.30878	1.53322	9.23233	16.60708	.24137
7	60.00000	20.84245	19.73645	1.10600	8.66000	12.77136	.38357
8	70.00000	20.69264	19.80555	.88709	8.72910	10.16245	.26089
9	80.00000	20.74261	20.03025	.71236	8.95380	7.95595	.22065
10	90.00000	20.93900	20.34169	.59731	9.26524	6.44678	.15092
11	100.00000	20.57721	20.05217	.52504	8.97572	5.84956	.05972
12	110.00300	18.68516	18.36110	.32406	7.28465	4.44853	.14010
13	120.00003	20.28695	19.94995	.33700	8.87350	3.79782	.06507

TABLE (A-2)

Q = 275 (L/M)

RESULTS OF
EXPERIMENT THREE FLUIDIZED BED DRYING
X(1)= 31.75

NO/	TIME MIN	WET (GM)	DRY(GM)	WATER G	SOLID GM	(X)(%)	RATE M(-1)
2	10.00000	22.01537	19.82624	2.18913	8.74979	25.01923	.67294
3	20.00000	21.48566	19.60136	1.88430	8.52491	22.10346	.29158
4	30.00000	21.37431	19.89862	1.47569	8.82217	16.72707	.53764
5	40.00000	20.89515	19.65542	1.23973	8.57897	14.45080	.22763
6	50.00000	20.33225	19.44635	.88590	8.36990	10.58436	.38664
7	60.00000	18.79205	18.29174	.50031	7.21529	6.93402	.36503
8	70.00000	21.61453	21.05868	.55585	9.98223	5.56840	.13656
9	80.00000	21.08722	20.61115	.47607	9.53470	4.99303	.05754
10	90.00000	20.20100	19.83618	.36482	8.75973	4.16474	.08283
11	100.00000	20.25114	19.92112	.33302	8.84467	3.73129	.04335
12	110.00000	21.37918	21.33831	.34087	9.96186	3.42175	.03095
13	120.00000	20.61433	20.28452	.32981	9.20807	3.58175	-.01600

TABLE (A - 3)

Q = 400 (L/M)

RESULTS OF
EXPERIMENT FOUR FLUIDIZED BED DRYING
X(1)= 29.55

NO/	TIME MIN	WET (GM)	DRY(GM)	WATER G	SOLID GM	(X)(..)	RATE M(-1)
2	10.00000	21.75855	19.73500	2.02355	8.65855	23.37054	.61799
3	20.00000	22.69534	20.78144	1.91390	9.70499	19.72078	.36498
4	30.00000	21.36721	19.86445	1.50276	8.78800	17.10014	.26206
5	40.00000	20.70300	19.78721	.91579	8.71076	10.51332	.65868
6	50.00000	20.66900	19.94600	.72300	8.86955	8.15148	.23618
7	60.00000	21.04000	20.52271	.51729	9.44626	5.47614	.26753
8	70.00000	21.14941	20.73877	.41064	9.66232	4.24991	.12262
9	80.00000	20.51735	20.14100	.37635	9.06455	4.15189	.00980
10	90.00000	20.73100	20.36777	.36323	9.29132	3.90935	.02425
11	100.00000	19.42858	19.13557	.29301	8.05912	3.63576	.02736
12	110.00000	20.07141	19.74500	.32641	8.66855	3.76545	-.01297
13	120.00000	19.60642	19.31871	.28771	8.24226	3.49067	.02748

TABLE (A - 4)

Q= 500 (L/M)

RESULTS OF
EXPERIMENT ONE FLUIDIZED BED DRYING
X(1)= 29.2

NO/	TIME MIN	WET (GM)	DRY(GM)	WATER G	SOLID GM	(X)(.)	RATE M(-1)
2	10.00000	22.67375	20.37118	2.30257	9.29473	24.77286	.43585
3	20.00000	22.03442	19.92945	2.10497	8.85300	23.776 1	.09959
4	30.00000	20.17942	18.52705	1.65237	7.45060	22.17764	.15992
5	40.00000	22.52225	20.64495	1.87730	9.56850	19.61959	.25581
6	50.00000	20.29816	18.92517	1.37299	7.84872	17.49317	.21264
7	60.00000	20.77831	19.50765	1.27066	8.43120	15.07093	.24222
8	70.00000	19.71245	18.72935	.98310	7.65290	12.84611	.22248
9	80.00000	20.65935	19.74400	.91535	8.66755	10.56065	.22855
10	90.00000	20.28300	19.60321	.67979	8.52676	7.97243	.25882
11	100.00000	19.05338	18.54015	.51323	7.46370	6.87635	.10961
12	110.00000	21.75518	21.14930	.61618	10.07255	6.11742	.07589
13	120.00000	21.77235	21.23085	.54150	10.15440	5.33266	.07848

B. TEMP= 60 (°C)

TABLE =(B-1)

Q = 150 (L/M)

RESULTS OF
EXPERIMENT TWO FLUIDIZED BED DRYING
X(1)= 29.24

NO/	TIME MIN	WET (GM)	DRY(GM)	WATER G	SOLID GM	(X)(./.)	RATE M(-1)
2	10.00000	23.73568	21.38122	2.35446	10.30477	22.8482	.63913
3	20.00000	23.18646	21.41885	1.76755	10.34240	17.09033	.57579
4	30.00000	21.87825	21.02660	.85165	9.95015	8.55917	.85312
5	40.00000	22.60309	22.04545	.55464	10.96900	5.05643	.35027
6	50.00000	20.46910	20.06242	.40668	8.98597	4.52572	.05307
7	60.00000	22.37772	22.05200	.32572	10.97555	2.96769	.15580
8	70.00000	18.87660	18.66691	.20969	7.59046	2.76255	.02051
9	80.00000	20.49616	20.26144	.23472	9.18499	2.55547	.02071
10	90.00000	20.43600	20.21717	.18883	9.14072	2.06581	.04897
11	100.00000	20.00594	19.90000	.10594	8.82355	1.20065	.08652
12	110.00000	21.05045	20.84890	.20155	9.77245	2.06243	-.08618
13	120.00000	20.92438	20.32765	.39673	9.45120	4.19767	-.21352

TABLE(B.2)

Q= 275 (L/M)

RESULTS OF
EXPLRIMENT THREE FLUIDIZED BED DRYING
X(1)= 33.67

NO/	TIME MIN	WET (GM)	DRY(GM)	WATER G	SOLID GM	(X)(.'.)	RATE M(-1)
2	10.00000	22.43074	20.39300	2.03774	9.31655	21.877 6	1.17932
3	20.00300	19.03982	17.81920	1.22062	6.74275	18.10270	.37696
4	30.00000	22.58355	21.71995	.86360	10.64350	8.11387	.99888
5	40.00000	20.19956	19.74852	.45004	8.67207	5.18953	.29243
6	50.00000	19.61911	19.33963	.27948	8.26318	3.38223	.18073
7	60.00000	20.35025	20.11842	.23183	9.04197	2.56393	.08183
8	70.00000	19.34920	19.16964	.17956	8.09319	2.21866	.03453
9	80.00000	16.22885	16.13325	.09560	5.05680	1.89052	.03281
10	90.00000	17.49177	17.38800	.10377	6.31155	1.64413	.02464
11	100.00000	20.86015	20.71790	.14225	9.64145	1.47540	.01687
12	110.00000	20.68470	20.54555	.13915	9.46910	1.46952	.00059
13	120.00000	22.14335	21.91600	.22735	10.83955	2.09741	-.06279

TABLE = (B . 3)

Q = 400 (L/M)

RESULTS OF
EXPERIMENT FOUR FLUIDIZED BED DRYING
X(1)= 31.54

NO/	TIME MIN	WET (GM)	DRY(GM)	WATER G	SOLID GM	(X)(.)	RATE M(-1)
2	10.00000	18.57772	17.27625	1.30147	6.19980	20.99 3	1.05453
3	20.00000	21.15843	19.74914	1.40929	8.67269	16.24974	.47424
4	30.00000	19.67830	18.90071	.77759	7.82426	9.93819	.63116
5	40.00000	21.85932	21.33850	.52082	10.26205	5.07520	.48630
6	50.00000	22.34200	21.00000	.34200	9.92355	3.44635	.16289
7	60.00000	19.28945	19.10000	.18945	8.02355	2.36117	.10852
8	70.00000	21.07931	20.84070	.23871	9.76385	2.44483	-.00837
9	80.00000	20.60530	20.36945	.23555	9.29300	2.53470	-.00899
10	90.00000	20.35067	20.11379	.23688	9.03734	2.62113	-.00864
11	100.00000	21.24920	21.01175	.23745	9.93530	2.38996	.02312
12	110.00000	20.62355	20.38461	.23894	9.30816	2.56699	-.01770
13	120.00000	19.23291	19.05223	.18068	7.97578	2.26536	.02016

TABLE (B.4)

Q= 500 (L/M)

RESULTS OF
EXPERIMENT ONE FLUIDIZED BED DRYING
X(1)= 32.05

NO/	TIME MIN	WET (GM)	DRY(GM)	WATER G	SOLID GM	(X)(%)	RATE M(-1)
2	10.00000	19.48725	17.88120	1.60605	6.80475	23.60 40	.84454
3	20.00000	21.46135	19.71247	1.74888	8.63602	20.25100	.33509
4	30.00000	22.07945	20.58362	1.49583	9.50717	15.73374	.45173
5	40.00000	17.21864	16.58186	.63678	5.50541	11.56644	.41673
6	50.00000	19.46331	19.02638	.43693	7.94993	5.49602	.60704
7	60.00000	18.91209	18.62471	.28738	7.54826	3.80724	.16888
8	70.00000	18.83279	18.66836	.16443	7.59191	2.16586	.16414
9	80.00000	18.12076	17.97937	.14139	6.90292	2.04825	.01176
10	90.00000	18.49993	18.40580	.09410	7.32935	1.28388	.07644
11	100.00000	15.51761	15.42761	.09000	4.35116	2.06841	-.07845
12	110.00000	17.69365	17.69365	0	6.61720	0	.20684
13	120.00000	17.14839	17.05381	.09458	5.97736	1.58230	-.15823

C. TEMP= 80 (°C)

TABLE (C_A 1)

Q = 150 (L/M)

RESULTS OF
EXPERIMENT TWO FLUIDIZED BED DRYING
Y(1)= 31.23

NO/	TIME MIN	WET (GM)	DRY(GM)	WATER G	SOLID GM	(X)(%)	RATE M(-1)
2	10.00000	22.85051	20.66939	2.18112	9.59294	22.73677	.84934
3	20.00000	21.45310	19.79435	1.65875	8.71790	19.02694	.37098
4	30.00000	23.53945	22.43340	1.10605	11.35695	9.73897	.92880
5	40.00000	21.62830	20.01565	1.61265	8.93920	18.04020	-.83012
6	50.00000	19.70137	19.49600	.20537	8.41955	2.43921	1.56010
7	60.00000	21.45300	21.25105	.20195	10.17460	1.98484	.04544
8	70.00000	20.97145	20.81210	.15935	9.73565	1.63677	.03461
9	80.00000	20.89710	20.75581	.14129	9.67936	1.45970	.01771
10	90.00000	22.11500	22.00091	.11409	10.92446	1.04435	.04154
11	100.00000	22.89150	22.74032	.15118	11.66387	1.29614	-.02518
12	110.00000	20.52165	20.38923	.13242	9.31278	1.42192	-.01256
13	120.00000	20.25072	20.13760	.11312	9.06115	1.24841	.01735

TABLE (C. 2)

Q= 275 (L/M)

RESULTS OF
EXPERIMENT THREE FLUIDIZED BED DRYING
X(1)= 29.53

NO/	TIME MIN	WET (GM)	DRY(GM)	WATER G	SOLID GM	(X)(-/	RATE M(-1)
2	10.00000	19.80680	18.88800	.91880	7.81155	11.76207	1.77647
3	20.00000	23.77380	22.61065	1.16315	11.53420	10.08436	.16777
4	30.00000	23.68690	23.04290	.62400	11.96645	5.21458	.48698
5	40.00000	19.34500	19.13700	.20800	8.06055	2.58047	.26341
6	50.00000	21.22625	21.03758	.18867	9.96113	1.89406	.06864
7	60.00000	22.53235	22.37905	.15380	11.32260	1.36075	.05333
8	70.00000	23.72710	23.55371	.17339	12.47726	1.38965	-.00289
9	80.00000	21.98071	21.82640	.15431	10.74995	1.43545	-.00458
10	90.00000	22.43330	22.29025	.14275	11.21380	1.27299	.01625
11	100.00000	21.33271	21.19176	.14095	10.11531	1.39343	-.01204
12	110.00000	19.74345	19.65132	.08913	8.57487	1.03943	.03540
13	120.00000	21.85264	21.67100	.19164	10.59455	1.80885	-.07694

TABLE (C.3)

Q = 400 (L/M)

RESULTS OF
EXPERIMENT FOUR FLUIDIZED BED DRYING
Y(1)= 27.71

NO/	TIME MIN	WET (GM)	DRY(GM)	WATER G	SOLID GM	(X)(%)	RATE M(-1)
2	10.00000	21.84513	20.29670	1.54843	9.22025	16.797-0	1.09209
3	20.00000	21.91700	20.89343	1.02357	9.81698	10.42653	.63673
4	30.00000	21.59615	21.24439	.35176	10.16794	3.45950	.69670
5	40.00000	22.02327	21.80669	.21658	10.73024	2.01841	.14411
6	50.00000	22.50615	22.34259	.16356	11.26614	1.45174	.05666
7	60.00000	22.95825	22.78500	.17325	11.70855	1.47969	-.00279
8	70.00000	20.21731	20.02449	.19282	8.94804	2.15489	-.06752
9	80.00000	20.95300	20.78300	.17000	9.70655	1.75139	.04035
10	90.00000	22.71524	22.52294	.19230	11.44649	1.67999	.06714
11	100.00000	22.79751	22.62954	.16797	11.55309	1.45390	.02261
12	110.00000	20.70858	20.57100	.13758	9.49455	1.44904	.00049
13	120.00000	21.90305	21.73446	.16559	10.65801	1.55367	-.01046

TABLE (C. 4)

Q= 600 (L/M)

RESULTS OF EXPERIMENT ON FLUIDIZED BED DRYING
X(1)= 32.31

NO/	TIME MIN	WET (GM)	DRY(GM)	WATER G	SOLID GM	(X)(%)	RATE M(-1)
2	10.00000	23.06220	20.91715	2.14505	9.84070	21.79174	1.05117
3	20.00000	23.72262	21.72475	1.99787	10.64830	18.76234	.30354
4	30.00000	24.40380	22.73909	1.66471	11.66264	14.27387	.44885
5	40.00000	23.07547	22.04230	1.03317	10.96585	9.42170	.48522
6	50.00000	22.04015	21.60185	.43830	10.52540	4.16421	.52575
7	60.00000	17.51617	17.36522	.15095	6.28877	2.40031	.17639
8	70.00000	18.83570	18.68370	.15200	7.60725	1.99809	.04022
9	80.00000	18.83965	18.68795	.15170	7.61150	1.99304	.00051
10	90.00000	16.42200	18.36137	.06063	7.28462	.83642	.11566
11	100.00000	22.14593	22.05065	.09525	10.97420	.86794	-.00315
12	110.00000	18.90631	18.84600	.06031	7.76955	.77624	.00917
13	120.00000	17.73866	17.75100	.03766	6.67455	.56423	.02120

D. TEMP.= 100 (°C)

TABLE(D . 1)
Q= 150 (L/M)

RESULTS OF
EXPERIMENT TWO FLUIDIZED BED DRYING
X(1)= 33.16

NO/	TIME MIN	WET (GM)	DRY(GM)	WATER G	SOLID GM	(X)(..)	RATE M(-1)
2	10.00000	23.12540	21.15200	1.97340	10.07555	19.58603	1.35769
3	20.00000	23.82325	22.23935	1.58390	11.16290	14.18897	.53971
4	30.00000	22.29630	21.56526	.73104	10.48881	6.9697	.72193
5	40.00000	21.69347	21.43605	.26242	10.35960	2.53311	.44366
6	50.00000	22.17817	22.17751	.10066	11.00106	.91500	.16181
7	60.00000	21.65318	21.62280	.03038	10.54635	.28806	.06269
8	70.00000	20.57680	20.54040	.03640	9.46395	.38462	-.00966
9	80.00000	20.01663	20.01154	.00509	8.93509	.05697	.03277
10	90.00000	21.74485	21.64475	.10010	10.56630	.94717	-.08902
11	100.00000	21.54837	21.52430	.02437	10.44755	.23326	.07139
12	110.00000	19.45366	19.44173	.01193	8.36528	.14261	.00966
13	120.00000	21.03725	21.01275	.02450	9.93630	.24657	-.01340

TABLE (D.2)

Q= 275 (L/M)

RESULTS OF
EXPERIMENT THREE FLUIDIZED BED DRYING
Y(1)= 26.90

NO/	TIME MIN	WET (GM)	DRY(GM)	WATER G	SOLID GM	(X)(.)	RATE M(-1)
2	10.00000	24.96416	22.97900	1.98516	11.90255	16.67844	1.02174
3	20.00000	22.03330	21.30565	.73335	10.22920	7.16918	.95093
4	30.00000	20.45300	20.23939	.21361	9.16294	2.33124	.48379
5	40.00000	21.37430	21.30511	.06889	10.22866	.67353	.16577
6	50.00000	20.94755	20.88430	.06325	9.80785	.64489	.00286
7	60.00000	20.94755	20.88430	.06325	9.80785	.64489	0
8	70.00000	20.94755	20.88430	.06325	9.80785	.64489	0
9	80.00000	20.94755	20.88430	.06325	9.80785	.64489	0
10	90.00000	20.94755	20.88430	.06325	9.80785	.64489	0
11	100.00000	20.94755	20.88430	.06325	9.80785	.64489	0
12	110.00000	20.94755	20.88430	.06325	9.80785	.64489	0
13	120.00000	20.94755	20.88430	.06325	9.80785	.64489	0

TABLE (D.3)

Q= 400 (L/M)

RESULTS OF
EXPERIMENT FOUR FLUIDIZED BED DRYING
X(1)= 36.92

NO/	TIME MIN	WET (GM)	DRY(GM)	WATER G	SOLID GM	(X)(.')	RATE M(-1)
2	10.00000	22.53655	21.32780	1.20875	10.25135	11.79113	2.51253
3	20.00000	21.59991	21.48820	.11171	10.41175	1.07282	1.07182
4	30.00000	22.89301	22.69400	.19901	11.61755	1.71301	-.06401
5	40.00000	20.39271	20.25299	.12972	9.17654	1.41361	.02994
6	50.00000	23.07021	22.97582	.09439	11.89937	.79324	.06204
7	60.00000	23.07021	22.97580	.09441	11.89935	.79340	-.00002
8	70.00000	23.07021	22.97580	.09441	11.89935	.79340	0
9	80.00000	23.07021	22.97580	.09441	11.89935	.79340	0
10	90.00000	23.07021	22.97580	.09441	11.89935	.79340	0
11	100.00000	23.07021	22.97580	.09441	11.89935	.79340	0
12	110.00000	23.07021	22.97580	.09441	11.89935	.79340	0
13	120.00000	23.07021	22.97580	.09441	11.89935	.79340	0

TABLE (D.4)

Q= 600 (L/M)

EFFECT OF (d_p) ON DRYING RATES

$A \cdot d_p = 106$ (1/H)

RESULTS OF EXPERIMENT ONE FLUIDIZED LED DRYING
X(1)= 21.95

NO/	TIME MIN	WET (GM)	DRY(GM)	WATER G	SOLID GM	(X)(. .)	RATE M(-1)
2	10.00000	18.84775	17.54375	1.30400	6.46730	20.16297	.18197
3	20.00000	18.58957	17.29625	1.29332	5.21980	20.79359	-.06306
4	30.00000	18.23646	17.01945	1.21701	5.94300	20.47800	.03156
5	40.00000	17.37415	16.34718	1.02697	5.27073	19.48440	.09936
6	50.00000	16.93633	15.97811	.95789	4.90166	19.54216	-.00578
7	60.00000	16.62233	15.74521	.87679	4.66876	18.77993	.07622
8	70.00000	17.30400	16.30111	1.00269	5.22466	19.19532	-.04154
9	80.00000	16.73865	15.64815	.78650	4.53170	17.22312	.19722
10	90.00000	20.13559	17.13424	1.00434	6.05779	16.57931	.06438
11	100.00000	18.36349	17.02340	1.04009	5.94695	17.48947	-.09102
12	110.00000	18.19435	17.24543	.98652	6.12903	15.99796	.14915
13	120.00000	17.19554	16.32758	.86796	5.25113	16.52901	-.05310

TABLE (A.1)

Q= 35 (L/M)

RESULTS OF
EXPERIMENT TWO FLUIDIZED BED DRYING
V(1)= 30.54

NO/	TIME MIN	WET (GM)	DRY(GM)	WATER G	SOLID GM	(X) /.)	RATE M(-1)
2	10.00000	18.10307	16.56812	1.53495	5.49167	27.95051	.26918
3	20.00000	18.24863	16.71075	1.53188	5.64033	27.15955	.07910
4	30.00000	18.52113	17.05521	1.46597	5.97876	24.51963	.26399
5	40.00000	18.75133	17.37950	1.37186	6.30305	21.76534	.27543
6	50.00000	17.12314	16.24075	.88239	5.16430	17.08634	.46750
7	60.00000	17.82955	17.05486	.77469	5.97841	12.95813	.41282
8	70.00000	17.23240	16.41745	.81495	5.34100	15.25838	-.23003
9	80.00000	16.88870	16.25500	.63370	5.17855	12.23762	.30214
10	90.00000	16.83525	16.23700	.59825	5.16055	11.59276	.06443
11	100.00000	16.74511	16.31430	.47181	5.23785	9.00776	.25851
12	110.00000	16.65134	16.54935	.40103	5.47290	7.32750	.16801
13	120.00000	16.60795	16.28895	.39900	5.21250	7.65468	-.03271

TABLE (A.2)

Q = 60 (L/M)

RESULTS OF
EXPERIMENT THREE FLUIDIZED BED DRYING
X(1)= 21.58

NO/	TIME MIN	WET (GM)	DRY(GM)	WATER G	SOLID GM	(X)(.)	RATE M(-1)
2	13.00000	17.98532	16.90609	1.07923	5.82964	18.51281	.30699
3	23.00000	18.00322	17.77765	1.12557	6.70120	16.79654	.17163
4	33.00000	19.00286	18.13541	.95745	7.05896	13.56361	.32329
5	43.00000	17.37480	16.76566	.60914	5.68921	10.70693	.28567
6	53.00000	18.17980	17.58520	.59360	6.50875	9.12003	.15869
7	63.00000	17.95835	17.00900	.48935	5.99255	8.16597	.09541
8	73.00000	17.85835	17.43651	.42184	6.36006	6.63264	.15333
9	83.00000	18.35768	17.96300	.39468	6.88655	5.73117	.09015
10	93.00000	18.50840	18.14690	.36150	7.07045	5.11283	.06183
11	103.00000	18.17500	17.84325	.33175	6.76680	4.90261	.02102
12	113.00000	17.57760	17.26025	.31735	6.18380	5.13196	-.02293
13	123.00000	17.67724	17.35311	.32413	6.27666	5.16405	-.00321

TABLE (A.3)

Q=85 (L/M)

RESULTS OF
EXPERIMENT FOUR FLUIDIZED BED DRYING
X(1)= 21.48

NO/	TIME MIN	WET (GM)	DRY(GM)	WATER G	SOLID GM	(X)(..)	RATE M(-1)
2	13.00000	17.84835	16.78356	1.06479	5.70711	18.65725	.28234
3	23.00000	17.37069	16.35106	1.01963	5.87461	17.35656	.13007
4	33.00000	17.27521	16.44000	.83521	5.36355	15.5719'	.17846
5	43.00000	15.73019	15.32924	.45695	4.25279	10.74471	.48273
6	53.00000	16.56962	16.20814	.36148	5.13169	7.04407	.37006
7	63.00000	16.34930	16.25211	.29639	5.17566	5.72661	.13175
8	73.00000	16.94648	16.64820	.29828	5.57175	5.35343	.03732
9	83.00000	17.01547	16.72409	.29138	5.64764	5.15932	.01941
10	93.00000	16.13295	15.89071	.23234	4.82326	4.81707	.03422
11	103.00000	16.93713	16.73447	.24253	5.62902	4.30933	.05077
12	113.00000	17.15433	16.96447	.29353	5.78802	5.07134	-.07620
13	123.00000	17.33335	17.02325	.27710	5.94630	4.65963	.04117

TABLE (A.4)

Q = 150 (L/M)

RESULTS OF
EXPERIMENT ONE FLUIDIZED BED DRYING
X(1)= 18.56

NO/	TIME MIN	WET (GM)	DRY(GM)	WATER G	SOLID GM	(X)(.)	RATE M(-1)
2	10.00000	20.16885	19.05535	1.11350	7.97890	13.95556	.46054
3	20.00000	18.69300	17.84015	.85285	6.76376	12 60922	.13463
4	30.00000	20.21309	19.24561	.96748	8.16916	11.84308	.07661
5	40.00000	18.37900	17.42947	.65053	6.35202	10.24131	16018
6	50.00000	19.58164	18.32265	.65899	7.84620	8.39884	.18425
7	60.00000	18.44945	18.01965	.42980	6.94320	6.19023	.22086
8	70.00000	18.13360	17.74034	.39326	6.66389	5.85634	.03339
9	80.00000	18.86700	18.46077	.34623	7.38432	4.66872	.11676
10	90.00000	17.97270	17.70600	.26670	6.62955	4.02290	.06658
11	100.00000	17.99930	17.68527	.31373	6.60882	4.74714	-.07242
12	110.00000	19.27720	18.95320	.32400	7.87675	4.11337	.06338
13	120.00000	19.23165	18.90368	.32797	7.82723	4.19012	-.00767

B. d_p 11 940 (μ)

TABLE (B.1)

Q = 85 (L/M)

RESULTS OF EXPERIMENT TWO FLUIDIZED BED DRYING
X(1)= 23.36

NO/	TIME MIN	WET (GM)	DRY(GM)	WATER G	SOLID GM	(X)(-/	RATE M(-1)
2	10 00000	19.75246	18.29270	1.45976	7.21625	20.22879	.31292
3	20.00000	20.17128	18.85100	1.32028	7.77455	16 9820.	32467
4	30.00000	19.19430	18.23000	.96400	7.15355	13.47583	.35062
5	40.00000	18.76475	18.14117	.62358	7.06472	8 82668	.46491
6	50 00000	17.46932	17.15575	.31357	6.07930	5.15800	.36687
7	60.00000	19.35573	19.58526	.37049	8.50881	4 35419	.08038
8	70.00000	19.79325	19.50664	.28661	7.43019	3.85737	.04968
9	80.00000	18.55415	18.30200	.25215	7.22555	3.48978	.03677
10	90.00000	17.66643	17.47500	.19143	6.39855	2.99177	.04979
11	100.00000	16.84425	16.64020	.20405	5.56375	3.66749	-.06757
12	110.00000	18.13925	17.87732	.26093	6.80087	3.83672	-.01692
13	120.00000	23.56333	18.26631	.29669	7.19986	4.12651	-.02898

TABLE (B.2)

Q= 150 (L/M)

RESULTS OF
EXPERIMENT THREE FLUIDIZED BED DRYING
X(1)= 25.27

NO/	TIME MIN	WET (GM)	DRY(GM)	WATER G	SOLID GM	(X)(..)	RATE M(-1)
2	13.00000	19.77730	18.52455	1.25245	7.44810	16.81570	84513
3	23.00000	20.03434	18.96725	1.06709	7.89085	13.52722	.32925
4	33.00000	18.40572	17.95975	.44597	6.88330	6.47901	.70442
5	43.00000	17.13125	16.86100	.27025	5.78455	4.67193	.18071
6	53.00000	18.51920	18.24525	.27395	7.16880	3.82142	.08505
7	63.00000	18.52625	18.28500	.24125	7.20855	3.34672	.04747
8	73.00000	18.49435	18.27024	.22411	7.19379	3.11533	.02314
9	83.00000	18.86164	18.63045	.23119	7.55400	3.06058	.00548
10	93.00000	19.13780	18.90461	.23319	7.82816	2.97886	.00816
11	103.00000	19.44435	19.20317	.24118	8.12672	2.96774	.00111
12	113.00000	19.41941	19.14535	.27306	8.06890	3.38418	-.04164
13	123.00000	18.40873	18.17066	.23807	7.09421	3.35584	.00283

TABLE (B.3)
Q= 275 (L/M)

RESULTS OF
EXPERIMENT FOUR FLUIDIZED BED DRYING
X(1)= 21.07

NO/	TIME MIN	WET (GM)	DRY(GM)	WATER G	SOLID GM	(X) (.)	RATE M(-1)
2	10.00000	18.13768	17.13853	.99915	6.06208	16.48197	.45838
3	20.00000	20.33234	19 32018	1.01216	8.24373	12.27 36	.42040
4	30 00000	18.17185	18.00000	.17185	6.92355	2.48215	.97958
5	40.00000	18.75519	18.46151	.29368	7.38506	3.97668	-.14945
6	50 00000	17.87350	17.68500	.18850	6.60855	2.85237	.11243
7	60.00000	18.59367	18.32605	.26762	7.24960	3 69151	-.08391
8	70 00000	18.52680	18.34300	.18380	7.26655	2.52940	.11621
9	80.00000	19.74096	19.50144	.23952	8.42499	2.84297	-.03136
10	90 00000	19.21742	19.02890	.18852	7.95245	2.37059	.04724
11	100.00000	17.64326	17.45110	.19216	6.37465	3.01444	-.06438
12	110.00000	18.54027	18.36800	.17227	7.29155	2.36260	.06518
13	120.00000	19.05225	18.84990	.20235	7.77345	2.60309	-.02405

TABLE (B.4)
Q = 500 (L/M)

RESULTS OF
EXPERIMENT ONE FLUIDIZED BED DRYING
X(1)= 22.02

NO/	TIME MIN	WET (GM)	DRY(GM)	WATER G	SOLID GM	(X)(...)	RATE M(-1)
2	10.00000	19.89825	18.10586	1.79239	7.02941	25.49844	-.34819
3	20.00000	20.42561	18.50770	1.91791	7.43125	25.81671	-.03103
4	30.00000	20.08325	18.20085	1.88240	7.12440	26.42187	-.06132
5	40.00000	20.07149	18.21577	1.85572	7.13932	25.99295	.04289
6	50.00000	20.53646	18.68938	1.84708	7.61293	24.26241	.17305
7	60.00000	20.37860	18.39942	1.46918	7.83297	18.75636	.55060
8	70.00000	19.81716	18.69815	1.11901	7.62170	14.68190	.40745
9	80.00000	19.20330	18.33300	.82980	7.30655	11.23376	.34481
10	90.00000	19.79428	19.03830	.75598	7.96185	9.49503	.17387
11	100.00000	19.70318	19.13800	.56518	8.06155	7.01061	.24842
12	110.00000	18.85500	18.35880	.49620	7.28235	6.81373	.01971
13	120.00000	19.53042	19.11655	.41387	8.04010	5.14757	.16662

TABLE(C.1)

Q=150(L/M)

$C_o \; d_p = 2471/\mu$

RESULTS OF
EXPERIMENT TWO FLUIDIZED BED DRYING
X(1)= 19.20

NO/	TIME MIN	WET (GM)	DRY(GM)	WATER G	SOLID GM	(X)(%)	RATE M(-1)
2	13.00000	19.28964	18.31700	.97264	7.24055	13.43323	.57620
3	23.00000	19.66515	18.69515	.97300	7.61870	12.77121	.06620
4	33.00000	19.25645	18.53985	.71660	7.46340	9.60152	.31697
5	43.00000	19.11500	18.46500	.65000	7.38855	8.79740	.08041
6	53.00000	18.91677	18.36717	.54960	7.29072	7.53835	.12590
7	63.00000	19.34961	19.40490	.46376	8.32845	5.83278	.17056
8	73.00000	18.62951	18.30354	.32497	7.22709	4.49655	.13362
9	83.00000	18.42200	18.11322	.30878	7.02677	4.39434	.01022
10	93.00000	18.08236	17.78881	.29355	6.71236	4.37328	.00211
11	103.00000	18.78231	18.42701	.27530	7.35056	3.74529	.06230
12	113.00000	18.55819	18.25342	.30477	7.17697	4.24650	-.05012
13	123.00000	18.76631	18.44855	.31776	7.37213	4.31031	-.00638

TABLE (C.2)

Q = 275 (L/M)

RESULTS OF
EXPERIMENT THREE FLUIDIZED BED DRYING
X(1)= 24.58

NO/	TIME MIN	WET (GM)	DRY(GM)	WATER G	SOLID GM	(X)	RATE M(-1)
2	10.00000	18.15745	16.93290	1.22455	5.85645	20 90942	36754
3	20 00000	19.80200	18.81165	.99035	7.73520	12.80226	.81063
4	30.00000	18.92378	18 22540	.69838	7.14895	9 76899	.30342
5	40 00000	19.38828	18.89717	.49111	7.82072	6.27960	.34894
6	50.00000	17.73918	17.38917	.35001	6.31272	5 54452	.07351
7	60 00000	18.58966	18.21900	.37066	7.14255	5.18945	.03551
8	70.00000	18.53190	18.21674	.32116	7.13429	4 50164	06878
9	80 00000	19.80075	19.46150	.33925	8.38505	4.04589	.04567
10	90.00000	19.23510	18.98965	.31545	7.89320	3.99648	.00494
11	100.00000	19.23476	18.88700	.34776	7.81055	4.45244	-.04560
12	110.00000	19.7.521	19.31673	.38548	8.24028	4.71440	-.02620
13	120.00000	19.58920	19.25600	.33320	8.17955	4.07357	.06408

TABLE (C.3)

Q= 375 (L/M)

RESULTS OF
EXPERIMENT FOUR FLUIDIZED BED DRYING
X(1)= 31.53

NO/	TIME MIN	WET (GM)	DRY(GM)	WATER G	SOLID GM	(X)(..)	RATE M(-1)
2	13.00000	19.19480	18.11780	1.07700	7.04135	15.29536	1.62390
3	23 00000	19.03362	19.02245	.88117	7.94603	11.089.3	.42059
4	33.00000	19.73940	19.14740	.59200	8.07095	7 33495	.37545
5	43 00000	18.66330	18.21090	.45240	7.13445	6.34106	.09939
6	53.00000	18.86939	18.45820	.41119	7.38175	5.57036	07707
7	63 00000	18.29730	17.95836	.33894	6.88191	4.92509	.06453
8	73.00000	18.31673	18.19515	.32158	7.11870	4 51743	04077
9	83 00000	19.09151	18.76790	.32361	7.69145	4.20746	-.03160
10	93.00000	19.24773	18.89505	.35273	7.81860	4 51142	-.03040
11	103.00000	18.74276	18.39905	.34371	7.32260	4.69382	-.01824
12	113.00000	19.62343	19.28397	.33943	8.20752	4.13560	05582
13	123.00000	18.75385	18.53200	.22685	7.45555	3.04273	.16929

TABLE (C.4)

Q = 500 (L/M)

RESULTS OF
EXPERIMENT ONE FLUIDIZED BED DRYING
X(1)= 31.17

NO/	TIME MIN	WET (GM)	DRY(GM)	WATER G	SOLID GM	(X)(./.)	RATE M(-1)
2	10.00000	20.31800	18.34589	1.97211	7.26944	27.12877	.40385
3	20.00000	21.05762	18.98000	2.07762	7.90355	26.28717	.03416
4	30.00000	20.10037	18.45251	1.64786	7.37606	22.34065	.39465
5	40.00000	20.07961	18.64081	1.43880	7.56436	19.02078	.33199
6	50.00000	21.84200	20.30878	1.53322	9.23233	16.60708	.24137
7	60.00000	20.84245	19.73645	1.10600	8.66000	12.77136	.38357
8	70.00000	20.69264	19.80555	.88709	8.72910	10.16245	.26089
9	80.00000	20.74261	20.03025	.71236	8.95380	7.95595	.22065
10	90.00000	20.93900	20.34169	.59731	9.26524	6.44678	.15092
11	100.00000	20.57721	20.05217	.52504	8.97572	5.84956	.05972
12	110.00000	18.68516	18.36110	.32406	7.28465	4.44653	.14010

TABLE (6.4.1)

TEMP = 40 (°C)

RESULTS OF
EXPERIMENT ONE FLUIDIZED BED DRYING
X(1)= 29.24

NO/	TIME MIN	WET (GM)	DRY(GM)	WATER G	SOLID GM	(X)(o/o	RATE M(-1)
2	10.00000	23.73568	21.38122	2.35446	10.30477	22.84825	.63913
3	20.00000	23.18643	21.41885	1.76755	10.34240	17.09833	.57579
4	30.00000	22.87825	21.02660	.85165	9.95015	8.55917	.85312
5	40.00000	22.60309	22.04545	.55464	10.96900	5.05643	.35027
6	50.00000	20.46911	20.06242	.40668	8.98597	4.52572	.05307
7	60.00000	20.37772	22.09293	.32572	10.97555	2.96709	.15580
8	70.00000	18.87660	18.66691	.20969	7.59146	2.76255	.62051
9	80.00000	20.49616	20.26144	.23472	9.18499	2.55547	.02671
10	90.00000	20.43666	20.21717	.18883	9.14072	2.06581	.04897
11	100.00000	20.03594	19.93000	.10594	8.82355	1.20065	.08652
12	110.00000	20.05045	20.04890	.20155	9.77245	2.06243	-.08618
13	120.00000	20.92438	20.52765	.39673	9.45120	4.19767	-.21352

TABLE (6.4.2)
TEMP.= 60 (°C)

RESULTS OF
EXPERIMENT ONE FLUIDIZED BED DRYING
X(1)= 31.23

NO/	TIME MIN	WET (GM)	DRY(GM)	WATER G	SOLID GM	(X)(./.)	RATE M(-1)
2	10.00000	22.85051	20.66939	2.18112	9.59294	22.73672	.84934
3	20.00000	21.45310	19.79435	1.65875	8.71790	19.02694	.37098
4	30.00000	23.53945	22.43340	1.10605	11.35695	9.73897	.92880
5	40.00000	21.62830	20.01565	1.61265	8.93920	18.04020	-.83012
6	50.00000	19.70137	19.49600	.20537	8.41955	2.43920	1.56010
7	60.00000	21.45300	21.25105	.20195	10.17460	1.98484	.04544
8	70.00000	20.97145	20.81210	.15935	9.73565	1.63677	.03481
9	80.00000	20.89710	20.75581	.14129	9.67936	1.45970	.01771
10	90.00000	22.11500	22.00091	.11409	10.92446	1.04435	.04154
11	100.00000	22.89150	22.74032	.15118	11.66387	1.29614	-.02518
12	110.00000	20.52165	20.38923	.13242	9.31278	1.42192	-.01258
13	120.00000	20.25072	20.13760	.11312	9.06115	1.24841	.01735

TABLE (6.4.3)

TEMP.=80 (°C)

RESULTS OF EXPERIMENT ONE FLUIDIZED BED DRYING
X(1)= 33.16

NO/	TIME MIN	WET (GM)	DRY(GM)	WATER G	SOLID GM	(X)(d.b.)	RATE M(-1)
2	10.00000	23.12540	21.15200	1.97340	10.07555	19.58603	1.35769
3	20.00000	23.82325	22.23935	1.58390	11.16290	14.18897	.53971
4	30.00000	22.29630	21.56526	.73104	10.48881	6.96971	.72193
5	40.00000	21.69847	21.43605	.26242	10.35960	2.53311	.44366
6	50.00000	22.17817	22.07751	.10066	11.00106	.91500	.16181
7	60.00000	21.65318	21.62280	.03038	10.54635	.28806	.06269
8	70.00000	20.57680	20.54040	.03640	9.46395	.38462	-.00966
9	80.00000	20.01663	20.01154	.00509	8.93509	.05697	.03277
10	90.00000	21.74495	21.64475	.10010	10.56833	.94717	-.08902
11	100.00000	21.54637	21.52400	.02437	10.44755	.23326	.07139
12	110.00000	19.45366	19.44173	.01193	8.36528	.14261	.00906
13	120.00000	21.03725	21.01275	.02450	9.93633	.24657	-.01040

TABLE (6.4.4)

TEMP. = 100 (°C)

APPENDIX (7)

(MODELLING)

APPENDIX (7.1) CALCULATIONS FOR GROUP(A) (106 - μ)

APPENDIX (7.2) CALCULATIONS FOR GROUP(B) (940 - μ)

APPENDIX (7.3) CALCULATIONS FOR GROUP(C) (2,247 - μ)

GAS ANALYSIS
SHALLOW BED MODEL(3)
EQM CURVE

NO/	XAV(•/•)	TEMP(OC)	P(MM HG)	(R.H.)(•/•)	Y EQM(GM/KGM)	Y MZ(GM/KGM)	Z=Y MZ/YEQM	$(1-\frac{Y_{EQ}}{Y})$
2	21.07204	30.00000	31.82400	.49897	13.33714	6.51795	.48871	.51129
3	20.47828	33.00000	37.72900	.48291	15.35144	5.27058	.34333	.65667
4	20.63582	31.00000	33.69500	.48717	13.79726	6.51795	.47241	.52759
5	19.98122	31.00000	33.69500	.46949	13.28606	6.51795	.49059	.50941
6	19.41428	33.00000	37.72900	.45686	14.90396	6.10216	.42072	.57928
7	19.16104	33.00000	37.72900	.44735	14.19518	6.10216	.42988	.57012
9	18.98762	33.00000	37.72900	.44267	14.04326	4.43900	.31609	.68391
9	18.20422	33.00000	37.72900	.42165	13.36226	4.43900	.33220	.66780
10	18.90122	33.00000	37.72900	.38633	12.22119	4.43900	.36322	.63678
11	17.03439	33.00000	37.72900	.38993	12.33718	4.43900	.35981	.64019
12	18.74372	33.00000	37.72900	.38208	12.08407	4.43900	.36734	.63266
13	18.26249	33.00000	37.72900	.36911	11.66633	4.43900	.38050	.61950

RESULTS OF
EXPERIMENT FOUR FLUIDIZED BED DRYING
X(1)= 21.98

TABLE (7.1.1)

Q= 90 (L/M)

GAS ANALYSIS
SHALLOW PBD MODEL(3)
EQM CURVE

NO/	XAV(%)	TEMP(OC)	P(MM HG)	(R.H.)(%)	Y EQM(GM/KGM)	Y MZ(GM/KGM)	Z=Y MZ/YEQM	$(1-\frac{Y_c}{Y^*})$
2	24.39665	32.00000	35.69500	1.00000	30.801084	11.92321	.38710	.61290
3	27.55526	33.00000	37.72900	.72394	23.299044	11.50742	.49390	.50610
4	25.43959	35.00000	42.17500	.64523	23.20964	10.67584	.45997	.54003
5	25.14248	38.00000	49.69200	.54813	23.23199	9.42847	.40584	.59416
6	19.42584	38.00000	49.69200	.45450	19.14195	9.42847	.49256	.50744
7	15.02224	40.00000	55.32400	.33560	15.65107	8.59689	.54928	.45071
8	14.10425	40.00000	55.32400	.31092	14.47355	4.43900	.30670	.69320
9	13.74770	40.00000	55.32400	.30595	14.23689	4.43900	.31180	.68818
10	11.91489	40.00000	55.32400	.26783	12.42766	4.43900	.35719	.64281
11	10.30023	40.00000	55.32400	.23424	10.84225	4.43900	.40942	.59058
12	8.16763	40.00000	55.32400	.18989	8.76031	4.43900	.50672	.49328
13	7.49112	40.00000	55.32400	.16864	7.76788	4.43900	.57146	.42854

RESULTS OF
EXPERIMENT FOUR FLUIDIZED BED DRYING
X(1)= 50.84

TABLE (7.1.2)

Q = 275 (L/M)

GAS ANALYSIS
SHALLOW BED MODEL(3)
EQM CURVE

NO/	XAV(%)	TEMP(OC)	P(MM HG)	(R.H.)(%)	Y EQM(GM/KGM)	Y MZ(GM/KGM)	Z=Y MZ/YEQM	$(1-\frac{Y_L}{Y^*})$
2	2[illegible].06895	35.00000	42.17500	.47186	16.80582	6.93374	.41258	.58742
3	[illegible].03691	39.00000	52.44200	.41519	18.47942	7.76532	.42021	.57979
4	[illegible].46426	47.00000	79.60000	.37454	25.51828	7.34953	.28801	.71199
5	[illegible].15834	47.00000	79.60000	.29369	19.83547	7.34953	.37052	.62948
6	8.89439	47.00000	79.60000	.20500	13.71409	4.43900	.32368	.67632
7	5.38534	47.00000	79.60000	.15482	10.30143	4.43900	.43091	.56909
8	5.54002	47.00000	79.60000	.14425	9.58755	4.43900	.46300	.53700
9	5.25638	47.00000	79.60000	.14070	9.34837	4.43900	.47484	.52516
10	4.98823	47.00000	79.60000	.13735	9.12240	4.43900	.48660	.51340
11	4.56320	47.00000	79.60000	.13204	8.76462	4.43900	.50647	.49353
12	4.69033	47.00000	79.60000	.13363	8.87160	4.43900	.50036	.49964
13	4.86549	47.00000	79.60000	.13382	9.01906	4.43906	.49218	.50782

TABLE (7.1.3)

Q = 150 (L/M)

GAS ANALYSIS
SHALLOW FED MODEL(3)
EQM CURVE

NO/	XAV(%)	TEMP(OC)	P(MM HG)	(R.H.)(%)	Y EQM(GM/KGM)	Y OUT(GM/KGM)	Z=YOUT/YEQM	$(1-\frac{Y_\zeta}{Y^*})$
2	21.79341	31.00000	33.69500	.51842	14.70327	15.00000	1.02018	.01941
3	18.60543	41.00000	59.00000	.43235	21.70588	21.00000	.96748	.23998
4	15.22895	46.00000	75.65000	.34118	21.97184	22.00000	1.00128	.39546
5	11.15125	46.00000	75.65000	.25195	16.07731	15.00000	.93299	.23939
6	6.99234	46.50000	77.60000	.16240	10.53871	6.30000	.59780	.17175
7	4.75609	56.00000	123.00000	.13445	13.90243	5.10000	.36684	.35172
8	4.10578	57.00000	129.82000	.12632	13.78357	4.43900	.32205	.67795
9	3.67354	55.00000	118.04000	.12092	11.96258	4.43900	.37107	.62893
10	3.24074	51.00000	97.20000	.11551	9.37158	4.43900	.47467	.52632
11	3.32963	51.00000	97.20000	.11662	9.46310	4.43900	.46909	.53191
12	3.75210	55.00000	118.40000	.12190	12.09911	4.43900	.36689	.63311
13	3.98161	51.00000	97.20000	.12477	10.13513	4.43900	.43798	.56201

TABLE (7.2.1)

Q = 200 (L/M)

GAS ANALYSIS
SHALLOW BED MODEL(3)
EQM CURVE

NO/	XAV(%)	TEMP(OC)	P(MM HG)	(R.H.)(%)	Y EQM(GM/KGM)	Y MZ(GM/KGM)	Z=Y MZ/YEQM	$(1-\frac{Y_S}{Y^*})$
2	18.77389	25.00000	23.75800	.43689	8.65417	14.83374	1.71406	———
3	14.37997	41.00000	58.34000	.31826	15.65148	16.49689	1.05401	Zero
4	7.38006	45.00000	71.88000	.16725	10.04540	6.51795	.64885	.35115
5	3.22941	48.00000	83.71000	.11537	8.04418	6.10216	.75858	.24142
6	3.41452	50.00000	92.51000	.11768	9.08300	4.43900	.48872	.51128
7	3.27194	51.00000	97.20000	.11590	9.40371	4.43900	.47205	.52795
8	3.11646	51.00000	97.20000	.11388	9.23751	4.43900	.48054	.51946
9	2.68618	51.00000	97.20000	.10858	8.80126	4.43900	.50436	.49564
10	2.60678	51.00000	97.20000	.10758	8.71968	4.43900	.50908	.49192
11	2.69252	51.00000	97.20000	.10866	8.80776	4.43900	.50399	.49601
12	2.68652	51.00000	97.20000	.10861	8.80366	4.43900	.50422	.49578
13	2.48284	51.00000	97.20000	.10604	8.59239	4.43900	.51662	.48338

RESULTS OF
EXPERIMENT FOUR FLUIDIZED BED DRYING
X(1)= 21.07

TABLE(7.2.3)

B=500(L/M)

GAS ANALYSIS
SHALLOW BED MODEL(3)
EQV CURVE

NO/	XAV(%)	TEMP(OC)	P(MM HG)	(R.H.)(%)	Y EQM(GM/KGM)	Y MZ(GM/KGM)	Z=Y MZ/YEQM	$(1-\frac{Y\zeta}{Y^*})$
2	23.75747	30.00000	31.82400	.57027	15.28965	9.01268	.58946	.41054
3	25.65358	30.00000	31.82400	.63853	17.17006	15.66532	.91236	.08764
4	26.11829	29.00000	30.04300	.65515	16.61677	13.58637	.81763	.18237
5	26.20741	34.00000	39.89600	.65847	22.37843	12.75479	.56996	.43004
6	25.12768	34.00000	49.69200	.61960	26.38895	10.26005	.38880	.61120
7	21.50938	34.00000	39.89800	.51075	17.21998	8.18111	.47509	.52491
8	16.71913	34.00000	39.89800	.38142	12.77030	4.43900	.34760	.65240
9	12.95783	34.00000	39.89800	.28952	9.64610	4.43900	.46019	.53981
10	10.36439	34.00000	39.89800	.23558	7.82635	4.43900	.56719	.43281
11	8.25292	34.00000	39.89800	.19166	6.35247	4.43900	.69878	.30122
12	6.91227	34.00000	39.89800	.16140	5.34104	4.43900	.83111	.16889
13	5.98065	34.00000	39.89800	.14976	4.95263	4.43900	.89629	.10371

RESULTS OF
EXPERIMENT FOUR FLUIDIZED BED DRYING
λ(1)= 22.02

TABLE (7.3.1)

Q= 3.25 (L/M)

GAS ANALYSIS
SHALLOW BED MODEL(3)
EQM CURVE

NO/	XAV(%)	TEMP(OC)	P(MM HG)	(R.H.)(%)	Y EQM(GM/KGM)	Y MZ(GM/KGM)	Z=Y MZ/YEQM	$(1-\frac{Y_c}{Y^*})$
2	5.31421	39.00000	52.44200	.37040	16.39690	11.92321	.72716	.27284
3	3.10222	35.00000	42.17500	.29253	10.31322	9.64426	.95453	.04547
4	2.18636	40.00000	55.39400	.25268	11.72645	9.01268	.76858	.23142
5	9.19946	41.00000	58.34000	.21135	10.30709	8.59689	.83408	.16592
6	8.10787	46.00000	75.65000	.18989	12.04118	4.43900	.36865	.63135
7	8.68556	46.00000	75.65000	.15857	10.02316	4.43900	.44287	.55712
8	8.16467	46.00000	75.65000	.13356	8.80454	4.43900	.50417	.49583
9	4.44545	46.00000	75.65000	.13057	8.22988	4.43900	.53938	.46062
10	4.38361	46.00000	75.65000	.12980	8.18068	4.43900	.54262	.45738
11	4.05928	46.00000	75.65000	.12574	7.92177	4.43900	.56035	.43965
12	3.99590	46.00000	75.65000	.12495	7.87123	4.43900	.56395	.43605
13	4.27840	46.00000	75.65000	.12848	8.09657	4.43900	.54826	.45173

TABLE (7.3.2)
Q = 500 (L/M)

S ANALYSIS
LLOW BED MODLL(3)
M CURVE

NO/	XAV(•/•)	TEMP(DC)	P(MM HG)	(R.H.)(•/•)	Y EQM(GM/KGM)	Y_{MZ}(GM/KGM)	Z=Y MZ/YEQM	$(1-\frac{Y_\zeta}{Y^E})$ =
2	22.74713	37.00000	47.06000	.53398	21.36859	9.84426	.46069	.53931
3	15.85629	43.00000	55.32400	.38512	18.02707	8.59689	.47689	.52311
4	11.28607	43.00000	55.32400	.25475	11.80930	8.59089	.72798	.27202
5	8.02429	45.00000	71.88000	.18691	11.24714	4.43900	.39468	.60532
6	5.91206	45.00000	71.88000	.14390	8.92752	4.43900	.49723	.50277
7	5.36699	45.00000	71.88000	.14209	8.51346	4.43900	.52141	.47859
8	4.84555	45.00000	71.88000	.13557	8.11784	4.43900	.54682	.45318
9	4.27377	45.00000	71.88000	.12842	7.68460	4.43900	.57765	.42235
10	4.02118	45.00000	71.88000	.12526	7.49341	4.43940	.59239	.40761
11	4.22446	45.00000	71.88000	.12781	7.64727	4.43900	.58047	.41953
12	4.58342	45.00000	71.88000	.13229	7.91915	4.43900	.56054	.43946
13	4.39399	45.00000	71.88000	.12392	7.77565	4.43900	.57089	.42911

TABLE (7.3.3)
Q= 375 (L/M)

APPENDIX (8)

MODELLING OF TOP SECTION IN FLUIDISED BED DRYING

Model (1) Dense-phase gas is perfectly mixed.

Model (2) Dense-phase gas in plug flow.

MODEL (1) DENSE-PHASE GAS IS PERFECTLY MIXED

Following the same analysis of Davidson and Harrison (1963), the top section in cylindrical bed dryer can be described in the following way:

(i) Material balance around rising bubble

$$V \frac{d\, Y_B}{dt} = Q \left(Y_p - Y_B \right) \qquad \text{(A-1)}$$

integrating over the top section

$$\left(Y_B \right)_{H'} = Y_p + \left(Y_\zeta - Y_p \right) e^{-X} \qquad \text{(A-2)}$$

where

$$X \quad : \text{N.T.U.} = \frac{Q}{V} \cdot \frac{H'}{U_A} = \frac{6.34\, H_o}{De\, (g\, D_o)^{\frac{1}{2}}} \left(U_o + \frac{1.3\, D_G^{\frac{1}{2}}\, g^{\frac{1}{4}}}{De^{\frac{1}{4}}} \right)$$

$$Q \quad : q + K_g S$$

$$H' \quad : H - \zeta$$

(ii) Material balance around the particulate phase, based on unit cross sectional area of the bed,

$$N V U_A \left(Y_\zeta - Y_p \right) \left(1 - e^{-X} \right) + U_o \left(Y_\zeta - Y_p \right) = - K_{g/p} \grave{A} \left(Y^* - Y_p \right) \qquad \text{(A-3)}$$

where

A' : particles surface area per unit cross sectionsl area of the bed (cm^2/cm^2).

$K_{g/p}$: Particle to gas mass transfer coefficient (cm/s).

Re-arranging (A-3) produces:

$$Y_p = Y_\zeta + \frac{1}{1 + C_1} (Y^* - Y_\zeta) \qquad (A-4)$$

where

$$C_1 = \frac{N V U_A (e^{-X} - 1) - U_o}{K_{g/p} A'} \qquad (A-5)$$

(iii) Overall material balance

$$U \cdot Y_o = (U - U_o) (Y_B)_{H'} + U_o \cdot Y_p \qquad (A-6)$$

Using equations (A-2) and (A-4) to replace $(Y_B)_{H'}$ and Y_p in equation (A-6), and after re-arrangement,

$$\frac{Y_o - Y_\zeta}{Y^* - Y_\zeta} = \frac{1}{(1 - C_1)} \left(1 - \left(\frac{U - U_o}{U} \right) e^{-X} \right) \qquad (A-7)$$

Equation (A-7) can represent the dryer performance(η) (as the ratio between the outlet air humidity to the equilibrium humidity), in the following form:

$$\eta = 1 - \beta_1 \left(1 - \frac{Y_\zeta}{Y^*} \right) \qquad \text{(A-8)}$$

where

η : Dryer performance $= \dfrac{Y_o}{Y^*}$

Y_ζ : air humidity at the end of entry zone

$$\beta_1 = 1 - \frac{K_{g/p}\, A'}{K_{g/p}\, A' + U_o + (U - U_b)\,(1 - e^{-X})} \left(1 - \left(\frac{U - U_g}{U} \right) \left(e^{-X} \right) \right) \qquad \text{(A-9)}$$

MODEL (2) DENSE-PHASE GAS IN PLUG FLOW

Following the same analysis of Davidson and Harrison (1963), the top section in cylindrical bed dryer can be described as follows:

(i) Differential material balance around rising bubble

$$\frac{d Y_B}{d Z} + \frac{X}{H'} \left(Y_B - Y_p \right) \quad 0 \qquad \text{(A-10)}$$

) Differential material balance on infinitesmal height (dZ) of the bed

$$U_0 \frac{d Y_p}{d Z} + (U - U_o) \frac{d Y_B}{d Z} - K_{g/p} A' (Y^* - Y_p) = 0 \quad (A-11)$$

solving equations (A-10) and (A-11) to find both of (Y_B) and (Y_p) as functions of bed height gives

$$A_1 \frac{d^2 \bar{Y}_B}{d Z^2} + A_2 \frac{d \bar{Y}_B}{d Z} + A_3 \bar{Y}_B = 0 \quad (A-12)$$

equation (A-12) is linear second order differentail equation where:

$$A_1 = \frac{U_o H'}{X}$$

$$A_2 = U + \frac{K_{g/p} A' H'}{X} \quad (A-13)$$

$$A_3 = K_{gp} A'$$

$$\bar{Y}_B = Y_B - Y^*$$

Solving equation (A-12) using the following boundary conditions:

$$\text{at } Z = 0 \qquad \bar{Y}_B = Y_\zeta - Y^* \tag{A-14}$$

$$Z = 0 \qquad \frac{d\,\bar{Y}_B}{d\,Z} = 0$$

The solution of (A-12) with the boundary conditions listed in (A-14) gives the bubble concentration (Y_B) as function of the bed height:

$$Y_B = Y^* + K_1\, e^{-m_1 Z} + K_2\, e^{-m_2 Z} \tag{A-15}$$

where

$$\left.\begin{aligned} K_1 &= \left(\frac{-m_2}{m_1 - m_2}\right)\left(Y_\zeta - Y^*\right) \\ K_2 &= \left(\frac{m_1}{m_1 - m_2}\right)\left(Y_\zeta - Y^*\right) \\ \begin{matrix} m_1 \\ m_2 \end{matrix} &= \frac{+A_2 \pm \sqrt{A_2^2 - 4 A_3 A_1}}{2 A_1} \end{aligned}\right\} \text{(A-16)}$$

Substituting the values of (Y_B) from equation (A-15) into equation (A-10), the dense-phase gas humidity (Y_p) can be obtained as a function of bed height,

$$Y_p = Y^* + \left(1 - \frac{m_1 H'}{X}\right) K_1\, e^{-m_1 Z} + \left(1 - \frac{m_2 H'}{X}\right) K_2\, e^{-m_2 Z} \tag{A-17}$$

Using equations (A-15) and (A-17) for (Y_B) and (Y_p), we can calculate the humidity of the gas leaving the bed,

$$U \cdot Y_o = U_o \cdot (Y_p)_{H'} + (U - U_o) \quad (Y_B)_{H'} \tag{A-18}$$

Substituting (A-15) and (A-17) into the last equation (A-18) we can express the bed performance in the following form:

$$\eta = 1 - \beta_2 \left(1 - \frac{Y_\zeta}{Y^*}\right) \tag{A-19}$$

where

η : dryer performance $= \dfrac{Y_o}{Y^*}$

$$\beta_2 = \left(\left(\frac{-m_2}{m_1 - m_2}\right)\left(1 - \frac{U_o}{U}\ \frac{m_1 H'}{X}\right) e^{-m_1 H'} + \left(\frac{m_1}{m_1 - m_2}\right)\left(1 - \frac{U_o\ m_2 H'}{U\ X}\right) e^{-m_2 H'}\right) \tag{A-20}$$

NOMENCLATURE

$\bar{A}$: Particle surface area per unit bed height

a : Bubble radius

$\bar{C}$: Average moisture concentration of solids

C^* : Water vapour concentration in equilibrium with solids

C_b : Concentration of water vapour in the bubble

C_g : Specific heat capacity of gas

C_H : Exit gas concentration

C_i : Inlet gas concentration

C_{in} : Water vapour concentration in the gas entering the bubble

C_s, C_p : Specific heat capacity of solids

D : Three-dimensional fluidised bed diameter

$\bar{D}_A$: Average agglomerate diameter

D_e : Equivalent bubble diameter

D_G : Molecular diffusion coefficient of moisture in air

D_p : Molecular diffusion coefficient of moisture in the pores

$\bar{D}_p$: Overall pore diffusion coefficient

D_t : Tube diameter

D_{Kp} : Knudson pore diffusion coefficient

D_{sp} : Surface pore diffusion coefficient

d_b : Bubble diameter

dp : Particle diameter

E_G : Axial diffusion coefficient

F_E : Electrostatic forces between particles

F_H : Hydrodynamic forces exerted by the fluid on particles

F_I : Overall inter-particle forces

F_S : Surface tension forces in the agglomerate

F_V : Van der Waal's forces

f_r : Bubble frequency in the bed

f_w : Wake fraction of the bubble

G : Air mass flow rate

$\acute{G}$: Gibbs free energy

g : Gravitional acceleration

H : Total bed height

H_o : Initial bed height

$h_{B/w}$: Bed to wall heat transfer coefficient

$h_{g/p}$: Gas to particle heat transfer coefficient

HTU : Height of transfer unit

$(\Delta H)_{vap}$: Latent heat of vaporization

i : Air enthalpy

J : Overall pore diffusion flux

K : Adsorption isotherm constant

$\acute{K}$: Number of reactor units

K_B : Overall bubble to dense-phase mass transfer coefficient

K_G : Mass transfer coefficient between bubble and its surface.

$\bar{K}_g$: Overall mass transfer coefficient between solids and gas

$K_{B/c}$: Bubble to cloud mass transfer coefficient

$K_{c/E}$: Cloud to emulsion-phase mass transfer coefficient

k : Air thermal conductivity

L : Bed height (expanded)

l : Pore depth of hygroscopic material

$\bar{l}$: Average film thickness around the particle

M : Molecular weight of diffusant

$\bar{M}$: Reduced free moisture content of solids

N : Number of particles in the agglomerate

$(NTU)_B$: Number of bubble transfer units (Exchange factor)

P : Bed operating pressure

(ΔP): Pressure drop across the bed

p^0 : Saturation vapour pressure of moisture at a given temperature

Q : Overall transfer between bubble and dense-phase gas

q : Convective transfer between the bubble and dense-phase gas

q_{HT} : Heat transfer rate

R : Solids drying rate

R_A : Ratio between agglomerate diameter and particle diameter

R_b : Bubble radius

R_c : Cloud radius

$(RH)^*$: Equilibrium relative humidity of air in contact with wet solids

S : Surface area of particles per unit volume of packing

T : Bed average temperature

T_g : Gas temperature

T_R : Room temperature

T_s : Solids temperature

T_{in} : Inlet air temperature

T_{out} : Outlet air temperature

t : Time

U : Air superficial velocity

U_A : Absolute bubble rising velocity $(= U_b + U - U_o)$

U_b : Bubble rising velocity $(= K \sqrt{g\ D_e})$

U_o : Minimum fluidising velocity of bone dry particles

U^* : Minimum fluidising velocity of moist particles

U_{cr} : Critical velocity at which the agglomerate breaks

$\bar{U}_{cr}$: Critical velocity for back mixing

u : Interstitial velocity $(= \frac{U}{\varepsilon})$

u_o : Interstitial velocity at incipient fluidisation

V : Bubble volume

W : Cumulative distribution function

w : Size distribution function

X : Solids moisture content

X_{cr} : Critical moisture content at which the agglomerate breaks

Y^* : Equilibrium air humidity

Y_B : Air humidity inside the bubble

Y_g : Overall air humidity

Y_p : Humidity of dense-phase air

Y_{in} : Air humidity at the inlet of the bed

Y_{out} : Air humidity at the outlet of the bed

Y_ζ : Air humidity at top of entry zone

Z : Bed height

Fr : Froude Number $(= \frac{U^2}{\varepsilon^2} \cdot \frac{1}{dp \cdot g})$

Jh : Heat transfer factor $(= \frac{hg}{C_g G} Pr^{\frac{2}{3}})$

Jd : Mass transfer factor $(= ST \cdot SC^{\frac{2}{3}} = \frac{kg\ \rho_g\ M}{G} \cdot (\frac{\mu}{\rho D_G})^{\frac{2}{3}})$

Nu : Nusselt number $(= \frac{h.dp}{k})$

Pr : Prandtl number $(= \frac{Cg \cdot \mu}{k})$

Pe : Peclet number $(= Re \cdot Pr)$

Re : Particle Reynolds number $(= \frac{\rho_g . U \cdot dp}{\mu})$

Sh : Sherwood number $(= \frac{K_g \cdot dp}{D_G})$

Sc : Schmidt number $(= \frac{\mu}{\rho_g \cdot D_G})$

St : Stanton number $(= \frac{Kg \cdot dp}{U})$

ε : Voidage fraction

ε_o : Voidage fraction at minimum fluidisation

ρ : Bulk density

$\rho_{f,g}$: Air density

ρ_s : Bone-dry solids density

ρ_s^* : Wet solids density

ϕ : Shape factor (sphericity)

α : Ratio of bubble velocity to interstitial velocity $(= \frac{U_b}{u_o})$

η : Bed performance $(= \frac{Y_{out}}{Y^*})$

ψ : Humidity driving force $(= Y^* - Y_g)$

ψ_0 : Relative humidity of air leaving the bed

μ : Air viscosity

ζ : Height of entry zone

β : Bubble factor defined in equations (7-5) and (7-7)

τ : Tortuosity factor

θ : Free fraction of cross sectional area of the pore

REFERENCES

(1) Baerg, A., Klassen, J. and Gishler, P.E., Can. J. Research, 28, 287, (1950).

(2) Baeyens, J. and Goossens, W.R., Powder Tech., 8, 91, (1973).

(3) Balakrishnat, A.R. and Pei, O.C.T., Can. J. Chem. Eng., 53, 231, (1975).

(4) Baskakov, A.P. et al, Powder Tech., 8, 273, (1973)

(5) Becker, H.A., J. Applied Polym. Sci., 1, 212, (1959)

(6) Becker, H.A. and Sallans, H.R., Chem. Eng. Sci., 13, 97, (1960)

(7) Beek, W.J., "FLUIDISATION", 449, ed. Davidson and Harrison, Academic Press, London, (1971)

(8) Beek, W.J. and Drinkenburg, A.A.H., "Proceeding Int. Symp. Fluid.", 507, ed Drinkenburg, A.A.H., Eindhoven, Netherland Univ.(196?).

(9) Beeken, D.W., The Ind. Chemist, 34, 329, (1958)

(10) Beeken, D.W., Brit. Chem. Eng., 5, 484, (1960).

(11) Bicknell, J.A., Whitmore, R.L., "Proc. of Int. Symp. Fluid.", 31, Eindhoven, ed. Drinkenburg, A.A.H., Netherland Univ. Press, (1967).

(12) Blake, F.C., Trans. Am. Inst. Chem. Engrs, 14, 415, (1922).

(13) Botterill, J.S.M., Powder Tech., 4, 19, (1970).

(14) Botterill, J.S.M., A.I.Ch.E. Symp. Ser., No 128, 69, 26, (1973)

(15) Botterill, J.S.M., "FLUID BED HEAT TRANSFER", 146, Academic Press, New York, (1975).

(16) Botterill, J.S.M. and Williams, J.R., Trans. Inst. Chem. Engrs, 41, 217, (1963).

(17) Botterill, J.S.M. et al, "Proceedings Int. Symp. Fluid.", 458, Eindhoven, ed Drinkenburg,A.A.H., Netherland Univ. Press, (1967).

(18) Calderbank, P.H. and Toor, F.D., "FLUIDISATION", 391, ed. Davidson, J.F. and Harrison, D., Academic Press, London, (1971).

(19) Capes, C.E., Powder Tech ., 10, 303, (1974).

(20) Capes, C.E. et al, Can. J. Chem. Eng., 47, 166, (1969).

(21) Carberry, J.J., A.I.Ch.E.J., 6, No 3, 460, (1960).

(22) Carmen, P.C., Trans. Inst. Chem. Engrs., 15, 150, (1937).

(23) Chang, T.M. and Wen, C.Y., Chem. Eng. Prog. Symp. Ser., No 67, 62, 111, (1966).

(24) Chavarie, C. and Grace, J.R., "Proceeding of Int. Fluid. Conference", 251, ed. Keairns, D.L., California, Hemisphere Publishing Co., Washington, (1975).

(25) Chavarie, C. and Grace, J.R., Chem. Eng. Sci., 31, 741, (1976)

(26) Cheng, D.C.H., Chem. Eng. Sci., 23, 1405, (1968).

(27) Chiba, T. and Kobayashi, H., Chem. Eng. Sci., 25, 1375, (1970).

(28) Chiba, T. and Kobayashi, H., "Fluidisation and its application", 468, ed. Angelino, H., Toulouse, (1973).

(29) Conway-Jones, J.M., Ph.D. thesis, 37, Imperial College, London, (1957).

(30) Corn, M., "Aerosol Science", 360, Academic Press, London, (1966).

(31) Davidson, J.F., Trans. Inst. Chem. Engrs., 39, 230, (1961).

(32) Davidson, J.F. and Harrison, D., "Fluidised Particles", 97, Cambridge Univ. Press, (1963).

(33) Davidson, J.F., Filla, M., Bates, J.F. and Eccles, M.A., Chem. Eng. Sci., 31, 359, (1976).

(34) Davis, W.L. and Glazier, W., A.I.Ch.E. Symp. Ser., 70, No 141, 131, (1965).

(35) Donsi, G. and Massimilla, L.,"Proc. of Int. Symp. Fluid. ", 41, ed Angelino, H., Toulouse, OCT.,(1973).

(36) Donsi, G. and Massimilla, L., Powder Tech., 10, 303, (1976).

(37) Dow, W. and Jackob, M., Chem. Eng. Prog., 47, 637, (1951).

(38) Drinkenburg, A.A.H., "Proceeding Int. Symp. Fluid.", Eindhoven, ed Drinkenburg, A.A.H., Netherland, Univ.Press, (1967).

(39) Drinkenburg, A.A.H. and Rietema, K., Chem. Eng. Sci., 27, 1765,(1972).

(40) Drinkenburg, A.A.H. and Rietema, K., Chem. Eng. Sci., 28, 259, (1973).

(41) Ergun, S., Chem. Eng. Prog., 48, 89, (1952).

(42) Ferron, J.R. and Watson, c.c., Chem. Eng. Progr. Symp. Ser., No 58, 38, 79, (1962).

(43) Frantz, J.F., Chem. Eng. Progr., 57, 35, (1961).

(44) Fryer, C. and Potter, O.E., "Fluidisation and its application", ed Angelino, H., Toulouse, (1973).

(45) Fryer, C. and Potter, O.E., A.I.Ch.E.J., 22, 38, (1976).

(46) Gabor, J.D., Chem. Eng. Prog. Symp. Ser., No 105, 66, 76, (1970)

(47) Geldart, D., Powder Tech., 6, 201, (1973).

(48) Geldart, D. and Baeyens, J., "Fluidisation and its application", 263, Toulouse, ed Angelino, H., (1973).

(49) Goren, S.L., J. Fluid Mech., 41, 619, (1970).

(50) Gupta, S.N., Chaube, R.B. and Upadhyay, S.N., Chem. Eng. Sci., 28, 839, (1973).

(51) Happel, J. and Bernner, H., "Low Re No. Hydrodynamics", 260, Prentic-Hall, (1965).

(52) Harrison, D. and Bhattacharya, S.C., Trans. Inst. Chem. Engrs., 54, 281, (1976).

(53) Harrison, D. and Guedes de Carvalho, J.R.F., "Proc. of Int. Fluid. Conf." ed Keairns, D.L., California, Hemisphere Publishing Co., Washington, (1975).

(54) Harrison, D. and Leung, L.S., Trans. Inst. Chem. Engrs., 40, 146,(1960).

(55) Harrison, D. and Pyle, D.L., Chem. Eng. Sci., 22, 531, (1967).

(56) Heertjes, P.M., Can. J. Chem. Eng., 40, 105, (1962).

(57) Heertjes, P.M., De Boer, H.G.J. and De Haas Van Dorsser, A.H., Chem. Eng. Sci., 2, 97, (1953).

(58) Heertjes, P.M. and McKibbins, S.W., Chem. Eng. Sci., 5, 161, (1956).

(59) Henszelmann, F. et al, "Proc. of Int. Symp. Fluid. ", Eindhoven, ed Drinkenburg, A.A.H., Netherland Univ. Press, (1967).

(60) Higbie, Trans. AICHE., 31, 365, (1935).

(61) Hovmand, S. and Davidson, J.F., "Fluidisation", 228, ed Davidson, J.F., and Harrison, D., Academic Press, (1971).

(62) Kato, K., Kubota, H. and Wen, C.Y., Chem. Eng. Prog. Symp. Ser., 66, No 105, 87, (1970).

(63) Keey, R.B., "Drying, Principles and Practice", 98, Pergamon Press, (1972).

(64) Kettenring, K.N., Mander Field, E.L. and Smith, J.M., Chem. Eng. Prog., 46, 139, (1950).

(65) Kunii, D. and Levenspiel, O., Ind. Eng. Chem. Fund., 7, 446, (1968)

(66) Latham, R. and Potter, O.E., Chem. Eng. J., 1, 152, (1970)

(67) Levenspiel, O. and Walton, J., Chem. Eng. Prog. Symp. Ser., No 9, 50, 1, (1954).

(68) Mathur, K.B. and Gishler, P.E., J. Appl. Chem., 5, 624, (1955).

(69) McConnachie, J.T.L. and Thodos, G., A.I.Ch.E.J., 9, No 1, 60, (1963).

(70) Mickley, H.S. and Fairbanks, D.F., A.I.Ch.E.J., 1, 374, (1955).

(71) Murray, J.D., J. Fluid Mech., 22, 57, (1965).

(72) Myklestad, O., Int. J. Heat and Mass Tran., 11, 675, (1968).

(73) Novak, L.T. and Coulman, G.A., Can. J. Chem. Eng., 53, 60, (1975).

(74) Orcutt, J.C., Davidson, J.F. and Pigford, R.L., Chem. Eng. Prog. Symp. Ser., 58, (38), 1, (1962).

(75) Partridge, B.A. and Rowe, P.N., Trans. Inst. Chem. Engrs., 44, T 335, (1966).

(76) Peck, R.E., Max, D.A. and Ahluwalia, M.S., Chem, Eng. Sci., 26, 389, (1971).

(77) Peck, R.E. et al, Can. J. Chem. Eng., 52, 201, (1974).

(78) Peterson, W.S., Can. J. Chem. Eng., OCT., 226, (1962).

(79) Petrovic, L.J. and Thodos, G., "Proceeding of Int. Symp. Fluid.", ed Drinkenburg, A.A.H., 586, Eindhoven, Netherland Univ.Press, (1967).

(80) Pfafflen, J.R., Shridhar, M. and Jullien, G.A., A.I.Ch.E. Symp. Ser., 70, No 141, 70, (1974).

(81) Philip, J.R. and De Vries, D.A., Trans. Am. Geophysical Union, 38, 222, (1957).

(82) Pyle, D.L., "Fluidised Bed Reactor - Reveiw", Imperial College, (1972), London.

(83) Pyle, D.L. and Haagreaves, J.H., Chem. Eng. Sci., 27, 433, (1972).

(84) Pyle, D.L. and Rose, P.L., Chem. Eng. Sci., 20, 25, (1965).

(85) Riccetti, R.E. and Thodos, G., A.I.Ch.E.J., 7, No 3, 442, (1961).

(86) Richardson, J.F., "Fluidisation", 34, Academic Press, ed Davidson and Harrison, London, (1971).

(87) Richardson, J.F. and Szekely, J., Trans. Inst. Chem. Engrs., 39, 212, (1961).

(88) Richardson, J.F. and Bakhtiar, A.G., Trans. Inst. Chem. Engrs., 36, 283, (1958).

(89) Rietema, K. and Hoebink, J., "Int. Symp. of Fluid. and its Application", 319, ed Angelino, H., Toulouse, (1973).

(90) Rietema, K. and Hoebink, J., "Proceeding of Int. Fluid. Conf.", 279, ed Keairns, D.L., California, Hemisphere Publishing Co., Washington,(1975).

(91) Rietema, K. and Mutsers, S.M.P., "Proc. of Int. Symp. Fluid. ", 28, ed Angelino, H., Toulouse,(1973).

(92) Rowe, P.N. and Claxton, K.T., Trans. Inst. Chem. Engrs., 43, T 321, (1965).

(93) Sastry, K.V.S. and Fuerstenau, D.W., Powder Tech., 7, 97, (1972).

(94) Scott, M.W., et al, J. of pharm. Tech., 52, No 3, 284, (1963).

(95) Sherwood, T.K., Pigford, R.L. and Wilke, C.R., "Mass Transfer", 39, McGraw Hill, New York,(1975).

(96) Shen, C.Y. and Johnstone, H.F., A.I.Ch.E.J., 1, 349, (1955).

(97) Smith, J.M., Chem. Eng. J., 5, 109, (1973).

(98) Stimson, M. and Jeffery, G.B., Proc. Royal Soc. London, 111, 110, (1926).

(99) Sunkoori, N.R. and Kaparthi, R., Chem.Eng.Sci., 12, 166, (1960).

(100) Thoenes, D. and Kramers, H., Chem. Eng. Sci., 8, 271, (1958).

(101) Tuot, J. and Clift, R, A.I.Ch.E.Symp. Ser., No 126, 69, 78,(1973).

(102) Vanecek et al, "Fluidised bed drying", London, Hill, (1966).

(103) Vanecek, V., Markuat, M and Drbahlav, R., "Proceedings Int. Symp. on fluidisation", 617, Netherland Univ. Press, ed Drinkenburg, A.A.H., Eindhoven, (1967).

(104) Van Heerden, C., Nobel, P. and Van Krevelen, P.W., Chem,Eng. Sci., 1, 51, (1951).

(105) Van Heerden, C., Nobel,P. and Van Krevelen, P.W., Ind. Eng. Chem., 45, 1237, (1953).

(106) Vitovec, J., Chem. Eng. J., 10, 235, (1975).

(107) Walker, B.V., Chem.Eng. J., 9, 49, (1975).

(108) Wall, C.J. and Ash, W.J., Ind. and Eng. Chem., 41, 1247, (1949).

(109) Wamsley, W.W. and Johanson, L.N., Chem. Eng. Prog., 50, 347, (1954).

(110) Wen, C. and Leva, M., A.I.Ch.E.J., 2, 482, (1956).

(111) Wender, L. and Cooper, G., A.I.Ch.E.J., 4, 15, (1958).

(112) Wormald, D. and Burnell, E.M.W., Brit. Chem. Eng., 16, 376, (1971).

(113) Yates, J.G. and Constans, J.A.P., "Fluidisation and its application", 481, ed Angelino,H., Toulouse, (1973).

(114) Yoon, P. and Thodos, G., Chem.Eng. Sci., 27, 15 49, (1972).

(115) Yoshida, K., Kunii, D. and Levenspiel, O., Int. J. Heat and Mass Transfer, 12, 529, (1969).

(116) Yoshida, K., Ueno, T. and Kunii,D., Chem. Eng. Sci., 29, 77, (1974).

(117) Zabrodsky, S.S., Antonishin, N.V. and Parnas, A.L., Can. J . Chem. Eng., 54, 52, (1976).

(118) Ziegler, E.N. and Homles, J.T., Chem.Eng.Sci., 21, 117, (1966).